Isolation, Characterisation and Reactivity of Five-Coordinate Pt^{IV} Complexes

By Paul Anthony Shaw

A thesis submitted for the partial fulfilment

of the requirements for the degree of

Doctor of Philosophy in Chemistry

Supervised by Dr Jon Rourke

Presented to

The University of Warwick

Department of Chemistry

November 2017

Table of Contents

Acknowledgements

I would first like to express my gratitude Dr. Jon Rourke, whose guidance shaped this thesis. Many thanks go, also, to Guy Clarkson for the many crystal structures determined and presented in this thesis. I greatly appreciate the funding from the EPSRC, which allowed me to conduct my research.

Thanks are also due to the many people I have shared office and lab space with over the course of my Ph.D. research, from whom I have been able to learn about chemistry beyond my own field of expertise, and gained friendships.

Lastly, I would like to thank friends and family who have often encouraged me to take a break from work, and pay them the occasional visit.

Declaration

I hereby declare that this thesis is my own work. To the best of my knowledge and belief, it contains neither material previously published or written by another person, nor material which has been accepted for the award of any other degree or diploma of a university or institute of higher education, except where due acknowledgement is made in the text.

Sections cotainining work carried out by past members of the Rourke group include "Section 2.2. Triphenylposphine derivative **1-Ph**" and "Section 2.3.1. Tributyl phosphine derivative **1-Bu**". Full aknowledgements to contributions are made in the paragraph directly below the respective section titles in the thesis text.

Paul Anthony Shaw

List of published journal articles based on the work presented in this thesis:

P. A. Shaw, J. M. Phillips, C. P. Newman, G. J. Clarkson and J. P. Rourke, *Chem. Commun.*, 2015, **51**, 8365-8368.

P. A. Shaw, J. M. Phillips, G. J. Clarkson and J. P. Rourke, *Dalton Trans.,* 2016, **45**, 11397-11406.

P. A. Shaw, G. J. Clarkson and J. P. Rourke, *Organometallics*, 2016, **35**, 3751–3762.

P. A. Shaw and J. P. Rourke, *Dalton Trans.*, 2017, **46**, 4768-4776.

P. A. Shaw, G. J. Clarkson and J. P. Rourke, *Chem. Sci.*, 2017, **8**, 5547–5558.

P. A. Shaw, G. J. Clarkson and J. P. Rourke, *J. Organomet. Chem.*, 2017, **851**, 115–121.

Abstract

The oxidative addition to square planar dicyclometallated C^N^C Pt^{II} 16 valence electron complexes (C^N^C= 2,6-di(4-fluorophenyl)pyridine and 2-(4-fluorophenyl)-6-*tert*butylpyridine) was studied with Cl_2 (via $PhICl_2$) and alkyl halides (e.g. MeI, BnBr and allylBr). The two-step nature of the process meant that Pt^{IV} 16 valence electron five-coordinate intermediates could be identified. The product of oxidation was an octahedral 18 valence electron product with the new groups added mutually *trans* across the metal, with isomerisation seen with time. However, in the case of the chlorine-based oxidant, $PhICl_2$, this was only part of the story, where further reactivity depended on the phosphine coordinated in the fourth coordination site. Oxidation of the PPh_3 derivative gave a long-lived five-coordinate intermediate (lasting about four hours) before combination with the second chloride. Complexes containing PBu_3, PPr_3 and P(*o*-Tol)$_3$ trapped the five-coordinate complex with agostic interactions, eventually leading to transcyclometallation products.

In parallel to these studies, abstraction of X^- from the octahedral Pt^{IV} oxidation products gave another path to the five-coordinate intermediates, and in most cases, they could be trapped with pyridine. Whilst we did not see any evidence of aryl-Cl coupling, we were able to isolate several three-coordinate monocyclometallated Pt^{II} products, which came about through aryl-R reductive elimination via a long-lived five-coordinate complex which were characterised in solution. Addition of a mild base led to the activation of the C(sp^2)-H bond, reforming the five-membered ring. Addition of another equivalent of the alkyl halide, and subsequent addition of $AgBF_4$ showed 100% regioselectivity for reductive coupling of the R group to the ring substituted previously. When C^N^C was 2-(4-fluorophenyl)-6-*tert*butylpyridine), the reductive elimination reaction was spontaneous under the reaction conditions for RX addition, showing complete selectivity of C(sp^3)-C(sp^2) over C(sp^3)-C(sp^3).

Further to these reactions, the PBn_3 derivative was also treated with $PhICl_2$, which led to the formation of a Pt^{IV} tricyclometallated product. When the halide was removed from the tricyclometallated complex (again with $AgBF_4$), reductive elimination of the coordinated benzyl and aryl group gave a three-coordinate complex with a strained nine-membered ring. Two distinct mechanisms were identified for the inversion of the ring, one of which included the breaking of the C-C bond to reform the five-coordinate intermediate. The fourth coordination site was open enough to allow chloride, CO and H_2 to coordinate. Coordination of H_2 was not seen directly, instead a product with no cyclometallation and a Pt-H bond was observed.

Abbreviations

Bn	Benzyl
C^N^C	Dicyclometallated ligand. ^ symbol denotes linkages
COSY	COrrelated SpectroscopY
d	doublet
e^-	electron
ESI-MS	ElectroSpray Ionisation Mass Spectrometry
FWHH	Full Width at Half Height
HMBC	Heteronuclear Multiple-Bond Correlation spectroscopy
HR-MS (ESI)	High Resolution Mass Spectrometry (ElectroSpray Ionisation)
HOMO	Highest Occupied Molecular Orbital
HSQC	Heteronuclear Single-Quantum Correlation spectroscopy
J	*J*-Coupling
LUMO	Lowest Occupied Molecular Orbital
m	multiplet
Me	methyl
NMR	Nuclear Magnetic Resonance
nOe	nuclear Overhauser effect
PBn_3	Tribenzylphosphine
PBu_3	Tri-^{n}butylphosphine
pen	pentet
Ph	Phenyl
P^oTol_3	Tri(*o*-tolyl)phosphine
PPh_3	Triphenylphosphine
ppm	parts per million
PPr_3	Tri-^{n}propylphosphine
py	pyridine
q	quartet
RT	Room Temperature
s	Singlet
sex	sextet
t	triplet

1.0 Introduction

1.1. Overview of Organometallic Chemistry

An organometallic compound is commonly defined as one containing a M-C bond. The existence of these compounds has been known for around 200 years, but only in the last 50 or so years has the study of these complexes been described within the emerging field of organometallic chemistry. The rise of interest in these compounds can be attributed to their use as catalysts and as reagents in organic synthesis, making them of high value to industry.

Arguably, the simplest organometallic complexes are those of main group metals, where only M-C σ-bonds are possible. These complexes are often seen in organic synthesis, used as strong bases, and anionic carbon synthons. Common examples include butyl lithium, Grignard reagents (general structure RMgX), diethyl zinc, and trimethyl aluminium (Figure 1.1).

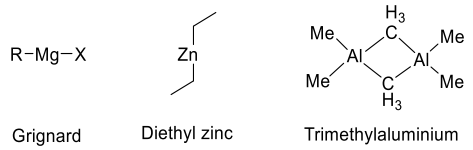

Figure 1.1 Examples of main group organometallic compounds.

More interesting, is the bonding of carbon to transition metals, which have d-orbitals and multiple stable oxidation states. The d-orbital lobes can overlap with carbon p-orbitals and therefore form multiple bonds to the same carbon. Compounds containing M-C multiple bonds (i.e. M=C and M≡C, known as alkylidene and alkylidyne complexes respectively) have been characterised (Figure 1.2). The original synthesis of these compounds was pioneered by Schrock and Fischer.[1–3]

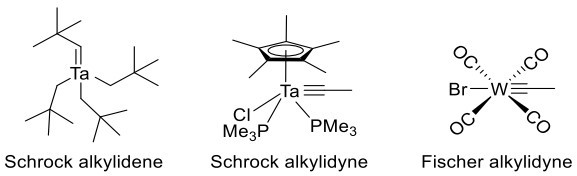

Figure 1.2 Examples of M-C single, double and triple bonds in transition metal organometallic complexes.

Alkenes can coordinate to metals, where the electrons of the π bond are donated to the metal. The first example was synthesized by Zeise in 1827.[4] Zeise's salt is a Pt^{II} trichloro complex with an η^2 coordinated ethene (Figure 1.4). The crystal structure showed that the ethene was coordinated to the platinum "side on" with the plane of the alkene orthogonal to the bond to the metal. Metals can also coordinate to extended π systems such as 1,3-butadiene. Figure 1.3 shows a complex with three equivalents of 1,3-butadiene (each coordinated η^4) coordinated to a single molybdenum (with two of the dienes omitted for clarity) exemplifying metals coordinating to extended π systems.[5]

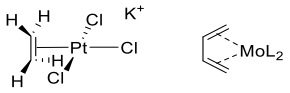

Figure 1.3 Structures of Zeise's salt (left) and molybdenum tris(butadiene) (right).

Aromatic rings can also coordinate to metals. When they coordinate via all of the carbons they form speces with names like sandwich complexes and piano stools. Ferrocene is one such organometallic complexes, and the first to be synthesized (Figure 1.4).[6] During the original synthesis of ferrocene, Pauson and Kealy reacted the cyclopentadienyl anion with an iron salt.[7] While they expected η^1 coordination of two cyclopentadienyl ligands, they were surprised to find that this was not the case when they realised that the complex was stable to air. It was later discovered that that the two cyclopentadienyl ligands were each coordinated η^5. This was based on the results of several spectroscopic techniques including infra-red spectroscopy where only one C-H stretching frequency was seen. The sandwich structure was later proven by NMR and crystal structure.[8]

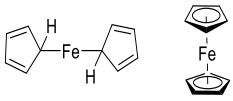

Figure 1.4 Incorrect (left) and correct (right) structures of ferrocene.

Organometallic complexes are very rare in nature, with the most well-known being vitamin B_{12}. This essential vitamin has a Co-R bond, and is responsible for several C-H/C-C bond forming and breaking reactions. In fact, most occurrences of M-C bonds in nature are short-lived intermediates.

Main group organometallic complexes are used in stoichiometric amounts, which creates a lot of metal waste, especially when industrial reaction scales are considered. Transition metals, however, are commonly used as catalysts, where a far smaller quantity of the metal is required.

There are a few exceptions to the "requirement of a M-C bond" definition for an organometallic complex, where the definition has been expanded to sometimes include metals with coordinated phosphines. This is more relevant for organometallic catalysts, where the inactive catalyst may not have a M-C bond, but will during the catalytic cycle.

A general catalytic cycle is shown in Figure 1.5. Typically, the catalytic cycles begin with an inactive pre-catalyst which is relatively easy to manipulate before the reaction. Activation can be spontaneous in situ, sometimes only requiring the dissociation of a ligand (or the coordination of the substrate). Next, a substrate might oxidatively add to the activated metal catalyst, followed by modifying steps to alter the added group. In the final step, the product can reductively eliminate, and the active catalyst is regenerated (completing the cycle). Note that the term "modification steps" is intentionally vague in this instance as the number of possible reactions that can occur at this step are too numerous to be explained here (also the focus of this thesis is on the oxidative addition and reductive elimination steps).

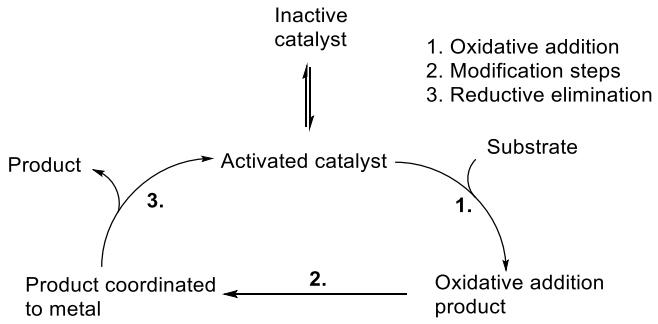

Figure 1.5 Illustration of a general catalytic cycle.

A good understanding of a catalytic cycle is important as to be able to design more specific catalysts, to improve yields, or reduce metal waste (lower catalyst loading). In asymmetric catalysis, chiral ligands are chosen in order to ensure the coordination of a pro-enantiomeric molecule coordinates more favourably on one face. The metal catalysed transformation is then enantioselective, meaning that the product mixture is enriched in one isomer over the other. In the reduction of ketones with hydrogen gas, Noyori catalysts

employ enantio-pure BINAP ligands to successfully select the desired enantiomer of the alcohol product (sometimes up to 100 % enantioselectivity), in a process called asymmetric hydrogenation (Scheme 1.1).[9]

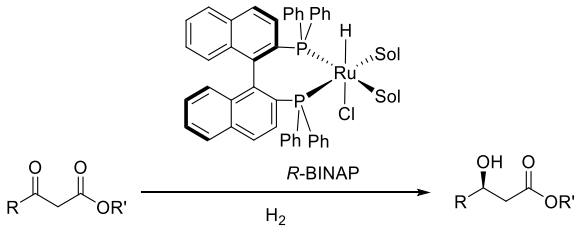

Scheme 1.1

Topics covered in the remainder of this chapter aim to give a broad overview of several important topics in organometallic chemistry relevant to the work in this thesis. This includes:

- Oxidative addition/reductive elimination
- Coordinatively unsaturated complexes
- Oxidative addition of alkanes
- Shilov chemistry

The chapter closes with the synthesis of the C^N^C dicyclometallated complexes synthesized previously in the Rourke group. Previous work (both from the Rourke group and elsewhere) that more closely resembles the work of a particular chapter are discussed in the introduction section of those chapters.

1.2. General Features of Oxidative Addition and Reductive Elimination Reactions

In the 1960s an effort was made to group similar organometallic transformations together. Oxidative addition emerged as a reactivity pattern of similar but distinct mechanisms.[10]

There are several distinct reaction mechanisms which can fall under the umbrella term of "oxidative addition", and may even compete, meaning that the reactions can be very sensitive to any change in the reaction. In the realm of organometallic chemistry, molecules like H_2 can be described as better oxidants than oxygen when reaction rates are compared.[11]

Oxidative addition and reductive elimination are connected by the microscopic reversibility principle.[12] This means that reductive elimination is the reverse of oxidative addition, and therefore the reactions share the same reaction mechanisms, just in the opposite order (relative to the other). Overall, in a typical oxidative addition reaction (including the reactions presented in the results chapters of this thesis) the oxidation state increases by two, the coordination number increases by two and the number of metal valence electrons is increased by two (Figure 1.6).[13] The opposite is true for reductive elimination.

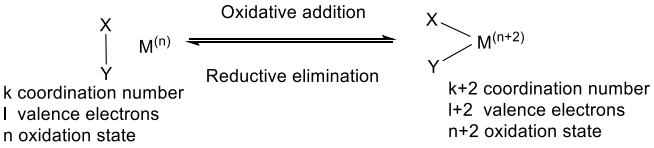

Figure 1.6 Illustration of a general oxidative adition and reductive elimination.

For an oxidative addition reaction to occur, the metal complex must have 16 valence electron or fewer (to allow the metal to accommodate the two extra electrons from the incoming group), and have a stable oxidation state two greater than the current oxidation state. Oxidative addition therefore favours lower oxidation states. A famous example includes the oxidative addition of RX compounds to magnesium to form Grignard reagents (RMgX).

Conversely, for reductive elimination reactions, the metal valence electron count is less of an issue. The complex requires an oxidation state two less than the current oxidation state, and so reductive elimination reactions favour higher oxidation states. Over the last 40 years C-C coupling reactions have gained a lot of attention (and Nobel prizes), as being able to form a C-C bond is very powerful in the synthesis of complex organic molecules. Important examples include the famous Suzuki and Heck cross-coupling reactions.[14–17] Reductive elimination of C-X[18] (where X is a halogen) and C-O[19,20] have also gained a lot of attention in the literature.

There are several known mechanisms of oxidative addition and reductive elimination including: ionic, radical, S_N2 and concerted. Radical and ionic mechanisms are not thought to be relevant to this project, and will not be explained here.

An S_N2 type oxidative addition is seen with more polar bonds such as alkyl halides and some non-polar diatomics such as Cl_2. Metals can donate electron density into the σ* orbital of X-Y (Figure 1.7). The metal forms a bond to Y, releasing an X^- leaving group,

which can later coordinate to the metal. Just like an S_N2 reaction for organic molecules the new M-Y bond forming, and the X-Y bond breaking are simultaneous, which has implications on the stereochemistry of Y (stereochemistry inversion). If Y-X adds to a square planar complex, the initial product is expected to have X and Y taking coordination sites on opposite sides of the metal, as this geometry would not require the movement of the other ligands.

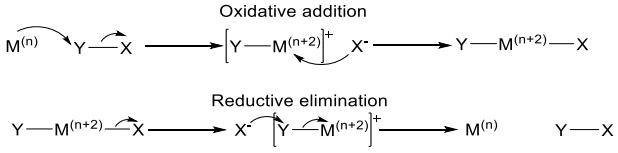

Figure 1.7 Illustration of a general S_N2-type oxidative addition or oxidative addition reaction.

An S_N2 type reductive elimination first requires the dissociation of X^- (Figure 1.7). The reaction therefore requires a labile M-X bond, where X^- can exist as a stable anion (e.g. halides). This reveals a coordinatively unsaturated complex. X^- then attacks the σ* orbital of Y to break the M-Y bond. Where there are many options for X^- to attack, the preference depends on many factors including accessibility of the M-Y σ* orbital, and the stability of the product (i.e. Br^- is unlikely to attack a phosphine or amine).

A concerted mechanism is seen for the oxidative addition of non-polar bonds. This includes C-H groups, dihydrogen and aryl halides. In a concerted mechanism, both of the new M-X and M-Y bonds are formed simultaneously with the breaking of the X-Y bond. This means that the initial product of a concerted oxidative addition reaction will have the added groups taking adjacent coordination sites. Figure 1.8 shows the concerted oxidative addition of a C-H bond.

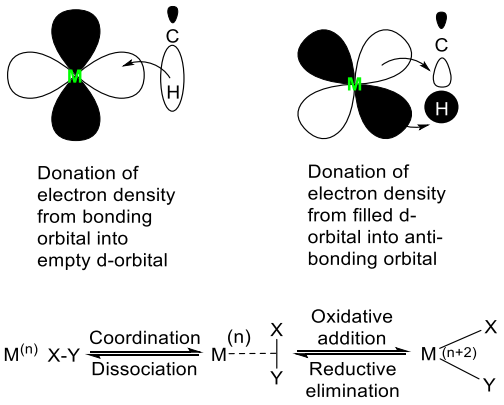

Figure 1.8 Illustration of the orbital overlap of d-orbitals and X-Y molecular orbitals and a general illustration of concerted oxidative addition and reductive elimination reactions.

X-Y can coordinate to the metal via the electron density of the X-Y σ-bond. Metals can also donate electron density back to X-Y into the σ* orbital. The greater the degree of this back-bonding, the more elongated the X-Y σ-bond becomes (as it becomes weaker). With enough back-bonding, the X-Y bond breaks to give the oxidatively added product. In a concerted reductive elimination mechanism, coupling groups must be in adjacent coordination sites, as the groups will be eliminated simultaneously (Figure 1.8).[21] The selectivity of a reductive coupling reaction depends heavily on kinetics (including proximity and availability of orbital overlap of coupling groups). Reductive elimination also requires that the product is a poor ligand, and so easily dissociates from the metal, as continued coordination may result in the group oxidatively adding to the metal again.

The product selectivity of concerted reductive eliminations is highly dependent on the geometry of the complex. The reason lies in the occupancy and geometry of the various d-orbitals, which has been rationalized computationally (Figure 1.9).[22,23] The results of the computational studies showed that a concerted reductive elimination mechanism is highly disfavoured at coordinatively saturated complexes.[24] The electrons from the leaving X-Y group would be donated into a highly antibonding orbital, which would destabilise the complex. If the complex can first lose a ligand (revealing a coordinatively unsaturated species), the electrons from the leaving X-Y group are instead donated into a lower energy non-bonding orbital. This therefore imposes conditions on the geometry of the complex, and the selectivity of reductive coupling reactions (explored further in Chapter 3).

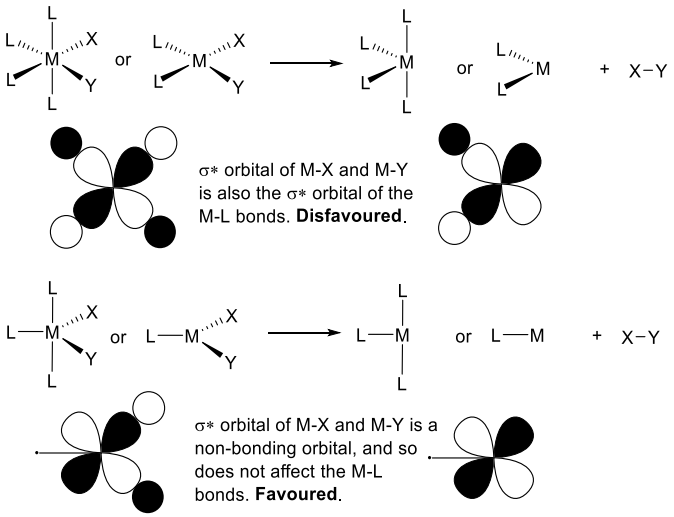

Figure 1.9 Illustration to describe the selectivity of reductive elimination reactions.[13]

Formation of a coordinatively unsaturated complex is therefore the initial step in both S_N2 and many concerted reductive elimination mechanisms. Recent work in the Sanford group looked at the competition between these two mechanisms. They studied a derivative of their complex where pyridine took the sixth coordination site of their complex (Scheme 1.2).[25] Pyridine was chosen as it is a labile ligand (which would reveal a coordinatively unsaturated complex), but also poorly nucleophilic (ruling out an S_N2 reductive elimination pathway). Heating the complex led only to the concerted reductive elimination of F-C_{alkyl}.

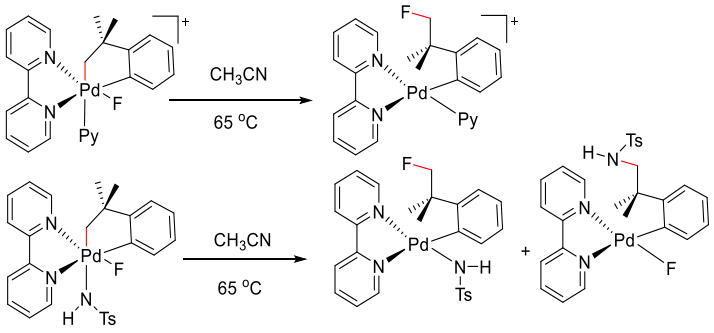

Scheme 1.2

The next step was to replace the pyridine with the nucleophilic pro-ligand 4-toluenesulfonamide.[26] Heating the complex gave the analogous F-C_{alkyl} reductive coupled product. Also seen was a N-C_{alkyl} reductive elimination product. Since the 4-toluenesulfonamide group was *trans* to the C(sp^3), a concerted N-C_{alkyl} reductive elimination mechanism is not possible. Instead, like the pyridine group, the 4-toluenesulfonamide group would have dissociated, and revealed a coordinatively unsaturated complex, allowing for attack of the C(sp^3) via an S_N2 type mechanism.

The S_N2 N-C_{alkyl} reductive coupling pathway was therefore in competition with the F-C_{alkyl} concerted reductive coupling pathway. The reaction can be pushed towards 100% conversion to the C-N reductive elimination product by adding excess 4-toluenesulfonamide. With more 4-toluenesulfonamide in solution, as soon as a 4-toluenesulfonamide ligand dissociates, another can attack the C-Pd bond (outcompeting the F-C_{alkyl} coupling pathway).

As in organic chemistry, an S_N2 attack at a chiral carbon results in the inversion of the stereocentre because the nucleophile attacks on the face opposite the leaving group. A concerted reductive elimination mechanism will instead give retention the stereocentre as the leaving group would just replace the metal on the same face. A recent paper describes an example in which the reductive elimination mechanism can be chosen by the inclusion of an additive (Scheme 1.3).[27] When XeF_2 (a source of F^-) was reacted with a cationic platinum alkyl complex, the fluoride coordinated to the metal, which was followed by the concerted reductive elimination of C-F.

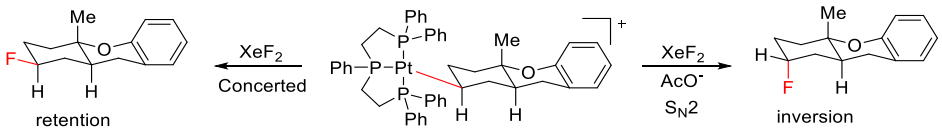

Scheme 1.3

When acetate was added before XeF_2, the acetate coordinated to the metal. The fluoride (unable to coordinate to the metal) attacked the cyclohexyl ring at the Pt-C via an S_N2 reductive elimination mechanism. Note that in each case the reactive platinum centre was five-coordinate before the reductive elimination of the fluorinated cyclohexyl ring.

1.3. Coordinatively Unsaturated Complexes

Oxidative addition and reductive elimination reactions are often seen to go via coordinatively unsaturated intermediates. These species are known to be highly reactive and short-lived, meaning that the study of these species is of academic interest.[28,29]

Of importance to the work presented in this thesis is the formation of 16 valence electron five-coordinate intermediates (Figure 1.10). Starting from a 16 valence electron square planar complex, a five-coordinate complex can be made via the addition of a positively charged species (e.g. H^+ or Cl^+). Conversely the same complex can be made by starting

with an 18 valence electron octahedral complex, and removing a negatively charged species (e.g. Cl^-) or a neutral species (e.g. phosphine or DMSO). The example in Figure 1.10 is modelled on work presented in this thesis.

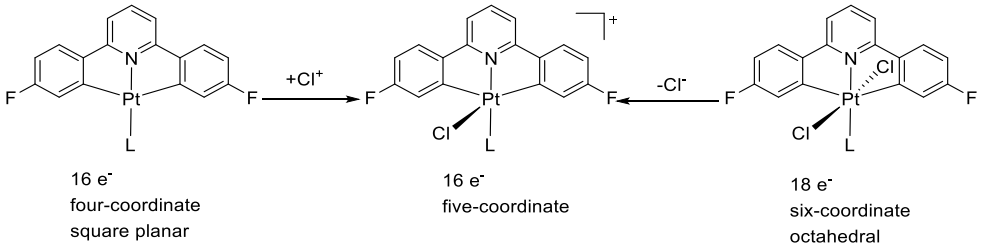

Figure 1.10 Illustration of the formation of a 16 valence electron coordinatively unsaturated species.

The Goldberg group have shown how stable five-coordinate complexes may be observed (Scheme 1.4).[30] By looking at the 16 valence electron complex with three methyl groups *cis* to each other (and a geometry which would favour reductive elimination), one would imagine that the evolution of ethane gas would be facile. However, it is completely stable at room temperature. They found that the complex required temperatures as high as 150 °C before it will begin to evolve ethane gas. The stability of the five-coordinate complex is thought to be because of the anionic nacnac ligand (nitrogen analogue of acetyl acetonate) making the complex neutral overall. The reductive elimination step led to the activation of one of the ^{i}Pr chains, forming a new five-coordinate species with a six-membered cyclometallated ring. Further elimination of methane gave a stable three-coordinate species.

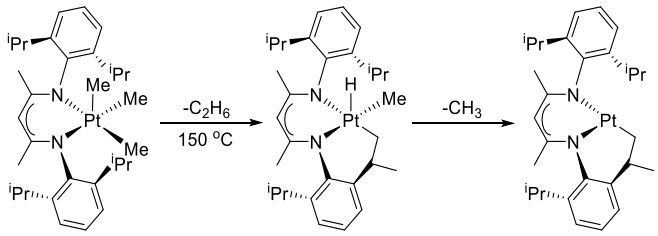

Scheme 1.4

A recent paper by Marta Roselló-Merino et al shows the formation of a five-membered platinacycle, via the formation of an C(sp^3)-Pt bond at a three-coordinate complex (Scheme 1.5).[31] After the addition of a silver salt to a Pt^{II} four-coordinate complex (to remove the iodide), the three-coordinate complex is revealed. When R' = H, no cyclometallation reactions took place, even with high temperatures and extended heating times.

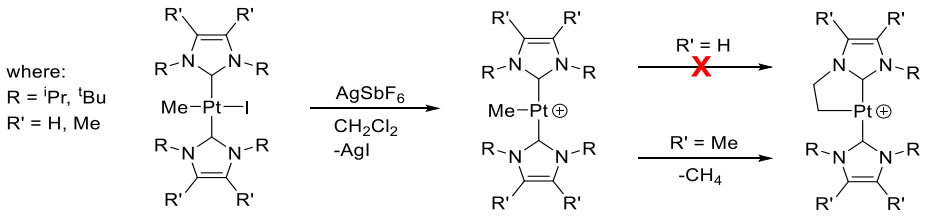

Scheme 1.5

When R' = Me, cyclometallation of the R group (and subsequent reductive elimination of methane) was seen. When R = ^{t}Bu the cyclometallation reaction occurred below -80 °C whilst when R = ^{i}Pr, full conversion to the cyclometallated complex required elevated temperatures (45 °C), with the reaction complete after 12h. The reaction is therefore driven by sterics, where the R' groups clash with the R groups. The larger the two groups, the closer the R group is to the metal, which encourages the C-H bond activation. This also explains why the ^{t}Bu derivative reacts faster than the ^{i}Pr derivative.

1.4. Dihydrogen Complexes

Stable dihydrogen complexes are quite common in the literature.[32] Like alkene complexes, the H-H bond lengths are shown to be elongated when compared to free H_2, showing a degree of back bonding to the hydrogen (and therefore requiring low metal oxidation state metals). The dihydrogen complex is therefore seen as an intermediary between an oxidatively added complex (i.e. a dihydride) and the free H_2. The range of typical H-H bods in dihydrogen complexes lies between 0.8 and 1.1 Å (the length of a "free" dihydrogen molecule is 0.74 Å).[32] Dihydrogen complexes with longer H-H bond lengths are described as stretched, but more commonly as compressed dihydrides, as the H-H σ-bond displays more characteristics of being broken. This can be measured by H-H (or H-D) coupling constants. As the H-H bond shows more "broken" character, the coupling constant drops dramatically (from around 30 Hz to around 2 Hz). However, the most precise method of determining bond lengths is neutron diffraction.

The earliest dihydrogen complexes were synthesized by the Kubas group in 1984 (Figure 1.11).[33,34] A feature of these complexes (which can also be seen in many more recent examples) is the presence of strong *trans* directing CO ligands, which sympathetically aid the coordination of the H_2 group. This effect plays into the antisymbiosis effect (which is an extension of the *trans* effect), where mutually *trans* soft ligands have a tendency to destabilise each other.[35]

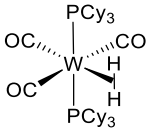

Figure 1.11 Illustration of a Kubas Complex.

Vaska's complex is the standard complex for the study of oxidative addition reactions (Scheme 1.6).[36] Various analogues have been synthesized, with different phosphines and X groups in order to probe oxidative addition reactions. In the coordination of H_2, Vaska's complex has shown to be able to reversibly add H_2 under relatively mild conditions. For example, under vacuum, the product of the oxidative addition of H_2 (an Ir^{III} octahedral complex) will lose H_2, and reform Vaska's complex.

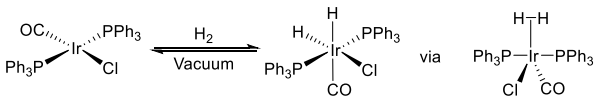

Scheme 1.6

Reaction of H_2 with Vaska's complex (a square planar 16 valence electron iridium complex) leads to an octahedral dihydride complex, with the two hydrogens mutually *cis*. The reaction is thought to go through a five-coordinate trigonal bipyramidal intermediate, where the H_2 group is part of the trigonal plane. This mechanism shows that square planar complexes are not inert to oxidative addition reactions via concerted mechanisms.

1.5. Oxidative Addition of C-H Bonds

C-H bonds are usually thought to be quite inert due to the high bond dissociation energy (~100 kcal/mol for an alkyl C-H bond).[37]. Before hydrocarbons are suitable for use in synthesis, they are currently functionalised first by oxidation or radical processes. These processes require vast amounts of energy, and are wasteful.

The holy grail of organometallic chemistry is in the selective functionalisation of C-H bonds in organic synthesis without the need for activated precursors.[38,39] There are already many papers that discuss methods of selective C-H bond activation.[40] In the famous Heck reaction, protons on terminal alkenes are selectively activated.[16] Large ligands coordinated to the metal can lead to activation of only the least sterically hindered protons of an organic molecule. In cyclometallation reactions, C-H activation is facilitated by the forced

proximity to the metal.[41] Other mechanisms besides oxidative addition exist[41–48] but with the exception of cyclometallation deprotonation (covered in section 1.5.2) these mechanisms will not be covered in this thesis.

Oxidative addition reactions of C-H can be split into two distinct types: intermolecular and intramolecular (Figure 1.12), which just describes whether the substrate is coordinated to the metal prior to activation. Oxidative addition of C-H bonds is directly comparable with that of H_2, except H_2 lacks the possibility of intramolecular assistance. Like the coordination of H_2, oxidative addition of a C-H bond is known to first require coordination of the C-H bond, forming a three-centred two-electron bond.[49] Efficient back-bonding lengthens the C-H bond until it breaks.

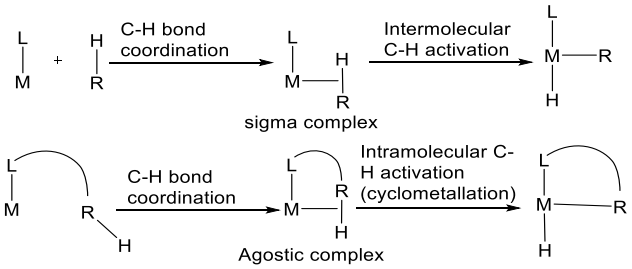

Figure 1.12 Illustration of general intra- and intermolecular C-H bond activation.

1.5.1. Oxidative Addition of Intermolecular C-H Bonds

Intermolecular coordination of a C-H bond gives a σ-complex (Figure 1.12). These are transient species, where the hydrocarbon is likely to simply dissociate from the metal. While there are many crystal structures of dihydrogen complexes. The weakness of the interaction for coordinated C-H bonds (compared to dihydrogen complexes) is because of the bulkiness of the alkane (compared to a tiny H_2 molecule). The Weller group reported the first unambiguous examples of X-Ray crystal structure of σ-complexes (**Error! Reference source not found.**).[50] The crystal was made by the addition of H_2 to a crystal of a rhodium norbornadiene complex (H_2 reduced norbornadiene to norbornane) at -173 °C. When the addition of H_2 was performed at RT, the norbornane was displaced by an aryl group of the $[BAr^F{}_4]^-$ counterion within hours. In the ^{13}C SSNMR, the characteristic peaks corresponding to the alkene carbons of norbornadiene disappeared quickly upon the addition of H_2 owing to the reduction of the C=C bond.

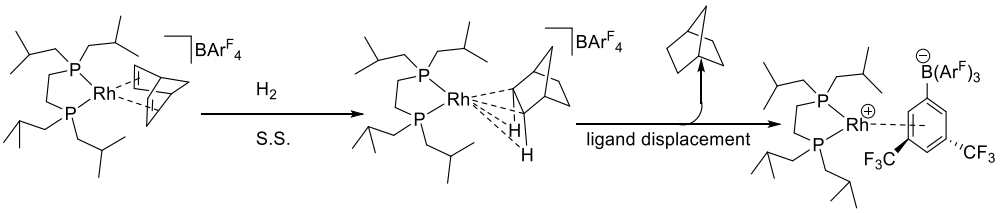

Scheme 1.7

The Weller group later reported the single crystal to single crystal synthesis of the norbornane rhodium complex which proved to be stable in air and at RT by using the analogous bidentate phosphine ligand 1,2-bis(dicyclopentylphosphino)ethane.[51,52] More recently Weller and co-workers have used similar techniques, alongside DFT calculations, to look at a pentane analogue of the previously mentioned structure.[53]

Previous to the Weller group's findings, the Meyer group reported an X-Ray crystal structure of an electro-rich uranium complex with a cyclohexane molecule in close proximety to the metal.[54] Alkanes (namely heptane) have also been reported to be trapped between porphyrin rings in the solid-state with short Fe-C distances.[55] The moieties around the porphyrin are thought to be responsible, "shielding" the heptane from solvent during the crystalisation.

Coordination of the terminal C-H bonds of an alkane has shown to be disfavoured, with a preference for coordination to C-H bonds nearer the middle of the alkane, which can be expected by the 10 kJ/mol difference in bond dissociation energy.[53,56,57] There is also evidence of preferential binding to axial vs equatorial C-H bonds.[58] Direct observation of intermolecular alkane σ complexes are still quite rare in the literature, but these transient species have been observed by NMR and IR at low temperatures (which decreases the rate of dissociation).[57,59]

Conversely, direct observation of the oxidative addition of saturated hydrocarbons is quite common. These are usually trapped by using metals complexes with very low oxidation states to make reductive elimination of the C-H bond unfavourable. This was first seen in complexes synthesized by Janowicz and Berman in 1982 (Scheme 1.8).[60]

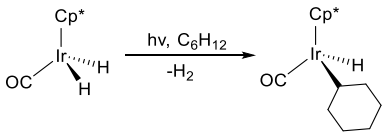

Scheme 1.8

The selectivity of alkane oxidative addition favours primary alkanes (the reverse of the trend seen for σ-complexes), likely due to the reduced steric crowding at the metal centre (as this would favour the reverse reaction). This can be seen in the borylation of alkanes, which is a topic too vast to be covered here, and has been covered in some depth in a review by Hartwig et al..[61]

After C(sp^3)-H bonds were shown to add to metals, the next step was to functionalise the alkane, and make the process catalytic. The most important process to mention at this point would be the Shilov system, which is explained in Section 1.7. A more recent example by Nishiyama, reporting an iridium complex that activates alkanes (namely octane) to form an alkane complex at 160 °C (Scheme 1.9).[62] The mechanism reported mechanism is via a concerted metalation deprotonation, where the oxidative addtion is assisted by the acetate groups which are coordinated to the metal deprotonating the alkane.[63,64] Goldberg and co-workers then found that upon heating the complex to 200 °C, the complex would eliminate octenes.[65] Most recently it has been reported that the starting material could be regenerated with O_2.[66]

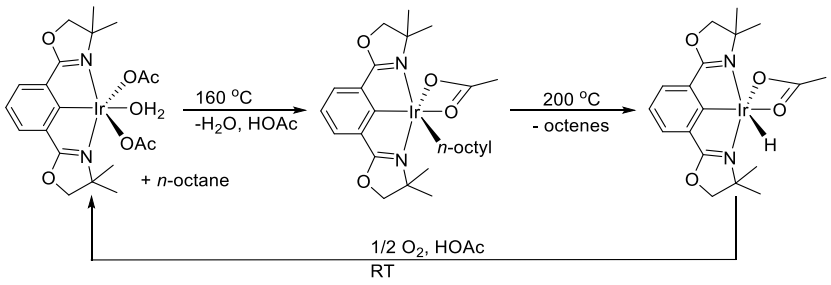

Scheme 1.9

Intermolecular oxidative addition of C(sp^2)-H bonds is much easier, owing to the relative stability of the oxidative addition product, examples of these were seen in the literature around 20 years earlier. To mention again the borylation of C-H bonds, C(sp^2)-H bonds will be activated in preference over C(sp^3)-H bonds.

An early example of arene C-H bond activation from 1965 by Chatt and Davidson showed the oxidative addition of naphthalene to a Ru(0) complex (Scheme 1.10). A Ru^{II} complex was first reduced with sodium metal to form a reactive Ru(0) species, followed by reaction with naphthalene.[67]

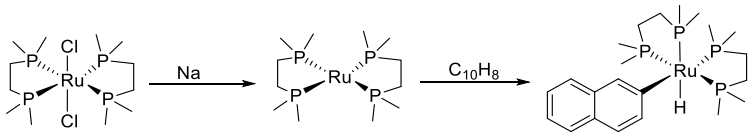

Scheme 1.10

Chatt and Davidson also discuss the reversibility of the C-H bond activation, noting that the complex also exists as a five-coordinate Ru(0) complex with an η^2 naphthalene group (Scheme 1.11). This was suggested by the reactivity of the complex towards I_2, and the liberation of naphthalene upon treatment with PEt_3 (where it is likely that the phosphine is displacing the neutral naphthalene). This was probably also one of the first observations of an η^2 arene complex (but without direct evidence, such as NMR data).

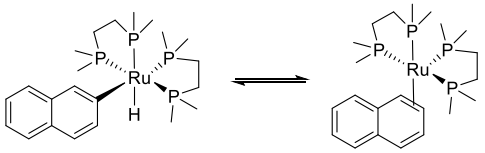

Scheme 1.11

Most commonly, an arene ligand will be seen coordinated via all of the carbon atoms of the aromatic ring (i.e. benzene will form an η^6 complex). Coordinating in this way forms a cap on the metal (e.g. sandwich and piano stool complexes). Greater hapticity leads to greater stability because of the chelate effect. η^2 coordinated arenes are relatively labile ligands, meaning that they are easier to displace (like the naphthalene in the earlier example). There are however, many examples of stable η^2 arene complexes in the literature, including complexes of rhenium (Figure 1.13),[68] osmium[69], ruthenium[70] and mixed metals (including ruthenium and osmium on the same aryl ring).[71]

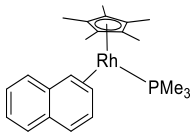

Figure 1.13 Illustration of an arene complex observed in solution.

These complexes provide a deep insight to the mechanisms of C-H activation in arenes, as they suggest that coordination of the arene would precede the C-H activation, rather than the coordination of the C-H bond.

1.5.2. Oxidative Addition of Intramolecular C-H Bonds

When σ-complexes form from C-H bonds which are tethered to the metal at a remote location, it is known as an agostic interaction (Figure 1.12). These interactions remain three-centre, two electron interactions.[72,73] Because the coordination of the C-H bond is assisted by the chelate effect (meaning that there is no entropic barrier of making one complex from two), it should be unsurprising that there are more examples of agostic interactions than intermolecular σ-complexes.[74–76] Agostic interactions can stabilize higher oxidation states via donation of electron density from the C-H σ-bond.[74] Agostic M-H bond lengths are around 1.8-2.3 Å, with M-H-C bond angles typically around 90 - 140°. Neutron diffraction studies have demonstrated that a standard M-H bond is a little shorter than this at around 1.6 – 1.7 Å.[60] The short M-H distance and small M-H-C bond angle suggests a greater involvement of the metal with the C-H σ-bond. In the ^{1}H NMR spectrum, the peak for the coordinated proton is likely to be seen upfield from that of the uncoordinated peak.

Agostic interactions are dynamic, with the coordinated hydrogen likely to exchange with symmetrically equivalent protons. In the ^{1}H NMR spectrum, a coordinated methyl group will typically only show a single resonance for that methyl group.[77] This also has implications on the $^{1}J_{\text{H-M}}$ coupling constant, as the true value of the coupling constant is shared across the equivalent protons. Agostic interactions have shown to favour the binding of C-H over C-D. Partial deuteration affects both the chemical shift and $^{1}J_{\text{H-Pt}}$ coupling constant.[78]

Anagostic interactions can be mistaken for agostic interactions, as both can be represented as M-H interactions (Figure 1.14). Anagostic interactions are identified by longer M-H bond lengths (2.3-2.9 Å) and larger M-H-C bond angles (110-170°), and the bonding is thought to be largely electrostatic (similar to a hydrogen bond) where the δ+ hydrogen is attracted to the electron rich metal. For some anagostic complexes (such as the example in Figure 1.14) the interaction can be forced by the geometric constraints of the ligands.

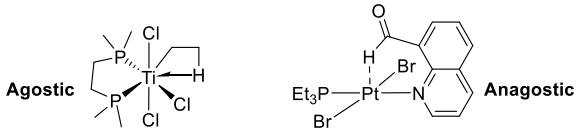

Figure 1.14 Illustration of the difference between agostic and anagostic interactions.

A C-H bond interaction can typically be assigned as agostic or anagostic with electron counting. In Figure 1.14 (left), the titanium of the octahedral complex (left) can be assigned as being Ti^{IV}, meaning a d^0 metal. There are six ligands (not counting the M-H interaction), each contributing two electrons. This means that the complex is 12 valence electron, which is low for a normal octahedral complex (where 18 valence electron is common). The donation of electrons from a C-H bond, would add an extra two electrons, making a 14 valence electron complex, which is closer to 18 valence electron. The C-H bond interaction is therefore agostic, as donation of electron density from the C-H bond is required to stabilize the low electron count of the complex.

In the square planar complex (Figure 1.14, right), the platinum can be assigned as Pt^{II}, meaning a d^8 metal. Four ligands contributing two electrons each, means this is a 16 valence electron complex. There are many examples of stable 16 valence electron square planar complexes, and so an extra two from a C-H bond is unnecessary. The M-H interaction here is therefore anagostic.

With this distinction between agostic and anagostic interactions only recently being identified, many previously reported agostic complexes are now being reclassified as anagostic. Yet, new research shows that the distinction between agostic and anagostic can be blurry.[79]

Agostic species are thought to play a role in some catalytic cycles. There are proposed mechanisms which suggest that the coordination of a C-H bond (from the substrate) is responsible for the enantioselectivity of the product. Zeigler-Natta catalysts are used in the polymerisation of alkenes. Agostic species are proposed as intermediates in chain propagation (Figure 1.15), and may be responsible for the retention of tacticity.[78]

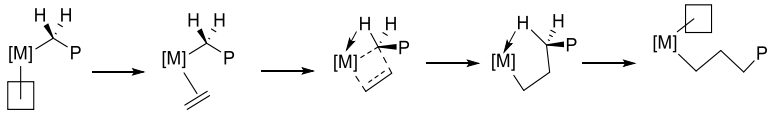

Figure 1.15 Illustration of a proposed alkene chain propagation mechanism including agostic interactions. The letter P represents the propagated chain.

Cyclometallation is an intramolecular C-H bond activation reaction (Figure 1.12).[80] Metallocycles are formed, which are organic rings in which the metal is a part. Initial complexation of the substrate increases the proximity of a particular C-H bond to a metal, increasing the chance of activation, and making cyclometallation reactions relatively facile

(and regiospecific). Cyclometallation reactions involving aryl C-H bond activation feature predominantly in the literature.

These reactions often occur without a change in oxidation state of the metal. Instead, the proton is removed by a base which may have even been previously coordinated to the metal. The three most important coordination assisted metalation (CAM) cyclometallation mechanisms are shown in Figure 1.16. One mechanism involves a concerted mechanism where the formation of M-C results in the elimination of HX. Overall, this can be seen as X^- being replaced by C^-. This is also the highest energy mechanism of the three, as the M-X bond is relatively strong. The remaining two mechanisms use a weak base, and differ by whether or not the base coordinates to the metal.[63,81]

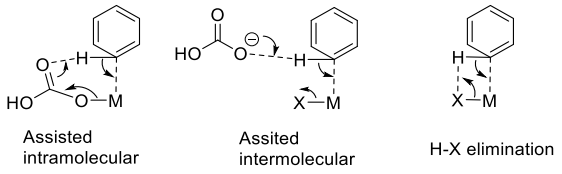

Figure 1.16 Illustrations of three important CAM reactions.

Although palladium is a relatively labile metal centre (required for its catalytic activity), cyclometallated complexes of palladium with four-[82] five-[83] six-[84] and even seven-[85] membered rings can be seen in the literature, with five-membered being most common. Ring sizes larger than six-membered are quite rare and tend to require stabilization, as reductive elimination pathways become more favourable.

The term "*Ortho*-metallation" (a special case of cyclometallation) was coined because of the prevalence of similar reactions in the literature. It describes the cyclometallation of bi-aryl rings, where the *ortho*- position of the second ring is commonly activated.[86] The metal first coordinates to a heteroatom (e.g. the nitrogen of bipy or 2-phenylpyridine), or a pre-existing ligand added earlier (e.g a biphenyl added via a prior intramolecular C-H activation, or transmetallation of M-R).[87] Because of the shape of these ligands, the *ortho* position of the second ring is held close to the metal, allowing for the formation five-membered metallocycles. Many examples for Pt^{II} and Pd^{II} can be seen in the literature, which are commonly isolated as halogen-bridged dimers (Scheme 1.12).[88–91]

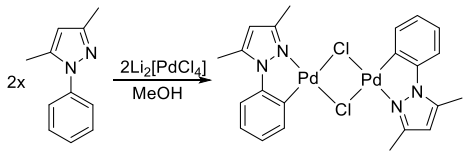

Scheme 1.12

Some of the earliest orthometallated complexes were synthesized in the 1960s. The Zelewsky group studied the electrochemical properties of dicyclometallated platinum complexes using mono-substituted pyridines. These were synthesized by reacting $Pt^{II}Cl_2(SEt_2)_2$ with 2-phenyl pyridines (lithiated at the ortho position) which gave only one product; ML_2, with the ligands in a N-N cis arrangement (Scheme 1.13).[92,93]

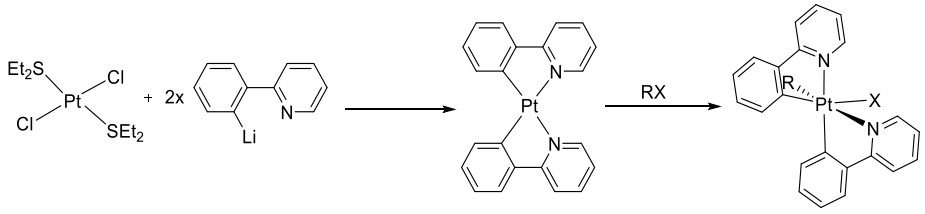

Scheme 1.13

These bis-cyclometallated complexes react cleanly with simple alkyl halides giving only one isomer, with the alkyl halide added *cis* to the metal (an octahedral complex with a *fac*-C_3 geometry).[94] The Pt^{IV} complex had a noticeable blue shift in the phosphorescence compared to the Pt^{II} starting material.[95] This has led to a great deal of research focussed on the role of these cyclometallated complexes in LEDs.[80,96–98] Cyclometallated platinum complexes have a number of applications in their own right, from chemical sensors to catalysts in the Fischer-Tropsch synthesis.[95,99,100] They also show promise as anti-cancer agents.[101,102]

With the synthesis of the first Pt-alkene complex (Zeise's salt)[4] in 1827, and the first Au^{I}-alkene complex in the late 1960s,[103] the synthesis of a stable Au^{III}-alkene complex remained elusive. Au^{III} has a high reduction potential (which is responsible for its use in catalysis), which meant past attempts to synthesize the Au^{III}-alkene complex instead led to the formation of Au^{I} or Au(0) products when exposed to alkenes. The Bochmann group were able to synthesize the first stable Au^{III}-alkene complex (Scheme 1.14).[104–106] The complex has a C^N^C dicyclometallated ligand filling the remaining three coordination sites, showing how dicyclometallated ligands improve stability to reduction.

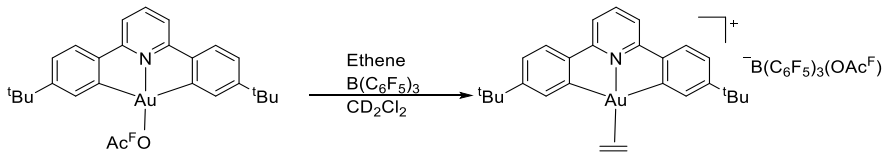

Scheme 1.14

N-heterocyclic carbene complexes of Au^{III} have proven to be efficient catalysts for a number of transformations.[107] The Bochmann group has probed the addition of a number of groups to their dicyclometallated (C^N^C)AuCl complexes (Scheme 1.15).

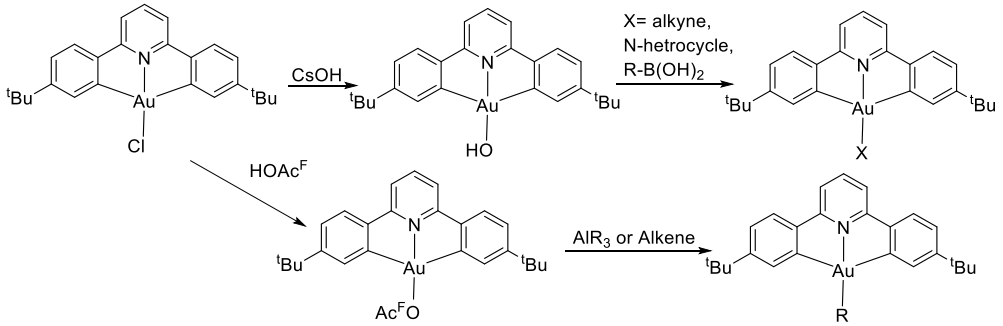

Scheme 1.15

This allows these complexes to be probed for catalytic ability, as addition of a group is the first step. Because Au^{I} and Au^{III} are isoelectronic with Pt(0) and Pt^{II} respectively, the chemistry of these cyclometallated compounds are of interest to this thesis.[108]

1.6. H/D Exchange at Metal Centres

Before the use of transition metals, the most efficient method of making benzene-d_6 was by boiling C_6H_6 in deuterated sulfuric acid (which was itself made by the reaction of deuterium oxide and H_2SO_4) at high temperatures, with long reaction times, giving 98 % deuterium incorporation, which equates to around 14 % being C_6D_5H. Leitch was able to reduce the amount of C_6D_5H to less than 4 % by using platinum black and deuterium oxide in the place of sulphuric acid.[109] Later Garnett found that sp^3 protons could be exchanged cleanly for deuterium in methyl-benzene compounds (from toluene all the way up to mellitene).[110–113] Garnett explained that the methyl hydrogens are also exchanged because the C(sp^3)-H bonds are activated by hyperconjugation, where the C(sp^3)-H bonds have some overlap with the π-system.

Alexander Shilov was the first to demonstrate that H-D exchange could also occur at alkanes. The discovery of both H/D exchange at metal centres and the Shilov system have been some of the most noteworthy additions to the research in C-H activation.[114] A recently published review celebrates 50 years since the initial contributions made by Shilov, and the research inspired from his work.[115] An example includes catalysts that can dehydrogenate alkanes (e.g. making benzene from cyclohexane).[116,117]

H/D exchange occurs through a concerted mechanism, shown in Figure 1.17. H/D exchange has since been observed at several different transition metal centres.[118] Deuterium labelling is now a standard technique to prove C-H bond activation where other techniques (e.g. NMR or IR) may be inconclusive. Because of the relative zero point energies between either side of the equilibrium, inverse kinetic effects have been seen.[119]

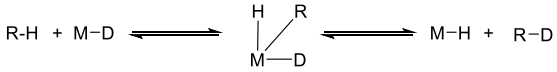

Figure 1.17 Illustration of H/D exchange at a metal centre.

The Goldberg group also showed that their three-coordinate complex seen in Scheme 1.4 would undergo H/D exchange in the presence of deuterated alkanes, exchanging the protons on the ^{i}Pr chains (Scheme 1.16).[120,121] The mechanism includes the oxidative addition of R-D, followed by reductive elimination of ^{i}Pr-D. When ^{i}Pr-H oxidatively adds to the metal, R-H can then reductively eliminate to leave the deuterium on the alkyl chain. These steps can then be repeated until all the protons on the ^{i}Pr chains have been exchanged.

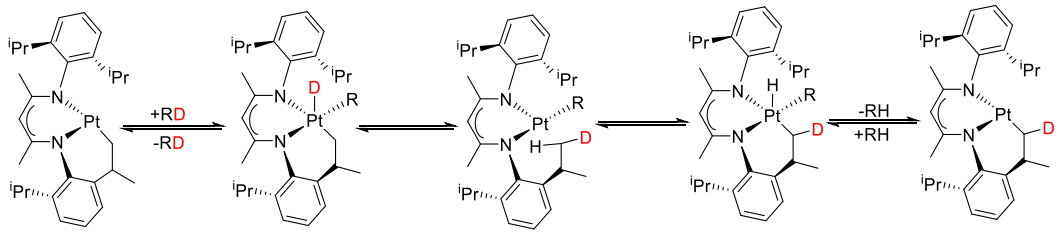

Scheme 1.16

1.7. The Shilov System

Shilov later discovered how to functionalise saturated hydrocarbons into more useful alcohols (and alcohol precursors including R-Cl). The Shilov system can functionalise hydrocarbons found in natural gas (Figure 1.18) as well as other unactivated alkanes. The initial functionalisation (C-H → C-X) is the most difficult step in making fine chemicals

from oil, because of the relative inertness of C-H bonds. Small alcohols are currently made by a steam reformation process, reacting CH_4 and H_2O to form methanol and hydrogen, and therefore requires high temperatures and pressures.

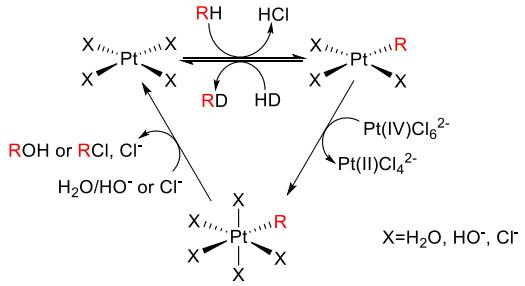

Figure 1.18 Illustration of a general Shilov cycle.

The Shilov system is somewhat selective, preferring to activate stronger C-H bonds. In longer chain alkanes, the Shilov system shows a preference for the chain ends. The hydrocarbon (such as methane or ethane) oxidatively adds to the Pt^{II} complex, followed by the reductive elimination of HCl (therefore no change in oxidation state overall). The Pt^{II}-R complex is then oxidised with an equivalent of a Pt^{IV} complex. Reductive elimination of ROH or RCl follows, giving the newly functionalized product. It was proven with isotope labelling that the Pt^{II} with the coordinated R group is oxidised, rather than the R group migrating onto the Pt^{IV} complex before the elimination of product (Figure 1.19).[122,123]

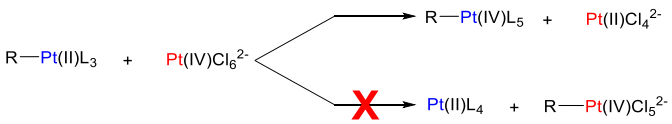

Figure 1.19 Illustrations of proposed mechanisms in the Shilov system.

The main drawback of the Shilov system is the price of the oxidant, requiring an equivalent of Pt^{IV} for every equivalent of product made. Because of this, a lot of research has been carried out in this area to improve the system, including different oxidants.[124–127] The oxidant must be selective (only oxidizing the Pt^{II} with the coordinated R group) in order to make the system catalytic.[128] A promising Pt^{II} complex with a bipyridyl ligand uses SO_3/H_2SO_4 as an oxidant, and produces methyl bisulphate from methane.[129] Yet, more recent research suggested that this can be easily outcompeted with simple $K_2[PtCl_4]$.[130]

All of the platinum species in the catalytic cycle of the Shilov system are surrounded by "X" groups (Figure 1.18) as the exact structure of any of the species is unknown, including

how many water, hydroxides or chlorides are attached at any given time. The arrangement of these groups could have a large effect on the efficacy of the catalyst, and so the exact mechanism of the Shilov system is also unknown.[131,132] More recent work has looked at the effect of bidentate ligands (including biphosphines) on the selectivity of the reductive elimination reaction.[20,131,133] Some ligand systems have also shown to be selectively oxidized by molecular oxygen.[134,135] There is also an example of the post-transition metal thallium (as $O{=}Tl(TFA)_3$, where TFA is trifluoro acetate) showing promise in the activation of methane, ethane and propane in the presence of a TFA solvent to give TFA esters.[136]

1.8. Past Work in the Rourke Group

This section focusses solely on the synthesis and derivatization of the starting materials **1-DMSO** and **21-DMSO**. Important past work in the Rourke group relevant to this thesis is presented in the introduction sections of the relevant results chapter.

1-DMSO is the Pt^{II} starting material for much of the chemistry discussed in this thesis (Scheme 1.17). Coordinated to the Pt^{II} metal centre is a dicyclometallated C^N^C pincer ligand (where both coordinated carbons are sp^2 hybridized) and a coordinated DMSO. The pro-ligand (2,6-di(4-fluorophenyl)pyridine) can be synthesized by reacting 2,6-dibromoropyridine with 4-fluorophenyl boronic acid, in a Suzuki-type reaction, to give 2,6-di(4-fluorophenyl)pyridine in close to quantitative yields.[137]

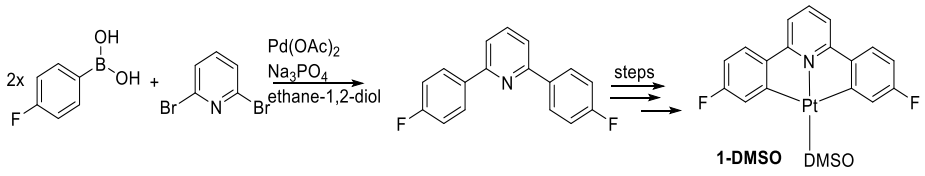

Scheme 1.17

The pro-ligand was reported to react with $K_2[PtCl_4]$ in acetic acid at reflux for a week, which gave an insoluble yellow powder (Scheme 1.18).[138–140] The powder was shown to be a chlorideibridged dimer **A** where one of the fluoro-phenyl rings has cyclometallated. The reported mechanism begins with the displacement of a chloride on the $PtCl_4^{2-}$ for the pyridyl nitrogen of the pro-ligand. As the 2- and 6- positions of the pyridine are substituted, the fluoro-phenyl rings are close enough to the platinum for one to become cyclometallated. It is quite possible that the cyclometallation reaction is assisted by the plentiful acetate in solution (Figure 1.16).

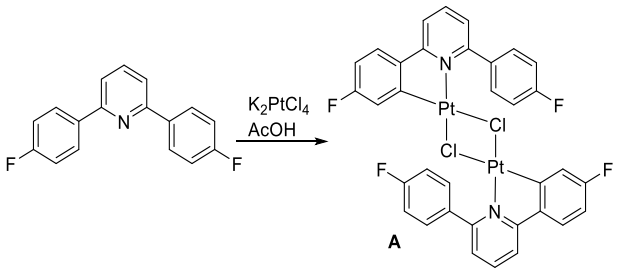

Scheme 1.18

The reported crystal structure of a Cl bridged dimer analogous to **A** (differing only by a substitution at the 4- position on the nitrogen) showed that the Pt-Cl bond for the Cl-C *trans* chloride was longer than the other Pt-Cl bond (Scheme 1.18). This was expected based on the *trans* effect, where an aryl ligand is a better *trans* labilising ligand than a pyridine.

The addition of DMSO to **A** displaces one of the chloride ligands, and therefore separates the dimer. Water and a mild base (e.g. K_2CO_3) are then added to the reaction mixture, resulting in full conversion to **1-DMSO** within a day (Scheme 1.19).

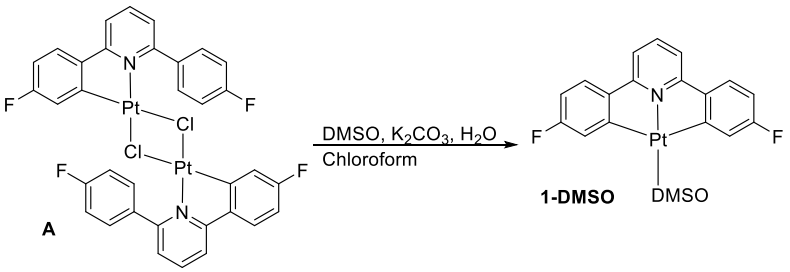

Scheme 1.19

DMSO is a relatively labile ligand, allowing it to be replaced with other ligands (including tripropyl- and tributylphosphine used in this project). Derivatization with trimethyl phosphine was reported to be clean and also high yielding allowing for the synthesis of the reported trimethylphosphine derivative (Scheme 1.20).[141] An equivalent of phosphine was added to a solution of **1-DMSO** under an inert atmosphere, with full conversion to the PMe_3 derivative **1-Me** within seconds. This is also a general scheme for the derivatization of **1-DMSO** for other air sensitive phosphines.

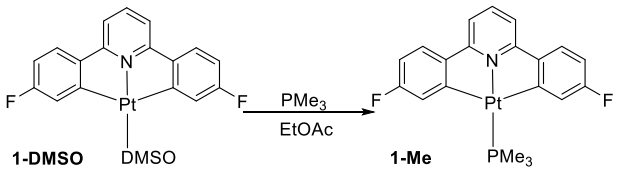

Scheme 1.20

Aryl-alkyl C^N^C complexes have been used extensively in the Rourke group. Synthesis and full characterization of the analogous dicyclometallated complex **21-DMSO** (with the pro-ligand 2-(4-fluorophenyl),6-*tert*butyl pyridine) has already been reported (Scheme 1.21).[142] In these complexes there is both a C(sp^3) and a C(sp^2) coordinated to the platinum. In this thesis, the chemistry of a derivative of **21-DMSO** is limited to Section 3.3.

Synthesis of the pro-ligand first involves the reaction of 2,6-dichloropyridine with ^{t}BuMgCl (a Grignard reagent) and a CuI catalyst, which replaces one of the chlorides on the pyridine ring with a ^{t}Bu group. Replacement of the other chloride is achieved (as before) with 4-fluorophenyl boronic acid in a Suzuki-type reaction which gave the pro-ligand in a modest 25 % overall yield.

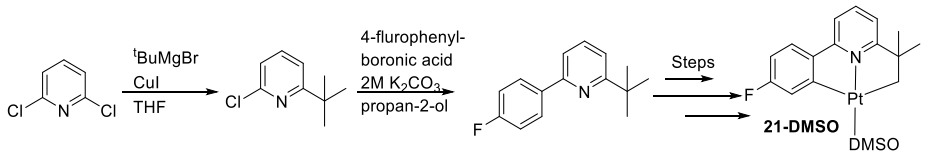

Scheme 1.21

After the pro-ligand was heated in acetic acid with $K_2[PtCl_4]$ at reflux for a couple of weeks, a monocyclometallated complex was collected **B**, where the platinum is also coordinated to the C(sp^2) (Scheme 1.22). A "dual-agostic" (or possibly an agostic and an anagostic) interaction from the ^{t}Bu protons was shown by the presence of platinum satellites ($^1J_{H\text{-}Pt}$ = 15.5 Hz) and a crystal structure which shows two hydrogens pointing towards the platinum. The fourth coordination site was taken by a chloride.

The reaction of analogous pro-ligands (where the ^{t}Bu group is replaced with a H, Et or ^{n}Pr) also give monocyclometallated complexes. When R was H, the remaining coordination sites were taken by a chloride and second equivalent of the pro-ligand (coordinated via the nitrogen), giving **C**. When R was Et or ^{n}Pr, chloride bridged dimers **D** were seen.

Addition of DMSO to **C** or **D** led to displacement of the second equivalent of pro-ligand to give **E**. The addition of DMSO to **B** instead led to the formation of **20-DMSO**. The C(sp^2)-

Pt bond has been exchanged for an C(sp^3)-Pt bond. Displacement of the agostic interaction for the DMSO ligand would be disfavoured due to the clash of the DMSO with the ^{t}Bu group. Even though the reaction forms a weaker Csp^3)-Pt bond, it is offset by the reduction of steric clash, where the flat fluoro-phenyl ring is free to rotate out of the way of the chloride.

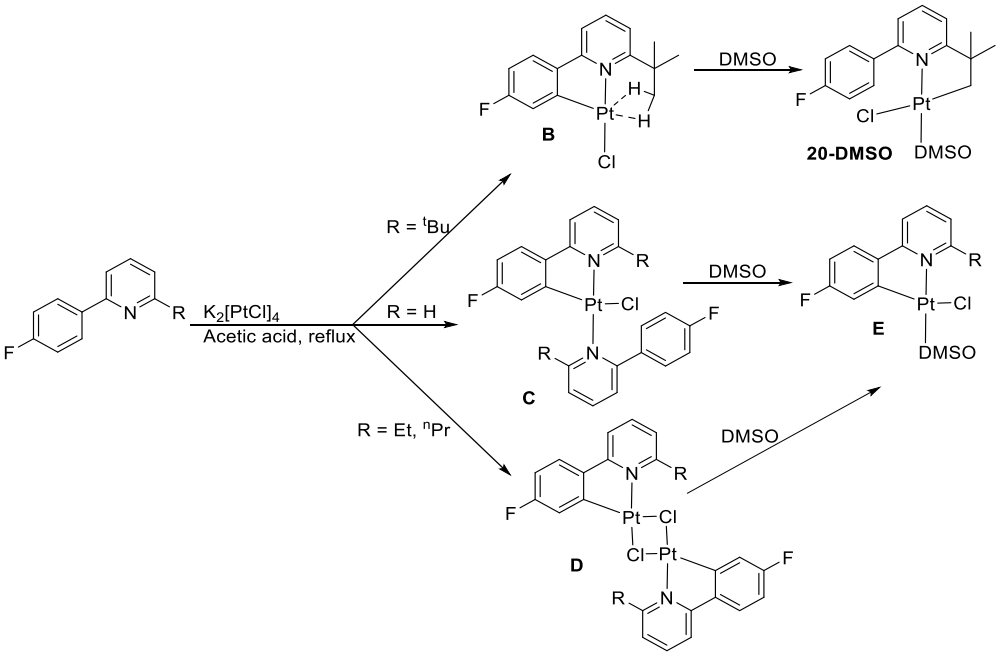

Scheme 1.22

A palladium complex analogous to **F** (where the third and fourth coordination sites are taken by a single acetyl acetonate group) showed an aryl-Pd bond being exchanged for an alkyl-Pd bond, where an isomerisation occurs at room temperature over the course of a couple of weeks (Scheme 1.23).[143] Because no new ligand was introduced, and the bond exchange still occurred, it is expected that steric clash of the acetyl acetone with the ^{t}Bu group was thought to be the driving force of the reaction.

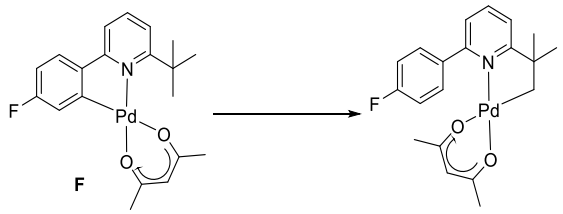

Scheme 1.23

Finally, to make complex **21-DMSO**, **20-DMSO** was reacted with a mild base to give the dicyclometallated complex. **21-DMSO** is analogous to the starting material **1-DMSO**, differing only by the C^N^C ligand (Scheme 1.24).

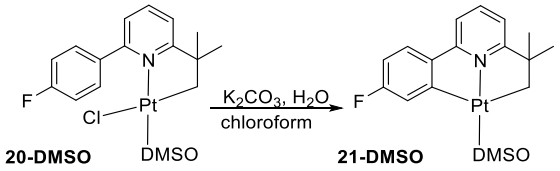

Scheme 1.24

1.9. Thesis Aims and Objectives, and Approach

1.9.1. The General Approach

Previous work in the Rourke group has looked at the oxidative addition of Cl_2 (delivered with $PhICl_2$) to square planar Pt^{II} complexes. Typically the products are simple Pt^{IV} dichlorides. The mechanism of reaction with $PhICl_2$, means that the two chlorides are added to the metal in a two-step process; initial addition of Cl^+, followed by the addition of Cl^-. Thus, before the Cl^- adds, a coordinatively unsaturated electrophilic Pt^{IV} intermediate is present. Another route to this same species would be the removal of Cl^- from the coordinatively saturated Pt^{IV} dichloride.

The study of reactive intermediates is of great interest academically as they are often not seen in more labile systems (such as where M = Pd or Au) but they are crucially important in determining both the reactivity and selectivity of catalysts. Therefore, the aim of this project was to look at oxidation reactions and to trap and control reactive five-coordinate intermediates. Coordinatively unsaturated complexes can by stabilised by steric hinderance, or trapped out by the coordination of a neutral entity (inter- or intra-molecular).

The platinum complexes previously studied by the Rourke group have planar C^N or C^N^C ligands, which are used as anchors to monitor isomerisation reactions at the metal centre. Ligands of this type have shown to reduce the reactivity of the metal centre, which allowed for the synthesis of the first Au^{III} alkene complex by the Bochmann group (Scheme 1.14). However, research from the Rourke group have shown that the C^N^C ligands are not just spectator ligands. As will be described in more detail in Section 3.3.1.,

steric crowding at the metal centre leads to the formation of a C(sp^3)-Cl reductive elimination product, where the C(sp^3) was initially coordinated to the metal as part of the C^N^C ligand.

1.9.2. General Thesis Aims and Objectives

- To investigate the products resulting from oxidative addition of $PhICl_2$, MeI, AllylBr and BnBr to doubly cyclometallated Pt^{II} complexes of C^N^C ligands.
- To investigate intercepting reactive Pt(IV) intermediates resulting from oxidative addition of $PhICl_2$, MeI, AllylBr and BnBr with intermolecular reactions and intramolecular interactions
- To investigate how complexes in which the reactive intermediates are stabilised by intramolecular interactions can be used to subsequently activate C-H bonds.
- To investigate reductive elimination reactions at Pt^{IV} complexes of doubly cyclometallated C^N^C ligands, initiated by halide abstraction reactions.

1.9.3. Characteristation Techiques

For both HR-MS (ESI) and ESI-MS the peaks quoted come from positive ion spectrometry as the complexes made in this thesis can form positive ions more easily. Some are already positively charged species, whilst others can lose negatively charged ligands (such as halogens), or gain positively charged ions (such as Na^+). Because the atoms present in the following compounds have several isotopes, a pattern appears in the shape of the natural abundance of these isotopes. It should therefore be noted that the values quoted from HR-MS (ESI) and ESI-MS spectra relate to the peak corresponding to the lightest natural weight (e.g. ^{12}C or ^{194}Pt).

The complexes reported in this thesis have many NMR active nuclei (with spin = ½): ^1H, ^{13}C, ^{19}F, ^{31}P and ^{195}Pt, which allows for relatively easy characterization of compounds. ^{13}C, ^{19}F and ^{31}P NMR experiments were run with ^1H decoupling (written as ^{13}C $\{^1H\}$, ^{19}F $\{^1H\}$ and ^{31}P $\{^1H\}$) to ensure that the resulting spectra are easier to interpret.

Because the relative abundance of ^{195}Pt is less than 100% (32.86 %), atoms close in connectivity (less than about five bonds) will have platinum satellites in their respective NMR spectra (where the area of the satellite peaks combined will be roughly half that of the main peak). ^{195}Pt chemical shifts vary over a large range (between around +9000 to

-6500 ppm)[144] and the shifts are very sensitive to the electron density at the metal centre. This means that we can infer changes in oxidation state from changes in the ^{195}Pt shift. In this thesis -1500 – -2400 ppm would suggest a Pt^{IV} species, whilst -3000 – -4500 ppm would suggest a Pt^{II} species.

The fluorine atoms present in the C^N^C ligands are for characterisation purposes, giving connectivity information, and are not thought to have any real effect on the ring (Figure 1.20). Presence of $^4J_{F\text{-}Pt}$ platinum satellites on the fluorine peaks indicates whether a fluoro-phenyl ring is coordinated. Figuring out the connectivity for the alkyl-aryl pyridine derivatives (such as **20** and **21**) is more difficult as the *tert*-butyl group does not have fluorines. However, the general idea of looking for platinum satellites in the $^{19}F\{^1H\}$ spectra was still implemented with good success.

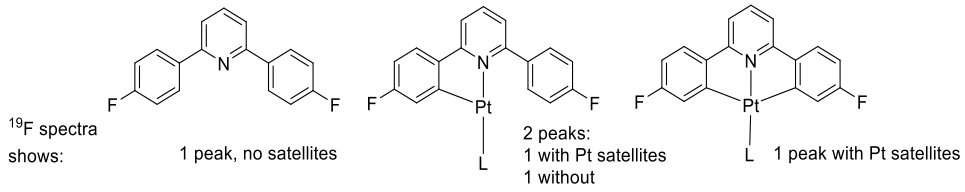

Figure 1.20 Illustration of the correlation of platinum satellites and fluoro-phenyl ring connectivity.

For the complexes in the following chapters, the phosphine ligand is rarely expected to be *trans* to anything other than a halogen or a pyridyl nitrogen (which have similar *trans* directing strength) implying that the Pt-P bond strength will remain consistent. The $^1J_{P\text{-}Pt}$ coupling constant of the platinum satellites seen in the $^{31}P\{^1H\}$ NMR spectrum can therefore also be used as an indicator of a change in the oxidation state of the platinum. Lower oxidation states have higher degrees of back bonding of electron density from the metal to phosphorus, increasing bond strength (therefore larger coupling constants, with the opposite being true for higher oxidation states). However, if the phosphorus is *trans* to a strong donating group (such as a carbon), the Pt-P bond is weakened, and therefore a smaller $^1J_{P\text{-}Pt}$ coupling constant is observed.

2.0 Oxidative Addition with $PhICl_2$

2.1. Introduction

The C^N monocyclometallated $Pt^{II}Cl$(DMSO) complex has been reported to react with the chlorine-based, oxidant iodobenzene dichloride ($PhICl_2$, a yellow solid that can be easily manipulated) shown in Scheme 2.1.[145] The Pt^{IV} product had the newly added chloride ligands mutually *trans*, which was expected as the oxidative addition of electrophilic reagent are known to add via an S_N2-type mechanism.[146,147] Addition of the two chlorides on opposite sides of the metal meant that the other ligands have not had to move, retaining the arrangement of the square-planar starting material. Formally this is an addition of Cl^+ to a 16 valence electron square planar Pt^{II} complex, giving a five-coordinate 16 valence electron Pt^{IV} complex, followed by combination with Cl^- to give an 18 valence electron Pt^{IV} octahedral complex.

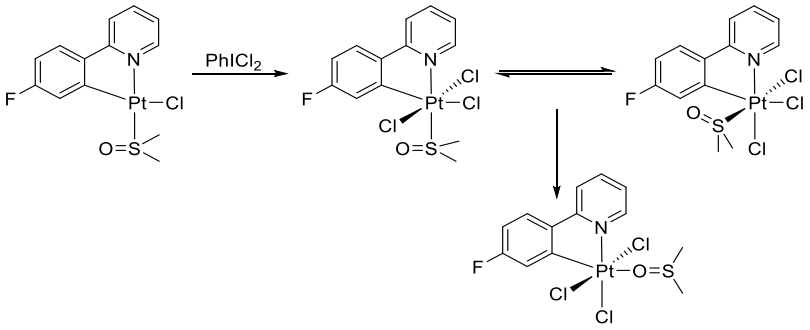

Scheme 2.1

In acetone new peaks begin to appear in the ^1H NMR spectrum, as the compound begins to isomerise, where the DMSO ligand is *cis* to both C and N of the C^N ligand. This isomerisation is reversible, giving a statistical mixture of the two isomers, showing that the energy difference between the two isomers is small. With further time in solution, both products eventually isomerised to a third and final product. The DMSO was shown to be *trans* to the aryl ring and bound via the oxygen. This can be explained by the relief of steric clash (by placing the methyl groups further away), but also by "transphobia" where placing a hard donor opposite a hard acceptor is preferred (the O is a stronger π donor than S).[148] Based on this principle, when DMSO was opposite the chloride or the pyridine, binding via the sulfur would have been preferred.

The related dicyclometallated (C^N^C) Pt^{II}DMSO complex **1-DMSO** was reported to react with $PhICl_2$, which also initially gave a *trans* dichloro- complex (Scheme 2.2).[141] Formation of a product with this geometry can again be rationalized by the two-step addition of the chlorine across the planar Pt^{II} starting material, requiring no movement of the other ligands. Full isomerisation to the *cis* dichloro- complex can be seen within a week in solution at room temperature.

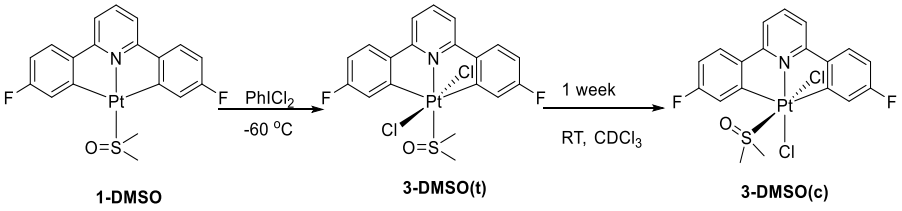

Scheme 2.2

Isomerisation of the *trans* dichloro- complexes to the *cis* geometry can be rationalized by the placing of the larger ligand out of the plane of the C^N^C ligand. The reported X-ray crystal structure of the S-N *trans* isomer **3-DMSO(t)** (left),[149] and the S-N *cis* isomer **3-DMSO(c)** (right) illustrates this preference (Figure 2.1).

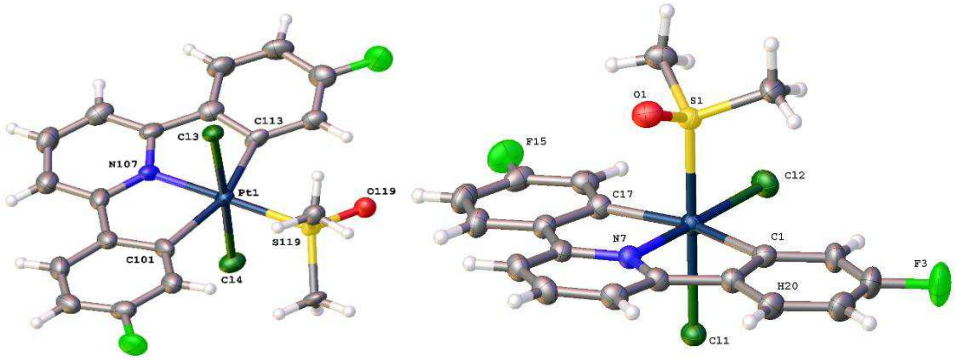

*Figure 2.1: Reported crystal structures of **3-DMSO(t)** (left) and **3-DMSO(c)** (right), thermal ellipsoids drawn at 50% probability level.*[149]

3-DMSO(t) has the smaller chloride ligands out of the main plane of the molecule. This leaves the larger DMSO to take up the space that has protons (*ortho* to Pt and F) pointing towards it, leading to crowding (Figure 2.2). In the S-N *cis* structure **3-DMSO(c)**, the larger group is positioned orthogonal to the planar dicyclometallated ligand. This allows more space, making it the thermodynamically favoured isomer, and the expected final product, assuming no other issues.

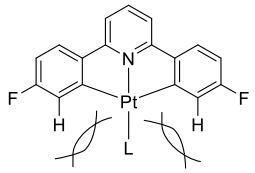

Figure 2.2 Illustration of steric clash with a L-N geometry.

A trapped five-coordinate intermediate has been reported, made by adding excess DMSO before the addition of oxidant, which gave the cationic "double-DMSO" complex (Scheme 2.3).[150] The presence of two DMSO peaks with platinum satellites in ^{1}H NMR spectrum led to the assigned geometry with the two DMSO groups *cis* to each other, both bound to platinum by sulfur. This complex quickly transformed into a mixture of the *cis* and *trans* dichloro- complex at room temperature by simple ligand substitution, giving the neutral complexes.

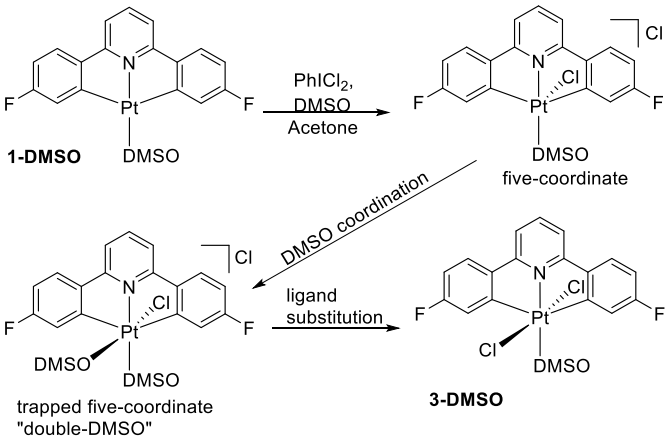

Scheme 2.3

To expand on this chemistry, different phosphine derivatives have been synthesised from **1-DMSO**, including: triphenyl, tributyl, tripropyl and tri(o-tolyl)phosphine (**1Ph**, **1-Bu**, **1-Pr** and **1-Tol**, respectively). Oxidizing these complexes allowed for the study of the effect of bulkier ligands and intramolecular interactions, where the two-step addition of Cl_2 (from $PhICl_2$) can be exploited. Reactions can be carried out and studied by NMR at low temperatures in order to study short-lived intermediates.

2.2. Triphenylphosphine Derivative **1-Ph**

It should be noted that the following section contains work incompletely explored by past members of the Rourke group.[149,151] Full NMR characterisation of **1-Ph**,**2-Ph**, **3-Ph(t)** and **3-Ph(c)** was completed previously, yet the absolute structure of **2-Ph** remained tentative. The work presented in this section aimed to remove this ambiguity.

Triphenylphosphine is used extensively in organic synthesis. Examples include the Mitsunobu reaction,[152] and as a ligand for palladium (e.g. tetrakis-(triphenylphosphine)palladium(0)) used in Suzuki coupling reactions. The C^N^C $Pt^{II}PPh_3$ complex **1-Ph** was synthesised from **1-DMSO** by simple ligand displacement (Scheme 2.4), as described earlier. Full characterisation was completed by a past member of the Rourke group.[151]

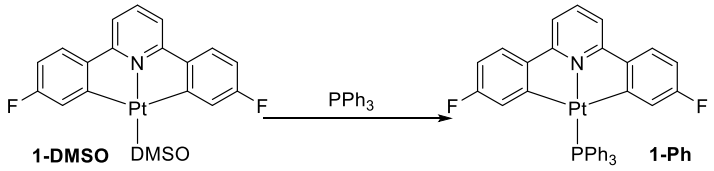

Scheme 2.4

The crystal structure (from crystals grown by a past member of the Rourke group)[151] can explain features in the ^1H NMR spectrum, in which the protons *ortho* to Pt and F are greatly upfield shifted relative to the other aryl peaks at 5.81 ppm (Figure 2.3).[150]

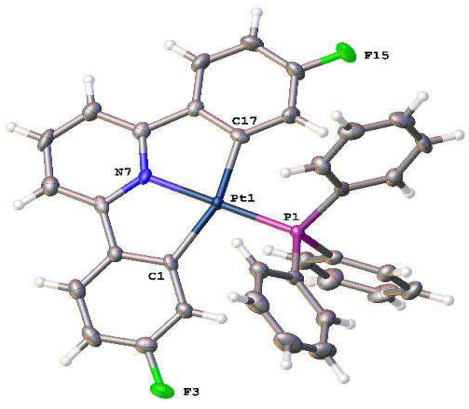

*Figure 2.3 Reported crystal structure of **1-Ph**, thermal ellipsoids drawn at 50% probability level.*[151]

The large Tolman cone angle of triphenylphosphine (145°) is due to the space requirements of the three aryl rings. This also means that, as shown in the crystal structure, the protons which are *ortho* to Pt and F are forced to point directly into the centre of the

aryl rings of the phosphine. The interference of the two ring currents has a shielding effect, shifting the peaks upfield. Other relevant NMR data includes a peak in the $^{31}P\{^{1}H\}$ NMR spectrum at 27.44 ppm ($^{1}J_{P\text{-}Pt}$ = 4020 Hz) and a doublet in the ^{195}Pt NMR spectrum at −4323 ppm ($^{1}J_{Pt\text{-}P}$ = ~4000 Hz).

To further investigate the oxidation of **1-Ph**, one equivalent of $PhICl_2$ was added to an acetone solution of **1-Ph** at -40 °C, which gave a single complex, **3-Ph(t)** (Scheme 2.5). The spectra showed a single peak in the $^{19}F\{^{1}H\}$ NMR spectrum at -107.91 ppm ($^{4}J_{F\text{-}Pt}$ = 16 Hz) and a pattern of peaks present by ^{1}H NMR spectroscopy which indicated that the C^N^C ligand remained dicyclometallated. In the $^{31}P\{^{1}H\}$ NMR spectrum, a peak at -4.09 ppm ($^{1}J_{P\text{-}Pt}$ = 2470 Hz) and a doublet in the ^{195}Pt NMR spectrum −2323 ppm indicated a Pt^{IV} species.

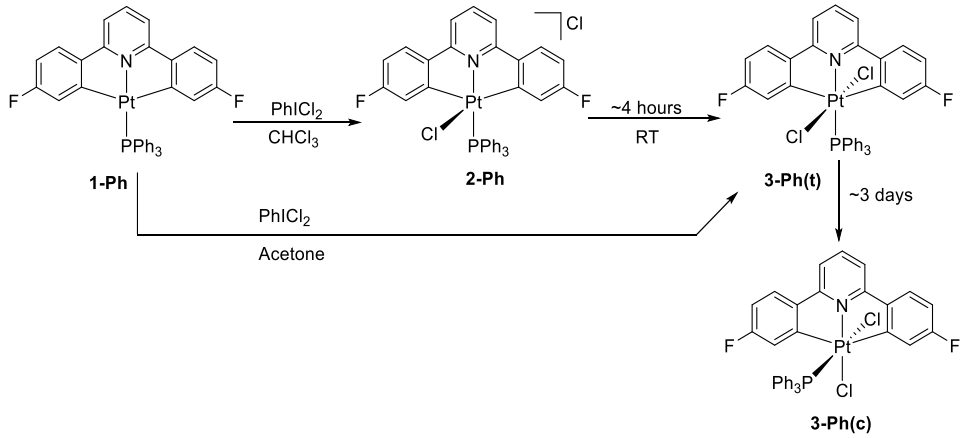

Scheme 2.5

With the precedence set by **1-DMSO**, **3-Ph(t)** would be expected to be a *trans* dichloro-complex. This assignment was backed up by nOe data, where irradiation of the proton *ortho* to Pt and F enhanced peaks corresponding to the phosphine aryl rings. A peak in the HR-MS (ESI) spectrum at 756.0921 m/z showed the mass of the starting material plus a chloride. To give a positively charged ion, the neutral **3-Ph(t)** can lose a negatively charged species (e.g. chloride). Loss of an electron or gain of a positively charged species (e.g. Na^{+}) are also possible for forming a positively charged species, but these are not seen for these dichloro- complexes.

Over the course of several days the amount of **3-Ph(t)** in solution decreased with the growth of a new compound **3-Ph(c)**. The spectra showed a single peak in the $^{19}F\{^{1}H\}$ NMR spectrum at -106.25 ppm ($^{4}J_{F\text{-}Pt}$ = 14 Hz) and a pattern of peaks present by ^{1}H NMR

spectroscopy which indicated that the C^N^C ligand remained dicyclometallated. In the $^{31}P\{^{1}H\}$ NMR spectrum, a peak at -7.95 ppm ($^{1}J_{P\text{-}Pt}$ = 2460 Hz) and a doublet in the ^{195}Pt NMR spectrum -2573 ppm indicated a Pt^{IV} species. This data shows that **3-Ph(c)** is the *cis* dichloro- complex, formed by isomerisation of **3-Ph(t)**, expected by the precedence set by **1-DMSO**, which was further supported by nOe data where irradiation of the protons *ortho* to Pt and F showed a greatly reduced effect on the aryl protons of the phosphine when compared to **3-Ph(t)**.

When one equivalent of $PhICl_2$ was added to a chloroform solution of **1-Ph** at -60 °C, clean conversion to a single new product **2-Ph** was seen (Scheme 2.5). This complex persisted in solution at -60 °C, with little difference over several hours. The spectra showed a single peak in the $^{19}F\{^{1}H\}$ NMR spectrum at -107.86 ppm ($^{4}J_{F\text{-}Pt}$ = 45 Hz) and a pattern of peaks present by ^{1}H NMR which indicated that the C^N^C ligand remained dicyclometallated. In the $^{31}P\{^{1}H\}$ NMR spectrum, a peak at 8.57 ppm ($^{1}J_{P\text{-}Pt}$ = 2810 Hz) and a doublet in the ^{195}Pt NMR spectrum −2339 ppm indicated a Pt^{IV} species. When **2-Ph** was allowed to warm to room temperature, **2-Ph** slowly disappeared from solution with the formation of **3-Ph(t)**. This disappearance can be quite slow, taking over four hours.

As **2-Ph** is a precursor to **3-Ph(t)**, it would suggest that the structure of **2-Ph** is that which precedes the coordination of the second chloride to form the six-coordinate **3-Ph(t)**. Without the coordination of the second chloride, and no other anions in solution, **2-Ph** is likely to be cationic The HR-MS (ESI) spectrum showed a peak at 756.0921 m/z which is the same position as for both **3-Ph(c)** and **3-Ph(t)** (cooresponding to $[M\text{-}Cl]^{+}$), but with greater intensity (relative to the baseline), which is unsurprising as they must first lose a chloride to become ionised. The possibility of **2-Ph** being an agostic intermediate was ruled out from the ^{195}Pt – ^{1}H correlation spectrum as no correlation was seen between platinum and the aryl protons of the phosphine.

As a five-coordinate intermediate species, **2-Ph** would also have to be accessible by removal of Cl^{-} from either isomer of **3-Ph**, which can be done performed silver salts. As addition of $AgBF_4$ to a chloroform solution of either isomer of **3-Ph** led only to degradation of the complex, and addition of $PhICl_2$ to **1-Ph** in acetone did not give **2-Ph**, a different approach was required. It was decided to add pyridine to trap the five-coordinate intermediate. Pyridine was added both before the addition of $PhICl_2$ to **1-Ph**, and before the addition of $AgBF_4$ to either isomer of **3-Ph**. Acetone was chosen as solvent to avoid the presence of degradation products.

To an acetone solution of either Pt^{IV} dichloro- complex **3-Ph**, pyridine was added (excess). $AgBF_4$ was then added at room temperature which gave a new complex **4-Ph** (Scheme 2.6). The resulting NMR spectra showed a single peak in the $^{19}F\{^1H\}$ NMR spectrum at -106.26 ppm ($^4J_{F\text{-}Pt}$ = 14 Hz) and a pattern of peaks present in the ^1H NMR spectrum which indicated that the C^N^C ligand remained dicyclometallated. In the $^{31}P\{^1H\}$ NMR spectrum, a peak at -11.23 ppm ($^1J_{P\text{-}Pt}$ = 2395 Hz) and a doublet in the ^{195}Pt NMR spectrum −2362 ppm ($^1J_{Pt\text{-}P}$ = ~2500 Hz) indicated a Pt^{IV} species.

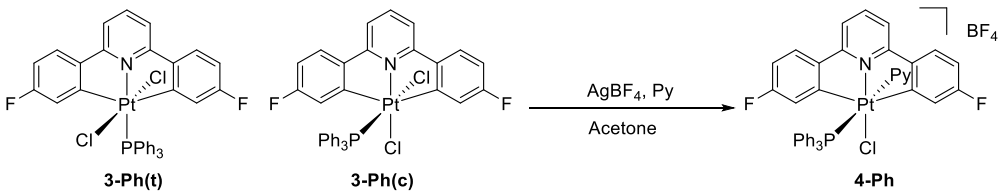

Scheme 2.6

In the ^1H NMR spectrum, pyridine was shown to be coordinated by the presence of platinum satellites ($^3J_{H\text{-}Pt}$ = 23.5 Hz) on peaks corresponding to pyridine-*o* protons. The HR-MS (ESI) spectrum also confirmed the addition of the hetrocycle with a peak at 835.1346 m/z which correlates to the mass of **2-Ph** plus pyridine. The stereochemistry of **4-Ph** was confirmed by nOe experiments, which showed no correlation between protons on the phosphine and pyridine ligands, and only a small effect on the protons of the phosphine and the proton *ortho* to Pt and F. This means that the pyridine and phosphine are *trans* to each other, and *cis* to the pyridine of the C^N^C ligand. The geometry is suggested further by comparison of the NMR spectra with those of **3-Ph(c)**. selected peaks include: the proton *ortho* to Pt and F at 7.64 ppm (cf. 7.73 ppm) in the ^1H NMR spectrum, and the peak at -11.23 ppm (cf. -7.95 ppm) in the $^{31}P\{^1H\}$ NMR spectrum.

The pyridine trapped complex **4-Ph** was also be synthesized by the treatment of **1-Ph** with $PhICl_2$ in chloroform, acetone or neat pyridine (provided pyridine is present in excess) (Scheme 2.7). Only the counterion differed between addition of $AgBF_4$ to **3-Ph** and the addition of $PhICl_2$ to **1-Ph**, and so it is unsurprising that there was no difference in the NMR spectra of **4-Ph** synthesised by either method. These reactions show that **2-Ph** is a five-coordinate intermediate as it is both capable of accepting another ligand, and can be formed from the Pt^{IV} dichloro- complexes by removal of a halide.

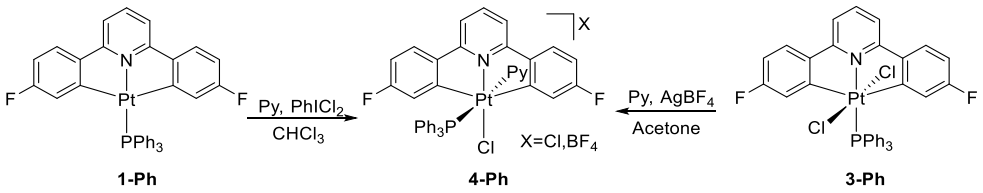

Scheme 2.7

2.3. Alkyl phosphines

Alkyl phosphine ligands are bulkier than DMSO. Oxidation of **1-Ph** with $PhICl_2$ gave a five-coordinate intermediate which persisted in solution. It was decided to study alkyl phosphine derivatives next, to see if a five-coordinate intermediate could be observed with other phosphines. The Tolman cone angles of ^{n}butyl and ^{n}propyl phosphine are about 15° smaller than PPh_3,[153] but with the presence of flexible alkyl chains, the five-coordinate intermediate might instead be trapped with intramolecular agostic interactions. Synthesis of **1-Bu** and **1-Pr** are identical, in which a small excess of phosphine is added to an EtOAc solution of **1-DMSO** under a nitrogen atmosphere (Scheme 2.8).

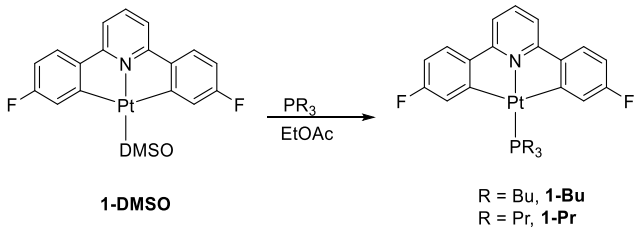

Scheme 2.8

2.3.1. Tributylphosphine Derivative **1-Bu**

It should be noted that the following section contains work initiated by a past member of the Rourke group.[149] Complex **1-Bu** lacked $^{13}C\{^{1}H\}$ NMR data. Preliminary oxidation experiments of **1-Bu** in chloroform were carried out at low temperature where the *trans* and *cis* dichloro- complexes **3-Bu(t)** and **3-Bu(c)** were observed, but not purified leading to incomplete NMR data (which was completed by the author of this thesis). The agostic complex **5-Bu** (observed at low temperature) led to the formation of a transcyclometallated complex. Neither complex was isolated, and the tentative NMR assignment of the transcyclometallation product (with a six-membered platinacycle) has since been disproven. Further characterisation of complex **5-Bu** by ^{1}H NMR was carried out by the

author of this thesis, meaning that it was entered into the experimental section. The aim of the work in this section was therefore to complete the preliminary work, and remove the ambiguity of the structure of the transcyclometallated complex.

Important NMR data for the tributylphosphine derivative **1-Bu** include: a single peak in the $^{19}F\{^{1}H\}$ NMR spectrum at -111.59 ppm ($^{4}J_{F\text{-}Pt}$ = 28 Hz), a single peak in the $^{31}P\{^{1}H\}$ NMR spectrum at 0.10 ppm ($^{1}J_{P\text{-}Pt}$ = 3713 Hz) and a doublet in the ^{195}Pt NMR spectrum at −4215 ppm.[141]

Oxidation of **1-Bu** at -60 °C in acetone with $PhICl_2$ gave a single product **3-Bu(t)** (Scheme 2.9). The spectra showed a single peak in the $^{19}F\{^{1}H\}$ NMR spectrum at -108.14 ppm ($^{4}J_{F\text{-}Pt}$ = 16 Hz) and a pattern of peaks present in the ^{1}H NMR spectrum which indicated that the C^N^C ligand remained dicyclometallated. In the $^{31}P\{^{1}H\}$ NMR spectrum, a peak at -13.74 ppm ($^{1}J_{P\text{-}Pt}$ = 2303 Hz) and a doublet in the ^{195}Pt NMR spectrum −2275 ppm ($^{1}J_{Pt\text{-}P}$ = ~2400 Hz) indicated a Pt^{IV} species. In the ^{1}H NMR spectrum, the proton *ortho* to Pt and F also couples to phosphorus, which is indicative of a P-N *trans* geometry. This geometry was backed up by nOe data, where irradiation of the proton *ortho* to Pt and F greatly enhanced the alkyl protons.

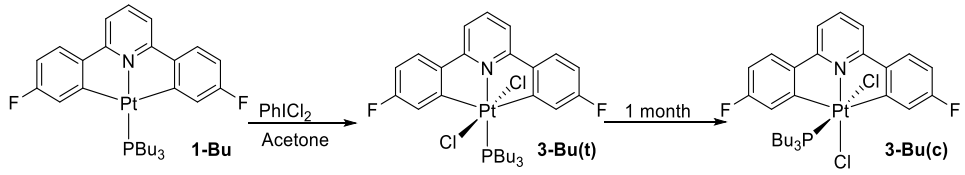

Scheme 2.9

With time at room temperature the NMR spectra gave evidence for a new compound, at the expense of **3-Bu(t)**, with the reaction being complete within two weeks. This new complex is the expected P-N *cis* dichloro- complex **3-Bu(c)**, shown in the $^{31}P\{^{1}H\}$ NMR where the peak is now shifted to 0.68 ppm whilst other NMR data show only minor changes. In the ^{1}H NMR spectrum, the proton *ortho* to Pt and F no longer couples to phosphorus. It was possible to separate the two complexes by column chromatography. Crystals were grown of each isomer, and the solved X-ray crystal structures further confirmed the expected geometries (Figure 2.4 and Figure 2.5).

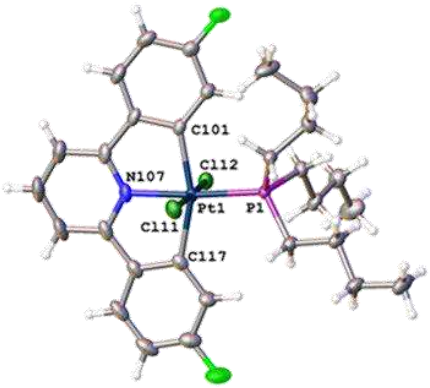

*Figure 2.4 Crystal structure of **3-Bu(t)**, thermal ellipsoids drawn at 50% probability level.*
***3-Bu(t)** selected bond lengths (Å) and angles (°): Pt-Cl11, 2.3327(9); Pt1-Cl12, 2.3267(8); Pt-C101, 2.102(4); Pt-N107, 2.043(3); Pt-C117, 2.123(4); Pt-P1, 2.3084(9); Cl12-Pt1-Cl11, 177.06(3);C101-Pt1-Cl11,,92.45(10); C101-Pt1-Cl12, 87.50(10); C101-Pt1-C117, 159.34(15); C101-Pt1-P1, 95.57(10); N107-Pt1-Cl11, 89.10(9); N107-Pt1-Cl12, 87.99(9); N107-Pt1-C101, 79.68(14); N107-Pt1-C117, 79.80(14); N107-Pt1-P1, 174.05(10); C117-Pt1-Cl11, 89.56(10); C117-Pt1-Cl12, 89.45(10); C117-Pt1-P1, 105.06(11); P1-Pt1-Cl11, 87.53(3); P1-Pt1-Cl12, 95.41(3).*

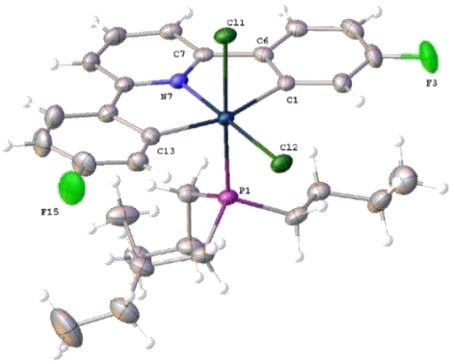

*Figure 2.5 Crystal structure of **3-Bu(c)**, thermal ellipsoids drawn at 50% probability level.*
***3-Bu(c)** selected bond lengths (Å) and angles (°): C1-Pt1, 2.066(3); Cl1-Pt1, 2.4098(7); P1-Pt1, 2.2901(7); Pt1-Cl2, 2.3324(7); Pt1-N7, 1.979(2); Pt1-C13, 2.074(3); C1-Pt1-Cl1, 87.62(8); C1-Pt1-P1, 92.41(8); C1-Pt1-Cl2, 98.27(9); C1-Pt1-C13, 162.29(12); P1-Pt1-Cl1, 178.12(3); P1-Pt1-Cl2, 85.55(3) Cl2-Pt1-Cl1, 92.58(3); N7-Pt1-C1, 81.41(11); N7-Pt1-Cl1, 88.78(7); N7-Pt1-P1, 93.08(7) N7-Pt1-Cl2, 178.58(7); N7-Pt1-C13, 81.50(11); C13-Pt1-Cl1, 87.43(8); C13-Pt1-P1, 93.08(8); C13-Pt1-Cl2, 98.93(9).*

The crystal structures of **3-Bu(t)** and **3-Bu(c)** further illustrate the preference for the *cis* geometry. The structure of **3-Bu(t)** (Figure 2.4) clearly shows the close proximity of the alkyl protons to the protons *ortho* to Pt and F, whilst **3-Bu(c)** (Figure 2.5) shows that the alkyl chains have a lot of space whilst orthogonal to the plane of the C^N^C ligand.

When $PhICl_2$ is added to a chloroform solution of **1-Bu** at -60 °C, **3-Bu(t)** is still seen, but now as a minor product, only makes up ~30% of the sample. The remainder was made up of a new Pt^{IV} species **5-Bu** (Scheme 2.10). The peak in the $^{31}P\{^{1}H\}$ NMR spectrum at 49.55 ppm ($^{1}J_{H\text{-}Pt}$ = 3064) is greater than 60 ppm downfield from the *trans* dichloro-

complex (-14.35 ppm). A paper by Vreize *et al.* shows that a shift of greater than 30 ppm can be indicative of the phosphorus being part of a ring, which suggested the same for the phosphorus of **5-Bu**.[154] In the ^{1}H NMR spectrum a triplet at 0.75 ppm had platinum satellites ($^{1}J_{H\text{-}Pt}$ = 15 Hz). This suggested the terminal methyl is involved in an intramolecular agostic interaction. The coupling constant is similar to those seen in agostic complexes previously seen in the Rourke group.[142] The spectra showed a single peak in the ^{19}F{^{1}H} NMR spectrum at -108.70 ppm ($^{4}J_{F\text{-}Pt}$ = 15 Hz), and a pattern of peaks present by ^{1}H NMR which indicated that the C^N^C ligand remained dicyclometallated. This species seemed to be stable at -60 °C, with little evidence of degradation within four hours.

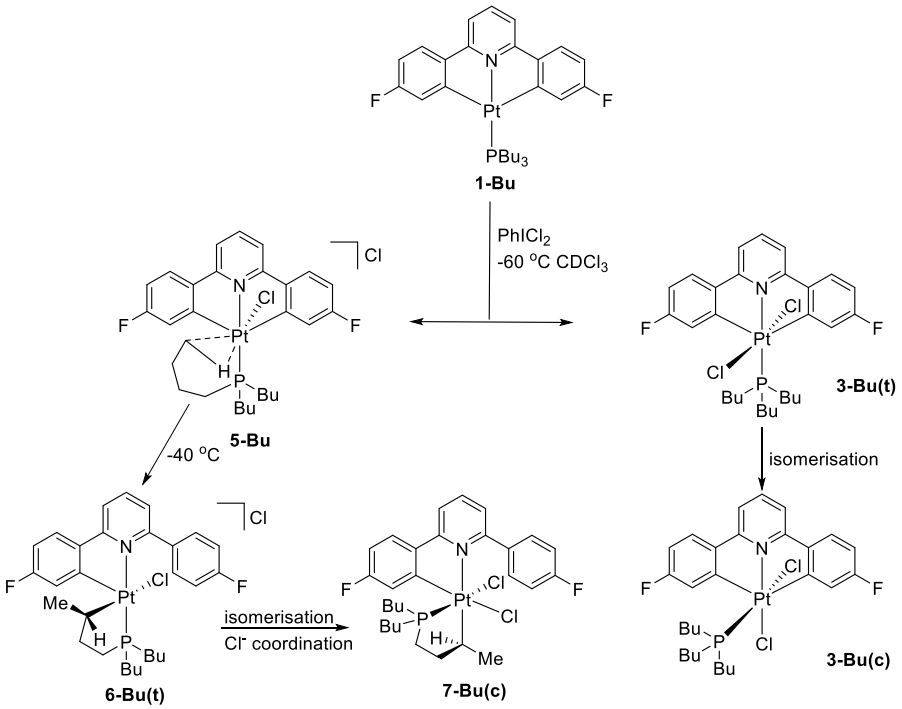

Scheme 2.10

When the sample was allowed to warm above -40 °C, the resonances for **5-Bu** disappeared with appearance of those for a new species **6-Bu(t)** (Scheme 2.10). The peak in the ^{31}P{^{1}H} NMR spectrum now at 39.34 ppm ($^{1}J_{P\text{-}Pt}$ = 3140 Hz), is too great a shift to attribute to the difference in temperature, can also be indicative of a smaller ring size. A P-N *trans* geometry was shown by the proton *ortho* to Pt and F also coupling to phosphorus in the ^{1}H NMR spectrum. This geometry is expected due to the temperature of the reaction (**3-Bu(t)** does not seem to isomerise at -60 °C). In the ^{19}F{^{1}H} NMR spectrum two resonances are seen (-112.37 ppm and -107.45 ppm, $^{4}J_{F\text{-}Pt}$ = 14 Hz) where one of the resonances lacks platinum coupling. This showed that the C^N^C ligand was

monocyclometallated. In the ^{1}H NMR spectrum a broad resonance at 2.45 ppm was seen, with an approximate $^{2}J_{H\text{-}Pt}$ ~100 Hz. The magnitude of this coupling showed that an alkyl C-Pt bond has been formed. A doublet at 0.42 ppm ($^{3}J_{H\text{-}Pt}$ = 38 Hz) which integrates to three protons showed that this is a terminal methyl peak and the adjacent carbon has only one proton attached. The platinum is therefore connected to the γ-C, meaning a five-membered platinacycle.

In an HR-MS (ESI) spectrum, a peak of high intensity (when compared to **3-Bu(t)** or **3-Bu(c)**) at 696.1868 m/z was seen (correlating to $[M\text{-}Cl]^{+}$), suggesting a cationic species as the height of the peak correlates with the ease of ionisation. This would further suggest that the second chloride has not filled the sixth coordination site. Instead, the sixth coordination site was shown to be filled by an agostic interaction from the decyclometallated ring. In the ^{195}Pt - ^{1}H correlation spectrum, an obvious correlation to the proton *ortho* to F on the decyclometallated ring was seen.

Therefore, the structure of **6-Bu(t)** comes about by formation of an alkyl-Pt bond at the expense of an aryl-Pt bond forming a five-membered platinacycle, where the carbon beside the terminal methyl group has been activated instead of the terminal methyl. The structure is cationic, with the sixth coordination site being taken up by an aryl agostic interaction. Formation of the five-membered ring is expected over the six-membered ring as five-membered rings are thermodynamically favoured due to favourable internal angles.

In an nOe spectrum, irradiation of the methyl adjacent to the cyclometallated carbon shows a weak interaction with the proton *ortho* to Pt and F, allowing the geometry to be assigned. The reaction gives a racemic mixture with stereospecificity (i.e. the methyl connected to the cyclometallated carbon always faces the cyclometallated aryl ring regardless of which "side" the cyclometallated carbon is bonded to). This is rationalized by the structure having the larger methyl group facing the less congested cyclometallated side.

The driving force of this transcyclometallation reaction is presumably the relief of ring strain, which offsets the exchange of a stronger Pt-C(sp^2) bond for a weaker Pt-C(sp^3). The phenyl rings of the C^N^C ligand have C-Pt-N angles of about 80° which is less than the ideal 90° (for a square planar complex) or 108° (the ideal internal angles of a pentagon). A similar driving force was seen in earlier work by the Rourke group, where exchange of an Pt-C(sp^2) bond for a Pt-C(sp^3) was facilitated by ligand exchange, described in Section 1.8.[142]

Over the course of a day at room temperature the amount of **6-Bu(t)** in solution decreased with the growth of a new compound **7-Bu(c)**, which has shown to be indefinitely air and

moisture stable. The NMR spectra of **7-Bu(c)** are very similar to **6-Bu(t)**, suggesting that the structure of the two complexes are similar. The peaks in the $^{19}F\{^{1}H\}$ NMR spectrum (-108.28 ppm, $^{4}J_{F\text{-}Pt}$ = 43.5 Hz and -112.88 ppm) show that the C^N^C ligand remains monocyclometallated. The peak in the $^{31}P\{^{1}H\}$ NMR spectrum shifted downfield by less than 1 ppm to 40.02 ppm ($^{1}J_{P\text{-}Pt}$ = 2945 Hz). In the ^{1}H NMR spectrum a peak at 3.59 ppm ($^{2}J_{H\text{-}Pt}$ = 75 Hz) relates to the proton attached to the alkyl carbon bonded to platinum which is a downfield shift of about 1 ppm compared to **6-Bu(t)**. The methyl adjacent had shifted to 1.44 ppm ($^{3}J_{H\text{-}Pt}$ = 36 Hz) showing a downfield shift of ~0.75 ppm.

A possible aryl-H agostic interaction was ruled out by the ^{195}Pt - ^{1}H correlation spectrum, where no correlation was seen to any of the protons of the dicyclometallated ring or alkyl protons of the phosphine. With no agostic interaction, and a peak of low intensity in the HR-MS (ESI) spectrum at 696.1863 m/z (corresponding to $[M\text{-}Cl]^{+}$), the sixth coordination site is proposed to be filled by the chloride to give a neutral species. The stereochemistry of the alkyl carbon directly attached to platinum was elucidated by use of nOe data, by irradiating separately the proton closest to the platinum on the cyclometallated aryl ring (*ortho* to Pt and F) and the proton attached to the alkyl carbon directly attached to platinum. The clear interaction of these protons allowed for the stereochemistry of this compound to be determined. It showed that the alkyl cyclometallated proton points towards the cyclometallated aryl ring. This shows that stereospecificity has been conserved within the isomerisation. Crystals suitable forstudyd by X-ray crystallography were grown from chloroform (Figure 2.6). The solved X-ray structure confirms the geometry, and the presence of two chloride ligands. Because the initial coordination of Cl^{+} could have happened on either face of **1-Bu** without preference, the resultant C-H activated product **7-Bu** is racemic. Study of the crystals but X-Ray crystallography showed pure crystals of a single enantiomer, and both enantiomers formed crystals. In all of the crystals studied by X-Ray crystallography, the methyl group points towards decyclometallated ring.

Conversion of **6-Bu(t)** to **7-Bu(c)** is thought to be a simple isomerisation by rotation of the platinacycle (the phosphorus is now *cis* to the nitrogen) followed by coordination of the second chloride to give a coordinatively saturated complex. The rationale for the isomerisation of the alkyl cyclometallated ring is the same argument used for the formation of the *cis* dichloro- complex **3-Bu(c)**, where having the phosphorus *cis* to the nitrogen allows the large butyl groups more space by positioning orthogonal to the plane of the C^N^C ligand. Even with the decyclometallated ring (which can rotate out of the plane of the C^N plane), a P-N *cis* geometry is greatly favourable, and allows for the chloride to fill the remaining coordination site.

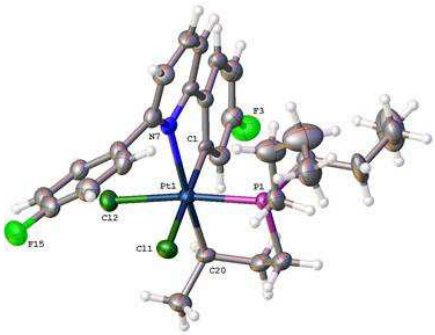

Figure 2.6 Crystal structure of ***7-Bu(c)****, thermal ellipsoids drawn at 50% probability level. Selected bond lengths (Å) and angles (°): C1-Pt1, 2.027(8); Cl1-Pt1, 2.432(2); P1-Pt1, 2.274(3); P1-C18, 1.832(10); Pt1-Cl2, 2.389(2); Pt1-N7, 2.274(7); Pt1-C20, 2.111(9); C18-C19, 1.518(13); C19 -C20, 1.518(14); C20-C21, 1.531(13); C18-P1-Pt1, 100.9(3); C1 Pt1-Cl1, 174.4(2); C1 Pt1-P1, 91.5(2); C1 Pt1-Cl2, 88.5(2); C1 Pt1-N7, 79.4(3); C1 Pt1-C20, 92.8(4); P1-Pt1-Cl1, 85.74(9); P1-Pt1-Cl2, 171.07(9); Cl2-Pt1-Cl1, 94.95(9); N7-Pt1-Cl1, 96.02(17); N7-Pt1-P1, 96.23(19); N7-Pt1-Cl2, 92.56(19); C20-Pt1-Cl1, 91.8(3); C20-Pt1-P1, 84.6(3); C20-Pt1-Cl2, 86.5(3); C20-Pt1-N7, 172.2(3); C19-C18-P1, 103.8(6); C18-C19-C20, 110.3(8); C19-C20-Pt1, 111.8(7); C19-C20-C21, 111.1(8); C21-C20-Pt1, 114.2(7).*

A recent paper has shown that nucleophiles can break alkyl C-Pt bonds.[155] If a chloride did attack the C(sp^3)-Pt (via the carbon), a monocyclometallated Pt^{II} species would have been observed, where one of the butyl chains is chlorinated. This was not observed, and thought to be because of the smaller ligands used and their greater flexibility which allowed the chloride to simply coordinate.

Restricted rotation about the aryl-py bond of the decyclometallated aryl ring can be seen by a broadening of the ^{1}H peaks *meta* to fluorine on the dicyclometallated ring caused by clash with the chloride pointing towards the aryl ring (Figure 2.7). By cooling the solution, the decyclometallated ring will rotate slower, and so exchange of the four resonances for the four protons present on the ring should be slow on an NMR timescale, as the protons on the side pointing towards the alkyl chains are in a different environment to those facing away. The chloroform solvent limited the temperature range of study to about -50 - +50 °C. At -40 °C four clear signals were observed, and lowering the temperature further does not resolve the peaks any further. Above 10 °C the exchange is fast enough on an NMR timescale. A COSY correlation between the protons *meta* and *ortho* to fluorine was only seen for these two resonances at temperatures over 40 °C.

An effort was made to increase yield of **7-Bu(c)** by changing the solvent, including the use of toluene and nitromethane. Chloroform gave the highest yield, as the others gave close to no conversion, which can be explained by chloroform being the best at solvating chlorides, keeping them away from the platinum long enough for an agostic interaction to form.

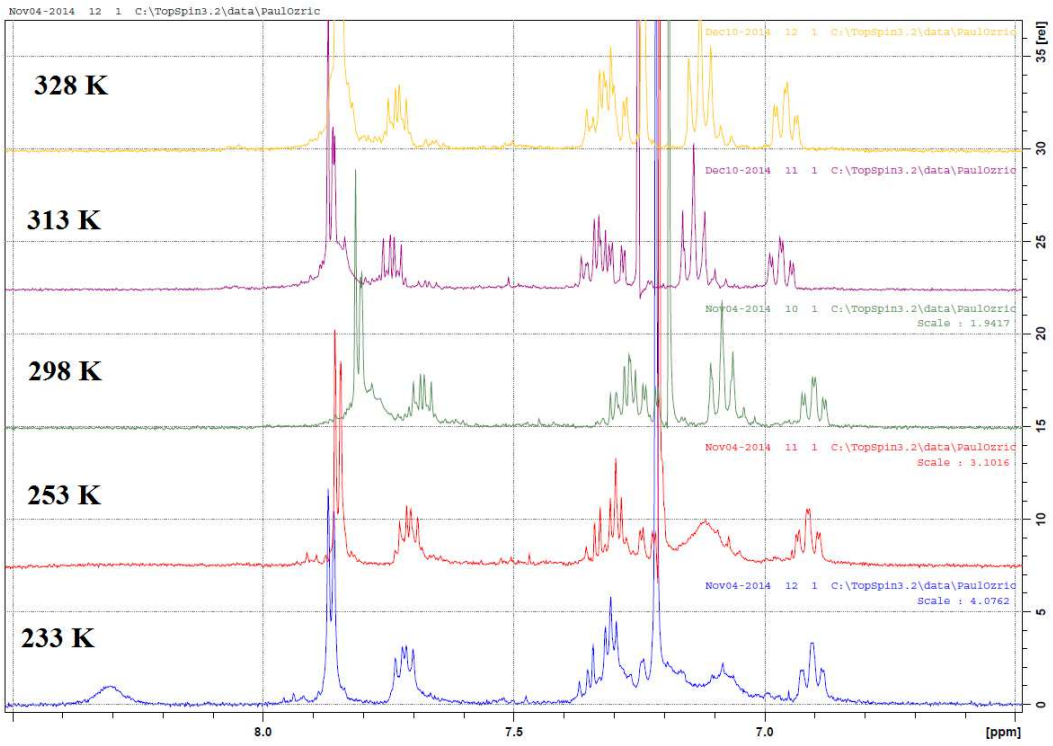

*Figure 2.7 ^{1}H NMR spectra of **7-Bu(c)** at various temperatures (233 – 328 K, aromatic region).*

2.3.1.1. Addition of $AgBF_4$

After the addition of $PhICl_2$ to a chloroform solution of **1-Bu** at -60 °C, there is no change in the relative amounts of **3-Bu(t)** or **5-Bu** with time, suggesting that it is not possible to displace the agostic interaction with a dissolved chloride counteranion. Instead, the second chloride would have to combine with an unobserved five-coordinate species. This suggests that the formation of the agostic interaction is in competition with the combination with the second chloride. To increase the amount of the agostic complex **5-Bu**, and the resulting transcyclometallation products **6-Bu(t)** and **7-Bu(c)**, the chloride counteranions must be removed from solution.

Silver salts (e.g. $AgBF_4$) can be used to remove halides from metal complexes, or from solutions, and form insoluble AgX compounds. By adding $AgBF_4$ before the addition of $PhICl_2$ to **1-Bu** at -60 °C in chloroform, 100% conversion to the transcyclometallated product **6-Bu(t)** was seen. This was followed by the addition of NaCl, which led to the eventual conversion of **6-Bu(t)** to **7-Bu(c)**. This shows that removal of chloride from solution removes the competition for the butyl groups to form agostic interactions, allowing for selective synthesis of **7-Bu(c)**.

$AgBF_4$ was added to a chloroform solution of the *cis* isomer **3-Bu(c)** in chloroform at -60 °C. Although the cloudiness of the solution led to poor NMR spectra with overly broadened peaks. The $^{31}P\{^1H\}$ and $^{19}F\{^1H\}$ spectra both indicated the presence of an alkyl transcyclometallated compound, seen by a large downfield shift in the $^{31}P\{^1H\}$ NMR spectrum and the presence of two peaks of equal intensity in the $^{19}F\{^1H\}$ NMR spectrum. Therefore, removal of a chloride ligand from coordinatively saturated Pt^{IV} dichloro-complexes is also a viable path to making a five-coordinate intermediate. The butyl chains are then able to coordinate. It is known that silver salts can be used to aid in transcylometallation reactions.[156] however, with the amount used in this reaction, and the solubility of the silver salts, it appears that the silver is just removing excess chloride from solution.

2.3.2. Tripropylphosphine Dervative **1-Pr**

Complex **7-Bu(c)** has a five-membered platinacycle, yet the agostic complex **5-Bu** has a six-membered platinacycle, where the terminal methyl of the butyl chain is coordinated. It was decided to see if oxidation of the PPr_3 derivative **1-Pr** (where the alkyl chains are one carbon shorter) would still give a transcyclometallated product without the ability to make an agostic complex with a six-membered ring, due to the shorter chain length. A crystal suitable for X-ray crystallography was grown from chloroform, which gave the structure in Figure 2.8.

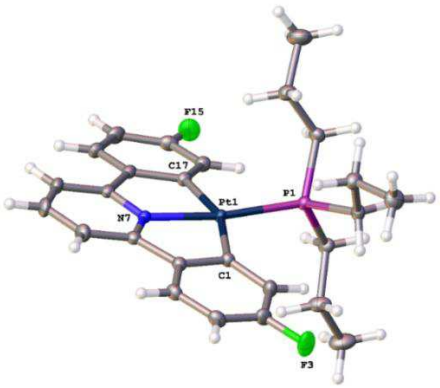

*Figure 2.8 Crystal structure of **1-Pr**, thermal ellipsoids drawn at 50% probability level. Selected bond lengths (Å) and angles (°): C1-Pt1, 2.0758(19); P1-Pt1, 2.2288(5); Pt1-N7, 2.0204(17); Pt1-C17, 2.0771(19); C1-Pt1-P1, 102.99(6); C1-Pt1-C17, 159.00(8); N7-Pt1-C1, 79.72(7); N7-Pt1-P1, 171.97(5); N7-Pt1-C17, 79.96(7); C17-Pt1-P1, 97.86(6).*

Important NMR data for the tripropylphosphine derivative **1-Pr** includes: a single peak in the $^{19}F\{^{1}H\}$ NMR spectrum at -111.44 ppm ($^{4}J_{F\text{-}Pt}$ = 28 Hz), a single peak in the $^{31}P\{^{1}H\}$ NMR spectrum at 1.34 ppm ($^{1}J_{P\text{-}Pt}$ = 3712 Hz) and a doublet in the ^{195}Pt NMR spectrum at -4212 ppm ($^{1}J_{Pt\text{-}P}$ = ~3750 Hz). As the alkyl chain differs from the butyl analogue by the absence of a CH_2, it is unsurprising that the NMR spectra of **1-Pr** is almost identical to the butyl derivative **1-Bu** for all nuclei studied.

Unsurprisingly, the products of oxidation of **1-Pr** with $PhICl_2$ in acetone were analogous to those of the oxidation of **1-Bu**. Oxidation of **1-Pr** with $PhICl_2$ at -40 °C in acetone gives mostly (>90%) the expected *trans* dichloro- complex **3-Pr(t)** (Scheme 2.11). This could be assigned easily by the presence of a peak in the $^{31}P\{^{1}H\}$ NMR spectrum at -13.96 ppm ($^{1}J_{P\text{-}Pt}$ = 2310 Hz), which is almost identical to that of **3-Bu(t)**. In the ^{1}H NMR spectrum, phosphorus coupling to the proton *ortho* to Pt and F was seen. The nOe spectra shoed that by irradiating this proton, the alkyl protons were alsoenhanced.

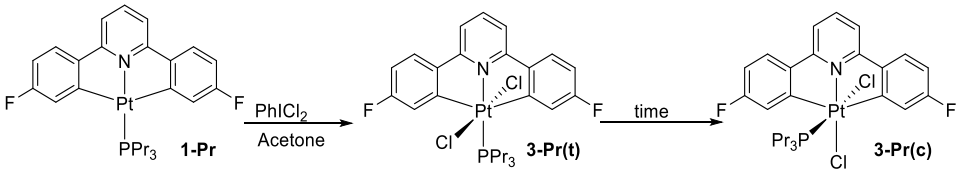

Scheme 2.11

The remainder of the product mass was the expected *cis* complex **3-Pr(c)**, which was also identified by the position of the peak in the $^{31}P\{^{1}H\}$ NMR spectrum at -1.42 ppm ($^{1}J_{P\text{-}Pt}$ = 2342 Hz). Allowing the product mixture to warm to room temperature gave a statistical mixture of *trans* and *cis* dichloro- isomers of around 5:3 (*trans*:*cis*) within two hours which made true isolation of **3-Pr(t)** impossible. In fact, NMR data were gathered from a mixture of the two complexes and the relative amounts were used to assign the spectra. Crystals of **3-Pr(c)** suitable for analysis have been grown via the sow evapouration of solvent from a chloroform solution, and the X-ray crystal structure elucidated, showing the expected *cis* geometry (Figure 2.9).

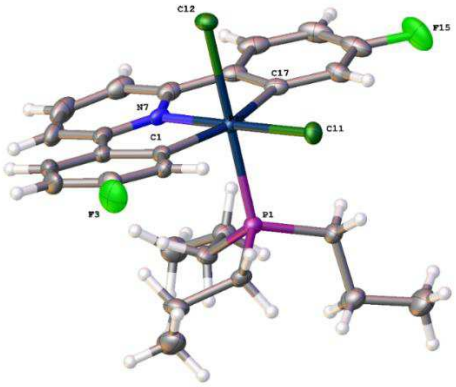

*Figure 2.9 Crystal structure of **3-Pr(c)**, thermal ellipsoids drawn at 50% probability level. Selected bond lengths (Å) and angles (°): Pt1-P1, 2.2944(11); Pt1-Cl2, 2.4116(10); Pt1-C1, 2.069(4); Pt1-C17, 2.083(4); Pt1-N7, 1.981(3); Pt1-Cl1, 2.3282(10); P1-Pt1-Cl2, 175.49(4); P1-Pt1-Cl1, 85.53(4); C1-Pt1-P1, 91.42(11); C1-Pt1-Cl2, 85.48(10); C1-Pt1-C17, 162.32(17); C1-Pt1-Cl1, 97.86(12); C17-Pt1-P1, 93.94(11); C17-Pt1-Cl2, 89.98(11); C17-Pt1-Cl1, 99.34(13); N7-Pt1-P1, 95.28(10); N7-Pt1-Cl2, 87.51(10); N7-Pt1-C1, 81.56(15); N7-Pt1-C17, 81.18(16); N7-Pt1-Cl1, 179.01(10); Cl1-Pt1-Cl2, 91.65(4).*

Addition of $PhICl_2$ to a chloroform solution at -60 °C gave **3-Pr(t)** as the major product, making up around 60% of the sample (Scheme 2.12). As soon as NMR data could be taken, a peak in the $^{31}P\{^{1}H\}$ NMR spectrum at 51 ppm ($^{1}J_{P\text{-}Pt}$ = 3080 Hz) was observed, and attributed to **5-Pr** (Scheme 2.12).

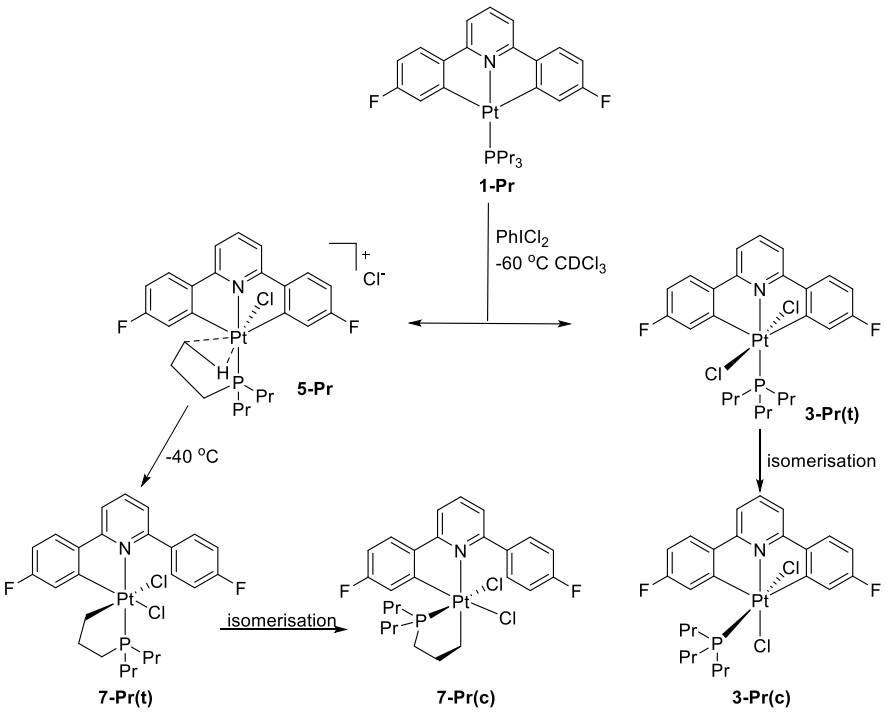

Scheme 2.12

The chemical shift and coupling constant are remarkably similar to **5-Bu**, however the complex disappeared quickly in solution without an increase in temperature to give a new complex **7-Pr(t)** before further NMR data could be recorded.

This alkyl-phenyl dicyclometallated complex **7-Pr(t)** was easily assigned due to its similarity to **6-Bu(t)**; a large downfield shift (relative to the *trans* dichloro- complexes) in the $^{31}P\{^{1}H\}$ NMR spectrum at 47.86 ppm, ($^{1}J_{P\text{-}Pt}$ = 3129 Hz) and two resonances in the $^{19}F\{^{1}H\}$ NMR spectrum (-111.90 ppm, -109.54, $^{4}J_{F\text{-}Pt}$ 45 Hz) where only one of the peaks has platinum coupling. In the ^{1}H NMR spectrum, a *trans* geometry could assigned by presence of phosphorus coupling on the proton *ortho* to Pt. As the alkyl chains of propyl phosphine are a carbon shorter, **7-Pr(t)** has two alkyl cyclometallated protons seen in the ^{1}H NMR spectrum at 3.09 ppm ($^{2}J_{H\text{-}Pt}$ = 102 Hz) and 2.37 ppm ($^{2}J_{H\text{-}Pt}$ = 56 Hz). The presence of **7-Pr(t)** shows that the five-coordinate intermediate can be stabilized by the shorter propyl chains, forming an agostic complex with a five-membered ring, **5-Pr**. It is unsurprising that the activation of the γ-carbon occurs at a lower temperature than for **5-Bu**. The methyl C-H bond is coordinated to platinum in **5-Bu**, and so requires a migration of the platinum to the adjacent carbon to activate the butyl γ-carbon.

7-Pr(t) has two chloride ligands, which was determined by a lack of ^{195}Pt - ^{1}H correlation with the protons on the dicyclometallated ring, and a relatively small mass peak in the positive mass spectrum. This is thought to be the reason for the much slower isomerisation to the final product **7-Pr(c)**, taking around 3-4 days for full conversion.

The isomerisation product **7-Pr(c)** was seen in the $^{31}P\{^{1}H\}$ NMR spectrum with an upfield shift from 47.86 ppm to 42.68 ppm ($^{1}J_{P\text{-}Pt}$ = 2938 Hz). In the ^{1}H NMR spectrum, a downfield shift of both alkyl cyclometallated protons to 3.70 ppm ($^{2}J_{H\text{-}Pt}$ = 95 Hz) and 3.10 ppm ($^{2}J_{H\text{-}Pt}$ = 65 Hz) was seen, an effect also seen for **7-Bu(c)**. Crystals suitable for analysis were grown from a chloroform solution, where the X-ray crystal structure showed the expected geometry (Figure 2.10). Again, enantiomerically pure crystals were grown from the racemic mixture (and crystals of both enantiomers were present).

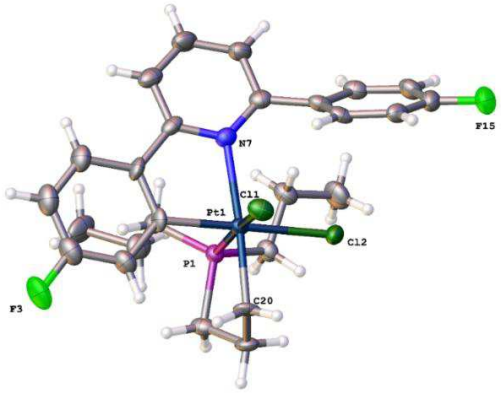

Figure 2.10 Crystal structure of ***7-Pr(c)****, thermal ellipsoids drawn at 50% probability level. Selected bond lengths (Å) and angles (°): Pt1-Cl1, 2.3953(15); Pt1-Cl2, 2.4072(16); Pt1-C1, 2.030(7); Pt1-N7, 2.246(5); Pt1-P1, 2.2650(15); Pt1-C20, 2.076(6); Cl1Pt1-Cl2, 91.68(6); C1-Pt1-Cl1, 89.54(19); C1-Pt1-Cl2, 178.72(19); C1-Pt1-N7, 79.7(3); C1-Pt1-P1, 87.46(19); C1-Pt1-C20, 96.2(3); N7-Pt1-Cl1, 91.74(14); N7-Pt1-Cl2, 100.66(15); N7-Pt1-P1, 95.20(14); P1-Pt1-Cl1, 171.83(5); P1-Pt1-Cl2, 91.29(6); C20-Pt1-Cl1, 87.93(19); C20-Pt1-Cl2, 83.4(2); C20-Pt1-N7, 175.9(3); C20-Pt1-P1, 84.84(19); C19-C18 P1, 106.0(6); C18-P1-Pt1, 101.2(2); C19-C20-Pt1, 112.9(4); C18-C19-C20, 110.6(6).*

Restricted rotation of the decylometallated ring about the aryl-py bond resulted in peak broadening in the ^{1}H NMR spectrum at room temperature. The complex was analysed by ^{1}H NMR between 208 K and 328 K at 10 K intervals (Figure 2.11).

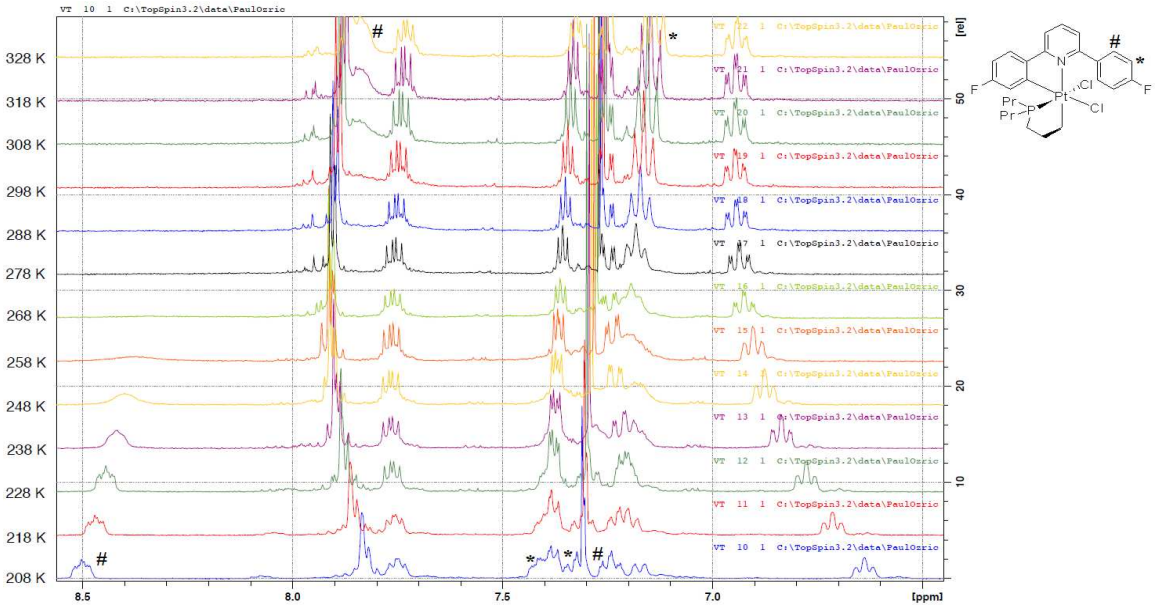

Figure 2.11 ^{1}H NMR spectra of ***7-Pr(c)*** *at various temperatures (208 – 328 K, aromatic region).*

Cooling a chloroform solution of **7-Pr(c)** to 208 K resulted in separation of all four protons of the decyclometallated ring. At this temperature, the rotation is very slow (on an NMR timescale). The two protons *meta* to fluorine on the ring shows the greatest separation as

one proton affected strongly by its proximity to the alkyl chains of the phosphine, whilst the other will be far from everything. The two peaks for the protons *meta* to fluorine are separated by 505 Hz at 208 K. Between 258 K and 298 K both lumps are sufficiently broad, even vanishing into the baseline at 278 K. By 328 K, even though two of the peaks have coalesced, the peak is very broad. The two protons *ortho* to fluorine are affected less, separated only by only 25 Hz at 208 K, and are easily identifiable as a single triplet at temperatures as low as 268 K. This gives a barrier to rotation of 61±5 $kJmol^{-1}$.

2.3.2.1. Trapping five-coordinate complexes using $AgBF_4$ and pyridine

The products of oxidation of **1-Ph**, **1-Bu** and **1-Pr** with $PhICl_2$ are solvent dependant. In chloroform the five-coordinate intermediates are either directly observable (**2-Ph**) or trapped with intermolecular interactions (**5-Bu** and **5-Pr**). In acetone, only the dichloro-complexes are observed. A possible reason for this is the complexation of acetone (or water) to the five-coordinate intermediate, which can be later displaced by the chloride. To test this, $AgBF_4$ was added to either isomer of **3-Pr** in an acetone solution to remove a chloride, and reveal a five-coordinate species. This species should effectively be the same as that before Cl^- or C-H bond coordination in the oxidation of **1-Pr** with $PhICl_2$. With no chloride in solution to form the dichloro- complexes **3-Pr**, only the solvent would be able to prevent C-H bond coordination.

Both **3-Pr(t)** and **3-Pr(c)** have poor solubility in acetone, and so solids were suspended in acetone. Obtaining pure **3-Pr(t)** had already proved fruitless, so a mixture of known composition was studied, alongside pure crystals of the *cis complex* **3-Pr(c)**. First pyridine-trapped complexes were made to allow for comparison with **4-Ph** (Scheme 2.6), and allow for the trapping of the five-coordinate complexes with less chance of seeing C-H activated products.

Pyridine was added (~20 eq) before the addition of $AgBF_4$ to the crystals of the *cis* isomer **3-Pr(c)**, and a new product was seen **4-Pr(c)** (Scheme 2.13). The spectra of **4-Pr(c)** showed a single peak in the $^{19}F\{^1H\}$ NMR spectrum at -106.15 ppm ($^4J_{F\text{-}Pt}$ = 14.5 Hz) and a pattern of peaks present by ^1H NMR which indicated that the C^N^C ligand remained dicyclometallated, and no reductive elimination of aryl-Cl had occurred. In the $^{31}P\{^1H\}$ NMR spectrum, a peak at 0.66 ppm ($^1J_{P\text{-}Pt}$ = 2213 Hz) and a doublet in the ^{195}Pt NMR spectrum −2240 ppm ($^1J_{Pt\text{-}P}$ = ~2550 Hz) indicated a Pt^{IV} species.

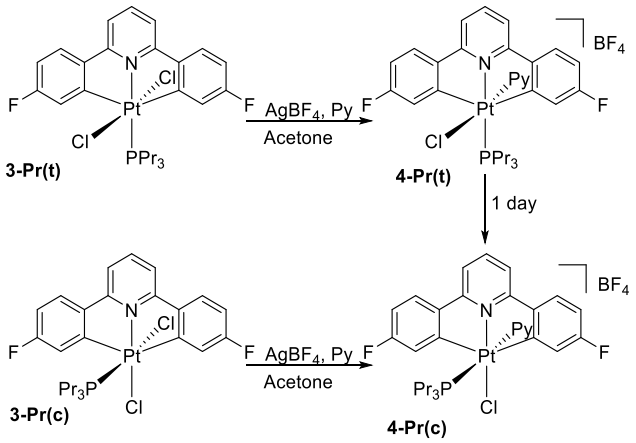

Scheme 2.13

Platinum coupling ($^3J_{H\text{-}Pt}$ = 20 Hz) on a peak corresponding to a py-*o* proton at 8.42 ppm in the ^{1}H NMR spectrum shows that pyridine is coordinated to platinum. A peak in the HR-MS (ESI) spectrum at 733.1826 m/z corresponded to the expected mass of the complex with including the coordinated pyridine. As with the reactions without pyridine (and the lack of any change with time), **4-Pr(c)** is expected to have a geometry in which the phosphorus is *cis* to the pyridine of the C^N^C ligand, and *trans* to the newly coordinated pyridine.

If pyridine is added (~20 eq) before the addition of $AgBF_4$ to the mixture of isomers, two products **4-Pr(t)** and **4-Pr(c)** were seen. The ratio of products was similar to that seen in the starting material (~5:3), where **4-Pr(c)** is the minor product. Adding pyridine straight after the addition of $AgBF_4$ to the mixture of isomers also gave only **4-Pr(t)** and **4-Pr(c)**.

4-Pr(t) could also be synthesised by oxidising **1-Pr** with $PhICl_2$ in the presence of pyridine (Scheme 2.14). The NMR spectra of **4-Pr(t)** showed a single peak in the ^{19}F{^{1}H} NMR spectrum at -103.75 ppm ($^4J_{F\text{-}Pt}$ = 11.5 Hz) and a pattern of peaks present by ^{1}H NMR which indicated that the C^N^C ligand remained dicyclometallated. In the ^{31}P{^{1}H} NMR spectrum, a peak at -9.03 ppm ($^1J_{P\text{-}Pt}$ = 2242 Hz) and a doublet in the ^{195}Pt NMR spectrum at −1966 ppm ($^1J_{Pt\text{-}P}$ = ~2350 Hz) indicated that a Pt^{IV} species was present. In the ^{1}H NMR spectrum the proton *ortho* to Pt and F showed coupling to phosphorus, which suggested that the phosphorus was *trans* to the pyridine of the C^N^C ligand, and *cis* to the newly coordinated pyridine. A peak at 8.65 ppm, relating to the py-*o* proton shows coupling to platinum ($^3J_{H\text{-}Pt}$ = 22 Hz) indicating that pyridine was coordinated. Further evidence in the HR-MS (ESI) spectrum at 733.1815 m/z corresponded to pyridine and chloride added (relative to the starting material, **1-Pr**). Isomerisation of **4-Pr(t)** to **4-Pr(c)** was seen over the course of weeks.

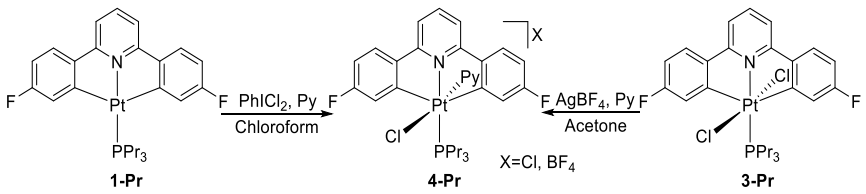

Scheme 2.14

This shows (analogous to the reactions with the PPh_3 derivative shown in Scheme 2.7) the five-coordinate intermediate can be trapped through both oxidation of the Pt^{II} starting material by adding oxidant in the presence of pyridine, or by adding pyridine directly to the five-coordinate when a chloride is removed from the Pt^{IV} dichloro- complexes. Whether pyridine is added before or after the addition of $AgBF_4$ to either isomer of **3-Pr**, no C-H activated products were observed.

Next, $AgBF_4$ was added to the dichloro- complexes **3-Pr(c)** and **3-Pr(t)** without any pyridine. Adding $AgBF_4$ to the suspension of crystals of the *cis* isomer at room temperature instantaneously gave one highly soluble platinum-containing product **2-Pr(c)** (Scheme 2.15), and the insoluble AgCl which was removed by filtration.

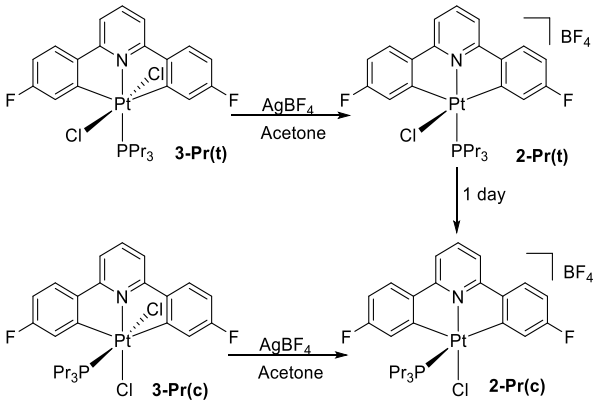

Scheme 2.15

The spectra of **2-Pr(c)** showed a single peak in the $^{19}F\{^1H\}$ NMR spectrum at -107.61 ppm ($^4J_{F\text{-}Pt}$ = 13 Hz) and a pattern of peaks present by ^1H NMR which indicated that the C^N^C ligand remained dicyclometallated, and no reductive elimination of aryl-Cl has occurred. In the $^{31}P\{^1H\}$ NMR spectrum, a peak at 13.74 ppm ($^1J_{P\text{-}Pt}$ = 2622 Hz) and a doublet in the ^{195}Pt NMR spectrum −2245 ppm ($^1J_{Pt\text{-}P}$ = ~2600 Hz) indicated a Pt^{IV} species. With no change over time a P-N *cis* geometry is expected. The tentative geometry assignment was

backed up by nOe spectra, where irradiation of the proton *ortho* to Pt and F showed very little correlation to the alkyl protons. No satellites on the terminal methyl protons, showed that there is also no sign of agostic interactions (the sixth coordination site is probably taken by acetone). Coordinated solvent was not shown in the HR-MS (ESI) spectrum, with a peak of high intesity relative to the baseline (relative to the neutral complex **3-Pr(c)**) at 755.1372 m/z which corresponds to the mass of **3-Pr(c)** missing one chloride ligand.

Adding $AgBF_4$ to the suspension of a mixture of isomers at room temperature instantaneously gave two highly soluble platinum-containing products, and the insoluble AgCl which was removed by filtration. As soon as NMR data could be taken, the proton spectrum shows two complexes in a ratio equal to the starting material (~5:3). The presence of **2-Pr(c)** as the minor product is further evidence of a *cis* geometry, and implies that the structure of **2-Pr(t)** is likely to have a P-N *trans* geometry.

The major product **2-Pr(t)** was then assigned from the remaining peaks in the NMR spectra. The spectra showed a single peak in the $^{19}F\{^1H\}$ NMR spectrum at -109.19 ppm ($^4J_{F\text{-}Pt}$ = 15.5 Hz) and a pattern of peaks present by ^1H NMR which indicated that the C^N^C ligand remained dicyclometallated, and no reductive elimination of aryl-Cl has occurred. In the $^{31}P\{^1H\}$ NMR spectrum, a peak at -12.10 ppm ($^1J_{P\text{-}Pt}$ = 2261 Hz) and a doublet in the ^{195}Pt NMR spectrum −2195 ppm ($^1J_{Pt\text{-}P}$ = ~2250 Hz) indicated a Pt^{IV} species. The proton *ortho* to Pt and F showed coupling to phosphorus, which suggested a P-N *trans* geometry. The HR-MS (ESI) spectrum of an aliquot taken from the reaction mixture showed no difference to that of **2-Pr(c)**. Within a couple of hours, the relative amount of the minor product **2-Pr(c)** grows noticeably, with full consumption of **2-Pr(t)** complete within a day.

With no signs of agostic complexes, or C-H activated products, the sixth coordination site is likely filled by solvent (shown in Scheme 2.16). Acetone is more coordinating than chloroform, and so might compete with the alkyl chains for the coordination site.

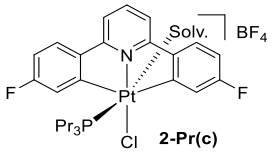

Scheme 2.16

It is known that having residual water in acetone is unavoidable, so water could also be coordinating. Neither acetone-d_6 nor water could be observed coordinating to the platinum in the ^{1}H NMR spectrum, and are expected to be constantly exchanging in solution. This was supported by adding $AgBF_4$ to **3-Pr(c)** in acetone-H_6 followed by removal of solvent and redissolving in acetone-d_6. Still no coordinated acetone was observed. The structure of **2-Pr(c)** can therefore be drawn more correctly by filling the remaining coordination site with a solvent molecule.

2.4. Tri(*o*-tolyl)phosphine Derivative **1-Tol**

Reactions of $PhICl_2$ with **1-Ph** in chloroform, gave a long-lived five-coordinate intermediate. The bulkiness of the phosphine meant a slow rate of combination of the second chloride. Reactions of $PhICl_2$ with the alkyl phosphines (**1-Bu** or **1-Pr**) in chloroform did not give a five-coordinate intermediate. However, it was possible for an alkyl chain to coordinate to platinum (forming an agostic interaction), where the γ-C of the phosphine was eventually activated, which gave transcyclometallated products.

Tri-orthotolyl phosphine (P(*o*-tol)$_3$) has a Tolman cone angle larger than 180°, and has C(sp^3) that are three carbons away from the phosphorus. With a larger Tolman cone angle, combination of the $[Pt^{IV}Cl]^+$ five-coordinate intermediate with the second chloride was expected to be even slower, allowing for a larger proportion of C-H activated products.

The Pt^{II} starting material **1-Tol** was synthesised from **1-DMSO** with one equivalent of P(*o*-tol)$_3$ (Scheme 2.17).[157] In the ^{1}H NMR spectrum, individual resonances for each proton (except the protons on individual methyl groups which appear to be able to rotate freely) are seen because of restricted rotation about the Pt-P bond (due to the steric bulk of the phosphine). VT NMR experiments (in toluene-d$_8$) showed that even heating to 80 °C the rotation is still slow on the NMR timescale.

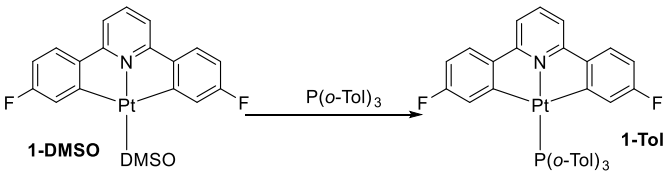

Scheme 2.17

With only one peak in the $^{31}P\{^{1}H\}$ NMR spectrum at 17.17 ppm ($^{1}J_{P\text{-}Pt}$ = 3942 Hz) and a single doublet in the ^{195}Pt NMR spectrum at -4227 ppm ($^{1}J_{Pt\text{-}P}$ = ~3800 Hz), we can be certain of a single phosphorus/platinum containing product. Despite having two peaks in the $^{19}F\{^{1}H\}$ NMR spectrum (-110.23 ppm, $^{4}J_{F\text{-}Pt}$ = 33 Hz and -111.79 ppm, $^{4}J_{F\text{-}Pt}$ = 27.5 Hz), the presence of platinum satellites on both peaks showed that the C^N^C ligand was dicyclometallated. A crystal suitable for X-ray analysis was grown from chloroform, and the crystal structure solved (Figure 2.12).

In the ^{1}H NMR spectrum one of the protons *ortho* to Pt and F is noticeably upfield shifted at 5.73 ppm; the other seems relatively unaffected. When the crystal is compared to that of **1-Ph**, it can be seen that only one of the protons *ortho* to Pt and F points towards the centre of a tolyl ring, and so the upfied shift can again be explained by conflicting ring currents.

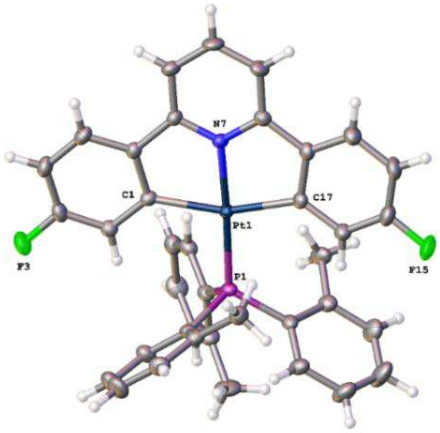

*Figure 2.12 Crystal structure of **1-Tol**, thermal ellipsoids drawn at 50% probability level. Selected bond lengths (Å) and angles (°): C1-Pt1, 2.094(3); Pt1-P1, 2.2548(8); Pt1-N7, 2.024(2); Pt1-C17, 2.085(3); C1-Pt-P,1 97.54(8); N7-Pt1-C1, 79.80(11); N7-Pt1-P1, 177.32(7); N7-Pt1-C17, 79.53(11); C17-Pt1-C1, 158.86(12); C17-Pt1-P1, 103.10(9).*

Also seen in the crystal structure is an *o*-tolyl aryl proton pointing directly at the Pt, with a Pt-H distance of 2.869Åbeing close enough to be considered a bond (the sum of the Van der Waals radii is 2.95Å). This proton was seen in the ^{1}H NMR spectrum at 8.99 ppm, the most downfield chemical shift. This anagostic interaction could also be seen in the ^{195}Pt – ^{1}H correlation spectrum.

Addition of $PhICl_2$ to a chloroform solution of **1-Tol** at -60 °C gave three new complexes; a dichloro- complex **3-Tol(c)** (15 %), and two C-H activated complexes **8** and **7-Tol(t)** (85 %) (Scheme 2.18). All products were stable at this temperature, with no change in product distributions over the course of several hours, which allowed for the collection of enough NMR data to be confident of the structure and geometry of all products present.

Allowing the reaction mixture to return to room temperature saw the C-H activated products precipitate, and become highly insoluble in all common solvents. The product distribution was unaffected by using acetone as the solvent. It could be assumed that the large *o*-tol groups prevent acetone from coordinating before a C-H activation reaction occurs because of the proximity of the methyl groups to the platinum (where as the smaller chloride ligands can still fit).

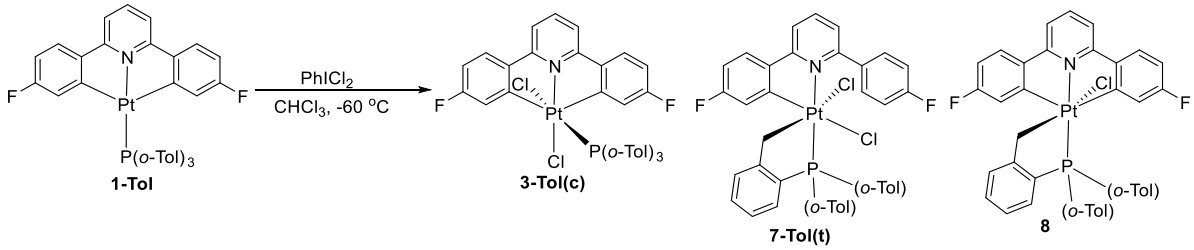

Scheme 2.18

Pure samples of **3-Tol(c)** could therefore be made by removal of the precipitate by filtration. In the $^{31}P\{^{1}H\}$ NMR spectrum, a peak at -13.96 ppm ($^{1}J_{P\text{-}Pt}$ = 2470 Hz) and a doublet in the ^{195}Pt NMR spectrum −2403 ppm ($^{1}J_{Pt\text{-}P}$ = ~2500 Hz) indicated a Pt^{IV} species. The spectra showed a single peak in the $^{19}F\{^{1}H\}$ NMR spectrum at -106.50 ppm ($^{4}J_{F\text{-}Pt}$ = 14 Hz) and a pattern of peaks present by ^{1}H NMR which indicated that the C^N^C ligand remains dicyclometallated, and that now the phosphine is able to rotate much more quickly (which suggests a *cis* geometry). The position of the proton *ortho* to Pt and F has also shifted far downfield to 7.69 ppm. A crystal grown from chloroform suitable for X-ray crystallography confirmed the *cis* geometry (Figure 2.13).

It was suspeced that the *trans* dichloro- complex is not seen because of the bulkiness of the phosphine, and the energy that could be gained from the phosphine moving to a P-N *cis* geometry, results in isomerisation before the coordination of Cl^{-}. After addition of the first chloride, rapid movement of the phosphine to a P-N *cis* position could precede combination with the second chloride.

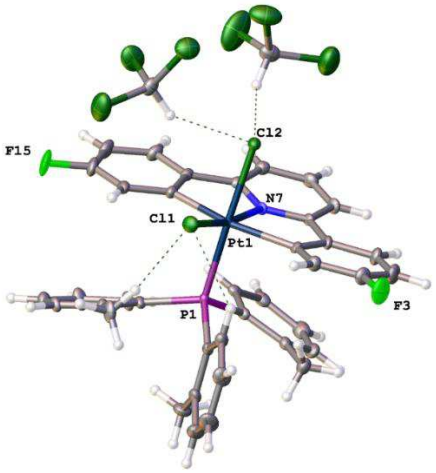

*Figure 2.13 Crystal structure of **3-Tol(c)**, thermal ellipsoids drawn at 50% probability level. Selected bond lengths (Å) and angles (°): C1-Pt1, 2.100(5); Cl1-Pt1, 2.3323(18); P1-Pt1, 2.3503(15); Pt1-Cl2, 2.3974(15); Pt1-N7, 1.985(5); Pt1-C17, 2.065(7); C1-Pt1-Cl1, 100.0(3); C1-Pt1-P1, 91.97(17); C1-Pt1-Cl2, 87.48(16); Cl1-Pt1-P1, 97.53(6); Cl1-Pt1-Cl2, 86.26(6); P1-Pt1-Cl2, 176.21(7); N7-Pt1-C1, 81.1(4); N7-Pt1-Cl1, 169.29(16); N7-Pt1-P1, 93.06(17); N7-Pt1-Cl2, 83.15(16); N7-Pt1-C17, 81.4(3); C17-Pt1-C1, 162.5(4); C17-Pt1-Cl1, 96.8(2); C17-Pt1-P1, 90.5(2); C17-Pt1-Cl2, 88.9(2).*

The minor C-H activation complex **8**, made up about 15 % of the product mass. In the ^{1}H NMR spectrum, two alkyl cyclometallated protons could be seen at 2.75 ppm ($^{2}J_{H\text{-}H}$ = 13 Hz, $^{2}J_{H\text{-}Pt}$ = 74 Hz) and at 3.77 ppm ($^{2}J_{H\text{-}H}$ = 13 Hz, $^{2}J_{H\text{-}Pt}$ = 90 Hz). The $^{2}J_{H\text{-}H}$ coupling show that the two protons are attached to the same carbon. A peak in the ^{31}P{^{1}H} NMR spectrum at 20.26 ppm ($^{2}J_{P\text{-}Pt}$ = 2818 Hz) indicated a Pt^{IV} species. The large downfield shift could suggest that the phosphorus is part of a ring (when compared with **3-Tol(c)**). In the ^{19}F{^{1}H} NMR spectrum, two peaks at -107.52 ppm ($^{4}J_{F\text{-}Pt}$ = 28 Hz) and -110.29 ppm ($^{4}J_{F\text{-}Pt}$ = 23 Hz) were seen. Satellites on both peaks shows that the C^N^C ligand is still dicyclometallated. Like **1-Tol**, the presence of two peaks suggested that the phosphorus is *trans* to the nitrogen. As the C^N^C remains dicyclometallated, and a methyl group has been activated, **8** is a tricyclometallated species. It is interesting to note the presence of two cyclometallated protons and two fluorine peaks with platinum satellites. It would be expected that **8** would have a plane of symmetry that would pass through the plane of the N-Pt-P and orthogonal to the C^N^C plane at thermodynamic equilibrium. At -40 °C any movement is frozen out and so the observed conformation of the *o*-tol platinacycle must break this plane of symmetry.

A likely mechanism for the formation of **8** would begin with initial addition of the first chloride to give a five-coordinate intermediate (Scheme 2.19). Before the phosphine moves to a position *cis* to the nitrogen, a methyl group close enough to platinum coordinates to the metal centre. Deprotonation of the methyl group will then give **8**.

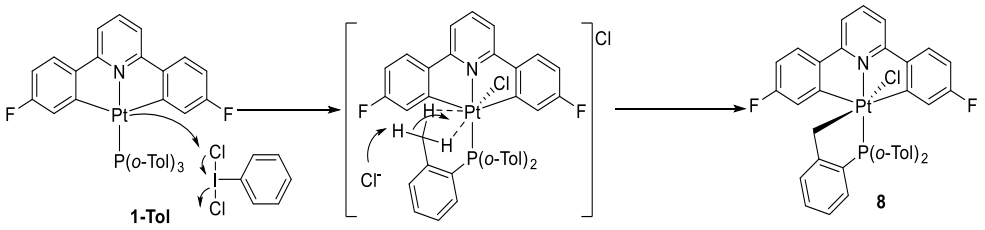

Scheme 2.19

A tricyclometallated complex was not seen upon the oxidation of **1-Bu** as the pK_a of alkyl protons is too high. The pK_a of tolyl-Me protons is ~40, about 20 lower than an alkyl chain (~60) due to stabilization from the aryl ring. Upon coordination to platinum, the pK_a would drop further, and so is likely the reason for the presnsece of this species.

The major C-H activation complex **7-Tol(t)**, made up the remaining 70 % of the sample. After the precipitation of the C-H activated products, serendipitously crystal was found in solution which proved to be suitable for X-ray crystallography. The solved X-ray crystal structure showed a P-N *trans* geometry and two chlorides coordinated to the metal (Figure 2.14).

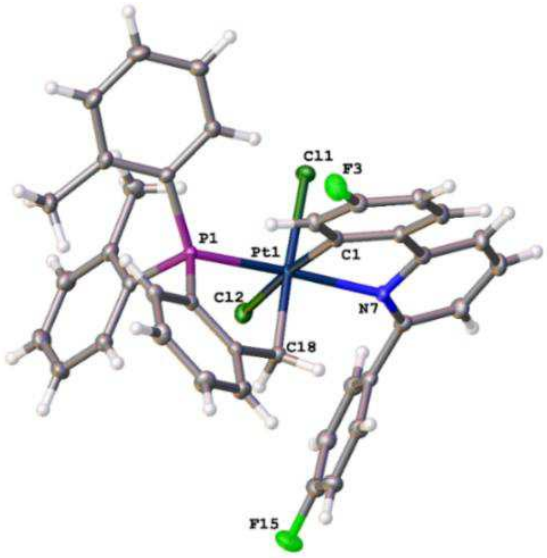

*Figure 2.14 Crystal structure of **7-Tol(t)**, thermal ellipsoids drawn at 50% probability level. Selected bond lengths (Å) and angles (°): Pt1-Cl1, 2.4429(6); Pt1-P1, 2.2906(6); Pt1-C1, 2.041(2); Pt1-Cl2, 2.4086(6); Pt1-N7, 2.179(2); Pt1-C18, 2.075(2); P1-Pt1-Cl1, 99.69(2); P1-Pt1-Cl2, 90.37(2); C1-Pt1-Cl1, 90.68(7); C1-Pt1-P1, 96.77(7); C1-Pt1-Cl2, 172.86(7); C1-Pt1-N7, 80.19(9); C1-Pt1-C18, 87.83(10); Cl2-Pt1-Cl1, 88.15(2); N7-Pt1-Cl1, 84.39(6); N7-Pt1-P1, 174.99(6); N7-Pt1-Cl2, 92.69(6); C18-Pt1-Cl1, 177.53(8); C18-Pt1-P1, 82.45(8); C18-Pt1-Cl2, 93.09(8); C18-Pt1-N7, 93.41(9); C19-C18-Pt1, 113.34(17); C24-C19-C18, 120.0(2); C19-C24-P1, 113.15(18); C24-P1-Pt1, 100.40(9).*

The solution NMR data that were assigned to **7-Tol(t)** was performed on the basis on similarity to **7-Bu(t)**. In the ^{1}H NMR spectrum there are two cyclometallated proton peaks at 4.07 ppm ($^{2}J_{\text{H-Pt}}$ = 76 Hz) and 4.66 ppm ($^{2}J_{\text{H-Pt}}$ = 102 Hz). A doublet in the ^{195}Pt NMR spectrum at -2527 ppm ($^{1}J_{\text{Pt-P}}$ = ~2900 Hz) is indicative of a Pt^{IV} species. In the ^{19}F{^{1}H} NMR spectrum there are two peaks, one without platinum satellites at -109.62 ppm ($^{4}J_{\text{F-Pt}}$ = 43 Hz) and -112.68 ppm.

Crystals of **7-Tol(t)** were collected and then suspended in acetone-d_6. The ^{1}H NMR spectrum of the suspension showed only solvent peaks, indicating that the crystals contained no soluble impurities. After a month, a new complex appeared in solution **6-Tol(c)** (Scheme 2.20). Due to the very low concentration of **6-Tol(c)** in solution, only some diagnostic peaks could be assigned.

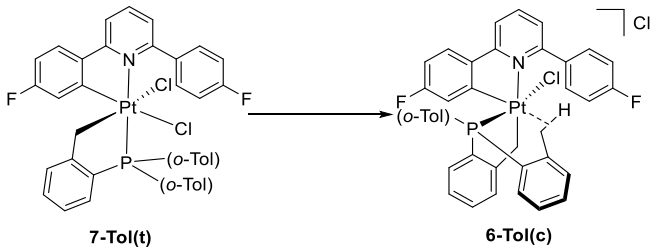

Scheme 2.20

With two peaks (including one without platinum satellites) in the ^{19}F{^{1}H} NMR spectrum at -109.33 ppm ($^{4}J_{\text{F-Pt}}$ = 45 Hz) and -115.18 ppm, no further reaction has happened with the C^N^C ligand. In the ^{31}P{^{1}H} NMR spectrum, a peak at 23.69 ppm ($^{1}J_{\text{P-Pt}}$ = 2969 Hz) and a doublet in the ^{195}Pt NMR spectrum −2583 ppm ($^{1}J_{\text{Pt-P}}$ = ~3000 Hz) indicated a Pt^{IV} species. In the ^{1}H NMR spectrum, the alkyl cyclometallated protons are further downfield (cf. **6-Tol(t)**) with smaller coupling constants at 5.12 ppm ($^{2}J_{\text{H-Pt}}$ = 95 Hz) and 4.25 ppm ($^{2}J_{\text{H-Pt}}$ = 45 Hz). A downfield shift of the alkyl cyclometallated protons was also seen for **7-Bu(c)** and **7-Pr(c)**, which would suggest that **6-Tol(c)** is formed by the isomerisation of the *o*-tolyl platinacycle. Due to the *trans* phobia (and the size of the tolyl rings), it is unlikely that the alkyl cyclometallated protons are *trans* to the cyclometallated aryl ring. An agostic interaction was seen in the ^{195}Pt - ^{1}H correlation spectrum with a clear correlation to the methyl protons at 1.22 ppm (Figure 2.15).

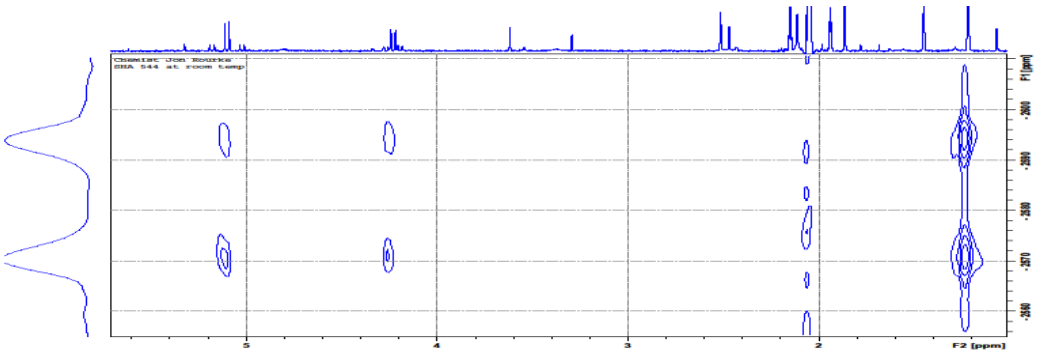

Figure 2.15 ^{195}Pt - ^{1}H correlation spectrum showing strong coupling to cyclometallated protons (left) and an agostic interaction (right).

2.5. Conclusion

Five-coordinate 16 valence electron complexes are known to be short-lived; some can only be speculated as reaction intermediates. The addition of oxidants that add via a two-step S_N2 mechanism allowed for these intermediates to be trapped. This included the use of auxiliary ligands, bulky ligands (to block coordination sites), and intramolecular interactions (such as agostic interactions). This chapter looked at the addition of the chlorine-based oxidant $PhICl_2$ to C^N^C dicyclometallated Pt^{II} complexes with larger and bulkier ligands, building on the past work in the Rourke group.[141,150,158]

After the addition of $PhICl_2$ to the various Pt^{II} starting materials, dichloro- complexes were observed in all cases. These are the expected products based on the initial addition of Cl^+ to the 16 valence electron Pt^{II} complex, followed later by combination with Cl^- to give coordinatively saturated 18 valence electron Pt^{IV} species.

However, the dichloro- complexes were not the only observed compounds. Oxidation of **1-Ph** gave a five-coordinate species which preceded the dichloro- complex, where the bulky phenyl groups blocked the open coordination site. Oxidation of **1-Bu**, **1-Pr** or **1-Tol** gave transcyclometallatation products formed by trapping the five-coordinate intermediate with an intramolecular agostic interaction.

The driving force in the formation of the transcyclometallation product is thought to be the release of bond strain in the five-membered ring. For this reason, future work should focus on monocyclometallated Pt^{II} starting materials, or less rigid dicyclometallated complexes. More specifically, it might be worth studying the oxidation of a triethylphosphine (or ethyldiphenylphosphine) to see if a four-membered ring can be synthesized.

3.0 Oxidative Addition with RX Compounds and Subsequent Reductive Elimination

3.1. Introduction

RX compounds (e.g. MeI) add to square planar Pt^{II} complexes via an S_N2-type reaction. An S_N2 reaction has been proved by the dependence of the rate on the concentration of both reagents, and the increase in reaction rate with polar solvents.[159] The rate of reaction is also greatly affected by the level of congestion at the metal centre, as the metal needs to be able to attack the R group. This also has implications for the size of the R group, as any congestion at the metal centre will reduce the rate of oxidative addition, and increase the rate of reductive elimination. The rate difference for increasing the size of the R group can be large; Puddephatt showed that some rates of oxidative addition of MeI were up to a hundred times faster than for comparable reactions with EtI.[160]

S_N2 reactions are by definition, a two-step mechanism. In the case of MeI undergoing oxidative addition to a 16 valence electron square planar complex, the metal first attacks the methyl carbon, which results in the breaking of the C-I bond. The oxidation state of the five-coordinate metal complex increases by two. The iodide later coordinates to form an 18 valence electron octahedral complex.

At low temperatures, Puddephatt *et al* have observed direct evidence of an intermediate of the oxidative addition reaction (Scheme 3.1).[161] After initial reaction of the platinum complex with MeI at -40 °C in a coordinating solvent (acetonitrile), the methyl group has added, but the remaining coordination site has been taken by a solvent molecule. Upon warming to room temperature, the anion displaces the solvent to form the expected product.

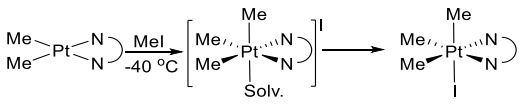

Scheme 3.1

Reductive elimination is the reverse of oxidative addition, and therefore shares the same mechanism pathways, but in reverse. Work in the Goldberg group looked at competing reductive elimination reactions at Pt^{IV} centres. They started with (P^P)$Pt^{IV}Me_3I$, where

there is a methyl group *trans* to the iodide. Heating the complex led to the formation of two Pt^{II} species. As the mechanism of an S_N2 reductive elimination reaction is expected to go via the reverse of the expected oxidation reaction, the natural first step is the dissociation of the iodide. The iodide would then abstract the methyl group from the metal, and reduce the oxidation state of the metal by two.[162]

Dissociation of the iodide reveals a coordinatively unsaturated intermediate. The coordinatively unsaturated complex allowed for the concerted reductive elimination of ethane, leading to the formation of the second Pt^{II} complex. The S_N2 reaction was therefore in competition with the concerted reaction, giving two possible products. Other work in their group demonstrated that methyl groups can be abstracted from five coordinate complexes by other five-coordinate complexes (also an S_N2 mechanism).[163]

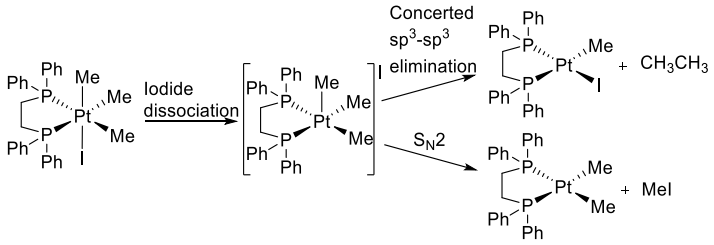

Scheme 3.2

Next, they synthesized the tetra-methyl derivative P^P $Pt^{IV}Me_4$. With no iodide to dissociate, an S_N2-type mechanism wasn't possible. With longer heating times and higher temperatures (50 h, 165 °C in benzene) ethane was still produced in a concerted reductive elimination reaction (Scheme 3.3).[164]

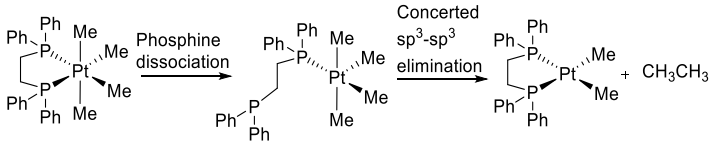

Scheme 3.3

A concerted reductive elimination mechanism is highly disfavoured at coordinatively saturated complexes because the electrons donated from the coupled group would be put into a highly antibonding orbital, which would destabilise the complex (Figure 1.9). Therefore, to allow a concerted mechanism to take place, a group would first have to leave to reveal a coordinatively unsaturated complex. Because methyl groups are unlikely to dissociate (as the carbanion would be highly unstable), it is likely that it is a phosphorus

that dissociates. Platinum-phosphorus bonds can be very strong, due to the phosphorus orbitals allowing efficient forward and back bonding. The strength of these bonds explains the need for the high temperatures and long reaction times, as the reductive elimination reaction is fast (and irreversible). Lower temperatures of reductive elimination could be achieved with monodentate-phosphines. Diphosphines will dissociate less readily than similar monodentate-phosphines because of the chelate effect, increasing the temperature required. In the examples mentioned above, all of the possible coupling groups were methyl groups. The methyl groups could move freely to different places on the metal (in the coordinatively unsaturated intermediate), and so there is no selectivity over which methyl groups would couple.

Cyclometallated ligands restrict the movement of other ligands by taking up two or more adjacent coordination sites. With less free movement in the coordinatively unsaturated intermediate, the products of reductive elimination will depend more on the original positions of the ligands before a group was removed (i.e. the starting material). Removal of a ligand from a six-coordinate 18 valence electron octahedral complex will give a five-coordinate reactive species which can take two different (but quite similar) geometries; square-based pyramidal and trigonal bipyramidal. Favoured and disfavoured coupling pathways are shown in Figure 3.1.[165]

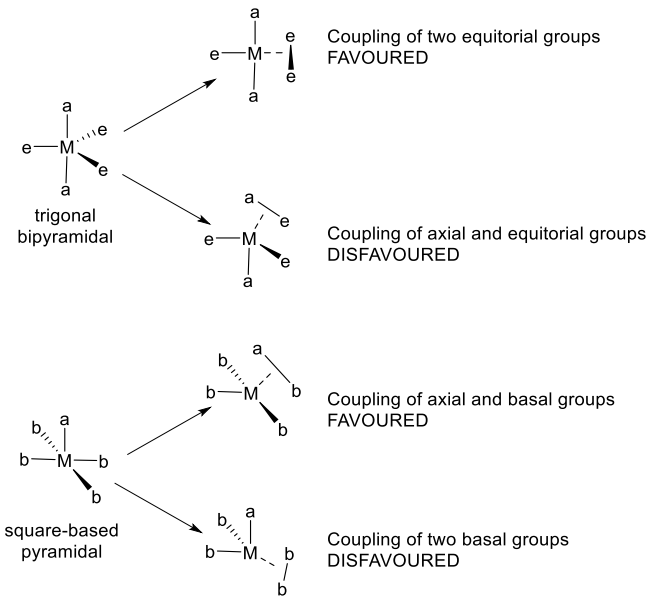

Figure 3.1 Illustration of favoured and disfavoured coupling geometries at five-coordinate metals.

L_e-L_e and L_a-L_b are favoured orientations for reductive coupling reactions because the reaction requires the coupling groups to be part of a trigonal plane, as electron density

donated from the coupling groups is donated into a non-bonding orbital. Conversely, L_a-L_e and L_b-L_b coupling reactions are disfavoured, because (like the coordinatively saturated complex) the electron density would be donated into a high energy anti-bonding orbital that would destabilise the complex. It has been shown computationally that alkenes may eliminate without the need of a coordinatively unsaturated intermediate, and without breaking the 18 valence electron rule. [166]

An example of the dependence of geometry for the selectivity of reductive coupling is shown in (Scheme 3.4). The monocyclometallated C^N complex of $Pt^{IV}(PPh_3)Me_2I$ has *fac*-PtC_3 geometry (aryl and two methyl groups) with the iodide *trans* to the aryl group.[167,168] Addition of $AgBF_4$ to this complex (to abstract the iodide) gave two isomers of a single product; the aryl group had coupled with a methyl. There was no evidence of methyl-methyl coupling, showing selectivity of $C(sp^2)$-$C(sp^3)$ coupling instead of $C(sp^3)$-$C(sp^3)$, forced by the geometry of the intermediate.

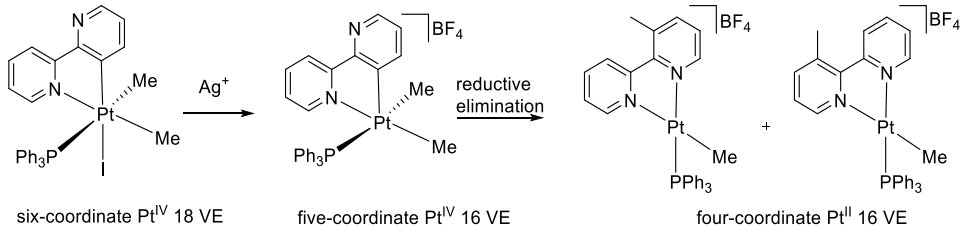

Scheme 3.4

The five-coordinate intermediate will have a square-based pyramidal geometry with the aryl group taking the axial position, and the other groups taking basal positions. Axial-basal reductive elimination reactions are favoured, whilst basal-basal are disfavoured. Without any rearrangement of the ligands taking place, the only favoured reaction is the coupling of an aryl and a methyl group, giving the observed Pt^{II} products. Axial-basal reductive elimination of aryl-P is favoured geometrically, however the product of the reductive coupling reaction is far less stable, and therefore not seen. Similar results have also been seen for tridentate N^N^C ligands.[169]

This chapter looks at the reaction of RX compounds with dicyclometallated C^N^C Pt^{II} complexes. The Pt^{IV} products were then treated with $AgBF_4$ to generate five-coordinate intermediates. As the C^N^C ligand is forced to take a *mer* geometry at the metal centre, movement of ligands about a five-coordinate species are even more restricted. The

products of reductive elimination have been rationalized, and the five-coordinate intermediates have been trapped.

3.2. C^N^C = 2,6-di(4-fluorophenyl)pyridine

This section focusses mainly on a series of reactions, beginning with the aryl-aryl dicyclometallated C^N^C $Pt^{II}L$ complexes **1-L** (where L = PPr_3, PBu_3 and PBn_3) and their reactivity with MeI. The three different phosphines used allowed for the effect of increasing cone angle to be studied with respect to oxidative addition and reductive elimination. Also shown is an analogous series of reactions of **1-Pr** with BnBr, allowing different alkylating agents to be compared. As the products of the following reaction are analogous, the main discussion will follow those where L = PPr_3 and RX = MeI. Only any interesting differences or crystal structures for the analogous complexes will be discussed separately.

3.2.1. Reactivity of Pt^{II} Complexes with RX Compounds

The $Pt^{II}PPr_3$ complex **1-Pr** was dissolved in MeI, and heated to reflux for 1 hour, after which time full conversion a single product **9-Pr(t)** was seen (Scheme 3.5).[165] The NMR spectra showed a single peak in the $^{19}F\{^1H\}$ NMR spectrum at -110.00 ppm ($^4J_{F\text{-}Pt}$ = 23 Hz) and a pattern of peaks present in the ^1H NMR spectrum indicated that the C^N^C ligand remained dicyclometallated. In the ^1H NMR spectrum a peak with a relative integral of three with platinum coupling at 1.02 ppm ($^2J_{H\text{-}Pt}$ = 67 Hz) indicated a Pt-Me bond.

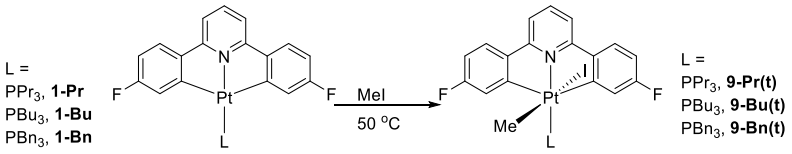

Scheme 3.5

A $[M\text{-}I]^+$ peak of of low intensity in the HR-MS (ESI) spectrum at 634.1934 m/z (corresponding to $[M\text{-}I]^+$) suggests that **9-Pr(t)** is a neutral species. A P-N *trans* geometry of **9-Pr(t)** was suggested by nOe data, where irradiation of the proton *ortho* to Pt and F enhanced the phosphine alkyl peaks, with no effect on the coordinated methyl group. A suitable crystal for X-ray analysis was grown from chloroform (Figure 3.2). The crystal

structure showed the expected P-N *trans* geometry, with the methyl and iodide groups coordinated *trans* across the metal.

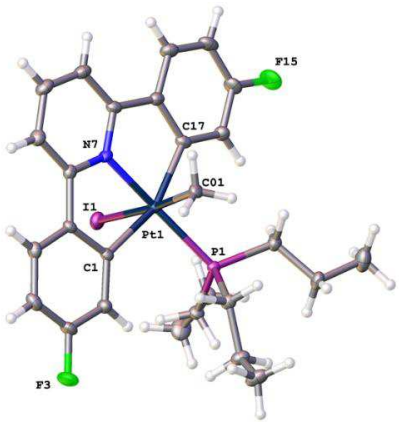

*Figure 3.2 Crystal structure of **9-Pr(t)**, thermal ellipsoids drawn at 50% probability level. Selected bond lengths (Å) and angles (°): C1-Pt1, 2.094(3); P1-Pt1, 2.2925(9); C01-Pt1, 2.117(4); I1-Pt1, 2.7497(3); Pt1-N7, 2.037(3); Pt1-C17, 2.101(4); C1-Pt1-P1, 95.81(10); C1-Pt1-C01, 91.40(14); C1-Pt1-I1, 89.44(10); C1-Pt1-C17, 159.43(15); P1-Pt1-I1, 97.72(2); C01-Pt1-P1, 87.11(11); C01-Pt1-I1, 175.00(11); N7-Pt1-C1 79.96(13); N7-Pt1-P1, 170.60(9); N7-Pt1-C01, 84.63(14); N7-Pt1-I1, 90.67(9); N7-Pt1-C17, 79.61(14); C17-Pt1-P1, 104.75(11); C17Pt1-C01, 89.05(14); C17-Pt1-I1, 88.43(10).*

The peak in the $^{31}P\{^{1}H\}$ NMR spectrum at -22.45 ppm is unusually upfield shifted when compared to the range of resonances in the previous chapter, and the position of the starting material **1-Pr** (1.34 ppm). The magnitude of the platinum constant ($^{1}J_{P\text{-}Pt}$ = 2650 Hz) is in keeping with Pt^{IV} complexes seen in the previous chapter. The peak in the ^{195}Pt NMR spectrum at -3520 ppm would suggest a Pt^{II} species when compared to the Pt^{II} starting material **1-Pr** (-4212 ppm), and the analogous Pt^{IV} dichloro- complex **3t-Pr(t)** (-2282 ppm). The chemical shift for **9-Pr(t)** is only 700 ppm downfield form **1-Pr**. However, the platinum must have beenoxidised to Pt^{IV} because the C^N^C remains dicyclometallated, and other coordination sites on the platinum are taken by a phosphorus, a methyl group and, as explained later, an iodide ligand.

A downfield shift is expected with an increase in oxidation state, as the platinum loses electron density. The magnitude of shift between the Pt^{II} and Pt^{IV} complexes will also depend on the ligands added to the metal. Chloride groups are strongly electronegative, withdrawing electron density away from the metal. Conversely, alkyl groups are donating, and will increase the electron density at the platinum centre. Although the iodide is also an electron withdrawing group, it is far less electronegative than chlorides.

With further heating in chloroform at 50 °C, the resonances for **9-Pr(t)** disappeared with the growth of a new complex **9-Pr(c)**, complete within 72 hours (Scheme 3.6). The spectra showed a single peak in the $^{19}F\{^1H\}$ NMR spectrum at -109.00 ppm ($^4J_{F\text{-}Pt}$ = 23 Hz) and a pattern of peaks present by ^1H NMR indicated that the C^N^C ligand remained dicyclometallated.

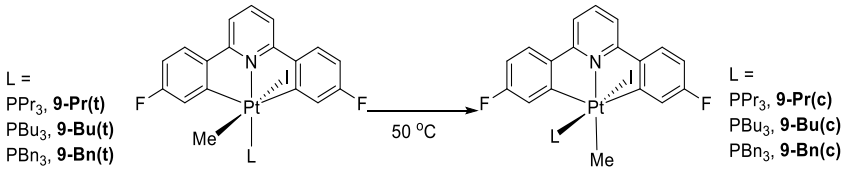

Scheme 3.6

A peak in the ^1H NMR spectrum with a relative integral of three at 1.02 ppm, and a large coupling constant ($^2J_{H\text{-}Pt}$ = 72 Hz) corresponded to Pt-Me. Because the connectivity is the same as **9-Pr(t)**, **9-Pr(c)** is therefore an isomerisation product. The change in geometry is also suggested by the downfield shift of the peak in the $^{31}P\{^1H\}$ NMR spectrum to -18.35 ppm ($^1J_{P\text{-}Pt}$ = 2482 Hz), an even larger upfield shift of the peak in the ^{195}Pt NMR spectrum at -3901 ppm (~350 ppm upfield cf. **9-Pr(t)**), and a large upfield shift of the Pt-Me peak in the $^{13}C\{H\}$ NMR spectrum to -15.16 ppm ($^1J_{C\text{-}Pt}$ = 502.5 Hz). The lack of coupling between the phosphorus and the methyl group (in the ^1H or ^{13}C NMR spectra) suggests that the methyl group is *cis* to the phosphorus. Irradiation of the proton *ortho* to Pt and F showed a far weaker enhancement of the alkyl chains (when compared to **9-Pr(t)**), and some enhancement of the Pt-Me protons, suggesting that the phosphorus is now *cis* to the nitrogen. This geometry can be explained, in much the same way as for **3-Pr(t)**, by placing the larger ligands orthogonal to the plane of the C^N^C ligand.

The rate of reaction of **1-Bn** with MeI was considerably slower, requiring two days under reflux for full consumption of **1-Bn** (Scheme 3.5). Although the reaction mixture contained mainly **9-Bn(t)**, some **9-Bn(c)** was seen, and separation of the two isomers was not possible. Full conversion to **9-Bn(c)** required a full week of heating **1-Bn** to reflux in MeI, as heating **9-Bn(t)** in chloroform led instead to full conversion to **1-Bn**.

Like in Scheme 3.2, the iodide is able to dissociate from **9-Bn(t)**, and abstract the methyl group in an S_N2-type reaction, forming **1-Bn** and MeI. The dissociation of the iodide also activated a concerted mechanism to give ethane gas from two adjacent methyl groups. For **9-Bn(t)** there are two aryl groups *cis* to the coordinated methyl group, but there was no

evidence of coupling of an aryl and a methyl group. This suggests that the concerted mechanism (discussed later) is relatively slow, compared to the competing S_N2 reaction.

A crystal of **9-Bu(c)** suitable for X-ray analysis was grown from chloroform (Figure 3.3). The crystal structure showed the expected P-N *cis* geometry, and the methyl and iodide groups coordinated *cis* across the metal.

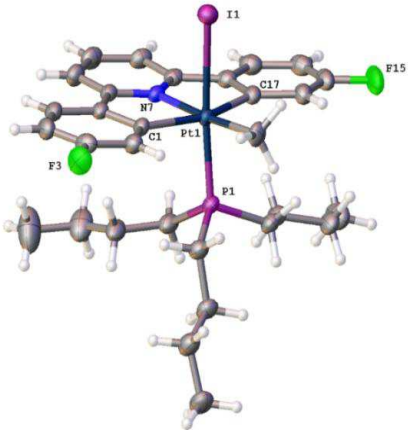

*Figure 3.3 Crystal structure of **9-Bu(c)**, thermal ellipsoids drawn at 50% probability level. Selected bond lengths (Å) and angles (°): Pt1-I1, 2.7124(2); Pt1-C100, 2.083(6); Pt1-I2, 2.6699(19); Pt1-C1, 2.094(3); Pt1-N7, 2.038(2); Pt1-C17, 2.079(3); Pt1-P1, 2.2836(8); C100-Pt1-I1, 87.30(15); C100-Pt1-C1, 100.91(16); C100-Pt1-P1, 87.12(15); C1-Pt1-I1, 87.48(8); C1-Pt1-P1, 94.35(8); N7-Pt1-I1, 88.55(7); N7-Pt1-C100, 175.77(16); N7-Pt1-C1, 79.75(11); N7-Pt1-C17, 80.28(11); N7-Pt1-P1, 97.01(7); C17-Pt1-I1, 89.30(8); C17-Pt1-C100, 98.82(16); C17-Pt1-C1, 159.84(12); C17-Pt1-P1, 90.77(8); P1-Pt1-I1, 174.36(2).*

The reaction of **1-Pr** with BnBr was not as clean as with MeI. After an hour of heating **1-Pr** in neat BnBr at 40 °C the dicyclometallated C^N^C Pt^{IV} dibromo- complex **15** was the only product observed, instead of the expected Pt^{IV} BnBr added complex **14** (Scheme 3.7).

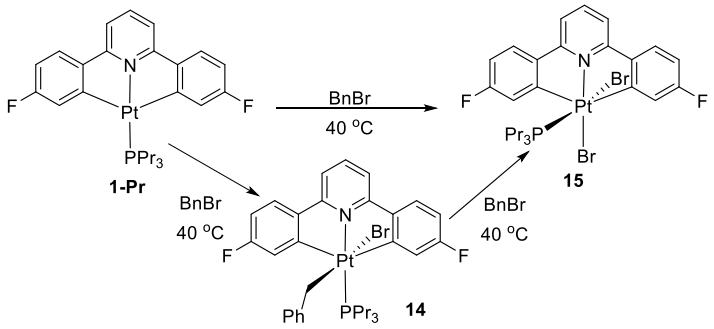

Scheme 3.7

In the ^{1}H NMR spectrum of the reaction mixture after an hour of heating (and not present in the starting materials) was a singlet peak at 2.91 ppm, and a broad multiplet peak at around 7.50 ppm, which suggested the presence of 1,2-diphenylethane.

Shorter reaction times did reveal the presence of **14** (discussed later), which suggests that **14** is used to form **15**. Therefore, a possible mechanism for the formation of **15** involves the S_N2 attack on another equivalent of BnBr (similar to the reaction of a organolithium reagent with an alkyl halide),[170] followed by coordination of the bromide (Scheme 3.8). This mechanism does not change the oxidation state of the platinum.

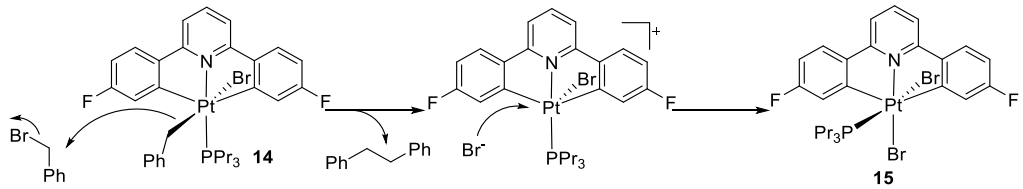

Scheme 3.8

The spectra of **15** showed a single peak in the ^{19}F{^{1}H} NMR spectrum at -106.40 ppm ($^{4}J_{F\text{-}Pt}$ = 16 Hz) and a pattern of peaks present by ^{1}H NMR spectrum which indicated that the C^N^C ligand remained dicyclometallated. In the ^{1}H NMR spectrum there were no peaks to suggest a coordinated benzyl group. Irradiation of the proton *ortho* to Pt and F showed little enhancement of any other peaks (such as the protons on the propyl chains), suggesting a P-N *cis* geometry. A peak in the ^{31}P{^{1}H} NMR spectrum at -6.66 ppm ($^{1}J_{P\text{-}Pt}$ = 2241 Hz) indicated a Pt^{IV} species. The chemical shift is more similar to that of the analogous dichloro- complex **Pr-3(c)** (-1.42 ppm) than to the analogous MeI added complex **Pr-9(c)** (-18.35). A crystal of **15** suitable for X-ray analysis was grown from chloroform (Figure 3.4). The crystal structure showed the expected P-N *cis* geometry, and two bromide ligands attached to the metal.

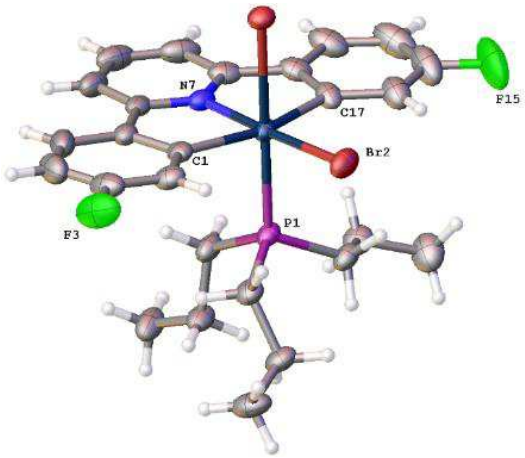

*Figure 3.4 Crystal structure of **15**, thermal ellipsoids drawn at 50% probability level. Selected bond lengths (Å) and angles (°): Br1-Pt1, 2.5407(4); C1-Pt1, 2.083(4); P1-Pt1, 2.2982(10); Pt1-Br2, 2.4520(5); Pt1-N7, 1.993(3); Pt1-C17, 2.075(4); C1-Pt1-Br1, 88.69(11); C1-Pt1-P1, 89.41(11); C1-Pt1-Br2, 99.79(12); P1-Pt1-Br1, 176.13(3); P1-Pt1-Br2, 87.13(3); Br2Pt1-Br1, 89.866(15); N7-Pt1-Br1, 88.20(9); N7-Pt1-C1, 81.05(16); N7-Pt1-P1, 94.84(10); N7-Pt1-Br2, 177.87(10); N7-Pt1-C17, 80.71(17); C17-Pt1-Br1, 88.71(11); C17-Pt1-C1, 161.65(18); C17-Pt1-P1, 94.14(12); C17-Pt1-Br2, 98.36(13).*

We have been able to isolate high yields of a Pt^{IV} di-bromo complex **15**, yet the presence of an iodo- analogue (which would have been synthesized via **9-Pr(t)**) has only been inferred from crystal structures. The crystal structure of **9-Bu(c)** shows some incorporation of a di-iodo impurity that we could not detect in solution. We believe this is partly because of the difference in solubility, as all analogues of **9-L** precipitate in the reaction mixture, whereas **14** does not. This means that **14** can more easily react further, giving the observed dibromo- species **15**.

Although small amounts of the expected BnBr adduct **14** were observed in solution with shorter reaction times, the yield of **14** was more easily maximized by reacting **1-Pr** with only a stoichiometric amount of BnBr. The spectra of **14** showed a single peak in the $^{19}F\{^{1}H\}$ NMR spectrum at -109.92 ppm ($^{4}J_{F\text{-}Pt}$ = 24 Hz) and a pattern of peaks present by ^{1}H NMR spectroscopy which indicates that the C^N^C ligand remains dicyclometallated. A peak in the ^{1}H spectrum at 3.36 ppm ($^{2}J_{H\text{-}Pt}$ = 88 Hz) showed that a benzyl group was coordinated to platinum. A peak in the $^{31}P\{^{1}H\}$ NMR spectrum at -20.50 ppm ($^{1}J_{P\text{-}Pt}$ = 2683 Hz), and a doublet in the ^{195}Pt NMR spectrum at -3056 ppm ($^{1}J_{Pt\text{-}P}$ = ~2800 Hz), are similar to the analogous **9-Pr(t)**. Irradiation of the proton *ortho* to Pt and F showed enhancement of the propyl chains, suggesting a P-N *trans* geometry. No attempt was made to isomerise **14** as even after purification small amounts of BnBr would remain.

3.2.2. Reaction of $Pt^{IV}RX$ Complex with $AgBF_4$

$AgBF_4$ was used to remove the halide from the complexes **9-L** and **14**, which revealed that five-coordinate species had been formed. This section looks at the structure and reactivity of these intermediates. The low solubility of $AgBF_4$ meant that reactions had to be carried out above 0 °C for a reaction to occur. For ease of reaction, the addition of $AgBF_4$ was carried out at room temperature, unless stated otherwise. Acetone solvent was used throughout the following experiments.

Addition of $AgBF_4$ to either **9-Pr(t)** or **9-Pr(c)** (or mixtures of the two isomers) gave full conversion to a single product **10-Pr** (Scheme 3.9). The spectra showed a single peak in the $^{19}F\{^1H\}$ NMR spectrum at -110.00 ppm ($^4J_{F\text{-}Pt}$ = 19 Hz) and a pattern of peaks present by ^1H NMR spectroscopy which indicated that the C^N^C ligand remained dicyclometallated. As the Pt-Me bond was still intact, as shown by a peak the ^1H NMR at 1.60 ppm ($^2J_{H\text{-}Pt}$ = 55 Hz), **10-Pr** is a five-coordinate species.

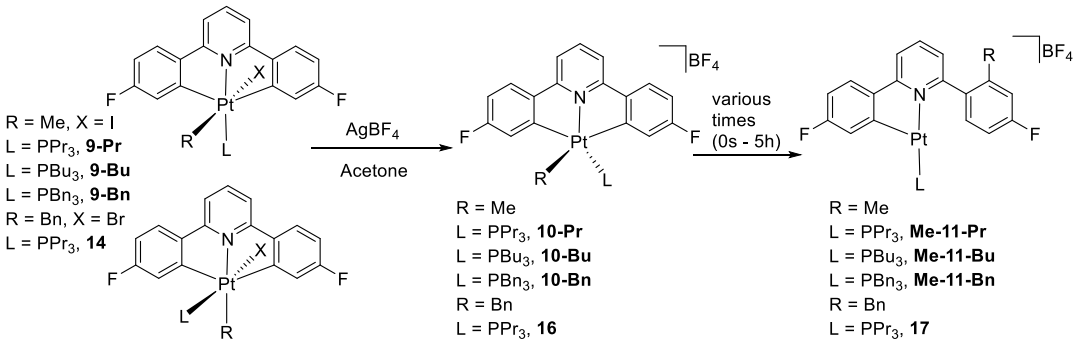

Scheme 3.9

Because **10-Pr** likely differs from **9-Pr** only by the lack of an iodide ligand, it was unsurprising that a peak of high intensity in the HR-MS (ESI) spectrum of **10-Pr** (when compared to **9-Pr**) at 634.1938 m/z (corresponding to $[M]^+$) was seen, suggesting a cationic species. Without the iodide ligand, the peak in the $^{31}P\{^1H\}$ NMR spectrum had shifted downfield to 1.89 ppm ($^1J_{P\text{-}Pt}$ = 3076 Hz). The doublet in the ^{195}Pt NMR spectrum at -2930 ppm ($^1J_{Pt\text{-}P}$ = ~3300 Hz) shows that the iodide has a larger effect on the ^{195}Pt chemical shift than the methyl group, as the peak is nearly 1000 ppm further downfield than that of **9-Pr(c)**.

Removing the iodide from the octahedral Pt^{IV} complex would initially give a structure with a square-based pyramidal geometry. However, in the nOe spectrum, irradiation of the proton ortho to Pt and F enhanced both the methyl and the phosphine protons. The

intensity of the enhancement in the nOe spectrum was less than that seen for when either group is *trans* to the nitrogen (**9-Pt(t)**: PPr_3, **9-Pr(c)**: Me) which suggests that neither group is *trans* to the nitrogen. The position of the peak corresponding to the Me-Pt in the $^{13}C\{H\}$ NMR spectrum at -4.37 ppm ($^1J_{C\text{-}Pt}$ = 508 Hz) lies between that of **9-Pr(t)** (3.55 ppm) and **9-Pr(c)** (-18.35 ppm) suggesting the geometry of the methyl group is between that of the two complexes. We therefore believe that the **10-Pr** has a trigonal bipyramidal geometry.

Within six hours at room temperature, the resonances for **10-Pr** disappear with the appearance of a new complex **Me-11-Pr** (Scheme 3.9). In the $^{31}P\{^1H\}$ NMR spectrum, a peak at 4.43 ppm ($^1J_{P\text{-}Pt}$ = 4018 Hz) and a doublet in the ^{195}Pt NMR spectrum at −3829 ppm ($^1J_{Pt\text{-}P}$ = ~4100 Hz) indicated a Pt^{II} species had formed. One of the fluoro-phenyl rings has also decyclometallated, shown by a lack of platinum coupling on one of the peaks in the $^{19}F\{^1H\}$ NMR spectrum (-110.54 ppm, $^4J_{F\text{-}Pt}$ = 61 Hz and -113.18 ppm). A singlet with relative intensity of three in the ^1H NMR spectrum at 2.64 ppm lacked platinum satellites, showing that the Pt-Me bond had been broken.

The methyl group is connected to the decyclometallated ring, shown by two the different fluoro-phenyl systems having the same pattern of peaks in the ^1H NMR spectrum (‘dd’, ‘dt’ and ‘dd’). This was also backed up by a correlation of the methyl protons to carbons on the decyclometallated ring in the $^1H/^{13}C$ HMBC spectrum. In the HR-MS (ESI) spectrum, a peak of high intensity (relative to **9-Pr**) at 634.1940 m/z (corresponding to $[M]^+$) suggested a cationic species.

Me-11-Pr was formed from the reductive elimination of aryl-Me, forming a $C(sp^2)$-$C(sp^3)$ bond, and reducing the platinum from Pt^{IV} to Pt^{II}, giving a three-coordinate species. Neither the proton *meta* to the fluorine, the Ph-Me or the phosphine alkyl chains showed any interaction with the platinum in the ^{195}Pt - ^1H correlation spectrum, allowing us to rule out a possible agostic complex. The magnitude of the platinum satellites on the peak in the $^{31}P\{^1H\}$ NMR spectrum ($^1J_{P\text{-}Pt}$ = 4018 Hz) showed that the phosphorus is *trans* to the nitrogen, which would also be expected on the grounds of reducing steric clash.

No evidence of coordinated water could be observed, leading us to believe that the fourth coordination site is likely filled by acetone (which quickly exchanges in solution).

As discussed in the introduction to this chapter, the geometry of the coordinatively unsaturated complex is important when considering the products of a concerted reductive elimination reaction. For five-coordinate intermediates, the coupling from two equatorial

positions is favoured in a trigonal bipyramidal complex, as is one axial and one basal position for square-based pyramidal complexes (Figure 3.5).

Complex **10-Pr** has been proposed to have a trigonal bipyramidal geometry. The rigidity of the C^N^C ligand ensures the aryl rings remain *trans* to one another and are, therefore, forced to take the axial positions of the trigonal bipyramid. The trigonal plane is occupied by a methyl, a phosphine, and pyridine ligands. The five-coordinate intermediate should therefore be indefinitely stable, as there are no viable reductive elimination products. However, within six hours, all **10-Pr** has converted into the reductive elimination product **Me-11-Pr**.

As described earlier, five-coordinate intermediate complexes can also adopt a square-based pyramidal geometry. When the phosphine is *trans* to the pyridine, the square base is complete (Figure 3.5). The basal positions are again taken by the phosphine and the nitrogen, but also by the two fluoro-phenyl groups. The axial position is taken by the methyl. Now there are viable reductive elimination products, where the methyl group can couple with either fluoro-phenyl group to give **Me-11-Pr**.

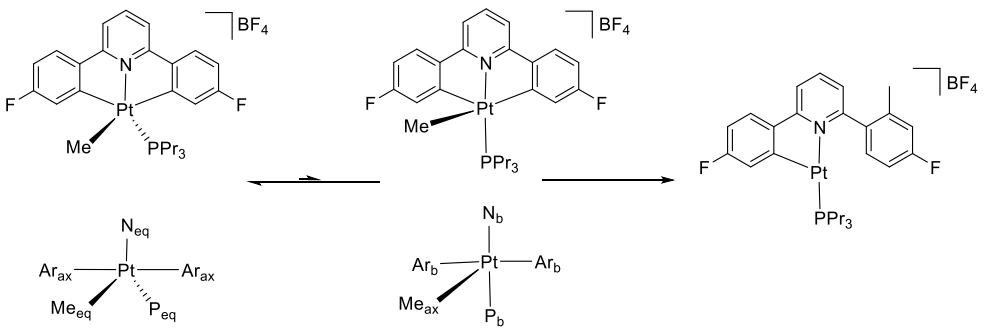

Figure 3.5 Illustration of geometry requirements for reductive elimination.

The trigonal bipyramidal geometry of **10-Pr** is likely to be lower in energy than the square-based pyramid (for the same reasons as discussed for the isomerisation of **3-Ph(t)** to **3-Ph(c)**) and so **10-Pr** is likely to have the trigonal bipyramidal geometry, slowing the rate of reaction. Because the reverse reaction is unlikely (under the conditions of this reaction) **10-Pr** is eventually progressed to **Me-11-Pr**.

Congested metal centres are known to have increased rates of reductive elimination.[13] The implication is that larger phosphines should increase the rate of reductive coupling, as the bulk of the phosphine will allow the methyl group less free space, making it more likely to be in a position to react. Even with a very small difference in phosphine size, the analogous

10-Bu is fully consumed within four hours. It is therefore no surprise that the analogous **10-Bn** (with a much larger phosphine) is not seen in solution under the same conditions, only giving the expected reductive elimination complex **Me-11-Bn**. We have observed mixtures of **Me-11-Pr** and **1-Pr** if the acetone is especially damp (or if water is added intentionally). We believe that water can attack the methyl group of **10-Pr** to form **1-Pr** and MeOH.

The analogous **16** is also not seen in solution, with reactions of **14** giving only the reductive elimination product **17**. With the smaller PPr_3 phosphine, the analogous **9-Pr(t)** gives a long-lived five-coordinate intermediate upon the addition of $AgBF_4$. We can then deduce that the size of the R group also has an effect on the rate of reductive coupling, and that the rate of reductive elimination is dependent on the level of crowding at the metal centre – more crowded metal centres eliminate faster. The fast rate of reductive elimination for **16** is expected, considering that the reaction of **14** with BnBr (Scheme 3.7) was thought to be stimulated by crowding at the metal centre).

3.2.3. Trapping the Five-Coordinate Intermediate with Pyridine

The five-coordinate intermediate **10-Pr** reacts slowly to form **11-Pr**. Pyridine was added to **10-Pr** to see if it could coordinate, to trap the five-coordinate complex, before attempting to trap the five-coordinate intermediates that were not seen in the previous experiments (such as **10-Bn**).

An excess of pyridine (~20 eq) was added to an acetone suspension of **9-Pr(t)** or **9-Pr(c)** (or, again a mixture). After adding $AgBF_4$, two highly soluble products **12-Pr(t)** and **12-Pr(c)** were seen (Scheme 3.10). The spectra of the major product **12-Pr(t)** (making up >90 % of the product mass) indicated full replacement of the iodide for a pyridine.

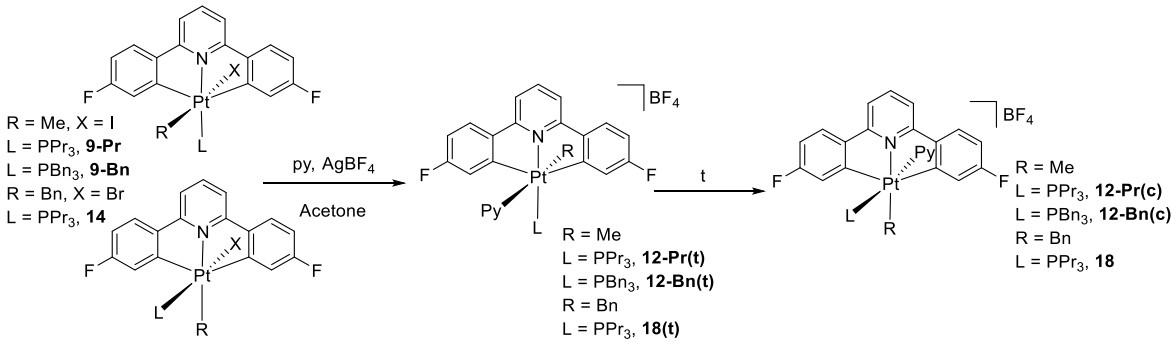

Scheme 3.10

The HR-MS (ESI) spectrum of the mixture showed a peak at 713.2371 m/z (corresponding to $[M]^+$) with high peak intensity. The patterns of peaks are identical to the starting material **9-Pr**, including a single peak in the $^{19}F\{^1H\}$ NMR spectrum at -107.87 ppm ($^4J_{F\text{-}Pt}$ = 20.5 Hz), a peak in the $^{31}P\{^1H\}$ NMR spectrum at -16.5 ppm ($^1J_{P\text{-}Pt}$ = 2600 Hz) and a methyl group coordinated to platinum (seen in the ^1H NMR spectrum at 1.06 ppm, $^2J_{H\text{-}Pt}$ = 66 Hz). Additionally, there are peaks in the ^1H NMR spectrum corresponding to the coordinated pyridine, including a peak with platinum satellites at 8.68 ppm ($^3J_{H\text{-}Pt}$ = 40 Hz). Irradiating the proton *ortho* to Pt and F showed a clear enhancement of the phosphine alkyl protons, which suggests a P-N geometry.

Within 30 minutes, full conversion of **12-Pr(t)** to **12-Pr(c)** was seen (Scheme 3.10). **12-Pr(c)** proved to be indefinitely air and moisture stable, and is expected to be the geometric isomer of **12-Pr(t)** as the NMR spectra are very similar. The peak in the $^{31}P\{^1H\}$ NMR spectrum at -9.05 ppm ($^1J_{P\text{-}Pt}$ = 2645 Hz) is a shift of >7 ppm downfield, which is expected for a change in geometry. The assignment of the geometry was backed up by nOe data, where irradiation of the proton *ortho* to Pt and F only affected the Pt-Me. This suggested that the phosphorus is *cis* to the to the methyl group. Again, the isomerisation can be rationalised by placing the larger groups perpendicular to the plane of the C^N^C ligand.

Pyridine was then added to separate acetone suspensions of **9-Bn(t)** and **14**. Addition of $AgBF_4$ gave full conversion to the analogous pyridine-coordinated P-N *cis* complexes **9-Bn(c)** and **18(c)**, and none of the reductive coupled complexes **11-Bn** or **17**. The rate of Me-aryl reductive elimination is therefore still slow enough to allow pyridine to coordinate.

3.2.4. Reaction with KX Salts

KX salts (KI, KBr and KCl) were added to separate acetone solutions of **11-Pr** to form four-coordinate Pt^{II} square-planar complexes. The halides slowly coordinated to the platinum forming **13-Pr**, with the reaction complete within 2 days at room temperature (Scheme 3.11). It was unsurprising that the peak intensity of the peak at 634.1928 m/z (corresponding to $[M\text{-}I]^+$ for **Me-13-Pr-I**) in the HR-MS (ESI) was comparable to other neutral species studied during the course of this body of work.

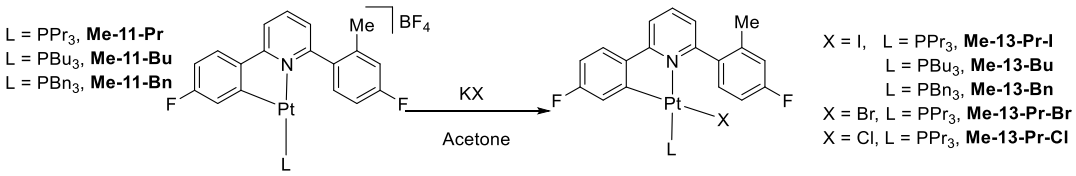

Scheme 3.11

A crystal suitable for X-ray analysis was grown from chloroform (Figure 3.6). The crystal structure showed the expected P-N *trans* geometry, and an iodide coordinated to the metal. The presence of the iodide has caused the decyclometallated fluoro-phenyl ring to be pushed back. The C-Pt-I bond angle of 151.59(13)° shows that there is steric clash between the iodide and fluoro-phenyl ring.

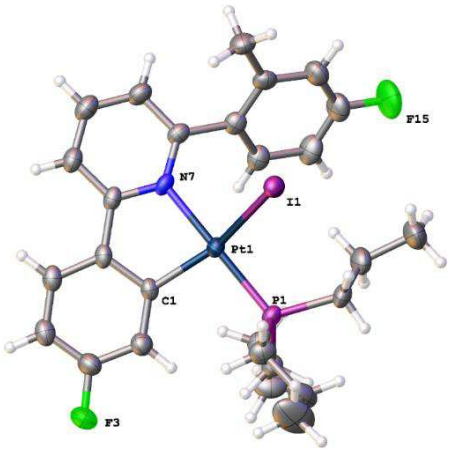

*Figure 3.6 Crystal structure of **Me-13-Pr-I**, thermal ellipsoids drawn at 50% probability level. Selected bond lengths (Å) and angles (°): Pt1-I1, 2.7083(3); Pt1-P1, 2.2347(11); Pt1-C1, 2.015(5); Pt1-N7, 2.112(4); P1-Pt1-I1, 91.01(3); C1Pt1-I1, 151.59(13); C1-Pt1-P1, 98.11(14); C1-Pt1-N7, 80.32(17); N7-Pt1-I1, 94.41(11); N7-Pt1-P1, 171.18(10).*

The addition of the halide to the metal has very little difference on the position of peaks in most of the NMR spectra (including ^{1}H and $^{19}F\{^{1}H\}$). The largest difference can be seen in the ^{195}Pt NMR spectrum. A pattern emerges that shows a correlation of the increasing size of the coordinated halide group with a more negative chemical shift (Table 3.1).

Table 3.1 Effect of substituent on chemical shift (ppm).

	halide	^{195}Pt (ppm)
Me-11-Pr (w/o halide)	N/A	-3829
Me-13-Pr-Cl	Cl	-3847
Me-13-Pr-Br	Br	-3879
Me-13-Pr-I	I	-3946

KI was also added to **Me-11-Bu** and **Me-11-Bn**, giving the analogous **Me-13-Bu** and **Me-13-Bn** (Scheme 3.11). For **Me-13-Bn**, coordination of the iodide led to restricted rotation about the P-Pt bond, which can be seen by the splitting of the benzyl CH_2 protons into two separate resonances. At 278 K the peaks resemble broad triplets (separated by about 423 Hz). At room temperature, the two peaks (FWHH of both peaks was about 55 Hz) were separated by about 320 Hz. By 333 K the peaks had coalesced, shown by the presence of only one broad peak at 3.60 ppm (FWHH around 100 Hz). This gives an approximate barrier to rotation of 70±5 $kJmol^{-1}$

A crystal of **Me-13-Bu** suitable for X-ray analysis was grown from chloroform (Figure 3.7). The crystal structure showed the expected P-N *trans* geometry, and an iodide coordinated to the metal. Because of the space requirements of the iodide, the decyclometallated ring is bent out of the way. A C-Pt-I bond angle of 153.15(8)° is slightly larger the analogous **Me-13-Pr-I**, suggesting that the size of the phosphine has some effect on this angle.

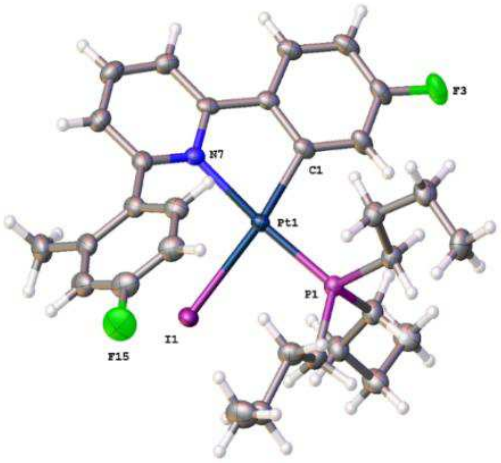

*Figure 3.7 Crystal structure of **Me-13-Bu**, thermal ellipsoids drawn at 50% probability level. Selected bond lengths (Å) and angles (°): C1-Pt1, 2.007(3); I1-Pt1, 2.7024(2); P1-Pt1, 2.2374(8); Pt1-N7, 2.122(2); C1-Pt1-I1, 153.15(8); C1-Pt1-P1, 97.38(9); C1-Pt1-N7, 80.52(11); P1-Pt1-I1, 92.48(2); N7-Pt1-I1, 93.17(6); N7-Pt1-P1, 171.06(6).*

3.2.5. Recyclometallation

Addition of K_2CO_3 to a $CHCl_3$ solution of **Me-11-Pr** gave full conversion to **Me-1-Pr** (Scheme 3.12). The spectra suggested a dicyclometallated complex, shown by the presence of two peaks with satellites of equal intensity in the $^{19}F\{^1H\}$ NMR spectrum at -111.01 ppm ($^4J_{F\text{-}Pt}$ = 24 Hz) and -113.45 ppm ($^4J_{F\text{-}Pt}$ = 27.5 Hz). In the $^{31}P\{^1H\}$ NMR spectrum, a peak at 2.70 ppm ($^1J_{P\text{-}Pt}$ = 3733 Hz) and a doublet in the ^{195}Pt NMR spectrum −4200 ppm ($^1J_{Pt\text{-}P}$ = ~3800 Hz) indicated a Pt^{II} species. A peak of intensity similar to other neutral complexes was seen in the HR-MS (ESI) spectrum at 634.1940 m/z (corresponding to $[M]^+$).

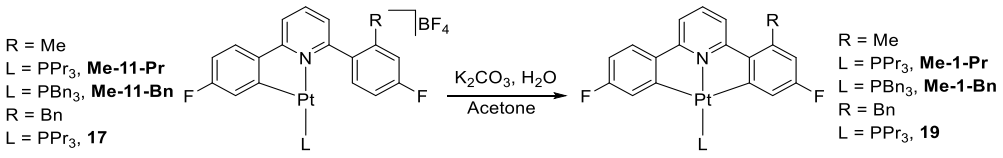

Scheme 3.12

A five- or six-membered ring can be expected through cyclometallation of the aryl or alkyl C-H bond, respectively.[171] Cyclometallation at the aryl ring (rather than the methyl group) was shown by the presence of two cyclometallated aryl C-H (protons *ortho* to Pt and F) peaks in the ^1H NMR spectrum (7.14 ppm, $^3J_{H\text{-}Pt}$ = 32 Hz and 7.07 ppm, $^3J_{H\text{-}Pt}$ = 36 Hz), and a singlet without satellites at 2.51 ppm corresponding to the aryl-Me.

Crystals of **Me-1-Pr** and **Me-1-Bn** suitable for X-ray analysis were grown from chloroform (Figure 3.8 and Figure 3.9). The crystal structures showed the expected dicyclometallated complex. The plane of the dicyclometallated ligand is unaffected by the inclusion of the methyl group. Shown in Figure 3.8, the proximity of the methyl group to one of the protons on 3- position of the pyridine ring, the methyl group has been pushed away, shown by a C-C-Me bond angle of about 124.6(7)° (normal bond angle at a C(sp^2) is 120°). The effect is expected to be the same for **Me-1-Bn**, however the crystal was more disordered, where no preference was seen for the position of the methyl group in the repeating unit.

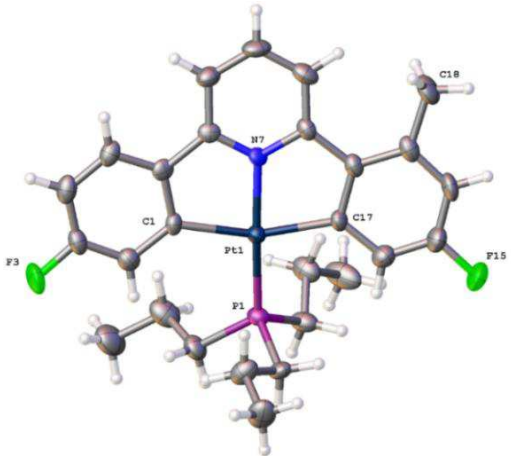

*Figure 3.8 Crystal structure of **Me-1-Pr**, thermal ellipsoids drawn at 50% probability level.*
***Me-1-Pr** selected bond lengths (Å) and angles (°): Pt1-C1, 2.074(6); Pt1-P1, 2.2298(16); Pt1-N7, 2.027(5); Pt1-C17, 2.050(6); C13-C18, 1.553(11); C6-C7, 1.457(9); C11-C12, 1.488(9); C1-Pt1-P1, 102.18(18); N7-Pt1-C1, 80.5(2); N7-Pt1-P1, 174.21(15); N7-Pt1-C17, 79.9(2); C17-Pt1-C1, 159.8(3); C17-Pt1-P1, 97.78(18); C8-C7-C6, 127.6(6); C10-C11-C12, 130.0(6); C13-C12-C11, 123.6(6); C12-C13-C18, 124.6(7).*

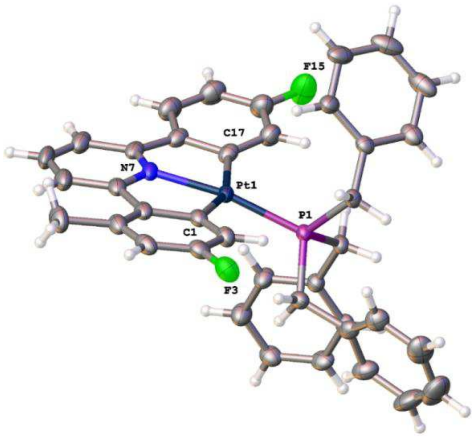

*Figure 3.9 Crystal structure of **Me-1-Bn**, thermal ellipsoids drawn at 50% probability level.*
***Me-1-Bn** selected bond lengths (Å) and angles (°): Pt1-P1, 2.2409(9); Pt1-C1, 2.062(4); Pt1-N7, 2.029(3); Pt1-C17, 2.071(4); C5-C5A, 1.529(6); C6-C7, 1.472(6); C11-C12, 1.466(6); C1-Pt1-P1, 98.67(11); C1-Pt1-*

C17, 158.79(15); N7-Pt1-P1, 169.79(8); N7-Pt1-C1, 79.69(14); N7-Pt1-C17, 80.22(14); C17-Pt1-P1, 102.30(10); C8-C7-C6, 128.7(4); C10-C11-C12, 127.4(4); C5-C6-C7, 124.1(3); C6-C5-C5A, 124.5(4).

3.2.6. Asymmetric Aryl-Aryl: Reaction of **Me-1-Pr** with a second equivalent of MeI

Through the reactions outlined in this chapter up to this point, it has shown that it is possible to modify **1-Pr** through the incorporation of an R group (Me or Bn) to a position *meta* to the fluorine (summarized in Scheme 3.13). Oxidative addition of an RX compound gives an octahedral Pt^{IV} complex (**9-Pr** or **14**). Removal of a halide using $AgBF_4$ then reveals a five-coordinate species, which eliminates aryl-Me. Recyclometallation is done using a weak base to activate the aryl C-H, giving **Me-1-Pr** and **19** respectively. This section looks at the reaction of **Me-1-Pr** with another equivalent of MeI to probe for any possible effect (if any) the incorporated methyl group has on the selectivity of the reductive elimination reaction.

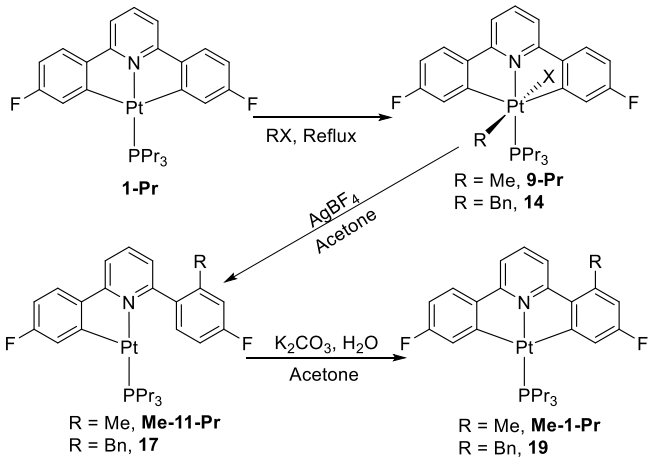

Scheme 3.13

As the methyl group is quite remote from the platinum, it is unsurprising that the reactivity of **Me-1-Pr** with MeI is almost identical to that of **1-Pr**. Oxidative addition of MeI to **Me-1-Pr** gave clean conversion to **Me-9-Pr(t)**, with conversion to **Me-9-Pr(c)** with further heating (Scheme 3.14). Addition of pyridine before the addition of $AgBF_4$ also gave the expected pyridine-trapped products **Me-12-Pr(t)** and **Me-12-Pr(c)**.

The effect of the methyl group only becomes apparent upon the addition of $AgBF_4$ without pyridine. NMR data recorded as soon as was possible after the addition of $AgBF_4$ showed only the reductive coupled product **Me$_2$-11-Pr**. To observe the five-coordinate intermediate **Me-10-Pr**, the reaction mixture was cooled to -50 °C after the addition of $AgBF_4$ (Scheme 3.14).

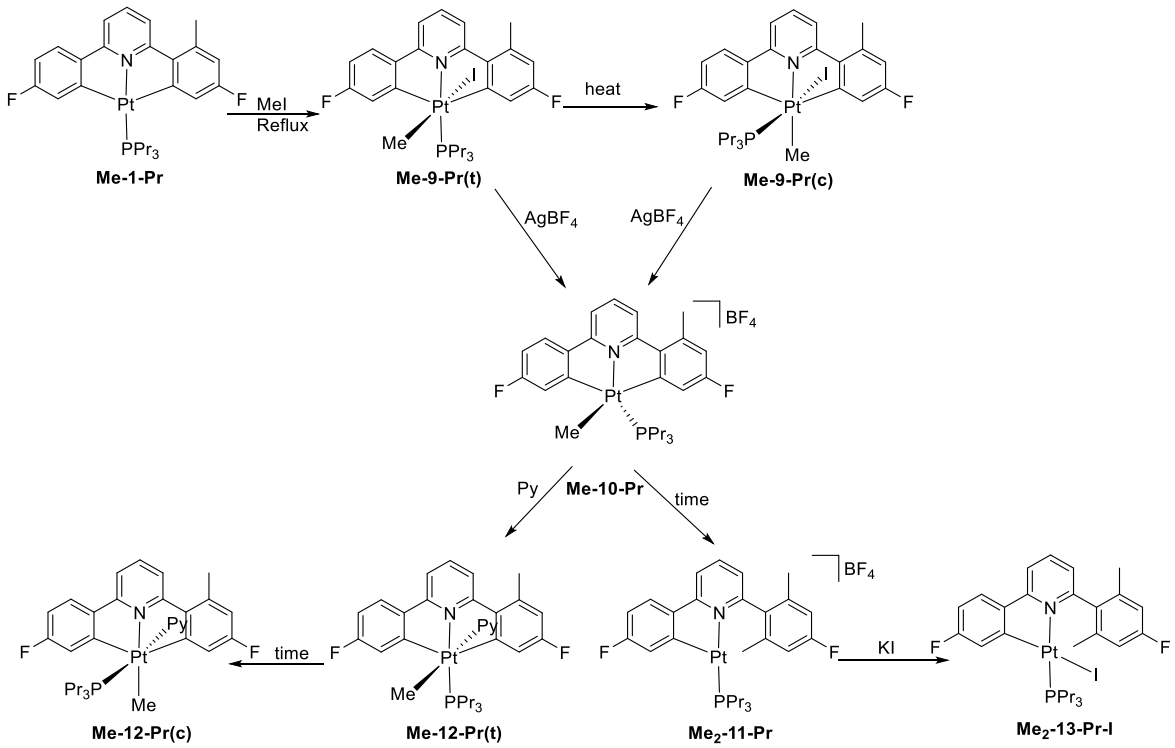

Scheme 3.14

The five-coordinate intermediate **Me-10-Pr** appeared to be stable at -50 °C, with no conversion to **Me$_2$-11-Pr** observed within two hours. The sample was allowed to warm to room temperature slowly in 15 °C increments. The reductive elimination reaction starts at around -20 °C. The spectra of **Me-10-Pr** were consistent with the analogous **10-Pr**. The spectra showed two peaks in the $^{19}F\{^1H\}$ NMR spectrum with satellites (-110.00 ppm, $^4J_{F\text{-}Pt}$ = 18 Hz and -112.33 ppm, $^4J_{F\text{-}Pt}$ = 21 Hz), a peak in the ^1H spectrum corresponding to the coordinated methyl (1.52 ppm, $^2J_{H\text{-}Pt}$ = 53 Hz), and a single peak in the $^{31}P\{^1H\}$ spectrum (1.36 ppm, $^1J_{P\text{-}Pt}$ = 3109 Hz). The structure of **Me$_2$-11-Pr** was made obvious by a doublet of relative height two in the ^1H NMR spectrum at 6.96 ppm, which would only be possible if both positions *meta* to a fluorine were substituted. This was confirmed by a singlet of relative height six at 2.54 ppm corresponding to the aryl-Me peaks. This shows that there is 100 % regioselectivity for the second methyl group to couple with the previously substituted ring.

The regioselectivity most likely caused by the release of steric strain (rather than any electronic effects caused by the donating nature methyl). As seen in the crystal structure of **Me-1-Pr** (Figure 3.8), the methyl group is bent away from the pyridine ring, due to a clash with a proton pointing directly towards it. Although crystals have not been grown for **Me-**

9-Pr(t) and **Me-9-Pr(c)**, the similar NMR data shows that the C^N^C ligand is not affected by the addition of MeI, and so the aryl-Me group is also expected to be bent back in these structures.

Removal of the halide allows the methyl-substituted aryl to react quickly with the methyl group, forming the dimethyl-substituted aryl ring and releasing the bond strain. Attempts to recyclometallate **Me$_2$-11-Pr** have failed, leading only to the degradation of the complex. In the recyclometallation of **Me-11-Pr** (Scheme 3.12), the complex has a C(sp^2)-H bond in a suitable position to form a five-membered ring. Activation of the weaker C(sp^3)-H of the methyl group, and possible formation of a six-membered ring is disfavoured on the basis of the reverse reaction (reforming the C-H bond) being more favourable. Conversely, in Section 1.5.2. the CAM mechanisms show facile C(sp^2)-H bond cleavage to form M-C(sp^2) bonds.

Addition of KI to **Me$_2$-11-Pr** gave the expected iodide adduct **Me$_2$-13-Pr-I**. A crystal suitable for X-ray analysis was grown from chloroform (Figure 3.10). The crystal structure showed the expected P-N *trans* geometry, two methyl groups on the same fluoro-phenyl ring, and an iodide coordinated to the metal. A close contact warning for the crystal structure between the iodide and a proton from the phosphine alkyl chains was seen in the crystal data suggesting that the additional methyl on the aryl ring has increased crowding at the metal centre. Although no indication of this can be seen in the ^{1}H NMR spectrum (possibly due to the plane of symmetry which runs through the plane of the C^N^C ligand), but it could explain the broadness of the peaks in the ^{19}F{^{1}H} NMR spectrum.

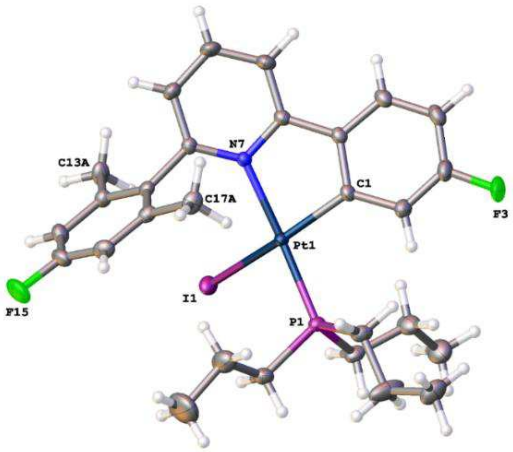

*Figure 3.10 Crystal structure of **Me$_2$-13-Pr-I**, thermal ellipsoids drawn at 50% probability level. Selected bond lengths (Å) and angles (°): Pt1-I1, 2.71245(16); Pt1-P1, 2.2454(6); Pt1-C1, 2.010(2); Pt1-N7, 2.1324(17); P1-Pt1-I1, 88.912(15); C1-Pt1-I1, 152.99(6); C1-Pt1-P1, 99.62(6); C1-Pt1-N7, 80.30(7); N7-Pt1-I1, 95.71(4); N7-Pt1-P1, 169.77(5).*

3.3. C^N^C = 2-(4-fluorophenyl)-6-*tert*butylpyridine

3.3.1. Introduction

(C^N) $Pt^{II}(Cl)PPh_3$ (where C^N is 2-(4-fluorophenyl)pyridine) was reported by the Rourke group which has a P-N *trans* geometry (Scheme 3.15).[158] Addition of $PhICl_2$ gave a Pt^{IV} complex, in which the new chloride ligands added *trans* across the metal. With time, isomerisation occurred, in which the PPh_3 moved to a position perpendicular to the plane of the molecule (fac-Cl_3).

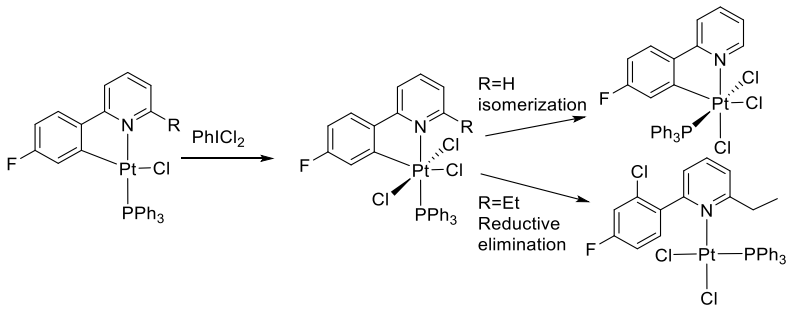

Scheme 3.15

If the hydrogen in the six-position of the pyridine was replaced by a larger group (e.g. ethyl), the isomerisation reaction did not occur. Instead, an aryl-Cl reductive elimination reaction took place, giving a Pt^{II} complex. The reaction shows that steric strain is a factor in the initiation of reductive coupling reactions.

Also synthesised was a similar (C^N^C) Pt^{II} dicyclometallated complex, where C^N^C is 2-(4-fluorophenyl)-6-*tert*butyl pyridine. They found that upon addition of $PhICl_2$ at -40 °C, the initial dichloro- product has a P-N *cis* geometry (i.e. the two new chlorides are *cis* to each other) (Scheme 3.16).[158] With time, the *cis* complex disappeared with the appearance on two new complexes, including a dichloro- complex with a P-N *trans* geometry.

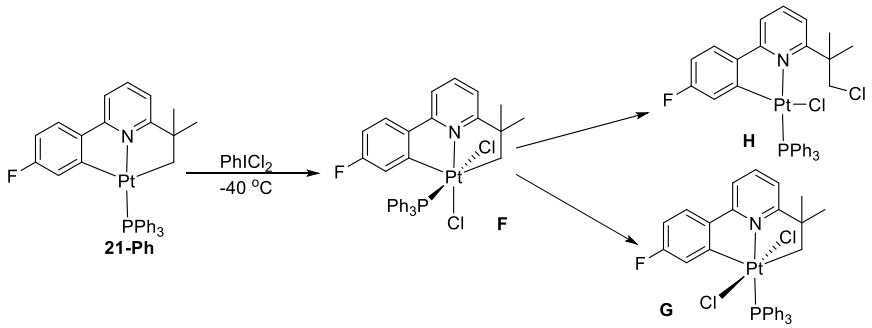

Scheme 3.16

As seen in Scheme 2.5, the oxidation of the analogous **1-Ph** (where the C^N^C ligand is 2,6-di(4-fluorophenyl)pyridine) with $PhICl_2$ initially gave a P-N *trans* **3-Ph(t)**, followed by isomerisation to P-N *cis* **3-Ph(c)**. The isomerisation is rationalized on the basis of putting the large phosphine out of the plane of the C^N^C ligand. However, when the C^N^C ligand is 2-(4-fluorophenyl)-6-*tert*butyl pyridine (such as **21-Ph**, seen in Scheme 3.16), the protons on the C(sp^3) coordinated to platinum point out of the plane of the C^N^C ligand. This not only makes the position *cis* to nitrogen more hindered, but also makes the position *trans* to nitrogen less hindered (as now only one aryl proton points towards this position).

The other product was shown to have resulted from reductive elimination where a chloride ligand had reductively coupled with the alkyl group **H**. It was shown that the mechanism of the reductive coupling was concerted, shown by a dependence on the geometry of the complex. Addition of Bu_4NCl made no difference to the rate of reductive elimination, meaning that the halide did not dissociate (Figure 3.11).

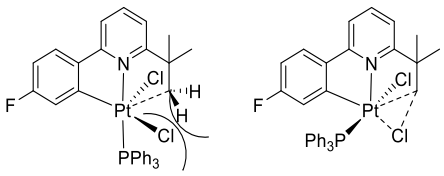

Figure 3.11 Illustration of the steric argument for Cl-N trans concerted coupling.

It was shown that only the P-N *cis* geometry (where there is a chloride *trans* to the pyridine) would reductively couple. This is because chlorides in positions *cis* to the pyridine would clash with the alkyl protons, whereas this is not the case for the N-Cl *trans* chloride. There was no evidence of an aryl-Cl coupled product.

This section first looks at the oxidative addition of RX compounds (namely MeI) with C^N^C dicyclometallated $Pt^{II}(PPr_3)$ complexes where C^N^C is 2-(4-fluorophenyl)-6-*tert*butyl pyridine. The C^N^C ligand has a C(sp^2) and a C(sp^3) coordinated to platinum,

and so this section also looks at the possible selectivity of reductive elimination reactions at C^N^C dicyclometallated Pt^{IV} complexes generally. It is already known that there is a preference for $C(sp^2)$-$C(sp^3)$ coupling over $C(sp^3)$-$C(sp^3)$ (usually explained by the directionality of the orbital lobes), however there have also been reports of exclusive $C(sp^3)$-$C(sp^3)$ coupling, with the main difference being the geometry of the ligand systems used.[169,172]

3.3.2. Addition of MeI

This section focuses on the addition of MeI to complex **21-Pr**, which can be synthsized from the known complex **21-DMSO**, or from **20-Pr** (Scheme 3.17).[173] The monocyclometallated PPr_3 derivative **20-Pr** was itself synthesized from the known DMSO complex **20-DMSO** via a simple ligand substitution reaction.[174] The synthesis of **20-DMSO** and **21-DMSO** was shown in Section 1.8. In order to avoid confusion, it should therefore be noted that both **20-Pr** and **21-Pr** (and all subsequent produts presented herin) were originally synthsised by the author of this thesis.

In the addition of PPr_3 to **20-DMSO** (or **21-DMSO**), the phosphine was diluted to ensure that the multiple addition did not occur (which has been seen in past work in the Rourke group). Heating **20-Pr** with K_2CO_3 gave the desired dicyclometallated complex **21-Pr**. Important data for **21-Pr** includes a single peak in the $^{19}F\{^1H\}$ NMR spectrum at -111.69 ppm ($^4J_{F\text{-}Pt}$ = 26.5 Hz), a peak the $^{31}P\{^1H\}$ NMR spectrum at 0.44 ppm ($^1J_{P\text{-}Pt}$ = 3813 Hz) and a doublet in the ^{195}Pt NMR spectrum −4026 ppm ($^1J_{Pt\text{-}P}$ = ~3800 Hz).

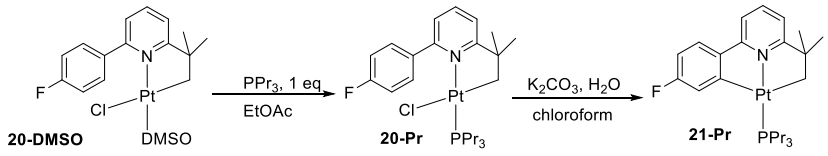

Scheme 3.17

The oxidative addition of MeI to **21** was carried out at 50 °C. A small excess of MeI was added to a chloroform solution of **21-Pr** and heated for an hour, after which time the solution had become much paler (starting out as a deep yellow). The NMR spectra showed full conversion of **21-Pr** to a single product **Me-23** (Scheme 3.18).

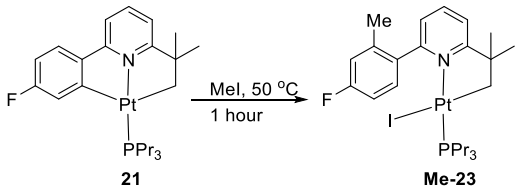

21 **Me-23**

Scheme 3.18

A peak in the $^{31}P\{^{1}H\}$ NMR spectrum at -2.05 ppm ($^{1}J_{P\text{-}Pt}$ = 4303 Hz), and a doublet in the ^{195}Pt NMR spectrum at -4339 ppm ($^{1}J_{Pt\text{-}P}$ = ~4300 Hz) indicated a Pt^{II} complex. A singlet without satellites in the $^{19}F\{^{1}H\}$ NMR spectrum at -113.28 ppm suggested that the fluoro-phenyl ring had become decyclometallated. A peak in the ^{1}H NMR spectrum at 2.45 ppm lacked platinum satellites also, and was shown to be connected to the aryl ring by $^{1}H/^{13}C$ HMBC.

The structure is therefore obvious, through comparison with **Me-11-Pr**. The fluoro-phenyl ring and the methyl have reductively coupled. Without the use of $AgBF_4$ to initiate the reaction, **Me-23** is likely to be a neutral species, where the iodide takes the fourth coordination site. This is backed up by the presense of a peak in the HR-MS (ESI) spectrum at 596.2353 m/z (corresponding to $[M\text{-}I]^{+}$) with intensity to other neutral complexes seen over the course of this body of work.

In the ^{1}H NMR spectrum at room temperature, the phosphine alkyl peaks are broad, and the ^{t}Bu methyl groups have separated into two broad resonances. In the $^{13}C\{H\}$ NMR spectrum, the resonanceces were not observed (probably too broad to be seen above the noise). The rotation of the fluoro-phenyl ring about its bond to pyridine is restricted because of steric clash with the iodide. By 55 °C the NMR spectra show coalescence of all the separated peaks, which allows us to calculate an estimated barrier to free rotation of 63 ± 5 kJ mol^{-1}.

The reductive elimination complex **Me-23** (by analogy to **Me-11-Pr**) is likely to have come from a Pt^{IV} complex, where the RX compound has added across the platinum, and the $C(sp^2)$-$C(sp^3)$ reductive elimination of reaction follows, and no sign of a $C(sp^3)$-$C(sp^3)$ reductive elimination product (Scheme 3.19). The reaction time was then shortened to 30 minutes, under the same conditions. This time, a mixture of complexes was seen, including **21-Pr** (25 %) and **Me-23** (10 %). The remainder was a new complex **22(Me)** (65 %). Complex **22(Me)** could not be separated from the other species. Shorter reaction times did lead to less of **Me-23**, but also less of **22(Me)**.

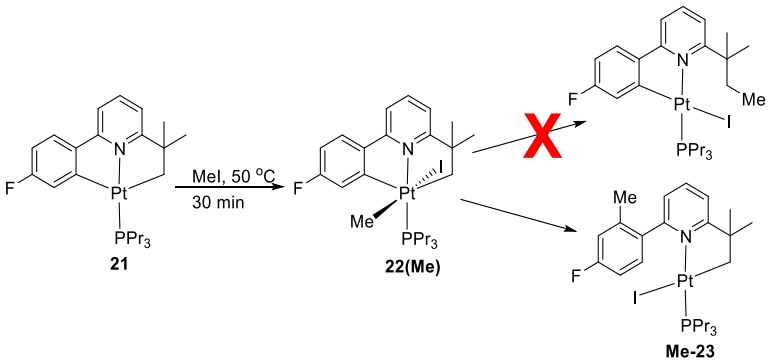

Scheme 3.19

The spectra of **22(Me)** shows a peak in the $^{19}F\{^{1}H\}$ NMR spectra at -110.33 ($^{4}J_{F\text{-}Pt}$ = 22 Hz), suggesting that the fluoro-phenyl ring is still cyclometallated. Two peaks with platinum satellites in the ^{1}H NMR spectrum (showing that the plane of symmetry through the plane of the C^N^C ligand has been broken) at 3.13 ppm ($^{2}J_{H\text{-}Pt}$ = 60 Hz) and 1.69 ppm ($^{2}J_{H\text{-}Pt}$ = 20 Hz) correspond to the protons attached to the C(sp^3) coordinated to platinum, which indicated that the C(sp^3) is also cyclometallated.

A peak of relative integral three at 1.08 ppm ($^{2}J_{H\text{-}Pt}$ = ~70 Hz) showed that there was a methyl group coordinated to platinum. A peak in the $^{31}P\{^{1}H\}$ NMR at -22.00 ppm ($^{1}J_{P\text{-}Pt}$ = 2704 Hz) and a doublet in the ^{195}Pt NMR spectrum at -3500 ppm ($^{1}J_{Pt\text{-}P}$ = ~2750 Hz) are consistent with similar complexes (cf. **9-Pr(t)**). A P-N *trans* geometry was assigned by nOe data, where irradiation of the phosphine alkyl protons enhanced both of the protons on the cyclometallated C(sp^3) equally.

Shown in Scheme 3.16, the reaction of **21-Ph** with $PhICl_2$ gives a P-N *cis* product **F**, which then disappears in solution to form a P-N *trans* complex **G**, and a reductive elimination complex **H**. Because neither a C(sp^3)-I or C(sp^3)-Me coupled product are seen in solution, it is possible to rule out a mechanism of oxidative addition of MeI which forms a *cis* isomer of **22(Me)**, which isomerises to form the observed *trans* isomer of **22(Me)**. Instead, it is more likely that the reaction of **21-Pr** with MeI is more similar to the analogous reaction of **1-Pr** with MeI, where MeI adds *trans* across the metal.

The reductive elimination reaction is 100 % selective, favouring C(sp^2)-C(sp^3) coupling over C(sp^3)-C(sp^3). The concerted mechanism for the formation of **Me-23** can be explained with similar arguments to that of the C(sp^3)-Cl coupling shown earlier (Figure 3.11). With a P-N *trans* geometry, and the methyl group is *cis* to the nitrogen. **22(Me)** therefore has a structure analogous to **G** (seen in Scheme 3.16), which was inert with respect to reductive elimination. Reductive elimination of C(sp^3)-I was only seen for **F**, as it required the

chloride to be in the position *trans* to the nitrogen (as the *cis* position leads only to clashing of the chloride with the protons). However, unlike **G**, **22(Me)** is not inert with respect to reductive elimination, with the geometry of the methyl group being favourable for the coupling of $C(sp^2)$-Me (Figure 3.12). Reductive elimination of $C(sp^2)$-Me over $C(sp^2)$-I can be explained by the difference in bond strengths (418 and 406 kJ/mol respectively), and the relative ease of oxidative addition of aryl-Cl to platinum.

We were able to rule out the dissociation of the iodide preceding the reductive elimination reaction. When Bu_4NI was added to solutions of **21-Pr**, the rate of formation of **Me-23** was unaffected. Excess iodide would have taken the place of any dissociated iodide, and would have therefore reduced the rate of reductive elimination.

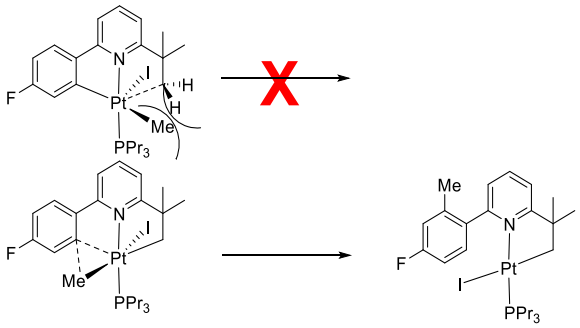

Figure 3.12 Illustration of the selectivity of $C(sp^3)$-$C(sp^2)$ over $C(sp^3)$-$C(sp^3)$ coupling.

When Bu_4NCl was added to solutions of **21-Pr**, only the expected iodo- product **Me-23** was observed. If the reductive elimination reaction was too fast to be trapped after the dissociation of the iodide, the chloride was present to compete with the iodide for the fourth coordination site. Although with enough time the iodide would eventually displace any chloride attached to the platinum, this replacement reaction is expected to be slow enough that a chloro- derivative of **Me-23** would have been observed.

There is also the possibility that a five-coordinate intermediate (by analogy with **12-Pr**) would have a trigonal bipyramidal structure, possibly allowing the methyl group to couple with either side of the C^N^C ligand. Yet, addition of $AgBF_4$ to a mixture of **22(Me)** and **Me-23** gave only a single product **24**. The structure of this complex is obvious, being the same as **Me-23**, but missing an iodide. In the HR-MS (ESI) spectrum, a relatively high intensity peak (relative to **21-Pr**) was seen at 596.2349 m/z (corresponding to $[M]^+$), suggesting that **24** is cationic. Without the iodide, there is no evidence of restricted rotation seen in the ^1H NMR spectrum. **Me-23** can also be made from **24** by the addition of KI (Scheme 3.20).

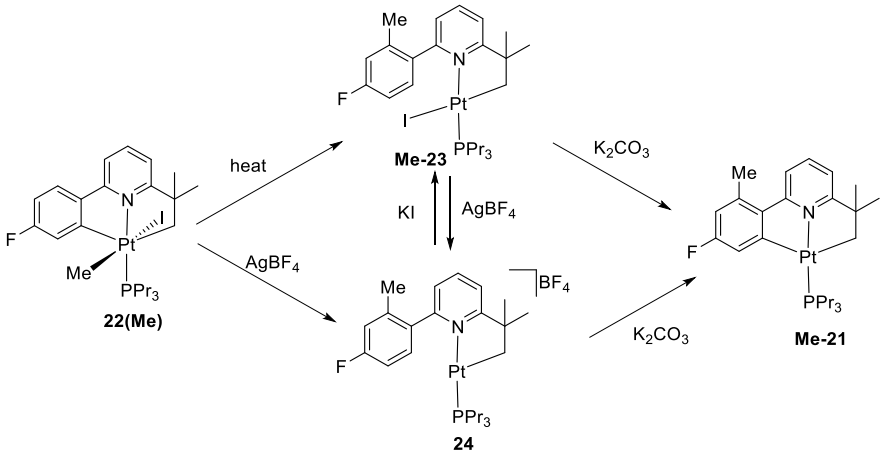

Scheme 3.20

Heating either **Me-23** or **24** in the presence of base gave the dicyclometallated complex **Me-21** (Scheme 3.20). The reaction time was much shorter for **24**, with the reaction complete within a day (cf. up to a week for **Me-23**). The spectra showed a single peak in the $^{19}F\{^{1}H\}$ NMR spectrum at -114.13 ppm ($^{4}J_{F\text{-}Pt}$ = 28 Hz), and a peak in the ^{1}H NMR spectrum with platinum satellites at 1.81 ppm ($^{2}J_{H\text{-}H}$ = 37 Hz) corresponding to the protons on the C(sp^3) attached to platinum, showed that the C^N^C ligand was dicyclometallated. A singlet at 2.63 ppm corresponded to the aryl-Me protons. In the $^{31}P\{^{1}H\}$ NMR spectrum, a peak at 0.96 ppm ($^{1}J_{P\text{-}Pt}$ = 3820 Hz) and a doublet in the ^{195}Pt NMR spectrum −3995 ppm ($^{1}J_{Pt\text{-}P}$ = ~3900 Hz) indicated a Pt^{II} species.

3.3.3. Addition of a second equivalant of MeI to **Me-21**, and One-Pot Synthesis

Now starting from **Me-21**, the same series of reactions could be repeated. After the same 30-minute reaction time, the reaction again showed two products: the analogous **Me-22(Me)**, and **Me$_2$-23** (Scheme 3.21). The rate of reaction with MeI is roughly the same as before (25 % of **Me-21** remained in the product mixture), which was expected on the basis of the remote location of the aryl-Me. However, now the relative amounts of each product was different. Instead of being the minor product, the reductive elimination complex **Me$_2$-23** is now the major product, making up 70 % of the product mixture.

We were unable to increase the relative amounts of **Me-22(Me)** in solution with different reaction times, and were only able to infer its existence from $^{19}F\{^{1}H\}$ and $^{31}P\{^{1}H\}$ NMR spectra by comparison with the analogous complex **22(Me)**. The increased rate of

reductive elimination was expected for the same reason as for the increased rate of formation of **Me_2-11-Pr**, where steric crowding of the methyl and pyridine protons were responsible. Although we were unable to grow crystals of **Me-21** or **Me-22(Me)**, it is believed that the same steric crowding is responsible here for the increased rate of reductive elimination.

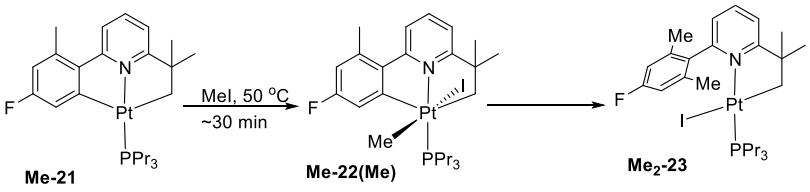

Scheme 3.21

The spectra of reductive elimination complex **Me_2-23** could be assigned, as a longer reaction time allowed for clean conversion to product. The spectra showed a peak in the $^{19}F\{^1H\}$ NMR spectrum without platinum satellites at -114.84 ppm, showing that the fluoro-phenyl ring had decyclometallated. In the ^1H NMR spectrum there was a peak of relative integral six at 2.35 ppm corresponding to the two methyl groups on the decyclometallated ring and a peak of integral two at 6.73 ppm corresponding to the two protons on the same ring (related by symmetry). A peak in the $^{31}P\{^1H\}$ NMR spectrum at -1.80 ppm ($^1J_{P\text{-}Pt}$ = 4292 Hz), and a doublet in the ^{195}Pt NMR spectrum at -4382 ppm ($^1J_{Pt\text{-}P}$ = ~4300 Hz) indicated a Pt^{II} complex. With the inclusion of another methyl group, rotation of the fluorophenyl ring is expected to be restricted further, but cannot be inferred by the ^1H NMR spectrum, due to symmetry.

As the reductive elimination reaction does not require the iodide to be removed (therefore requiring $AgBF_4$ to remove it), an effort was made to make **Me_2-23** from **Me-21** in a one-pot synthesis. MeI and K_2CO_3 were added to a chloroform solution of **Me-21**. After a week of heating to 50 °C, full clean conversion was seen to the expected product **Me_2-23** (Scheme 3.22). NMR spectra taken over the course of time showed differing amounts of the various intermediary complexes.

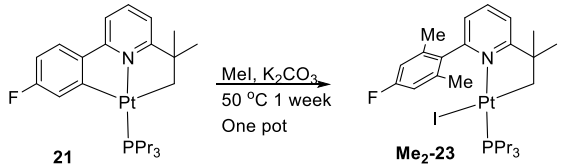

Scheme 3.22

3.3.4. Addition of BnBr and AllylBr, and One-Pot Synthesis

Different RX compounds (BnBr and allylBr) were reacted with **21-Pr** in order to compare the relative speed of oxidative addition and reductive elimination. Pseudo first order reactions were carried out by using a large excess of the chosen RX compound, while keeping the amount of **21-Pr** equal between experiments. The selected RX compound gave the expected analogous complexes upon heating with **21-Pr**, including the six-coordinate (**22(Bn)** and **22(allyl)**), and the reductive elimination complex (**Bn-23** and **allyl-23**) (Scheme 3.23).

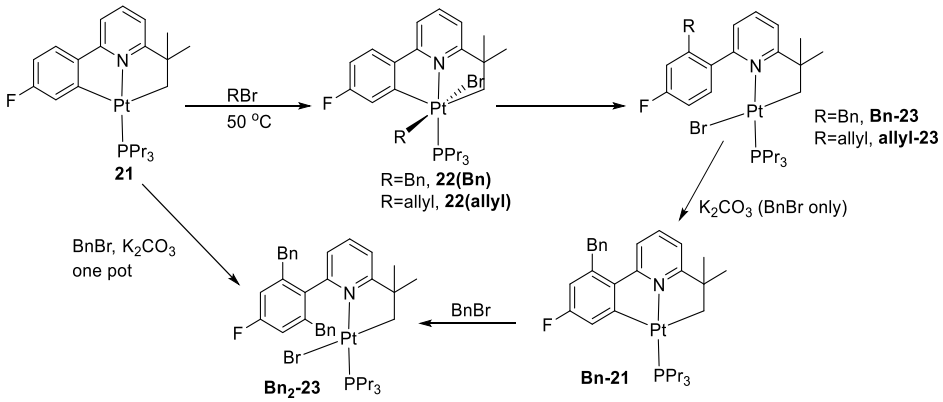

Scheme 3.23

After 30 minutes of heating at 50 °C, the proportions of each species was calculated from the integration of peaks in the $^{19}F\{^{1}H\}$ NMR spectra shown in Table 3.2.

Table 3.2 Relative amounts of the starting material, $Pt^{IV}RX$ complex, and the reductive complex after 30 minutes of heating.

		21	22	23	Ratio of 22:23
21-Pr	MeI	25	65	10	6.5 : 1
21-Pr	Allyl bromide	30	55	15	3.7 : 1
21-Pr	Benzyl bromide	75	19	6	3.2 : 1
Me-21	MeI	25	5	70	0.1 : 1

The rate of oxidative addition of the different RX compounds follows the expected trend where smaller RX compounds (i.e. MeI) add faster to the metal (the small MeI and AllylBr add to **21** at similar rates, showing a small dependence on the halide leaving group). The difference between the fastest and slowest is only a factor of three, suggesting that the platinum centre is relatively unhindered, allowing a variety of sizes of RX compounds to react, but the rate of reaction did increase with larger R groups.

Restricted rotation of the decyclometallated fluro-phenyl ring was seen for complexes **Bn-23** and **allyl-23** (like **Me-23**) In the case of **Bn-23** at room temperature, the two benzyl CH_2 protons, the two methyl groups and protons attached to the C(sp^3) coordinated to platinum are separated by 103, 60 and 102 Hz respectively (600 MHz spectrometer). We estimate a coalescence of about 338 K, and a barrier to rotation of about 68.0 ±5.0 kJ mol^{-1}. In the case of **allyl-23**, we did not calculate a coalescence temperature, but at room temperature we observed that the two methyl groups and protons attached to the carbon coordinated to platinum are separated by 75 Hz and 183 Hz respectively (600 MHz spectrometer).

As there was so little difference in rates (both oxidative addition and reductive elimination, shown by the ratio of complex **22** to the respective complex **23**) between compounds with different R groups, only **Bn-23** was taken further in which analogous products to the MeI reactions were seen (and could be assigned based on very similar NMR spectra). Again, by heating in the presence of base, the analogous **Bn-21** was made. Addition of another equivalent of BnBr to **Bn-21** gave full conversion to **Bn_2-23**. This meant that **Bn_2-23** could also be made with the one-pot method, with the reaction complete within a week (Scheme 3.23). Although BnBr adds slower to the metal, recyclometallation of **Bn-23** was marginally faster, meaning that the overall reaction time is comparable to that for **Me_2-23**.

3.4. Conclusion

Building on Chapter 2, this chapter focused on the addition of RX compounds to dicyclometallated Pt^{II} complexes; RX compounds are also expected to add via an S_N2-type mechanism. Complexes with the di-aryl C^N^C ligand, **1-L** and **Me-1-Pr**, reacted very differently when compared to complexes with the alkyl-aryl C^N^C ligand, **21-Pr** and **Me-21**, in the reductive elimination step.

Pt^{II} complexes of the form **1-L** (where L = PPr_3, PBu_3 or PBn_3) react with RX compounds (MeI and BnBr) forming six-coordinate Pt^{IV} complexes with the R and X groups taking the open coordination sites, analogous to the dichloro- complexes seen in Chapter 2. These were the only observed products, with no evidence of C-H activation products. The addition of $AgBF_4$ was required to initiate a reductive elimination reaction (coupling R and a fluoro-phenyl ring). This reaction proceeded via a long-lived five-coordinate intermediate (up to four hours), which could be trapped with pyridine. The reductive elimination product was then recyclometallated at the sp^2 C-H to give an asymmetric Pt^{II} complex, such as **Me-1-Pr**, which was reacted with further equivalents of MeI. Addition of $AgBF_4$ to these Pt^{IV} complexes led to the 100% regioselective reductive elimination with

the R group coupling with the methyl substituted fluoro-phenyl ring. The reductive elimination reaction was also much faster (requiring the reaction to be carried out at low temperatures to observe the intermediate) due to the steric clash of the methyl group and the hydrogen at the 3- position of the central pyridine.

The observation of long-lived five-coordinate intermediates can be explained by the geometric requirements for reductive eliminations. With the C^N^C ligand having a restricted geometry, both the R group and the phosphine to adopt a complementary geometry that is able eliminate R-aryl.

Complexes of the form **21-Pr** (having the alkyl-aryl C^N^C ligand) also react with RX complexes (MeI, BnBr and allylBr), initially forming the analogous six-coordinate complex. It has been shown that this complex will then selectively eliminate aryl-R without the requirement of a five-coordinate intermediate. Addition of $AgBF_4$ to the six-coordinate complex gave the same R-aryl substituted product. Recyclometallation was carried out and, like with **Me-1-Bn**, a further equivalent of RX was added. As predicted, the R group coupled with the aryl ring. The simplicity of this synthesis lent itself to a one-pot synthesis of the complexes with the di-substituted fluoro-phenyl rings.

Without a five-coordinate intermediate, the argument for the reductive coupling reaction is instead based on the steric bulk at the metal centre. With the alkyl side of the C^N^C ligand having protons which protrude out of the plane of the C^N^C ligand the platinum centre is more congested. This initiates the reductive elimination reaction (as the Pt^{II} is less congested). We believe that the selectivity of the reductive coupling is forced by the geometry of the six-coordinate complex. Future work should, therefore, look at ways to add an RX compound which would also have the R group *trans* to the nitrogen. Better still, to look at having two of the same R groups coordinated to the platinum, taking positions both *cis* and *trans* to the nitrogen, but could also result simply in the reductive elimination of R-R.

Future work could look at the reactivity of sterically demanding RX compounds, which could result in the reductive elimination of aryl-R before the coordination of X. Also, reactions should be carried out at low concentrations of RX to see if C-H activation products can be isolated. Another option is the addition of $PhICl_2$ to **Me-11-Pr** and **Me_2-11-Pr** to see is the aryl-Me can be activated through an oxidative process.

4.0 Activation of $C(sp^2)$-H bonds at Electrophilic Five-Coordinate Pt^{IV} centres and subsequent reductive elimination

4.1. Introduction

The Suzuki reaction is a famous example of a $C(sp^2)$-$C(sp^2)$ bond formation reaction. An aryl halide and an aryl-substituted boronic acid are coupled together using a palladium catalyst (e.g. $Pd(OAc)_2$) forming an aryl-aryl bond. The versatility of this reaction won Suzuki a share of the 2010 Nobel prize in Chemistry.[15,17] The prevalence of this reaction in both academic and industrial scale reactions has prompted academic interest to better understand the mechanism involved, including (relevant to this chapter) the reductive elimination step.[175,176]

The focus of this project was to study what effect a dicyclometallated C^N^C ligand has on the products of oxidative addition and reductive elimination, as the C^N^C ligand can only adopt a *mer* geometry at the metal centre. Similar work from the Sanford group showed the formation of a $C(sp^2)$-$C(sp^2)$ bond via reductive elimination at a dicyclometallated complex $(C^N)_2Pd^{IV}Cl_2$ (Scheme 4.1).[177] They showed that the dicyclometallated complex Pd^{II}(2-phenylpyridine)$_2$ reacted first with $PhICl_2$, which gave a stable Pd^{IV} dichloro- species. The geometry of the product had the newly added chlorides *cis* to each other, and the two nitrogens mutually *trans*. The geometry matched similar work by Zelewsky *et al.*, who used different electrophilic reagents such as MeI (Scheme 1.13).[94] Heating the complex in pyridine at 80 °C initiated a C-C bond forming reaction, where the aryl groups coupled, followed by the displacement of this C-C coupled product by solvent.[178,179]

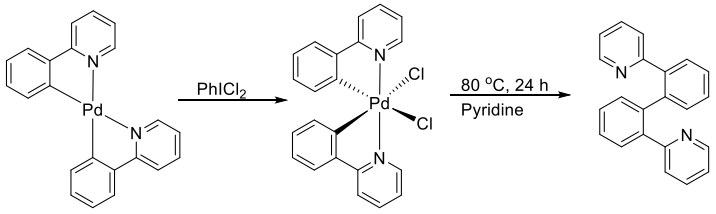

Scheme 4.1

The Dutton group then showed that the same dicyclometallated Pd^{II} complex could be oxidized by the new $PhI^{III}Py_2(OTf)_2$ compound (Scheme 4.2).[180] The oxidant was

consumed, but no Pd^{IV} complex was seen. Instead, two Pd^{II} complexes were observed: $Pd(py)_4^{2-}$ and $Pd(L)_2^{2-}$ (where L is the C-C coupled product). They suggest that the pyridine groups were unable to stabilize the Pd^{IV} complex, which led to the observed reductive coupling reaction at room temperature. Without a great excess of pyridine in solution, the ligands redistributed to form the observed complexes, instead of displacing the C-C coupled product (which was observed for Sanford).

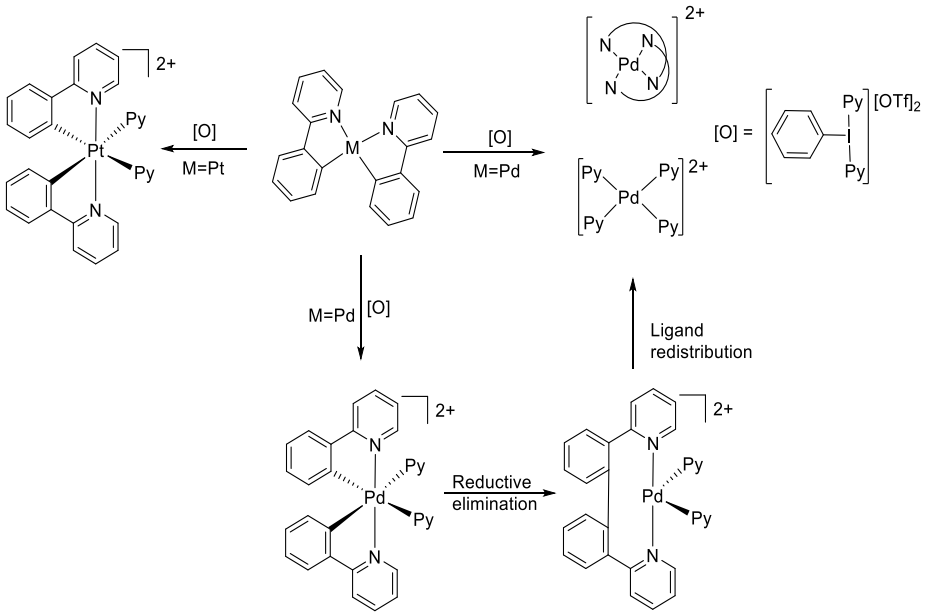

Scheme 4.2

The coordinated C-C coupled product gives a nine-membered ring from a starting material with two five-membered rings. In the formation of the nine-membered ring, two bonds break and one forms, giving an overall nine-sided shape. Also, Pd is counted in both of the five-membered rings, and only once in the nine-membered ring. The two five-membered rings are expected to be lower energy (in terms of ring strain) when compared to the nine-membered ring. However, the energy difference is offset by the formation of a strong C-C bond, and the reduction of Pd^{IV} to Pd^{II}. The C-C coupled product was shown to be coordinated with the nitrogens *trans* to each other, which has been seen with a similar platinum complex.[181]

The analogous dicyclometallated Pt^{II} complex Pt(2-phenylpyridine)$_2$ reacted with $PhI^{III}Py_2(OTf)_2$ and gave an observable Pt^{IV} species, which did not subsequently reductively couple, likely because Pt^{IV} is relatively inert compared to Pd^{IV}.

Past work in the Rourke group has shown that two 2-(4-fluorophenyl)pyridine pro-ligands will coordinate to platinum (from $K_2[PtCl_4]$), yet only one of these ligands will cyclometallate, even when the reaction mixture was heated for extended periods of time (greater than one month) in acetic acid (Scheme 4.3).[145,182]

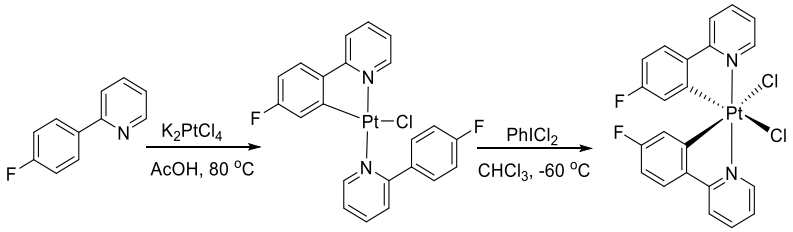

Scheme 4.3

The singly cyclometallated complex reacted with $PhICl_2$, giving a Pt^{IV} dicyclometallated species. Instead of just adding Cl_2 across the molecule (cf. the trichloro- complex seen in Scheme 2.1) a C(sp^2)-H bond was also activated. The geometry of the phenylpyridine ligands was like that of the Zelewsky complexes (but with mutually *trans* nitrogens).[94] Unlike the alkyl phosphines (Section 2.3), formation of the new C-Pt bond does not come at the cost of another, and so led to the formation of a stable dicyclometallated Pt^{IV} complex.

The expected mechanism for the formation of the dicyclometallated product is shown in Scheme 4.4. First the platinum attacks the oxidant in an S_N2 type mechanism (adding Cl^+), to give a Pt^{IV} five-coordinate intermediate. The fluoro-phenyl ring then attacks the highly electrophilic platinum (similar to a Friedel-Crafts mechanism) activating the *ortho* position and giving a Wheland-type intermediate, which are known to be very acidic.[183] The loss of the proton will then give the dicyclometallated product.

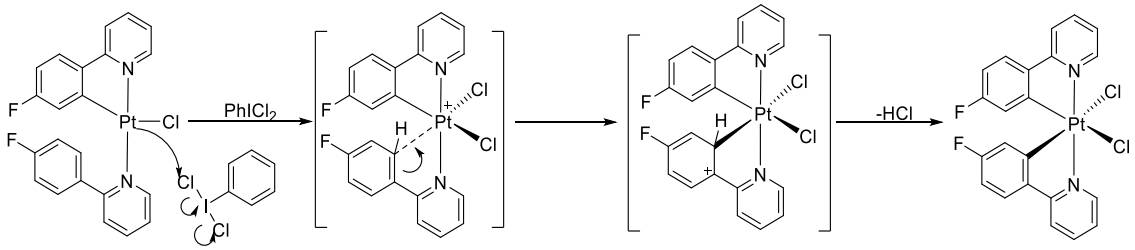

Scheme 4.4

This chapter looks at the synthesis of tricyclometallated complexes, starting from the diaryl C^N^C dicyclometallated Pt^{II} complex **1-Bn**, and oxidized using $PhICl_2$ (as seen in Chapter 2). Because the chloride was unlikely to dissociate spontaneously from the tricyclometallated products, the tried-and-tested-method of adding $AgBF_4$ to the Pt^{IV} (as seen in Chapter 3) was attempted, which initiated a reductive coupling reaction, giving a stable three-coordinate complex with a nine-membered ring. Small molecules such as chloride, CO and H_2 have shown to coordinate to the metal centre, each having very different effects on the geometry and structure of the molecule.

The same methodology of oxidative addition was then attempted starting with the methyl substituted diaryl C^N^C dicyclometallated Pt^{II} complex **Me-1-Bn**. In Chapter 3, the presence of the aryl-Me was shown to affect regioselectivity. Adding $AgBF_4$ to these analogous tricyclometallated complexes allowed us to study the possible effect on the regioselectivity of the reductive coupling reaction products, and then compare with the results of Chapter 3.

4.2. Symmetric Diaryl C^N^C Dicyclometallated Pt^{II} Complex **1-Bn**

The $Pt^{II}Bn_3$ derivative **1-Bn** was synthesized from **1-DMSO** by simple ligand displacement, as described in Section 2. Important NMR data for the tribenzyl phosphine derivative **1-Bn** includes: a single peak in the $^{19}F\{^1H\}$ NMR spectrum at -110.54 ppm ($^4J_{F\text{-}Pt}$ = 28 Hz), a single peak in the $^{31}P\{^1H\}$ NMR spectrum at -1.23 ppm ($^1J_{P\text{-}Pt}$ = 3847 Hz) and a doublet in the ^{195}Pt NMR spectrum at −4151 ppm ($^1J_{Pt\text{-}P}$ = ~3900 Hz).

A crystal suitable for crystal structure determination was grown from chloroform (Figure 4.1). The X-ray crystal structure showed that the phenyl rings have more space (cf. **1-Ph**) as the methylene groups allow the phenyl groups to point out of the way of the C^N^C ligand.

PBn_3 has a Tolman cone angle of around 165°, almost 30° smaller than P(*o*-tol)$_3$, but also about 20° larger than PPh_3, though a recent paper has shown that the effective cone angle might actually be smaller than PPh_3.[184] Also (unlike **1-Ph**), the protons *ortho* to Pt and F do not point into the centre of the benzyl rings, which is reflected in the ^1H NMR, where there are no unusually upfield shifted peaks.

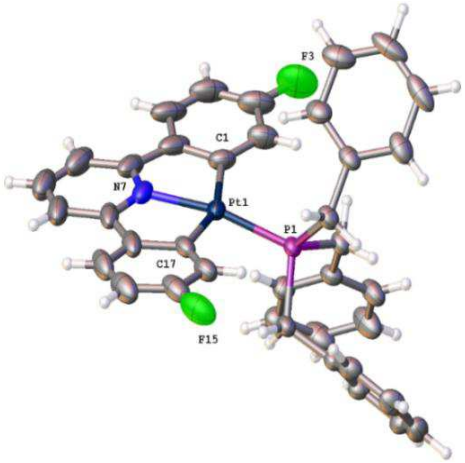

*Figure 4.1 Crystal structure of **1-Bn**, thermal ellipsoids drawn at 50% probability level. Selected bond lengths (Å) and angles (°): Pt1-P1, 2.2200(8); Pt1-N7, 2.033(3); Pt1-C1, 2.075(4); Pt1-C17, 2.085(4); N7-Pt1-P1, 168.72(10); N7-Pt1-C1, 80.05(17); N7-Pt1-C17, 79.84(16); C1-Pt1-P1, 103.82(12); C1-Pt1-C17, 159.19(17); C17-Pt1-P1, 96.93(11).*

4.2.1. Oxidation of **1-Bn** with $PhICl_2$

Oxidation of **1-Bn** with one equivalent of $PhICl_2$ at -60 °C gave two new complexes **(26** and **27(t)**) in equal proportions (Scheme 4.5).[185] Further reactions of **1-Bn** with $PhICl_2$ showed that the proportions of the two products was unaffected by the choice of solvent (such as acetone and toluene), or whether the reaction was carried out at room temperature. Adding diethyl ether to the reaction mixture allowed the insoluble **27(t)** to be removed by filtration. The solution spectra of **27(t)** showed a single peak in the $^{19}F\{^1H\}$ NMR spectrum at -108.45 ppm ($^4J_{F\text{-}Pt}$ = 20 Hz) and the pattern of peaks present in the ^1H NMR spectrum indicated that the C^N^C ligand remained dicyclometallated. In the $^{31}P\{^1H\}$ NMR spectrum, a peak at 19.37 ppm ($^1J_{P\text{-}Pt}$ = 2649 Hz) and a doublet in the ^{195}Pt NMR spectrum −2911 ppm ($^1J_{Pt\text{-}P}$ = ~2700 Hz) indicated a Pt^{IV} species had been formed.

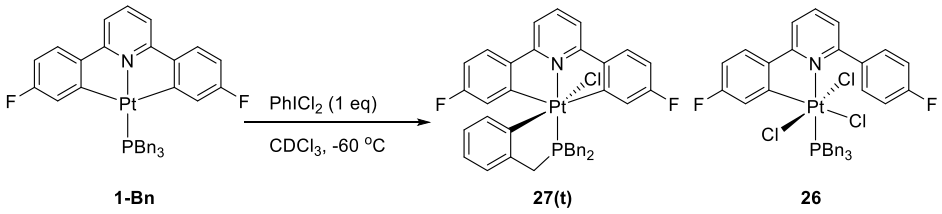

1-Bn **27(t)** **26**

Scheme 4.5

A peak in ^{1}H NMR spectrum at 6.19 ppm, which integrated to one proton with platinum satellites ($^{3}J_{H\text{-}Pt}$ = 47 Hz), showed that one of the benzyl rings had been activated (a C-Pt bond had formed). Further evidence of the phosphorus being part of a ring came from the downfield shift of peak in the ^{31}P{^{1}H} NMR spectrum, which had shifted by over 20 ppm (when compared to **1-Bn**). As the C^N^C ligand remained dicyclometallated, and a benzyl ring had been activated, **27(t)** is a tricyclometallated complex. The pattern of the three resonances for the Ph*CH*$_2$ protons can be explained by the plane of symmetry imposed by the coordinated benzyl ring (the plane of symmetry is perpendicular to the C^N^C ligand). A P-N *trans* geometry could be assigned by nOe data where irradiation of protons *ortho* to Pt and F showed weak interactions with all the CH_2 resonances. A crystal suitable for X-ray crystallography was grown from chloroform (Figure 4.2). The crystal structure confirms the connectivity and the P-N *trans* geometry.

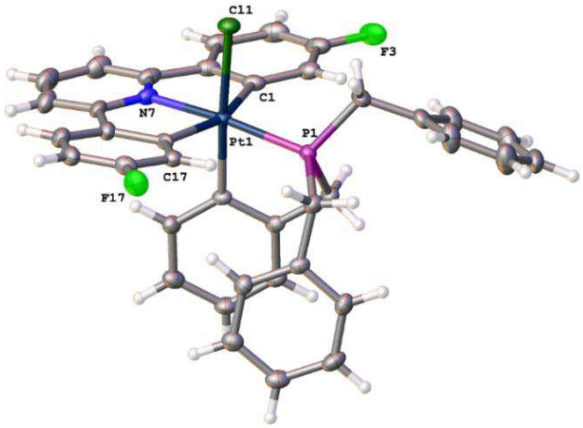

*Figure 4.2 Crystal structure of **27(t)**, thermal ellipsoids drawn at 50% probability level. Selected bond lengths (Å) and angles (°): Pt1-Cl1, 2.4425(8); Pt1-P1, 2.2609(9); Pt1-C1, 2.106(3); Pt1-N7, 2.039(3); Pt1-C17, 2.097(3); Pt1-C20, 2.057(3); P1-Pt1-Cl1, 96.45(3); C1-Pt1-Cl1, 91.42(9); C1-Pt1-P1, 96.30(11); N7-Pt1-Cl1, 91.88(8); N7-Pt1-P1, 170.83(8); N7-Pt1-C1, 79.61(14); N7-Pt1-C17, 79.78(13); N7-Pt1-C20, 90.93(13); C17-Pt1-Cl1, 86.02(9); C17-Pt1-P1, 104.57(10); C17-Pt1-C1, 159.13(15); C20-Pt1-Cl1, 176.97(10); C20-Pt1-P1, 80.68(10); C20-Pt1-C1, 87.96(12); C20-Pt1-C17, 95.61(12); C19-C20-Pt1, 117.8(2); C20-C19-C18, 119.6(3); C19-C18-P1, 104.4(2); C18-P1-Pt1, 100.67(12).*

The other product **26** is also a Pt^{IV} species, shown by a single peak in the ^{31}P{^{1}H} NMR spectrum at 9.14 ppm ($^{1}J_{P\text{-}Pt}$ = 2434 Hz) and a doublet in the ^{195}Pt NMR spectrum at −1719 ppm ($^{1}J_{Pt\text{-}P}$ = ~2450 Hz). In the ^{19}F{^{1}H} NMR spectrum the presence of two peaks of equal intensity (one with and one without platinum satellites) at -107.92 ppm ($^{4}J_{F\text{-}Pt}$ = 29.5 Hz) and -111.26 ppm showed that the C^N^C ligand had become monocyclometallated. A pattern of peaks in the ^{1}H NMR spectrum showed that the decyclometallated ring did not have a chloride attached (a doublet of doublets and a triplet, both with a relative integral of

two). A P-N *trans* geometry was suggested by nOe data, where irradiation of the proton *ortho* to Pt and F greatly enhanced the alkyl protons of the benzyl.

As **26** is a monocyclometallated Pt^{IV}, it is likely to be the product of the oxidation of the monocyclometallated Pt^{II} complex **25**. Upon oxidation of **1-Bn** with half of an equivalent of $PhICl_2$ at -60 °C, the monocyclometallated complex **25** and the tricyclometallated complex **27(t)** were seen (Scheme 4.6). The amount of **27(t)** in solution equalled that of the monocyclometallated products combined (**25** and **26**).

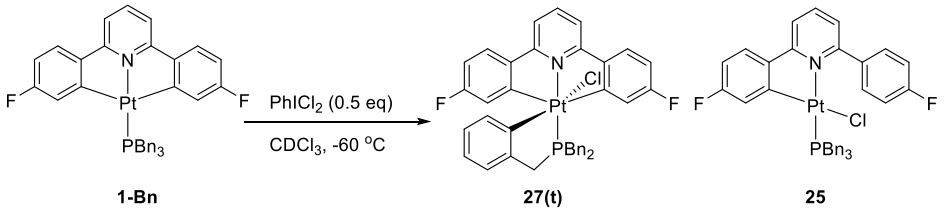

1-Bn **27(t)** **25**

Scheme 4.6

The solution spectra of **25** showed two peaks in the $^{19}F\{^1H\}$ NMR spectrum (only one of which had platinum satellites) at -110.84 ppm ($^4J_{F\text{-}Pt}$ = 64 Hz) and -111.36 ppm and a similar pattern of peaks in the ^1H NMR spectrum showed that the connectivity of **25** is very similar to **26**. A peak in the $^{31}P\{^1H\}$ NMR spectrum at -1.76 ppm ($^1J_{P\text{-}Pt}$ = 4272 Hz) and a doublet in the ^{195}Pt NMR spectrum −3807 ppm ($^1J_{Pt\text{-}P}$ = ~4300 Hz) indicated a Pt^{II} species. A peak of intensity similar to other neutral species was seen in the HR-MS (ESI) spectrum at 764.1779 m/z (corresponding to $[M\text{-}Cl]^+$) suggesting that **25** is a neutral species. Crystals suitable for X-ray analysis of **25** were grown from chloroform (Figure 4.3). The crystal structure showed the decyclometallated fluoro-phenyl ring and a chloride in the fourth coordination site.

The formation of **27** is expected to go through a similar Wheland-type intermediate as seen in Scheme 4.4. Dissolved chlorides or even **1-Bn** are possible bases used in the removal of the acidic proton of the Wheland-type intermediate (to give **27**).

The mechanism of the formation of **25** requires the coordination of H^+ to **1-Bn** (which is quickly followed by reductive elimination of aryl-H), but the strength of the acid required to protonate **1-Bn** was unknown. The susceptibility was tested by adding a drop of 1M HCl to a chloroform solution of **1-Bn** in an NMR tube. The sample was shaken and monitored by NMR. As no reaction was observed over several hours, it is unlikely that HCl in solution was able to protonate **1-Bn**.

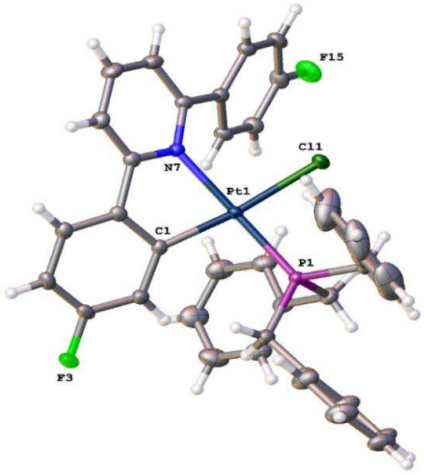

*Figure 4.3 Crystal structure of **25**, thermal ellipsoids drawn at 50% probability level. Selected bond lengths (Å) and angles (°): Pt1-Cl1, 2.3884(4); Pt1-C1, 1.9947(17); Pt1-P1, 2.2384(4); Pt1-N7, 2.1274(13); C1-Pt1-Cl1, 172.43(5); C1-Pt1-P1, 99.70(5); C1-Pt1-N7, 79.14(6); P1-Pt1-Cl1, 86.424(16); N7-Pt1-Cl1, 94.32(4); N7-Pt1-P1, 174.23(4).*

Therefore the 50:50 ratio is explained by the use of two equivalents of **1-Bn** to synthesize **27(t)** (Scheme 4.7). One equivalent is oxidised by $PhICl_2$, whilst the other is used sacrificially as a base, forming **25**.

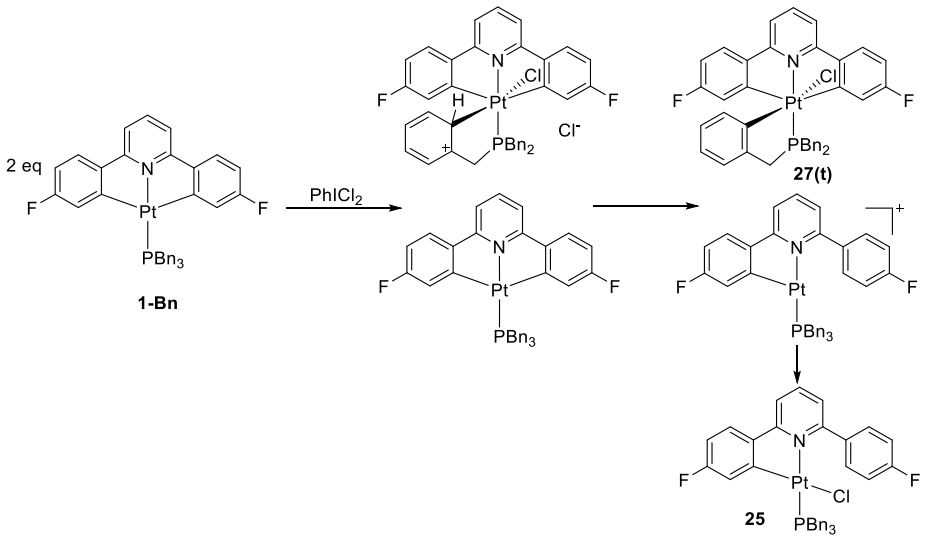

Scheme 4.7

When a drop of 5M HCl was added to a chloroform solution of **1-Bn** and heated to 50 °C, HCl added twice to the molecule, once to break a Pt-C bond, and another to protonate the central pyridine. Lack of this product in the reactions mentioned earlier further suggests that Cl^- is not the base. Before the chloride coordinates to the platinum in the formation of

25, there is a positively charged species. No evidence of a benzyl phenyl attacking this platinum was observed. The platinum is likely not sufficiently electrophilic to activate the phenyl ring as it is in a low oxidation state.

To prevent the formation of **25** in solution, another base is required to outcompete **1-Bn** in the deprotonation of the Wheland-type intermediate. Adding inorganic bases (e.g. K_2CO_3) to the reaction mixture before addition of oxidant made no difference, likely because of their inherent insolubility in organic solvents. Instead, it was found that water was the best choice of base. When water was stirred into a chloroform solution of **1-Bn** followed by addition of $PhICl_2$ a ratio of **27(t)**:**25** of 9:1 was seen. When water was stirred an acetone solution of **1-Bn**, followed by addition of $PhICl_2$, only **27(t)** was seen (Scheme 4.8). The greater yield in acetone can be explained by the greater miscibility of water in acetone.

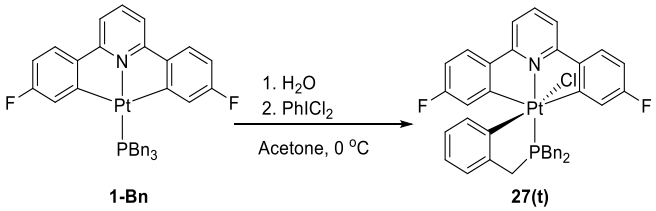

Scheme 4.8

4.2.2. Initiation of a Reductive Elimination Reaction with a Lewis Acid

Purification of **27(t)** was not possible by column chromatography, as it changed with time whilst adsorbed to the silica (shown by 2D TLC). When samples of **27(t)** were left on the column long enough, full conversion to two new products **27(c)** and **28** was seen, with a ratio of around 1:4 (**27(c)**:**28**) (Scheme 4.9). The mechanism of formation of the new products is unclear, but the likely cause is the Lewis acidity of the silica.

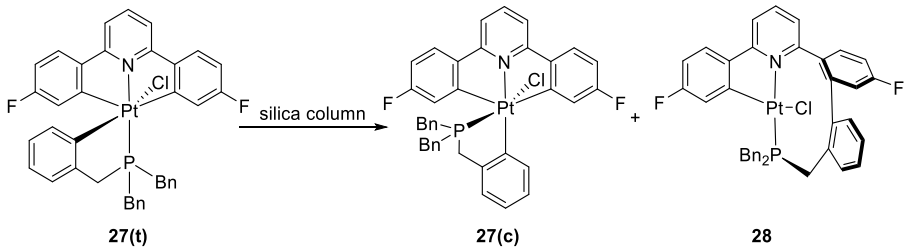

Scheme 4.9

The minor product **27(c)** is the P-N *cis* tricylometallated complex. The spectra of **27(c)** showed a single peak in the $^{19}F\{^{1}H\}$ NMR spectrum at -108.14 ppm ($^{4}J_{F\text{-}Pt}$ = 21 Hz) and the pattern of peaks present in the ^{1}H NMR indicated that the C^N^C ligand remained dicyclometallated. The benzyl ring was shown to be cyclometallated by a peak in the ^{1}H NMR spectrum at 8.34 ppm ($^{3}J_{H\text{-}Pt}$ = 31 Hz), making it the most downfield peak in the spectrum. In the $^{31}P\{^{1}H\}$ NMR spectrum, a peak at 29.00 ppm ($^{1}J_{P\text{-}Pt}$ = 2692 Hz) and a doublet in the ^{195}Pt NMR spectrum at −3144 ppm ($^{1}J_{Pt\text{-}P}$ = ~2700 Hz) indicated a Pt^{IV} species. In solution **27(c)** does not change with time, nor is there any change upon repeated silica columns, which showed that **27(c)** does not react on the column to form **28**.

The major product **28** had two peaks (and only one having platinum satellites) in the $^{19}F\{^{1}H\}$ NMR spectrum at -110.38 ppm ($^{4}J_{F\text{-}Pt}$ = 57 Hz) and -112.08 ppm, which indicated that one of the rings of the C^N^C had become decyclometallated. In the $^{31}P\{^{1}H\}$ NMR spectrum, a peak at -9.29 ppm ($^{1}J_{P\text{-}Pt}$ = 4552 Hz) and a doublet in the ^{195}Pt NMR spectrum at −3985 ppm ($^{1}J_{Pt\text{-}P}$ = ~5500 Hz) indicated a Pt^{II} species. The only peak in the ^{1}H NMR spectrum with platinum satellites at 6.55 ppm ($^{3}J_{H\text{-}Pt}$ = ~60 Hz) corresponded to the proton *ortho* to Pt and F. The benzyl C-Pt bond had therefore been broken, which was also suggested by the large upfield shift of the peak in the $^{31}P\{^{1}H\}$ NMR spectrum of around 30 ppm (cf. **27(t)**). In the $^{1}H/^{13}C$ HMBC, through bond coupling was seen between a benzyl aryl ring and the decyclometallated fluoro-phenyl ring, showing that the two aryl rings have reductively coupled together. The magnitude of the platinum satellites on the peak in the $^{31}P\{^{1}H\}$ NMR spectrum suggested that the phosphorus was *trans* to the nitrogen. A peak (with intensity to the other neautral species discussed in this thesis) was seen in the HR-MS (ESI) spectrum at 762.1622 m/z (corresponding to $[M\text{-}Cl]^{+}$) is consistant with a neutral species, where the fourth coordination site is expected to be taken by a chloride. A crystal suitable for X-ray analysis was grown from chloroform. The crystal structure confirmed the expected connectivity, and P-N *trans* geometry (Figure 4.4).

The bond angles in the crystal structure shows that the nine-membered ring is highly strained. The N-Pt-P bond angle of 155.83(5) and the Pt-P-C bond angle of 96.81(8) are quite different to the expected angles of 180° and 109.5° respectively. The strain can also be seen in the distortion from an ideal square planar geometry at the platinum centre, where the C-Pt-Cl bond angle of 158.48(6) is >20° smaller than the ideal 180°. It is believed that the C-Pt-Cl bond angle is not caused by the proximity to the nine-membered ring, as the chloride is visibly distant from the ring. Instead, it is more likely because of the nine-membered ring bending the nitrogen towards the phosphorus, much like the beginning of the transition of square planar to tetrahedral geometry, which in turn causes a

sympathetic reduction of the C-Pt-Cl bond angle. The complex can be characterised as a distorted square planar, as the molecule remains NMR active (a tetrahedral complex would be paramagnetic).

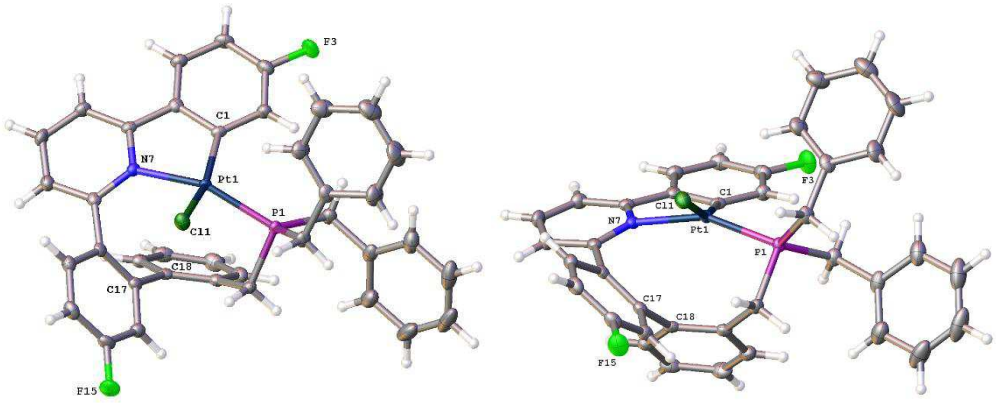

Figure 4.4 Crystal structure of ***28*** *from different angles, thermal ellipsoids drawn at 50% probability level. Selected bond lengths (Å) and angles (°): C1-Pt1, 1.987(2); Cl1-Pt1, 2.4001(6); P1-Pt1, 2.2346(6); P1-C24, 1.857(2); Pt1-N7, 2.095(2); C24-P1-Pt1, 96.81(8); C1-Pt1-Cl1, 158.48(6); C1-Pt1-P1, 104.44(7); C1-Pt1-N7, 80.56(9); P1-Pt1-Cl1, 87.97(2); N7-Pt1-Cl1, 95.35(6); N7-Pt1-P1, 155.83(5).*

The formation of **28** can be explained by the reductive elimination of two C(sp^2) (one of the fluoro-phenyl groups and the coordinated benzyl group) in a C-C bond forming reaction. Like the reductive elimination reactions seen in Chapter 3, there is no evidence of the two fluoro-phenyl ring coupling, because of the constraints of the C^N^C ligand. Unlike the reaction seen in Scheme 4.1, the benzyl R group is tethered to the phosphorus, and so the coupled carbons become part of a nine-membered ring.

The geometry of **28** and the conformation of the nine-membered ring is restricted by the imposed geometry of a square planar complex for a Pt^{II} species. Only two geometries are allowed (P-N *cis* and P-N *trans*). As an octahedral geometry would allow more freedom for the nine-membered ring, $PhICl_2$ was added to **28**, and gave clean conversion to a single product **29** (Scheme 4.10). The NMR data for **29** are similar to **28**, suggesting that the connectivity of the molecule was unaffected.

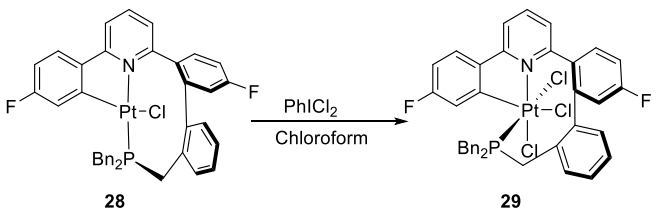

Scheme 4.10

The solution spectra of **29** showed two peaks in the $^{19}F\{^1H\}$ NMR spectrum at -103.68 ppm ($^4J_{F\text{-}Pt}$ = 28.5 Hz) and -111.13 ppm, which showed that the C^N^C ligand was still monocyclometallated. In the $^{31}P\{^1H\}$ NMR spectrum, a peak at -0.41 ppm ($^1J_{P\text{-}Pt}$ = 2271 Hz) and a doublet in the ^{195}Pt NMR spectrum at −1902 ppm ($^1J_{Pt\text{-}P}$ = ~2300 Hz) indicated a Pt^{IV} species. The downfield shift of the peak in the $^{31}P\{^1H\}$ NMR spectrum of about 10 ppm suggested a change in the P-N geometry. The magnitude of the platinum satellites on the peak in the $^{31}P\{^1H\}$ NMR spectrum showed that the phosphorus was not *trans* to the aryl ring. A P-C *trans* geometry is also likely to increase to ring strain energy. Data from nOe experiments was difficult to interpret due to overlapping peaks in the ^1H NMR spectrum. Luckily a crystal of **24** suitable for X-ray analysis was collected from a chloroform solution (Figure 4.5). The crystal structure showed a P-N *cis* geometry, where the phosphorus is also *cis* to the cyclometallated aryl ring (*fac*-Cl_3). The complex has a standard octahedral geometry, with the angles between adjacent ligands being very close to the ideal 90°.

The N-Pt-P bond angle of 99.46(5) and the Pt-P-C bond angle of 115.49(7) are also much closer to the expected angles of 90° and 109.5° respectively, suggesting that the internal angles of the nine-membered ring of **29** are less strained than for **28**. We expect that the P-N *trans* isomer is not formed in the reaction. The reduced N-Pt-P bond angle, and the aryl rings on the nine-membered ring make one side of the molecule highly congested, and so the chlorides are more likely to add individually to the to the less congested side.

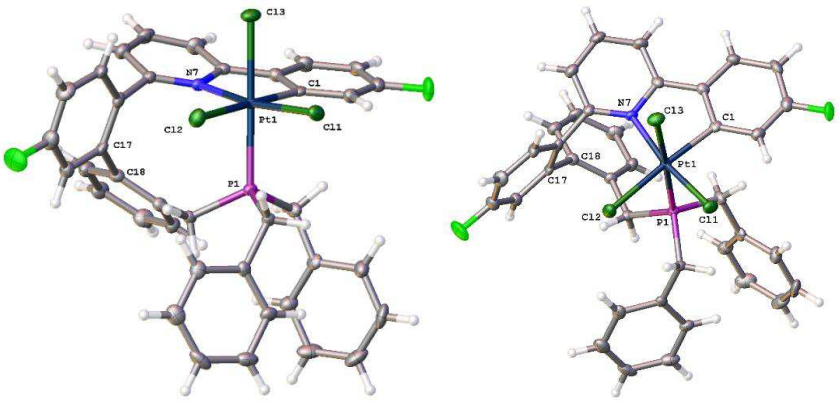

*Figure 4.5 Crystal structure of **29** from different angles, thermal ellipsoids drawn at 50% probability level. Selected bond lengths (Å) and angles (°): Pt1-Cl1, 2.3060(5); Pt1-P1, 2.3162(5); Pt1-Cl3, 2.3870(5); Pt1-Cl2, 2.4175(5); Pt1-N7, 2.1070(16); Pt1-C1, 2.031(2); Cl1-Pt1-P1, 87.370(19); Cl1-Pt1-Cl3, 90.032(19); Cl1-Pt1-Cl2, 85.42(2); P1-Pt1-Cl3, 175.622(19); P1-Pt1-Cl2, 84.619(19); Cl3-Pt1-Cl2, 91.66(2); N7-Pt1-Cl1, 169.78(5); N7-Pt1-P1, 99.46(5); N7-Pt1-Cl3, 83.59(5); N7-Pt1-Cl2, 102.69(5); C1-Pt1-Cl1, 90.83(6); C1-Pt1-P1, 95.26(6); C1-Pt1-Cl3, 88.30(6); C1-Pt1-Cl2, 176.26(6); C1-Pt1-N7, 81.03(7); C24-P1-Pt1, 115.49(7); C23-C24-P1, 122.04(15).*

4.2.3. Initiation of a Reductive Elimination Reaction with $AgBF_4$

Based on the methodology of Chapter 3, $AgBF_4$ was then added to a colourless acetone solution of either tricyclometallated complex (**27(t)** or **27(c)**) to initiate a reductive elimination reaction, and gave a vivid yellow product **30** (Scheme 4.11). Such a large colour change suggested a change in oxidation state from Pt^{IV} to a Pt^{II} species. The product was the expected C-C coupled product with the same connectivity as **28**. Without the chloride, **30** is a three-coordinate species.

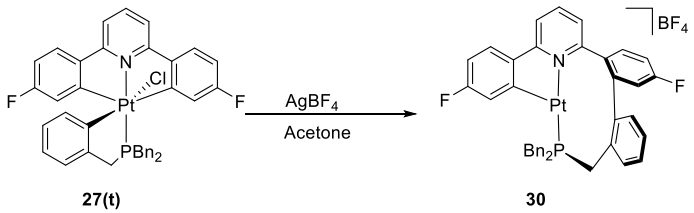

Scheme 4.11

The solution spectra of **30** showed two peaks (only one of which had platinum satellites) in the $^{19}F\{^1H\}$ NMR spectrum at -108.51 ppm ($^4J_{F\text{-}Pt}$ = 55 Hz) and -110.60 ppm, which indicated that one of the rings of the C^N^C had become decyclometallated. In the $^{31}P\{^1H\}$ NMR spectrum, a peak at -9.49 ppm ($^1J_{P\text{-}Pt}$ = 4119 Hz) and a doublet in the ^{195}Pt NMR spectrum at −3612 ppm ($^1J_{Pt\text{-}P}$ = ~4200 Hz) indicated a Pt^{II} species. The only peak in the ^1H NMR spectrum with platinum satellites at 6.46 ppm ($^3J_{H\text{-}Pt}$ = ~90 Hz) corresponds to the proton *ortho* to Pt and F. The benzyl C-Pt bond has therefore been broken, which was also seen in a large upfield shift of the peak in the $^{31}P\{^1H\}$ NMR spectrum of around 30 ppm (compared to **27(t)**). In the $^1H/^{13}C$ HMBC, through bond coupling was seen between a benzyl aryl ring, and the dicyclometallated ring. In the HR-MS (ESI) spectrum of the reaction mixture apeak of high intensity (relative to **27(t)**) at 762.1637 m/z (corresponding to $[M]^+$) was seen, suggesting a cationic species. The magnitude of the platinum satellites on the peak in the $^{31}P\{^1H\}$ NMR spectrum showed that the phosphorus is *trans* to the nitrogen. No obvious signs of coordinated water were seen by NMR, even if the solution was cooled to -60 °C, suggesting the structure is three-coordinate (or has coordinated acetone).

4.2.4. Comparison of the Two Reductive Elimination Products **(28** and **30**)

The connectivity of **28** and **30** is identical, where both have a five-membered ring (because of an o*rtho*-metallated fluoro-phenyl ring) and a nine-membered ring (connected to the platinum by a nitrogen and a phosphorus). The nine-membered ring is the result of a reductive elimination reaction where the other o*rtho*-metallated fluoro-phenyl ring coupled with the coordinated benzyl-aryl, originating from either tricyclometallated complex (Scheme 4.12). **28** differs from **30** by a chloride, which can be removed from **28** using silver salts (Scheme 4.12). Conversely, **28** can be made from **30** via the addition of KCl.

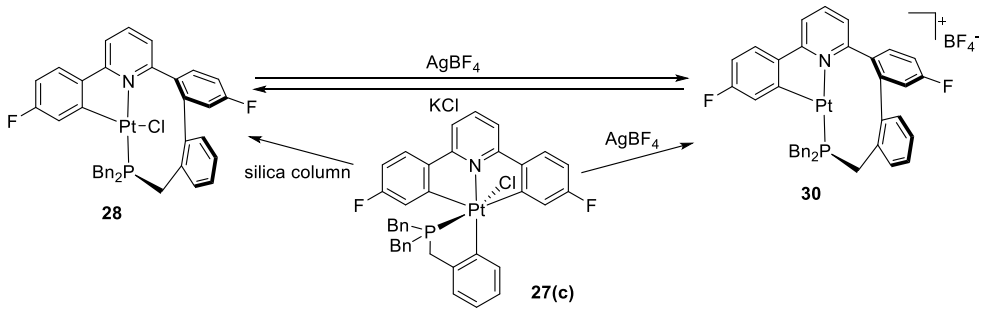

Scheme 4.12

The crystal structure of **28** (Figure 4.4) shows that the chloride is pushed far out of the plane by the ring strain of the nine-membered ring (C-Pt-Cl bond angle of 158.5°). Variable temperature NMR (in which a toluene-d_8 solution of **28** was heated at 25 °C intervals up to 100 °C (shown in Figure 4.6) showed that the positions of the peaks in the ^{1}H NMR spectra move very little, which suggested that the structure is very rigid.

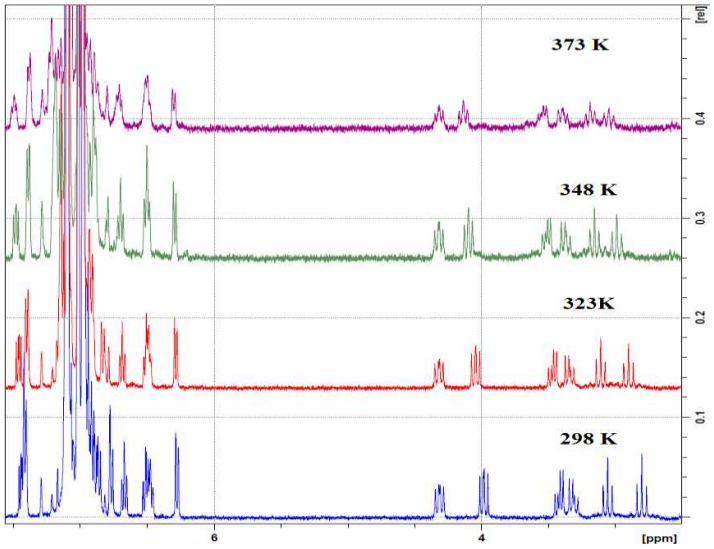

*Figure 4.6 ^{1}H NMR spectra of **28** at various temperatures (298 – 373 K).*

The six resonances between 2.5-4.5 ppm correspond to the six PhCH_2 protons, showing that there is no symmetry in the molecule (as all six protons are different). As there are already six different resonances at room temperature, it is highly unlikely that there will be any difference at lower temperatures. Any movement of peaks can be explained more by effects of solvent.

The geometry of **30** (lacking the chloride) is not expected to be very different to **28** as it is believed that it is the rigidity of the nine-membered ring that has the largest effect on the geometry of the molecule. This is backed up by the positions of the peaks in the $^{31}P\{^{1}H\}$ NMR spectrum (-9.49 for **30**, and -9.29 for **28**), as the position of phosphorus peaks has a greater dependence on the surrounding charge (and therefore geometry) compared to ^{1}H NMR (where the nucleus is more affected by the surrounding atoms). In the ^{1}H NMR spectrum (unlike **28**), the positions of peaks were observed to shift with temperature, suggesting a much less rigid structure. Variable temperature experiments ($CDCl_3$) were carried out between 208 K and 328 K (Figure 4.7). The complex degraded quickly on heating, so experiments at higher temperatures were excluded.

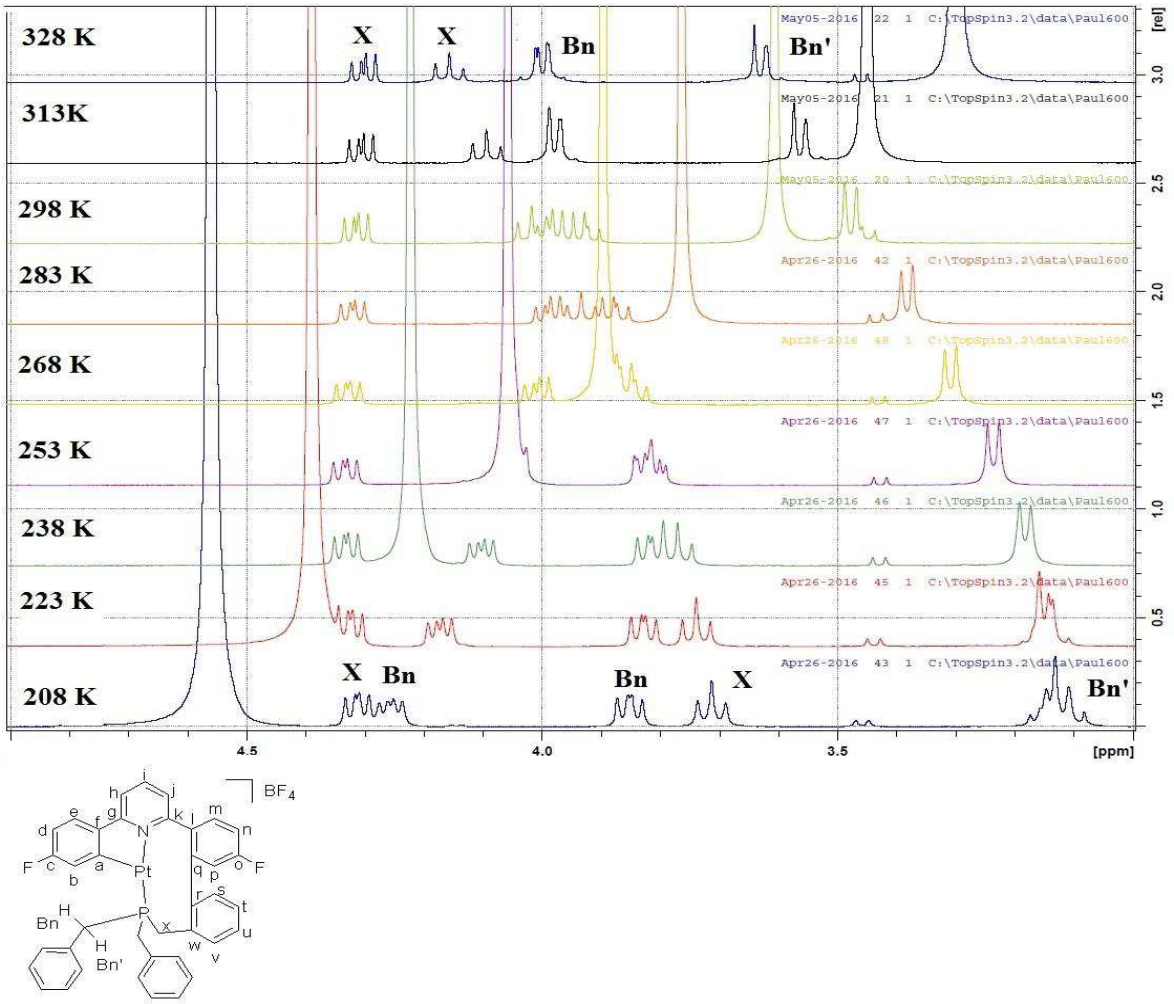

*Figure 4.7 ^{1}H NMR spectra of **30** at various temperatures (208 – 328 K, aliphatic region).*

Looking upfield at the benzyl alkyl protons, a lot of peak movement can be seen over the temperature range. at 208 K the Ph*CH₂* protons are largely separated into six individual peaks. The two H_x protons are separated by 360 Hz, Bn peaks are peaks separated by 230 Hz (600 MHz spectrometer). The separation of the Bn' protons is negligible, coalescing to a single doublet by 238 K. At 213 K, Bn also coalesces into a single doublet. Although coalescence is not seen for the H_x protons, the trend in the movement of the two peaks would suggest a coalescence temperature of around 360 K. The temperatures required would degrade the complex, implying a relatively large energy barrier.

In the ^{1}H NMR spectrum of **30** at 298 K, irradiating the proton *ortho* to Pt and F showed interactions with only one of the free Ph*CH₂* protons, and two of the CH_2 protons on the nine-membered ring (H_x). Irradiating the proton three bonds away from H_x (H_v) showed correlation the remaining Ph*CH₂* protons and no correlation to H_x. These interactions suggest a twisted geometry where the phosphorus is oriented in such a way to bring the (H_x) protons close to the proton *ortho* to Pt and F.

Looking downfield, the positions of H_b and H_s show the most change over the temperature range (Figure 4.8). With increasing temperature, we see greater amounts of deshielding of H_s, and greater shielding of H_b (with both peaks moving about 1 ppm between the highest and lowest temperatures).

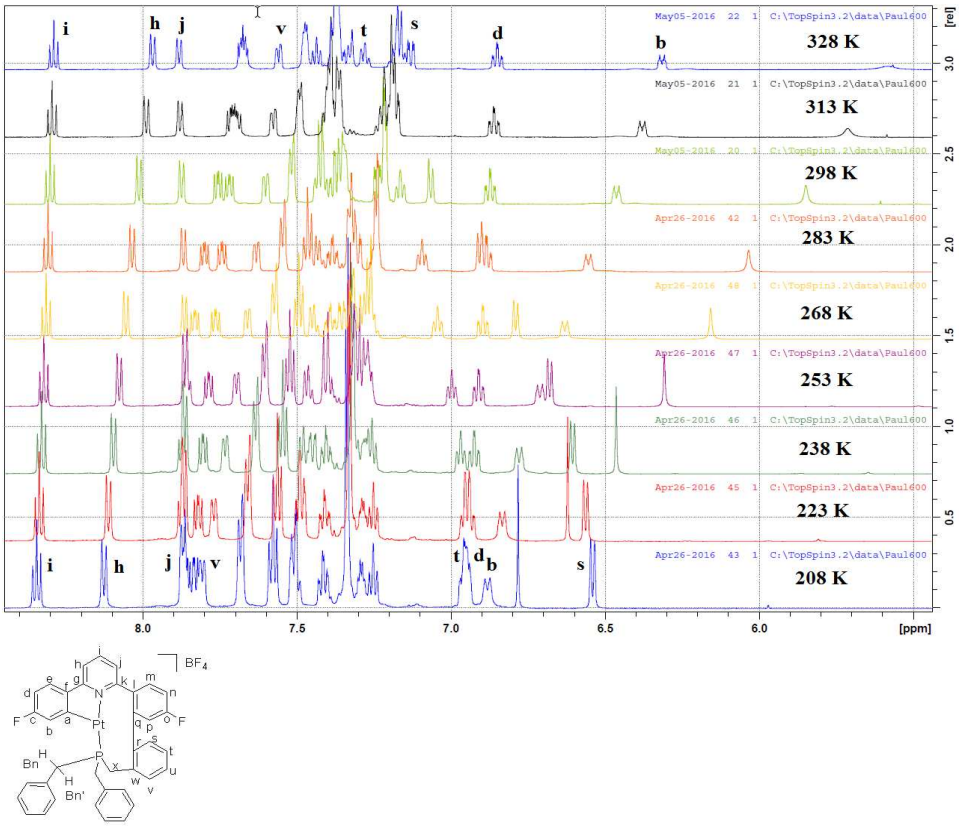

*Figure 4.8 ^{1}H NMR spectra of **30** at various temperatures (208 – 328 K, aromatic region).*

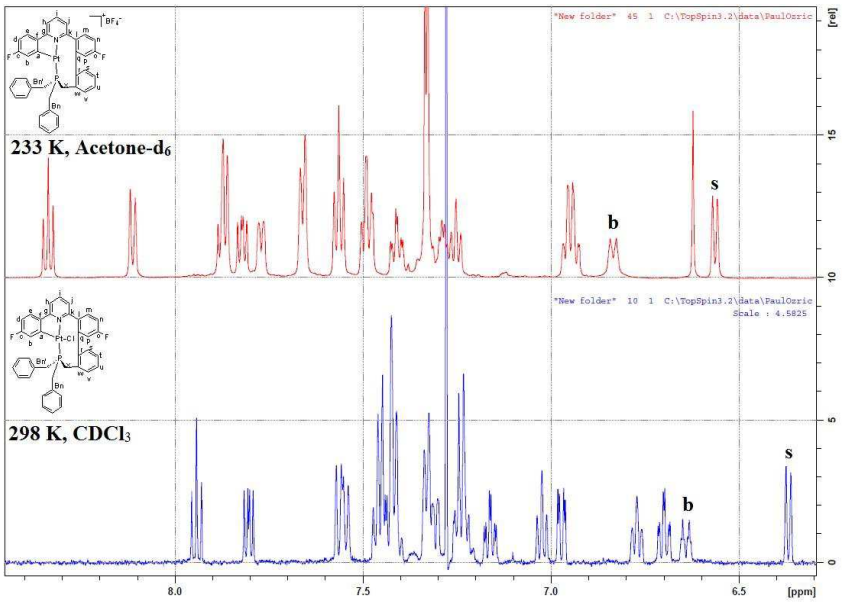

*Figure 4.9 ^{1}H NMR comparison of **30** and **28** (at 233 K and 298 K respectively, aromatic region).*

Conversely, many other peaks (including the peaks of the central pyridine H_{h-j}) show very little movement over the same temperature range. Comparison of the ^1H spectra of **30** at different temperatures with **28** at room temperature (by comparing the separation of H_b and H_s) shows that **28** at room temperature is similar to **30** at around 238 K (Figure 4.9).

There are two possible methods of ring inversion. Firstly (and most likely) the coupled aryl rings move between the two sides of the square plane, shown in Figure 4.10 (The top and bottom diagrams show different parts of the molecule pruned from the diagram to aid clarity).

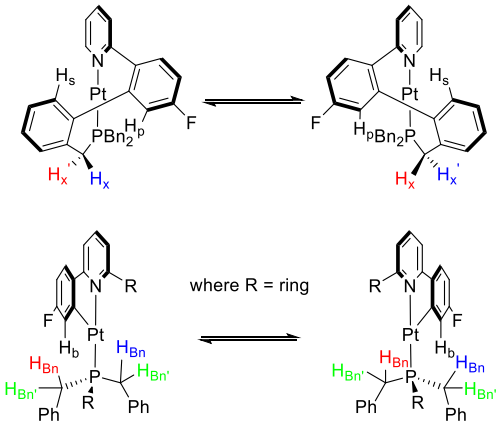

Figure 4.10 Illustration of the inversion of the nine-membered ring.
Top: cyclometallated fluorophenyl ring pruned.
Bottom: aryl rings from the nine-membered ring pruned.

This inversion mechanism requires rotation of the two aryl rings about the C-C bond formed by the reductive elimination reaction. This means that protons H_p and H_s are brought into proximity during the inversion. Therefore, it is obvious as to why the chemical shift of H_s moves so much with temperature. At low temperatures (where the inversion is effectively frozen out on an NMR timescale) H_s will be affected less by its proximity to H_p.

Also shown in Figure 4.10 (where the nine-membered ring is pruned back), is the explanation for the other phenomena seen over the temperature range. The resonance corresponding to H_b moves because at low temperatures (and low rates of ring inversion) H_b is held close to one of the Bn protons, whereas at higher temperatures (and higher rates of ring inversion) on average H_b will be between the two Bn protons. The implication of this average position means that the Bn protons are in the same environment, and the two resonances for Bn coalesce. Bn' doesn't interact strongly with any other protons, and is

therefore largely unaffected by the temperature range. The separation of Bn' in **28** could be because of the presence of the chloride, and its proximity to a Bn' proton. The second mechanism involves activation of the C-C bond formed during the reductive coupling, followed by reductive coupling of the benzyl ring with the other fluoro-phenyl ring. Evidence against this mechanism is presented in Section 4.3.3.

The rigidity of the aryl rings increases the energy required for the interconversion (seen by the high estimated coalescence temperature), giving an approximate barrier to interconversion of around 62±8 kJmol^{-1}.

4.3. Asymmetric Diaryl C^N^C Dicyclometallated Pt^{II} Complex **Me-1-Bn**

In Chapter 3, the Pt^{II}PBn$_3$ complex **Me-1-Bn** was synthesised via a series of steps, beginning with **1-Bn** (Scheme 3.13). The C^N^C ligand has a methyl group on one fluoro-phenyl ring, *meta* to Pt and F. The presence of the methyl group destroys the plane of symmetry that is perpendicular to the plane of the C^N^C ligand. Important NMR data for the asymmetric Pt^{II} tribenzyl phosphine **Me-1-Bn** includes: two peaks in the ^{19}F{^{1}H} NMR spectrum with platinum coupling at -110.69 ppm ($^4J_{F\text{-}Pt}$ = 26.5 Hz) and -113.14 ppm ($^4J_{F\text{-}Pt}$ = 29 Hz), a single peak in the ^{31}P{^{1}H} NMR spectrum at 1.18 ppm ($^1J_{P\text{-}Pt}$ = 3893 Hz) and a doublet in the ^{195}Pt NMR spectrum at −4097 ppm ($^1J_{Pt\text{-}P}$ = ~3900 Hz). The crystal structure can be seen in Figure 3.9.

Oxidation of **Me-1-Bn** with PhICl$_2$ was expected to give products analogous to those seen for the symmetric complex **1-Bn** as the methyl group is in a remote location from the metal centre. This section looks at the selectivity of the reductive elimination reaction, and comparisons are made to similar reactions seen in Chapter 3, where reductive elimination of methyl-aryl (from **Me-9-Pr**, initiated with AgBF$_4$) gave 100 % regioselectivity for the previously substituted side.

4.3.1. Oxidation of **Me-1-Bn** with PhICl$_2$

With the only difference between **1-Bn** and **Me-1-Bn** being the extra methyl group on the C^N^C ligand, it is unsurprising that the reaction with PhICl$_2$ yields similar results. Addition of half of an equivalent of PhICl$_2$ to a chloroform solution of **Me-1-Bn** at -60 °C gave the expected tricyclometallated complex **Me-27(t)**, yet only one Pt^{II} monocyclometallated complex **Me-25(b)** with the same 50:50 ratio (Scheme 4.13). The

structure of **Me-25(b)** was assigned from the mixture of **Me-25(b)** and **Me-27(t)**. The solution spectra showed two peaks of equal intensity in the $^{19}F\{^{1}H\}$ NMR spectrum (where only one of the peaks had at platinum satellites) at -110.96 ppm, ($^{4}J_{F\text{-}Pt}$ = 63 Hz) and -112.78 ppm. A peak in the $^{31}P\{^{1}H\}$ NMR spectrum at -1.96 ppm ($^{1}J_{P\text{-}Pt}$ = 4253 Hz) and a doublet in the ^{195}Pt NMR spectrum at −3821 ppm ($^{1}J_{Pt\text{-}P}$ = ~4300 Hz) indicated a Pt^{II} species. In the ^{1}H NMR spectrum there was no evidence of an activated benzyl ring. The Pt^{IV} complex **Me-26** was present in trace amounts, and was assigned based on diagnostic peaks in the NMR spectra.

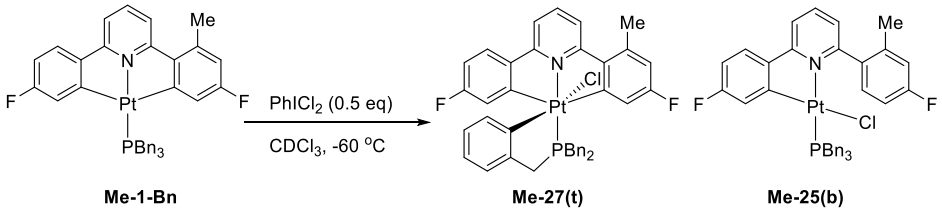

Scheme 4.13

It was clear enough in the solution NMR of **Me-25(b)** which fluoro-phenyl ring had become decyclometallated by looking at the pattern of peaks in the ^{1}H NMR spectrum. The patterns of peaks observed for the two fluoro-phenyl rings were both "dd, td and dd", which would only be possible for **Me-25(b)** (Scheme 4.14).

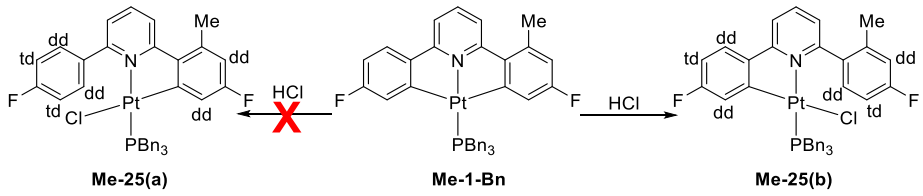

Scheme 4.14

The coordination of H^{+} to **Me-1-Bn** would give a five-coordinate intermediate, which is capable of coupling to either fluoro-phenyl ring. The presence of only one Pt^{II} monocyclometallated complex can therefore be explained by analogy with the mechanism of the formation of **Me-11-Pr** (Section 3.2.6.), where relief of the steric clash between the methyl group, and the central pyridine directed the regioselectivity.

Me-27(t) is a tricyclometallated complex analogous to **27(t)**. The solution spectra of **Me-27(t)** showed two peaks in the $^{19}F\{^{1}H\}$ NMR spectrum with platinum satellites at -108.61 ppm ($^{4}J_{F\text{-}Pt}$ = 19 Hz) and -111.30 ppm ($^{4}J_{F\text{-}Pt}$ = 22 Hz), which indicated the C^N^C ligand

remained dicyclometallated. A peak in the $^{31}P\{^{1}H\}$ NMR spectrum at 19.76 ppm ($^{1}J_{P\text{-}Pt}$ = 2657 Hz) and a doublet in the ^{195}Pt NMR spectrum at −2885 ppm ($^{1}J_{Pt\text{-}P}$ = ~2700 Hz) indicated a Pt^{IV} species. A peak with platinum satellites that integrated to one proton in ^{1}H NMR spectrum at 6.18 ppm ($^{3}J_{H\text{-}Pt}$ = 47 Hz), showed that a benzyl ring had been activated, and a C-Pt bond formed. A suitable crystal could not be grown of **Me-27(t)**, but further evidence of the structure can be found in the comparison of NMR data with **27(t)**. The peak in the $^{31}P\{^{1}H\}$ NMR spectrum at 19.76 ppm for **Me-27(t)** is almost identical to that of **27(t)** (19.37 ppm). The peak for the proton *ortho* to platinum on the benzyl ring in the ^{1}H NMR spectrum at 6.18 ppm for **Me-27(t)** is almost identical to that of **27(t)** (6.19 ppm). A peak (with instensity consistant with other neutral species seen during this body of work) in the HR-MS (ESI) spectrum at 776.1787 m/z (corresponding to $[M\text{-}Cl]^{+}$) is consistant with **Me-27(t)** being a neutral species.

Following the methodology for the selective synthesis of **27(t)** (Scheme 4.8), stirring water into an acetone solution of **Me-1-Bn** before the addition of $PhICl_2$ gave selective synthesis of **Me-27(t)** (Scheme 4.15).

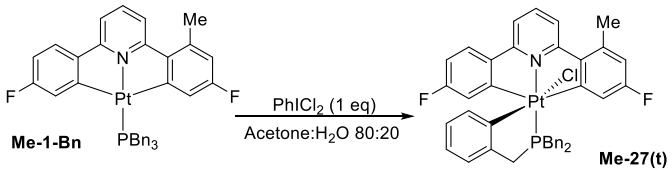

Scheme 4.15

4.3.2. Initiation of a Reductive Elimination Reaction with a Lewis Acid or Heat

Like the P-N *trans* tricyclometallated complex **27(t)**, the analogous **Me-27(t)** could not be purified by column chromatography, as it was shown to react on the silica. The reaction gave the P-N *cis* tricyclometallated complex **Me-27(c)**, and the reductive elimination complexes **Me-28(a)** and **Me-28(b)** (Scheme 4.16).

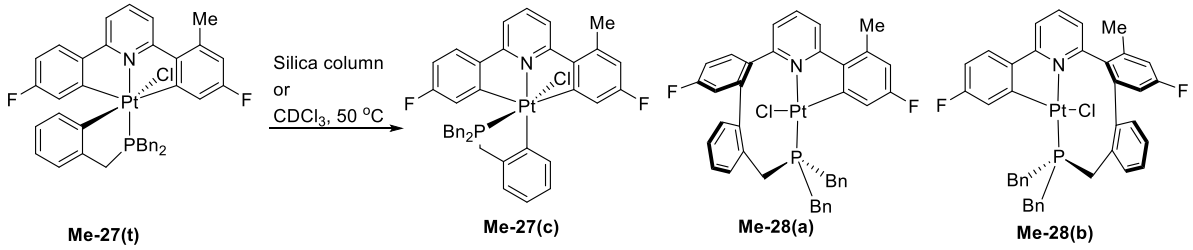

Scheme 4.16

A ratio of 6:1:1 for **Me-27(c)**:**Me-28(a)**:**Me-28(b)** (or 3:1 ratio for the isomerisation product vs reductive elimination products) shows **Me-27(c)** is the major recovered product. The total mass recovered from the column was far less than expected, and so degradation on the column can be assumed.

Complex **Me-27(c)**, the P-N *cis* tricyclometallated complex, was formed by the isomerization of **27(t)**. The solution spectra showed two peaks in the $^{19}F\{^{1}H\}$ NMR spectrum at -108.24 ppm ($^{4}J_{F\text{-}Pt}$ = 20 Hz) and -110.153 ppm ($^{4}J_{F\text{-}Pt}$ = 23 Hz) which indicated that the C^N^C ligand remained dicyclometallated. The benzyl ring was shown to be cyclometallated by a peak in the ^{1}H NMR spectrum at 8.27 ppm ($^{3}J_{H\text{-}Pt}$ = 31 Hz). A peak in the $^{31}P\{^{1}H\}$ NMR spectrum at 29.03 ppm ($^{1}J_{P\text{-}Pt}$ = 2723 Hz) and a doublet in the ^{195}Pt NMR spectrum at −3120 ppm ($^{1}J_{Pt\text{-}P}$ = ~3100 Hz) indicated a Pt^{IV} species. A crystal suitable for X-Ray analysis could not be grown, but further evidence of the structure can be found in the comparison of NMR data with **27(c)**. The peak in the $^{31}P\{^{1}H\}$ NMR spectrum at 29.03 ppm for **Me-27(c)** is almost identical to that of **27(c)** (29.00 ppm). The peak for the proton *ortho* to platinum on the benzyl ring in the ^{1}H NMR spectrum at 8.27 ppm for **Me-27(c)** is almost identical to that of **27(t)** (8.34 ppm). A peak (with height consistant with other neautral species observed during the course of this body of work) in the HR-MS (ESI) spectrum at 776.1787 m/z (corresponding to $[M\text{-}Cl]^{+}$) showed that **Me-27(c)** is a neutral species. Heating a chloroform solution of pure **Me-27(c)** at 50 °C showed no sign of change with time, and so it does not convert into **Me-28(a)** or **Me-28(b)**.

*Complexes **Me-28(a)** and **Me-28(b)** are structurally analogous to **28**, differing only by the presence of a methyl group on one of the fluoro-phenyl rings. NMR data for **Me-28(a)** and **Me-28(b)** were collected from a vial containing a non-equal amount of the two isomers collected during column chromatography. A summary of similar peak positions in the NMR spectra is shown in*

Table 4.1. Although the peak in the ^{195}Pt NMR spectrum of **28** appears about 500 ppm further upfield from **Me28(a/b)**, the peaks for **Me28(a/b)** are similar.

Table 4.1 Selected NMR data for comparison (chemical shifts quoted in ppm and coupling constants in Hz).

	28	**Me-28(a)**	**Me-28(b)**
^{1}H	6.55 ($^{3}J_{H\text{-}Pt}$ = ~60) (for H_b)	6.39	6.51
$^{19}F\{^{1}H\}$	-110.38 ($^{4}J_{F\text{-}Pt}$ = 57), -112.08	-112.37, -113.51 ($^{4}J_{F\text{-}Pt}$ = 52)	-110.49 ($^{4}J_{F\text{-}Pt}$ = 53), -113.73
$^{31}P\{^{1}H\}$	-9.29 ($^{1}J_{P\text{-}Pt}$ = 4552)	-6.91 ($^{1}J_{P\text{-}Pt}$ = 4622)	-8.22 ($^{1}J_{P\text{-}Pt}$ = 4527)
^{195}Pt	−3985	-3466	-3439

Assignment of structures of **Me-28(a)** and **Me-28(b)** with the available NMR data was more difficult than that of **Me-25(b)** (Scheme 4.14). In the ^{1}H NMR spectrum, the C^N^C ligands of either isomer have the same patterns of peaks (i.e. “dd, dt, dd” and “dd, dd”) for the fluoro-phenyl rings (Scheme 4.17). The assignment of the structures can be made by interpretation of the COSY spectrum, where the peak with platinum satellites (corresponding to the proton *ortho* to Pt and F) will couple to a “dd” for **Me-28(a)** and a “dt” for **Me-28(b)**.

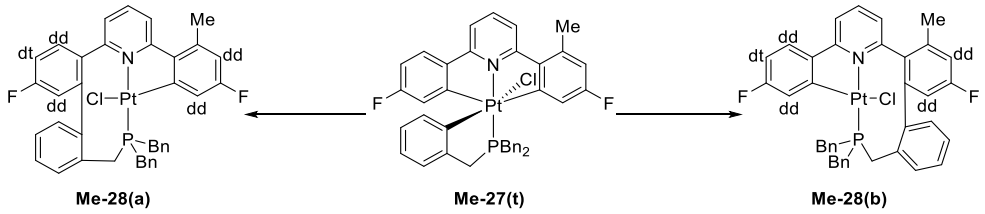

Scheme 4.17

As mentioned earlier, column chromatography gave poor yields to which insoluble degradation products are thought to be responsible. The ratio of **27(c)**:**28** recovered from the column was 1:4, showing a large excess of the reductive coupled product. In contrast, the ratio of **Me-27(c)**:**Me-28(a/b)** was 3:1, showing a greater amount of the tricyclometallated product. We believe that initially, the ratio of **27(c)**:**Me-28(a/b)** would be 1:4 (same as the symmetric). However, degradation of the reductive coupled products **Me-28(a/b)** gives the observed ratio. Further iterations of column chromatography of clean showed no reduction in yield, and so only **Me-28(a/b)** are sensitive to silica and **Me-27(c)** does not react with the silica.

Degradation of **Me-28(a/b)** continued after elution from the column, until full consumption of **Me-28(a/b)** (Scheme 4.18). The single degradation product **33** proved to be highly insoluble, and quickly formed crystals, which meant that only limited NMR data were obtained.

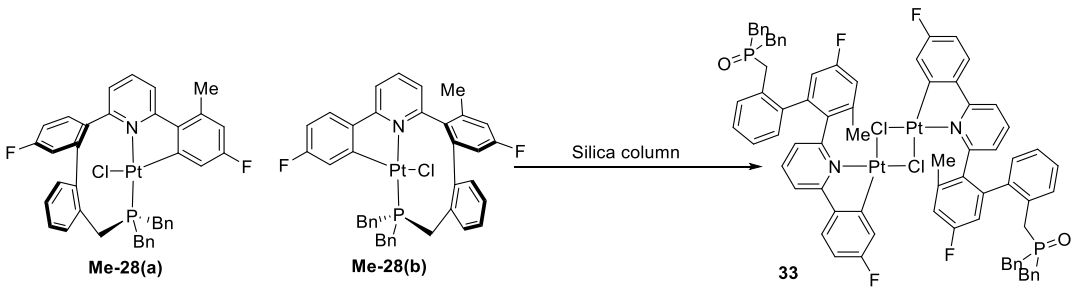

Scheme 4.18

A suitable crystal for X-ray analysis was found, and the crystal structure solved (Figure 4.11). The structure showed that **33** is a chloride bridged-dimer, and the dissociated phosphorus atoms have oxidised.

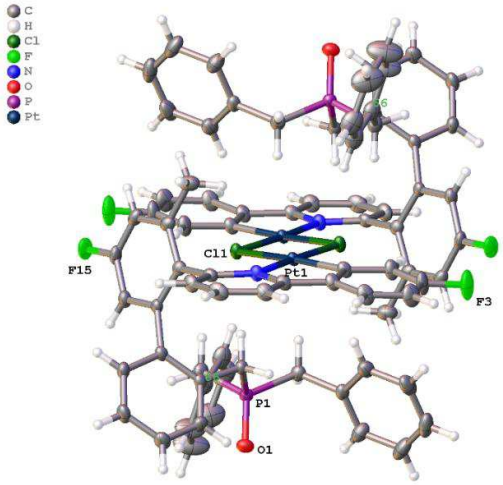

*Figure 4.11 Crystal structure of **33**, thermal ellipsoids drawn at 50% probability level.*
Selected bond lengths (Å) and angles (°): C1-Pt1, 1.968(4); C1-C2, 1.406(6); C1-C6, 1.401(5); O1-P1, 1.490(3); Pt1-Cl1^{1}, 2.4607(9); Pt1-Cl1, 2.2982(9); Pt1-N7, 2.052(3); C1-Pt1-Cl1, 93.50(12); C1-Pt1-Cl1, 171.00(13); C1-Pt1-N7, 81.59(15); Cl1-Pt1-Cl1^{1}, 79.15(3); N7-Pt1-Cl1^{1}, 105.73(9); N7-Pt1-Cl1, 175.09(9).

The solution spectra showed a peak in the $^{31}P\{^{1}H\}$ NMR spectrum without platinum satellites at 59.78 ppm, which suggested that the phosphorus had dissociated from the metal and had become oxidized. The peaks in the $^{19}F\{^{1}H\}$ NMR spectrum at -108.83 ppm ($^{4}J_{F\text{-}Pt}$ = 49 Hz) and -112.66 ppm showed that at least one fluoro-phenyl ring was still cyclometallated. Many other peaks were seen in the ^{1}H NMR spectrum, but they could not be assigned with certainty.

Unlike **27(t)**, **Me-27(t)** changed in solution with time. A chloroform solution of **Me-27(t)** was heated to 50 °C, and monitored by NMR. ^{1}H NMR spectra were recorded every hour for the first 24 hours, and then every other hour for the next 48 hours. The reaction gave

Me-27(c), **Me-28(a)** and **Me-28(b)** forming in a consistent 3:1:1 ratio (Scheme 4.16). The consistency of the product ratio over the reaction time suggests that the products do not interconvert. The relative amount of each complex was calculated by the integration of a peak in the ^{1}H NMR spectra corresponding to the methyl protons, which were then normalized to an unchanging peak (Figure 4.12). After 3-4 days, the presence of a degradation product had become significant (>10 %), and so only the results for the first 62 hours are shown. The points for **Me-28(a)** are obscured by **Me-28(b)**, as the relative amounts of each are almost identical.

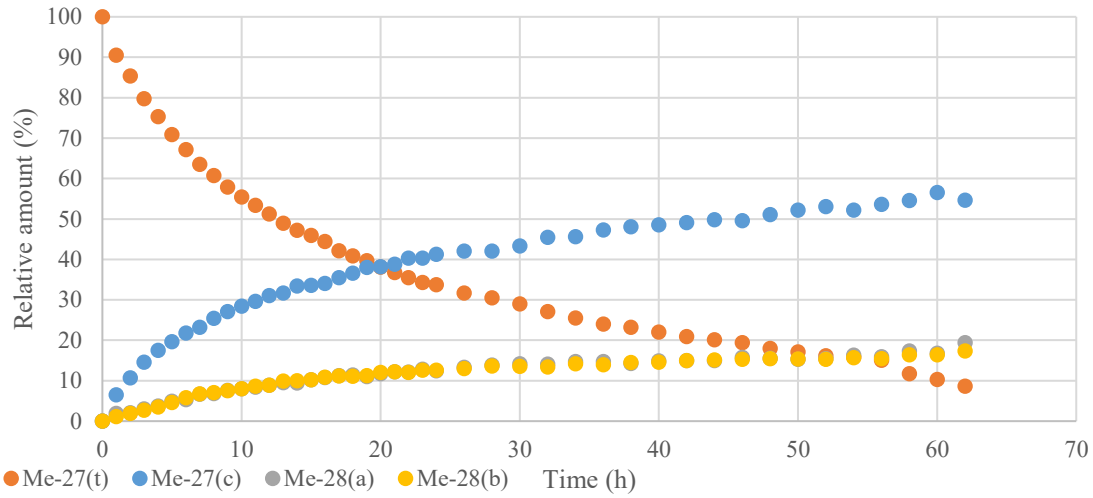

Figure 4.12 Plot of the relative amount of each complex against time.

4.3.3. Initiation of a Reductive Elimination Reaction with $AgBF_4$

Analogous to **27(t)**, reaction of **Me-27(t)** with $AgBF_4$ at 0 °C led to the reductive elimination of the benzyl ligand and a fluoro-phenyl in a C-C forming reaction. As soon as NMR data could be recorded, two products were seen with a ratio of about 3:1 **Me-30(a)**:**Me-30(b)** (Scheme 4.19).

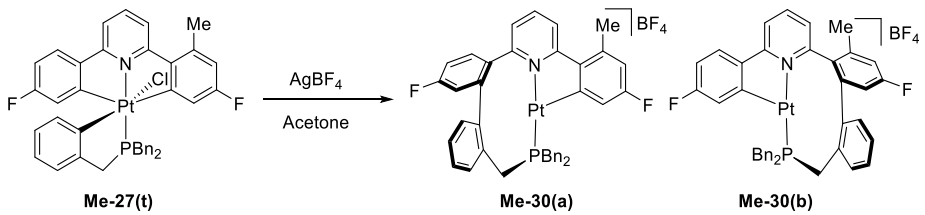

Me-27(t) **Me-30(a)** **Me-30(b)**

Scheme 4.19

The NMR data of **Me-30(a)** and **Me-30(b)** are very similar as they are structural isomers, differing only in the position of the methyl in the molecule. Table 4.2 shows some selected peaks in the NMR spectra which shows the similarities of the two isomers. Also shown is the analogous complex **30**. This time, the positions of the peaks in the ^{195}Pt are relatively similar, but the peaks in the $^{31}P\{^{1}H\}$ spectra vary by 9 ppm. This is likely to be because the methyl group is now likely to affect the conformation of the nine-membered ring.

Table 4.2 Selected NMR data for comparison (chemical shifts quoted in ppm and coupling constants in Hz).

	30	**Me-30(a)**	**Me-30(b)**
^{1}H	6.46 ($^{3}J_{H\text{-}Pt}$ = ~90) (for H_b)	6.19 (1H, m, $^{3}J_{H\text{-}Pt}$ = 110)	6.58
$^{19}F\{^{1}H\}$	-108.51 ($^{4}J_{F\text{-}Pt}$ = 65), -110.60	-109.64, -110.18 ($^{4}J_{F\text{-}Pt}$ = 72)	-109.95 ($^{4}J_{F\text{-}Pt}$ = 63), -112.68
$^{31}P\{^{1}H\}$	-9.49 ($^{1}J_{P\text{-}Pt}$ = 4119)	-7.73 ($^{1}J_{P\text{-}Pt}$ = 4043)	-0.55 ($^{1}J_{P\text{-}Pt}$ = 4463)
^{195}Pt	-3612	-3632	-3478

As the two complexes were made in non-equal proportions, they were easily distinguished, using the same method used to assign **Me-28(b)** and **Me-28(a)** (Scheme 4.17). The peak with platinum satellites (corresponding to the proton *ortho* to Pt and F) will couple to a "dd" for **Me-30(a)** and a "dt" for **Me-30(b)**.

In the $^{31}P\{^{1}H\}$ NMR, the peaks of **Me-30(a)** and **Me-30(b)** are about 7 ppm apart, suggesting that the methyl group effects the overall structure, yet it is unlikely that the structures are greatly different. The $^{1}J_{P\text{-}Pt}$ coupling constant for both complexes are both >4000 Hz, showing that both cases have a P-N *trans* geometry. It is more likely that the methyl group has a larger effect on the conformation of the nine-membered ring. It is already known that the methyl group clashes with the central pyridine in **Me-1-Bn**. If the methyl group is present on the nine-membered ring, the conformation may change to accommodate the relief of steric clash.

The relative amounts of **Me-30(a)** and **Me-30(b)** changed with time in solution at room temperature, and were monitored by NMR. The ^{1}H NMR data were recorded every hour for the first 24 hours, every other hour for the next 96 hours, followed by twice a day thereafter (Figure 4.13). The relative amounts of each complex were calculated by the integration of the aryl-Me protons in the ^{1}H NMR spectra, which were then normalized to an unchanging peak.

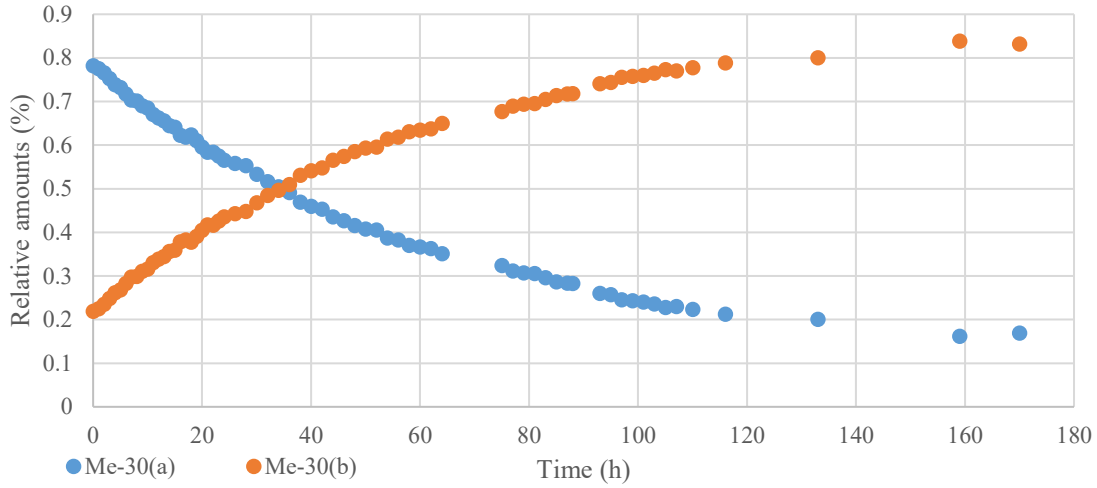

*Figure 4.13 Plot of the relative amounts of **Me-30(a/b)** with time.*

After about 8 days, the presence of a degradation product had become significant, and so only the results for the first 180 hours are shown. At 50 °C total degradation of both complexes was seen within an hour. Over the course of ~180 hours, the initial product ratio of 3:1 (**Me-30(a)**:**Me-30(b)**) eventually forms a dynamic equilibrium ratio of ~12:88. At equilibrium, the majority product **Me-30(b)** was the product predicted by the results of Chapter 3, where the methyl-substituted fluoro-phenyl eliminated with the R group. As the ratio does not appear to approach 100 % of either isomer, there must not be a large difference in energy between the two isomers.

Conversion between the two isomers would have to go through a five-coordinate intermediate (Scheme 4.20). The aryl-aryl bond formed during the reductive elimination reaction must be able to oxidatively add to the platinum, making a five-coordinate tricyclometallated intermediate, followed by reductive elimination of the coordinated benzyl with the other fluoro-phenyl ring.

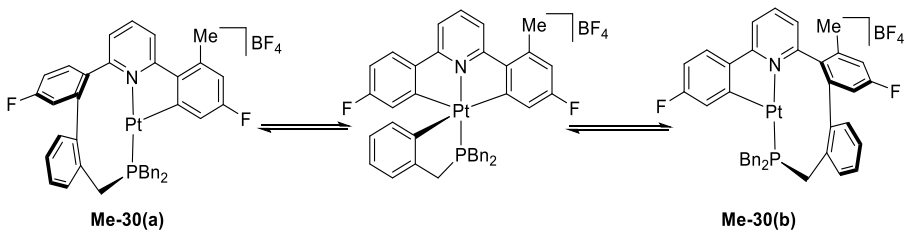

Scheme 4.20

The rates of conversion between isomers followed an exponential decay. The data was then manipulated to adjust for the fact that the reaction was not approaching full consumption of **Me-30(a)**, followed by a plot of $\ln(x-x_0)$ which gave a straight-line graph, showing first

order dependence (Figure 4.14). The slope is equal to the sum of the forward and back reaction of a reversible reaction (k_{obs} = k + k'). the final product ratio is equal to the relative ratio of the products and reactants (K = k/k'). Rearranging these equations allowed for the forward rate to be calculated at 0.0145 h^{-1} at 298 K.

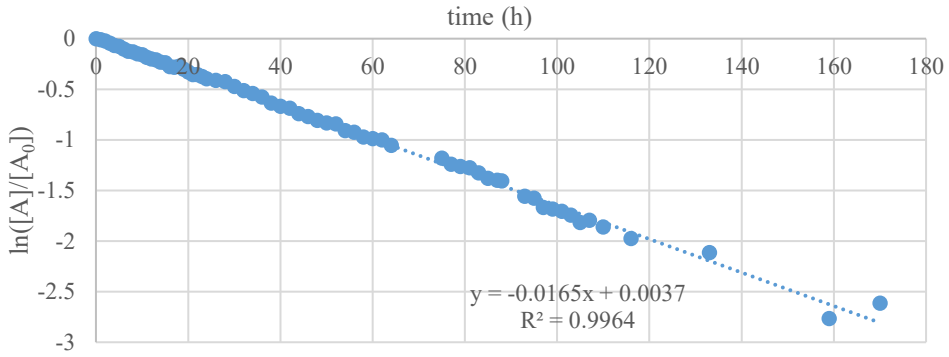

Figure 4.14 Plot of ln([A]/[A_o]) against time.

The rate limiting step is the C-C bond activation (formation of the five-coordinate intermediate), because the reductive elimination reaction had already proven to be too fast to observe. Now, to return to the interconversion of peaks seen in the ^{1}H NMR spectrum of **30** (Section 4.2.3), an interconversion via a five-coordinate intermediate can now be ruled out. The rate of interconversion at 298 K is relatively slow on the NMR timescale (as the separation of H_x is 180 Hz), but fast on a scale of minutes and hours. The rate of conversion between **Me-30(a)** and **Me-30(b)** through a five-coordinate intermediate is much slower (half-life of about 48 hours) and so the interconversion between the two states of **30** must be an inversion of the nine-membered ring. We see no evidence of a C-C agostic interaction in the ^{13}C NMR. Both carbons are quarternary, and so the peak heights are already too small without looking for platinum satellites. We did not attempt to run a ^{13}C NMR spectrum at a lower temperature, which should be done if we are to rule out a C-C agostic interaction.[186]

In Chapter 3, reductive elimination of methyl-aryl was 100% regiospeciffic to the previously substituted side. As the initial ratio of **Me-30(a)** and **Me-30(b)** is not 50:50 ratio, it is apparent that in the case of C(sp^2)-C(sp^2) coupling, the preference appears to be reversed. It is not obvious why this is the case, but it is suggested that the same "twisting" of the methyl substituted fluoro-phenyl (because of the steric clash of the methyl group and the central pyridine) is again responsible, as the directionality of the orbitals of a C(sp^2) are very different to that of a C(sp^3) (i.e. the p-orbital of the Pt-C on the fluoro-phenyl ring in the plane of the C^N^C ligand will overlap better with the benzyl Pt-C p-orbital).

4.4. Further Reactivity of the Three-Coordinate Complex **30**

Complex **30** is a three-coordinate species, and is therefore coordinatively unsaturated. In previous chapters, coordinating ligands have been shown to coordinate to some five-coordinate intermediates. Low temperature ^{1}H NMR spectra of **30** shows that the fourth coordination site is not taken by water. The open coordination site could be exploited to coordinate other small groups. CO and H_2 were used as they are good ligands for low oxidation states and are of great industrial importance. It was not known if further reactions would take place, or even if the ligands would coordinate at all.

Complex **30** was synthesized in the same way as shown in Scheme 4.11, with the resulting acetone-d_6 solution being transferred to an NMR tube fitted with a J. Young's tap. Reactions of either gas were carried out by freezing the solution with liquid nitrogen, followed by removal of air, and replacing with the gas of choice.

4.4.1. Addition of CO

The colour of the solution quickly lightened upon the addition of CO to the acetone solution of **30**, which eventually became colourless. NMR data taken as soon as was possible showed full conversion to a new product **31** (Scheme 4.21). A peak in the HR-MS (ESI) spectrum at 762.1606 m/z (corresponding to $[M]^+$) and an absorbance in the IR spectrum at 2097 cm^{-1} (which is similar to CO stretches in related complexes) showed that CO had coordinated to the metal.[140]

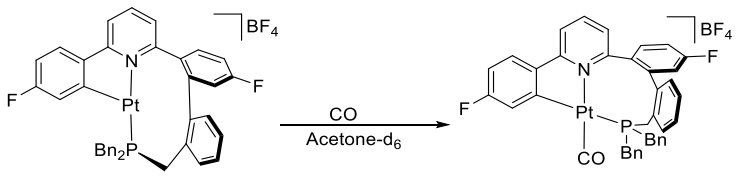

30 **31**

Scheme 4.21

In the ^{195}Pt spectrum, a doublet at -3976 ppm indicated a Pt^{II} species. The spectra showed two peaks in the ^{19}F{^{1}H} NMR spectrum at -105.85 ppm and a doublet with platinum satellites at -109.55 ppm (d, $^{5}J_{F\text{-}P}$ = 5.5 Hz, $^{4}J_{F\text{-}Pt}$ = 36 Hz). The doublet was shown to be because of long-range coupling from the phosphorus by the presence of a doublet in the ^{31}P{^{1}H} NMR spectrum at 11.50 ppm (d, $^{5}J_{P\text{-}F}$ = 5.5 Hz, $^{1}J_{P\text{-}Pt}$ = 1694 Hz) with the same

coupling constant. Coupling between the fluorine and phosphorus, and a large reduction in the $^{1}J_{P\text{-}Pt}$ coupling constant suggests that the phosphorus is now *trans* to the cyclometallated aryl ring. The pyridine nitrogen was shown to still be attached to platinum due to residual phosphorus coupling seen in the carbons adjacent to the nitrogen on the pyridine ring. Therefore, the CO resides *trans* to the nitrogen.

Data from nOe experiments could neither prove nor disprove the proposed structure. No further reactions took place with time, and therefore **31** proved to be indefinitely moisture and air stable even after removal from the J. Youngs tube. The CO would have originally added to **30** at the coordination site opposite the cyclometallated fluorophenyl ring. Isomerisation of the complex (where the CO and phosphorus swap places) would follow because of transphobia, where C-M-P is more favoured than C-M-C.[148] Ring strain is expected to be even higher in the nine-membered ring in **31**, but this will be offset by having the CO *cis* to the cyclometallated fluorophenyl ring.

4.4.2. Addition of H_2

Upon adding H_2 to an acetone solution of **30**, the colour lightened before turning dark orange. As soon as NMR data could be recorded, only a single product **32** was observed (Scheme 4.22).

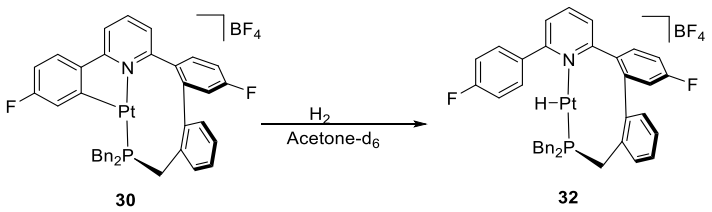

30 **32**

Scheme 4.22

A broad singlet in the $^{31}P\{^{1}H\}$ NMR spectrum at 1.31 ppm ($^{1}J_{P\text{-}Pt}$ = 5015 Hz) indicated a Pt^{II} complex. Neither of the peaks in the $^{19}F\{^{1}H\}$ NMR spectrum at -110.40 ppm and -112.62 ppm had Pt satellites, and therefore neither fluoro-phenyl was coordinated to platinum. A broad peak in the ^{1}H NMR spectrum at -24.34 ppm ($^{1}J_{H\text{-}Pt}$ = 1230 Hz) indicated a Pt-H bond.[187]

The peak in the HR-MS (ESI) spectrum at 764.1772 m/z is two mass units larger than **30** further suggesting that H_2 had added. Coordination of the pyridine was inferred by the

pattern of PhCH_2 peaks in the ^{1}H NMR spectrum, where individual peaks for each PhCH_2 proton suggested that (like **30**) ring flipping of the nine-membered ring is restricted. Initially the H_2 would have taken the fourth coordination site of **30**, forming a dihydrogen species (Scheme 4.23).[34]

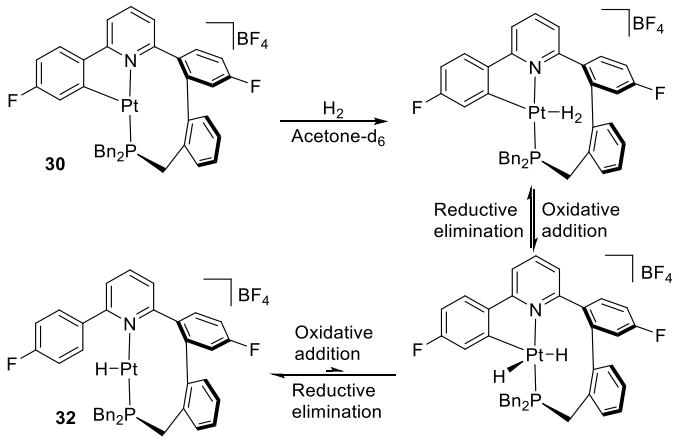

Scheme 4.23

Oxidative addition of hydrogen would have led to a Pt^{IV} five-coordinate di-hydride complex which would quickly eliminate Ar-H (but could also return to the dihydrogen complex) to give the observed product **32**. Although the dihydrogen species was not observed by NMR, the presence of this species could explain the initial colour change seen upon the addition of H_2.

4.4.3. H/D Exchange

No agostic interaction was seen in the ^{195}Pt - ^{1}H correlation spectrum of **30** at room temperature. However, it is likely that the proton *meta* to the fluorine on the aryl ring that is not part of the nine-membered ring interacts with the platinum, because of its proximity to the metal, and similarity to complexes such as **6-Bu(t)**. As seen in Scheme 4.23, **32** is formed by reductive elimination from a Pt^{IV} five-coordinate di-hydride complex. Although **32** is the thermodynamic product, it is possible that the elimination is reversible, with the reaction heavily favouring the formation of **32**.

This hypothesis was tested by studying the H/D exchange of not only the Pt-H bond, but also that of the protons on the fluoro-phenyl ring that could be *ortho*-metallated. As the incorporation of each deuterium increases the mass by one mass unit, the relative amounts deuterium incorporation was monitored by ESI-MS. Direct monitoring of peak heights was

not possible as platinum has several isotopes, which gives a distinctive pattern of peaks for platinum-containing compounds. The natural abundance of each isotope shown in Table 4.3. ^{194}Pt – ^{195}Pt are 1 unit apart, which means that addition of deuterium atoms would overlap with these peaks in the ESI-MS.

Table 4.3 Natural abundances of platinum isotopes

Isotope	Natural abundance
192	0.782
194	32.86
195	33.78
196	25.21
198	7.36

The relative amount of ^{192}Pt is small enough to be ignored. The mass of the complexes in this thesis are defined by the peak in the ESI-MS that includes the ^{194}Pt isotope. The atomic mass of **32** (~764) means that the platinum is ^{194}Pt, all protons are ^{1}H, all carbons are ^{12}C etc. Before the addition of D_2O, the distribution (and height) of the peaks in the ESI-MS line up well with the pattern for the natural abundance of platinum isotopes, as the amount of naturally occurring ^{2}H and ^{13}C is very low. The degree of labelling can therefore be estimated based on the peak heights in the ESI-MS.

With no deuterium atoms incorporated (**32-0D**), the peak at ~765 m/z will be 33.78 arbitrary units high relative to the peak at ~764 m/z which would be 32.86 arbitrary units high. The exchange of a proton for a deuterium increases the mass of the complex by one, as a deuterium atom weighs one unit more than hydrogen. Therefore, if the peak at ~765 m/z is greater than 33.78 arbitrary units (relative to 32.86 arbitrary units high for the peak at ~764 m/z) then a deuterium has been incorporated (**32-1D**), and **32-1D** is entirely responsible for remaining height. The degree of H/D exchange can then be calculated as a percentage based on the amount of 0D and 1D. This method can then be extended to include the incorporation of two (**32-2D**) and three (**32-3D**) deuterium atoms.

D_2O (excess) was added to an acetone solution of **32-0D**. The mixture was then shaken, and the reaction monitored by ESI-MS, monitored by recording a mass spectrum hourly for the first nine hours, followed by 24 hourly intervals for a total of two weeks, showing the incorporation of up to three deuterium atoms (Figure 4.15).

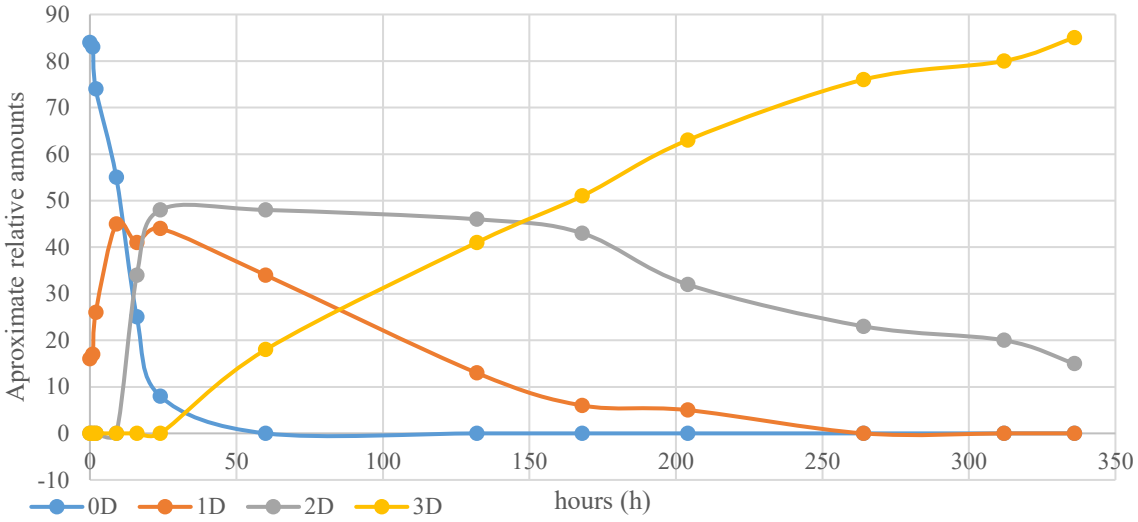

Figure 4.15 Plot of the relative amounts of deuterium replaced species in a deuterated solvent with time.

The first proton is exchanged quickly (>90 % consumption within the first 24 hours, and full consumption within 50 hours) shown by a steep decrease in the relative amount of **32-0D**. The relative amount of **32-1D** grew in line with the decrease of **32-0D** until around 12 hours, where the relative amount of **32-1D** reaches 50 %. The relative amount of **32-1D** does not exceed 50 % as **32-2D** begins to grow at roughly the same rate as **32-1D** disappears. When **32-0D** had been fully consumed, the relative amount of **32-1D** began to decrease, as **32-3D** began to appear. The relative amount of **32-2D** has reached a plateau (also at roughly 50 %) as the rate of formation from **32-1D** is roughly equal to its conversion to **32-3D**. After 150 hours (when **32-1D** had almost been fully consumed), the relative amount of **32-2D** began to decrease. The relative amount of **32-3D** increases quite linearly throughout the reaction time.

The proposed mechanism for the formation of **32-3Da** from **32-0Dc** is shown in Scheme 4.24. As the mechanism is a series of repeated steps, the reaction can be reduced to four paths (labelled **a**-**d**) which are all reversible. There are several complexes for **32-1D** and **32-32-2D** that would not be distinguished by ESI-MS, and therefore the numbering system has been further expanded to accommodate these complexes. As with the numbering system of the reaction paths, the numbering of the complexes also infers similarity.

Path **a** is where we expect the Pt-H bond to be exchanged for Pt-D (forming **Da**), increasing the number of deuterium atoms on the molecule by one.[188] The reaction is relatively slow, taking roughly a day for conversion of all Pt-H bonds (Figure 4.15) The replacement of the Pt-H with Pt-D is also reversible, but unlikely due to there being a large excess of D_2O in solution. Path **b** shows the oxidative addition of the available fluoro-phenyl ring, forming a five-coordinate monocyclometallated dihydride Pt^{IV} species **Db**

(although one of the hydrides is a deuterium). **Db** is not expected to stay in solution long, and will quickly eliminate aryl-H or aryl-D. Path **c** shows the reductive elimination of aryl-D to give **Dc**, a complex with a Pt-H bond, and the deuterium has been transferred to the decyclometallated fluoro-phenyl ring. These complexes can exchange with D_2O again. Path **d** leads to **Dd**, which are dead-end complexes. **Dd** must revert back to **Da** for the reaction to continue forwards. As a dihydride species is not expected to last long in solution (because of the possibility of reductive elimination reactions), it is unlikely that Pt-H H/D exchange occurs at complexes **Db** or **Dd**.

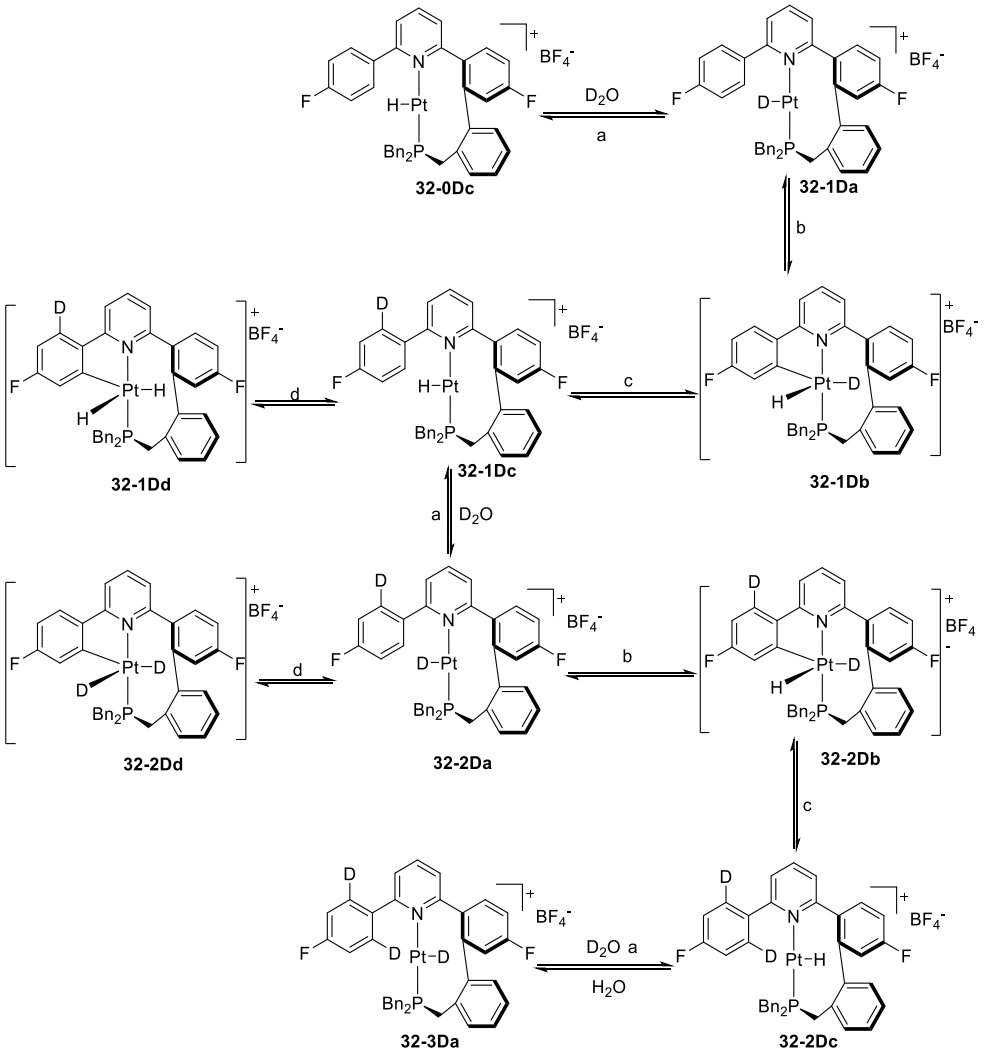

Scheme 4.24

After full conversion to **32-3Da**, H_2O was added to a sample of **32-3Da** and the exchange was monitored by ESI-MS for the first day, which showed full incorporation of the first hydrogen, giving **32-2D**. It should be noted that ^2H NMR experiments should be run to remove ambiguity of the positions of the incorporated deuterium atoms.

4.5. Conclusion

With Chapter 2 focussing on the activation of C(sp^3)-H bonds, this chapter instead uses a ligand with an C(sp^2)-H bond in a position that could afford a five-membered ring if activated. This also builds on previous work done in the Rourke group.[182] This work goes further by adding silver to the octahedral Pt^{IV} C-H activation products to initiate reductive elimination, similar to that seen in Chapter 3. Reductive elimination from a Pt^{IV} complex having an asymmetric C^N^C ligand gave insight into the selectivity of the reductive elimination reaction, with results comparable to those in Chapter 3.

C(sp^2)-H bonds were activated by electrophilic five-coordinate Pt^{IV} centres to form tricyclometallated octahedral complexes. Removal of the halide from these complexes with silver salts initiated a C-C reductive elimination in which two aryl rings coupled to give a three-coordinate product with a nine-membered ring. Variable temperature NMR showed that the conformation of the ring is strained, meaning that inversion of the ring is a relatively high energy process. The large ring size left enough space for small molecules such as chloride, CO, and H_2 to coordinate to the remaining coordination site.

In the case of the asymmetric C^N^C ligand (e.g. **Me-1-Bn**), removal of the halide from the analogous tricyclometallated complex gave two complexes with nine-membered rings (differing only by whether the methyl is on the nine-membered ring) in a ratio of 4:1 (favouring benzyl coupling with the fluoro-phenyl ring without the methyl). With time, the relative quantities changed to give a dynamic equilibrium of 85:15 which instead favoured the product with the methyl substituted fluoro-phenyl ring being coupled to the benzyl ring. This product was predicted by the results of Chapter 3. The change of the relative amounts with time invoked a mechanism in which the C-C bond breaks across the platinum centre (forming a five-coordinate intermediate) followed by the benzyl group coupling with the other fluoro-phenyl ring.

Future work could look at the reductive elimination of an C(sp^3)-C(sp^2) bond, forming a structurally similar nine-membered ring to see if the C(sp^3)-C(sp^2) bond could also be activated by the platinum (cf. dynamic bond activation seen in this chapter).

5.0 Conclusions and Future Work

Coordinatively unsaturated complexes, known for being short-lived and highly reactive, are thought to be critical intermediates in catalytic cycles, making the study of these complexes important to both industry and academia. Five-coordinate complexes can be generated via the addition of Y^+ to a 16 valence electron square planar complex, or the removal of X^- from an 18 valence electron octahedral complex. These happen to be the initial steps of the S_N2 mechanisms of oxidative addition and reductive elimination reactions, respectively.

Dicyclometallated square planar complexes were studied with the general form of C^N^C $Pt^{II}(PR_3)$, which had been studied previously in the Rourke group.[138,145,149,151] In this project, C^N^C typically referred to 2,6-di(4-fluorophenyl)pyridine.. These complexes were used to synthesize the Pt^{IV} 18 valence electron octahedral complexes through oxidative addition of $PhICl_2$ or alkyl halides.

Preliminary oxidative addition experiments completed by previous members of the Rourke group showed that the addition of Cl_2 (via treatment with $PhICl_2$) gives octahedral dichloro- Pt^{IV} complexes.[149,151] Initially a P-N *trans* dichloro- complex forms, followed by isomerisation to a *cis* dichloro- complex. Initial formation of P-N *trans* complex is kinetically driven, and expected, given the S_N2 type mechanism. The isomerisation of P-N *trans* to *cis* was noted routinely throughout this thesis, and was argued on the basis of putting the large phosphine out of the plane of the C^N^C ligand. Isomerisation to the P-N *cis* complex was therefore expected on the basis of being the thermodynamic product, assuming no other issues (e.g. competing ligands).

The work presented in this thesis has shown that with careful choice of L, steric hindrance (when L = PPh_3), intramolecular interactions (when L = PBu_3, PPr_3, P^oTol_3 and PBn_3), and auxiliary ligands (added pyridine) are factors that can be manipulated to trap five-coordinate intermediates. In each case the second equivalent of chloride is outcompeted for, or blocked from, the sixth coordination site, and so the initial complex is a chloride salt. Where the sixth coordination site was taken by an intramolecular interaction, C-H bond activation was seen. The activation of $C(sp^3)$ and $C(sp^2)$ leads to transcyclometallation and tricyclometallation complexes, respectively. It has also been shown that solvent choice is also a factor; chloroform is preferred as a non-coordinating solvent, whilst a mixture of acetone and water allow for the deprotonation of acidic intermediates.

The oxidative addition of MeI to square planar complexes did not display such variety. Only the octahedral Pt^{IV} products with the separate methyl and iodide groups added across the metal were observed, a product which may be considered analogous to the dichloro-complexes.

Removal of a chloride from octahedral dichloro- complexes led the formation of stable five-coordinate species. Removal of the iodide from (C^N^C) $Pt^{II}(PR_3)MeI$ led to a long-lived five-coordinate complex, which could be identified in solution, and could also be trapped with pyridine. Over time (about five hours), the methyl group coupled irreversibly with the fluorophenyl ring to give a three-coordinate complex. The rate of this reductive elimination was increased with larger phosphines. The relative slowness of this reductive coupling is due to the forced *mer* geometry of the rigid C^N^C ligand.

Removal of the chloride from the tricyclometallated complex (derived from the oxidation of the (C^N^C) $Pt^{II}(PBn_3)$ starting material did not give an observable five-coordinate intermediate (and could not be trapped with pyridine). Instead, a three-coordinate complex formed in which the coordinated benzyl group, and a flurophenyl group, coupled to give a nine-membered ring. Small mlecules such as chloride, CO, and H_2 were shown to coordinate to the fourth coordination site. NMR experiments with the methyl derivative of the complex with a nine-membered ring showed that the nine-membered ring occasionally oxidatively adds to the platinum, forming a five-coordinate intermediate, but also quickly reductively eliminates.

In summary, this body of work probes a broad range of reactivity for 16 valence electron five-coordinate Pt^{IV} C^N^C dicyclometallated intermediates. These intermediates were accessed through the oxidation of 16 valence electron Pt^{II} square planar complexes (with $PhICl_2$ or MeI), or the abstraction of a halide from an 18 valence electron Pt^{IV} octahedral complexes. Formation of these intermediates led to C-H bond activation and C-C bond formation reactions which are of industrial importance.

The work presented in this thesis has focussed heavily on the 2,6-di(4-fluorophenyl) pyridine ligand. Future work could explore different C^N^C ligands (including the 2-(4-fluorophenyl)-6-*tert*butyl pyridine ligand seen in Section 3.3) to further probe the selectivity of the mechanisms seen throughout this thesis.

6.0 Experimental

6.1. General Considerations

All chemicals were used as supplied, unless noted otherwise. $PhICl_2$ was synthesised using the established method.[189] All NMR spectra were obtained on a Bruker Avance 400, 500 or 600 MHz spectrometers and were recorded at room temperature, in chloroform, unless stated otherwise. ^{1}H and $^{13}C\{H\}$ are referenced to external TMS, assignments being made with the use of decoupling, nOe and the DEPT and COSY pulse sequences. $^{31}P\{^{1}H\}$ spectra were referenced to external 85% H_3PO_4. $^{19}F\{^{1}H\}$ chemical shifts are quoted from the directly observed signals referenced to external $CFCl_3$. ^{1}H-^{195}Pt correlation spectra were recorded using a variant of the HMBC pulse sequences with the ^{195}Pt chemical shifts quoted taken from the 2D HETCOR spectra and referenced to external Na_2PtCl_6. Coupling values to the ^{195}Pt nucleus are quoted, however platinum satellites are excluded from stated multiplicities. Column chromatography was carried out on silica 40-63 μ, 60 Å (Fluorochem). All elemental analyses were performed by Warwick Analytical Services. All mass spectra were run on either a Bruker maXis or maXis plus, running in positive ion mode. The peaks recorded for the calculated and observed m/z correspond to peak where all atoms in the molecule have isotopes of the lowest naturally abundant mass. The platinum isotope ^{194}Pt was used instead of ^{192}Pt as the low natural abundance of ^{192}Pt could mean that the peak is not seen above the baseline. Infrared spectra were recorded with a Bruker ALPHA.

X-ray crystal structures were collected on an Oxford Diffraction Xcalibur Gemini diffractometer with a Ruby CCD area detector or Rigaku Oxford Diffraction SuperNova diffractometer with a duel source (Cu at zero) equipped with an AtlasS2 CCD area detector with individual details given in the appendix. CIFs for all X-ray crystal structures are attached electronically. Using Olex2,[190] the structure was solved with the XS structure solution program[191] using Direct Methods and refined with the ShelXL[191] refinement package using Least Squares minimisation.

While elemental analysis (CHN) data was obtained, many fall outside the acceptable 4% margin of error. It is not well understood why this is the case. Most samples were recovered after purification by column chromatograpy. All samples were shown to dissolve fully in an organic solvent, demonstrating that common inorgaic salts such as K_2CO_3 or NaCl are unlikely to be present. Samples were dried for extended periods of time under high vacuum. It could still be likely that errors in the elemental analysis are due to residual solvents, however, this was not proven.

6.2. Starting Materials (C^N^C = 2,6-di(4-fluorophenyl)pyridine)

6.2.1. Synthesis of **1-Bu** and **1-Pr** (air sensitive phosphines)

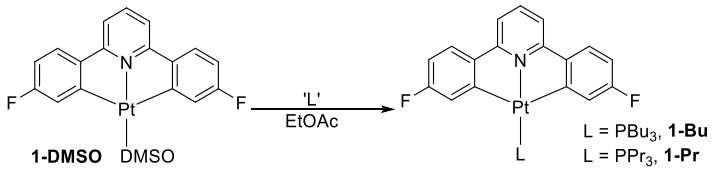

Synthesized from the previously reported **1-DMSO**.[138] To an EtOAc (20 ml) solution of **1-DMSO** (100 mg, 1.85 x 10^{-4} mol) in a Schlenk flask under nitrogen, was added the required phosphine (0.1 ml, excess) with vigorous stirring. After 5 minutes the solvent was removed by vacuum (the trap was rinsed with an iodide solution after to neutralise any phosphine that had distilled across). The crude product was then purified by column chromatography, loading and eluting with toluene to give product as a bright yellow solid (**1-Bu:** 125 mg, 1.84 x 10^{-4} mol, 99% **1-Pr:** 112 mg, 1.80 x 10^{-4} mol, 97%).

Complex - **1-Bu**

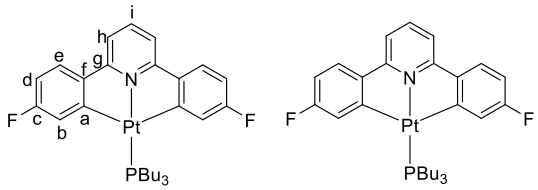

δ_H = 7.56 (1H, t, $^3J_{H\text{-}H}$ = 8 Hz, H_i), 7.45 (2H, dd, $^3J_{H\text{-}H}$ = 8.5 Hz, $^4J_{H\text{-}F}$ = 5.5 Hz, H_e), 7.2 (4H, m, $H_{b,h}$), 6.71 (2H, dt, $^3J_{H\text{-}F}$ = $^3J_{H\text{-}H}$ = 8.5 Hz, $^3J_{H\text{-}H}$ = 2.7 Hz, H_d), 2.09 (6H, m, P*CH*$_2$), 1.57 (6H, m, PCH$_2$*CH*$_2$), 1.44 (6H, sex, $^3J_{H\text{-}H}$ = 7.5 Hz, PCH$_2$CH$_2$*CH*$_2$), 0.89 (9H, t, $^3J_{H\text{-}H}$ = 7.5 Hz, PCH$_2$CH$_2$CH$_2$*Me*) ppm.

δ_C = 12.62 (s, PCH$_2$CH$_2$CH$_2$*Me*), 23.13 (d, $^1J_{C\text{-}P}$ = 15 Hz, $^2J_{C\text{-}Pt}$ = 40 Hz, P*CH*$_2$), 23.35 (s, $^3J_{C\text{-}Pt}$ = 32 Hz, PCH$_2$CH$_2$*CH*$_2$), 25.83 (s, $^4J_{C\text{-}Pt}$ = 32 Hz, PCH$_2$*CH*$_2$), 109.30 (d, $^2J_{C\text{-}F}$ = 22 H, C_d), 113.44 (d, $^6J_{C\text{-}F}$ = 2.5 Hz, $^3J_{C\text{-}Pt}$ = 25 Hz, C_h), 123.18 (d, $^2J_{C\text{-}F}$ = 16.5, $^2J_{C\text{-}Pt}$ = 62 Hz, C_b), 124.84 (d, $^3J_{C\text{-}F}$ = 8.5 Hz, $^3J_{C\text{-}Pt}$ = 31 Hz, C_e), 138.91 (s, C_i), 146.07 (m, C_f), 163.00 (d, $^1J_{C\text{-}F}$ = 254 Hz, $^3J_{C\text{-}Pt}$ = 52 Hz, C_c), 164.00 (s, $^2J_{C\text{-}Pt}$ = 61 Hz, C_g), 167.87 (m, $^1J_{C\text{-}Pt}$ = 714 Hz, C_a) ppm.

δ_F = -111.59 ($^4J_{F\text{-}Pt}$ = 28 Hz) ppm.

δ_P = 0.10 ($^1J_{P\text{-}Pt}$ = 3713 Hz) ppm.

δ_{Pt} = -4215 (d, $^1J_{Pt\text{-}P}$ = ~3700 Hz) ppm.

Elemental analysis found (calculated): C 51.00 (52.56), H 5.31 (5.48), N 1.96 (2.11).

Complex - **1-Pr**

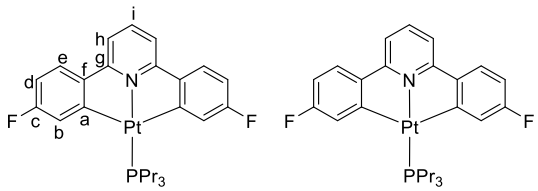

δ_H = 7.58 (1H, t, $^3J_{H\text{-}H}$ = 8 Hz, H_i), 7.47 (2H, dd, $^3J_{H\text{-}H}$ = 8.5 Hz, $^4J_{H\text{-}F}$ = 6 Hz, H_e), 7.22 (4H, m, $H_{b,h}$), 6.73 (2H, dt, $^3J_{H\text{-}F}$ = $^3J_{H\text{-}H}$ = 8.5 Hz, $^3J_{H\text{-}H}$ = 2.7 Hz, H_d), 2.09 (6H, m, P*CH₂*), 1.66 (6H, m, PCH₂*CH₂*), 1.05 (9H, t, $^3J_{H\text{-}H}$ = 7.5 Hz, PCH₂CH₂*Me*) ppm.

δ_C = 15.72 (d, $^3J_{C\text{-}P}$ = 16 Hz, PCH₂CH₂*Me*), 17.61 (s, $^3J_{C\text{-}Pt}$ = 31.5 Hz, PCH₂*CH₂*), 26 (d, $^1J_{C\text{-}P}$ = 35 Hz, $^2J_{C\text{-}Pt}$ = 34 Hz, P*CH₂*), 109.34 (d, $^2J_{C\text{-}F}$ = 23 Hz, H_d), 113.46 (d, $^6J_{C\text{-}F}$ = 3 Hz, $^3J_{C\text{-}Pt}$ = 27 Hz, H_h), 123.12 (d, $^2J_{C\text{-}F}$ = 17 Hz, $^2J_{C\text{-}Pt}$ = 64, H_b), 124.88 (d, $^3J_{C\text{-}F}$ = 8.5 Hz, $^3J_{C\text{-}Pt}$ = 31 Hz, H_e), 139 (s, H_i), 146.07 (m, $^2J_{C\text{-}Pt}$ = 26 Hz, H_f), 163.34 (d, $^1J_{C\text{-}F}$ = 255 Hz, $^3J_{C\text{-}Pt}$ = 54 Hz, H_c), 163.98 (s, $^2J_{C\text{-}Pt}$ = 67 Hz, H_g), 167.80 (d, $^3J_{C\text{-}F}$ = 8 Hz, $^1J_{C\text{-}Pt}$ = 718 Hz, H_a) ppm.

δ_F = -111.44 ($^4J_{F\text{-}Pt}$ = 28 Hz) ppm.

δ_P = 1.34 ($^1J_{P\text{-}Pt}$ = 3712 Hz) ppm.

δ_{Pt} = -4212 (d, $^1J_{Pt\text{-}P}$ = ~3750 Hz) ppm.

HR-MS (ESI): found 620.1783 m/z, calculated 620.1782 m/z = $C_{26}H_{30}F_2NP^{194}Pt$ = $[M]^+$.

Elemental Analysis found (calculated): C 50.04 (50.32), H 4.84 (4.87), N 2.27 (2.26).

Crystals suitable for X-ray analysis were grown by the slow evaporation of solvent from a chloroform solution – ps9.

6.2.2. Synthesis of **1-Tol** and **1-Bn** (air stable phosphines)

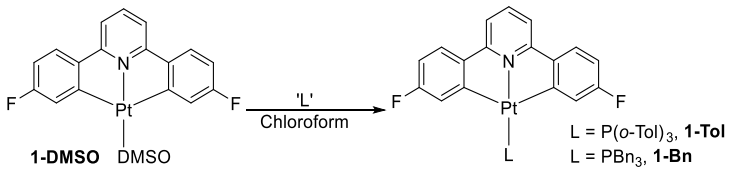

Synthesized from the previously reported **1-DMSO.**[138] To a chloroform (20 ml) solution of **1-DMSO** (100 mg, 1.85 x 10^{-4} mol) was added the required phosphine (1 eq). The mixture was allowed to stir for 5 minutes before removal of the solvent by evaporation. The crude product was purified by column chromatography loading and eluting with toluene to give pure product as a bright yellow powder (**1-Tol:** 142 mg, 1.85 x 10^{-4} mol, quantitative yield, **1-Bn:** 142 mg, 1.85 x 10^{-4} mol, quantitative yield). **1-Ph** was made in a similar way, and was characterised by a past member of the Rourke group.[151]

Complex - **1-Tol**

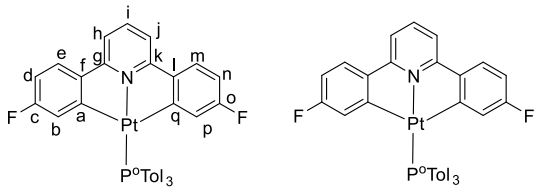

δ_H = 8.99 (1H, dd, $^3J_{H\text{-}H}$ = 16 Hz, $^3J_{H\text{-}H}$ = 8 Hz, H_{Ar})*, 7.67 (1H, dd, $^3J_{H\text{-}H}$ = 11 Hz, $^3J_{H\text{-}H}$ = 8 Hz, H_{Ar}), 7.63 (1H, dd, $^3J_{H\text{-}H}$ = 8 Hz, H_i), 7.23-7.47 (9H, m, H_{Ar}) 7.41 (1H, H_e), 7.38 (1H, H_m), 7.26 (2H, dd, $^3J_{H\text{-}H}$ = 8 Hz, $H_{h,j}$), 7.14 (2H, m, H_{Ar}), 6.62 (1H, dt, $^3J_{H\text{-}H}$ = $^3J_{H\text{-}F}$ = 8 Hz, ^4J = 2 Hz, H_d), 6.58 (1H, dt, $^3J_{H\text{-}F}$ = $^3J_{H\text{-}H}$ = 8 Hz, $^4J_{H\text{-}H}$ = 2 Hz, H_n), 6.55 (1H, dd, $^3J_{H\text{-}F}$ = 11 Hz, $^4J_{H\text{-}H}$ = 2 Hz, $^3J_{H\text{-}Pt}$ = 29 Hz, H_p), 5.73 (1H, dd, $^3J_{H\text{-}F}$ = 11 Hz, $^4J_{H\text{-}H}$ = 2 Hz, $^3J_{H\text{-}Pt}$ = 26 Hz, H_b), 2.99 (3H, s, Me), 1.88 (3H, s, Me), 1.75 (3H, s, Me) ppm.

*This proton shows a correlation to platinum when the coupling constant is set to 10 Hz.

δ_C = 22.19 (d, $^4J_{C\text{-}P}$ = 9 Hz,C_{Me}), 23.39 (d, $^4J_{C\text{-}P}$ = 4 Hz,C_{Me}), 25.03 (d, $^4J_{C\text{-}P}$ = 9 Hz, C_{Me}),110.27 ($C_{d,n}$), 114.27, (C_{Ar}), 121.29 (H_b), 124.72-125.75 ($C_{h,j,p,Ar}$), 125.75-127.00 ($C_{g,k,Ar}$) 133.15 ($C_{e,m}$), 140.12 (C_i), 143-147 ($C_{f,l,Ar}$) 144.56 (C_{Ar}), 162.89-165.36 ($C_{c,o,Ar}$) 167.78 (m, $C_{a/q}$) 170.74 (m, $^1J_{C\text{-}F}$ = 737 Hz, $C_{a/q}$) ppm.

δ_F = -110.23 ($^4J_{Pt\text{-}F}$ = 32.5 Hz), -111.79 ($^4J_{Pt\text{-}F}$ = 27.5 Hz) ppm.

δ_P = 17.17 ($^1J_{P\text{-}Pt}$ = 3942 Hz) ppm.

δ_{Pt} = -4227 (d, $^1J_{Pt\text{-}P}$ = ~3800 Hz) ppm.

HR-MS (ESI): found = 764.1784 m/z, calculated = 764.1784 m/z = $C_{38}H_{30}F_2N^{194}PtP$ $[M]^+$.

Crystals suitable for X-ray analysis were grown by the slow evaporation of solvent from a chloroform solution – ps7.

Complex - **1-Bn**

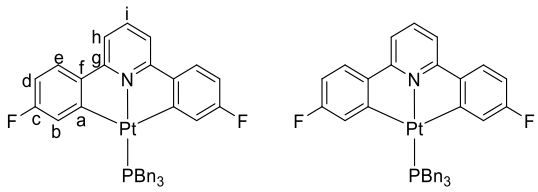

δ_H = 7.67 (1H, t, $^3J_{H\text{-}H}$ = 8 Hz, H_i), 7.50 (2H, dd, $^3J_{H\text{-}H}$ = 8.5 Hz, $^4J_{H\text{-}F}$ = 5.5 Hz, H_e), 7.41 (6H, d, $^3J_{H\text{-}H}$ = 7.5 Hz, Bn-*o*), 7.29 (2H, d, $^3J_{H\text{-}H}$ = 8 Hz, H_h), 7.23 (9H, m, Bn-*m,p*), 7.01 (2H, dd, $^3J_{H\text{-}H}$ = 11 Hz, $^4J_{H\text{-}H}$ = 3 Hz, $^3J_{H\text{-}Pt}$ = 25 Hz, H_b), 6.70 (2H, td, $^3J_{H\text{-}H}$ = $^3J_{H\text{-}F}$ = 9 Hz, $^4J_{H\text{-}H}$ = 3 Hz, H_d), 3.54 (6H, d, $^2J_{H\text{-}P}$ = 10 Hz, $^3J_{H\text{-}Pt}$ = 31 Hz, Bn-*CH*$_2$) ppm.

δ_C = 29.59 (d, $^1J_{C\text{-}P}$ = 32 Hz, $^2J_{C\text{-}Pt}$ = 32 Hz, Bn-*CH*$_2$), 109.36 (d, $^2J_{C\text{-}F}$ = 23.5 Hz, C_d), 113.57 (d, $^4J_{C\text{-}P}$ = 3 Hz, $^3J_{C\text{-}Pt}$ = 26.5 Hz, C_h), 123.26 (d, $^2J_{C\text{-}F}$ = 17 Hz, $^2J_{C\text{-}Pt}$ = 56 Hz, C_b), 124.86 (d, $^3J_{C\text{-}F}$ = 8 Hz, $^3J_{C\text{-}Pt}$ = 28 Hz, C_e), 125.8 (s, Bn-*p*), 127.47 (s, Bn-*m*), 129.336 (d, $^3J_{C\text{-}P}$ = 6 Hz, Bn-*o*), 132.66 (d, $^2J_{C\text{-}P}$ = 5.5 Hz, $^3J_{C\text{-}Pt}$ = 17 Hz, Bn-*i*), 139.07 (s, C_i), 145.82 (t, $^3J_{C\text{-}P}$ = $^4J_{C\text{-}F}$ = 2 Hz, $^2J_{C\text{-}Pt}$ = 27.5 Hz, C_f), 163.20 (d, $^1J_{C\text{-}F}$ = 253 Hz, $^3J_{C\text{-}Pt}$ = 53 Hz, C_c), 164.13 (s, $^2J_{C\text{-}Pt}$ = 67 Hz, C_g), 168.53 (m, $^1J_{C\text{-}Pt}$ = 719 Hz, C_a) ppm.

δ_F = -110.54 ($^4J_{F\text{-}Pt}$ = 28 Hz) ppm.

δ_P = -1.23 ($^1J_{P\text{-}Pt}$ = 3847 Hz) ppm.

δ_{Pt} = -4151 (d, $^1J_{Pt\text{-}P}$ = ~3900 Hz) ppm.

HR-MS (ESI): found 764.1774 m/z, calculated 764.1784 m/z = $C_{38}H_{30}F_2PN^{194}Pt$ = $[M]^+$.

Elemental analysis found (calculated): C 59.43 (59.68), H 3.99 (3.95) N 1.72 (1.83).

Crystals suitable for X-ray analysis were grown by the slow evaporation of solvent from a chloroform solution – ps28.

6.3. Starting materials (C^N^C = 2-(4-fluorophenyl)-6-*tert*butyl pyridine)

6.3.1. Synthesis of **20-Pr**

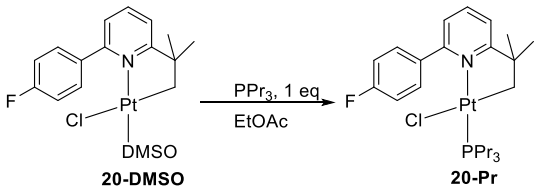

20-DMSO **20-Pr**

In a Schlenk flask under nitrogen, the previously reported **20-DMSO**[142] (50 mg, 9.31 x 10^{-5} mol) was dissolved in EtOAc (20 ml). Separately, also under an atmosphere of nitrogen, tripropylphosphine (16 mg, 1.00 x 10^{-2} mol, 1 eq) was dissolved in freshly distilled and degassed EtOAc (20 ml). The solution of phosphine was added slowly to the solution **1-DMSO** over 10 minutes at 0 °C. The reaction mixture was then left to stir for a further 10 minutes. Solvent was then removed, followed by purification of the crude mixture by column chromatography loading and eluting with toluene to give **20-Pr** as a yellow solid (46 mg, 7.43 x 10^{-5} mol, 80%).

Complex - **20-Pr**

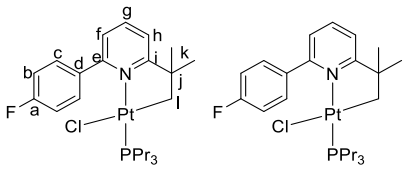

δ_H = 7.99 (2H, m, H_c), 7.81 (1H, t, $^3J_{H-H}$ = 8 Hz, H_g), 7.35 (1H, d, $^3J_{H-H}$ = 8 Hz, H_f), 7.25 (1H, d, $^3J_{H-H}$ = 8 Hz, H_h), 7.06 (2H, m, H_b), 1.85 (2H, d, $^3J_{H-P}$ = 1.5 Hz, $^2J_{H-Pt}$ = 50 Hz, H_l), 1.75 (6H, m, P*CH₂*), 1.62 (6H, m, PCH₂*CH₂*), 1.54 (9H, s, H_k), 1.04 (9H, t, $^3J_{H-H}$ = 7.5 Hz, PCH2CH2Me) ppm.

δ_C = 15.76 (d, $^3J_{C-P}$ = 15.5 Hz, PCH₂CH₂*Me*), 17.82 (s, $^3J_{C-Pt}$ = 34.5 Hz, C PCH₂*CH₂*), 23.58 (d, $^2J_{C-P}$ = 4.5 Hz, $^1J_{C-Pt}$ = 738 Hz, C_l), 25.74 (d, $^1J_{C-P}$ = 38 Hz, $^2J_{C-Pt}$ = 47.5 Hz, P*CH₂*), 33.41 (s, $^3J_{C-Pt}$ = 45 Hz, C_k), 49.74 (s, $^2J_{C-Pt}$ = 20 Hz, C_j), 114.47 (d, $^2J_{C-F}$ = 22 Hz, C_b), 119.66 (s, $^3J_{C-Pt}$ = 25 Hz, C_h), 123.95 (d, $^4J_{C-P}$ = 4 Hz, $^3J_{C-Pt}$ = 13 Hz, C_f), 130.99 (d, $^3J_{C-F}$ = 8 Hz, C_c), 136.84 (d, $^4J_{C-F}$ = 2.5 Hz, C_d), 137.71 (s, C_g), 159.49 (s, C_e), 163.44 (d, $^1J_{C-F}$ = 246 Hz, C_a), 174.81 (d, $^3J_{C-P}$ = 2.5 Hz, C_i) ppm.

δ_F = -112.38 ppm.

δ_P = -0.18 ($^1J_{P-Pt}$ = 4367 Hz) ppm.

δ_{Pt} = -4113 (d, $^{1}J_{Pt\text{-}P}$ = ~4350 Hz) ppm.

HR-MS (ESI): found 582.2181 m/z, calculated 582.2191 m/z = $C_{24}H_{36}FNP^{194}Pt$ = [M-HCl]$^{+}$.

Elemental analysis found (calculated): C 46.56 (48.94), H 5.86 (6.14), N 2.26 (2.20).

6.3.2. Synthesis of **21-Pr**

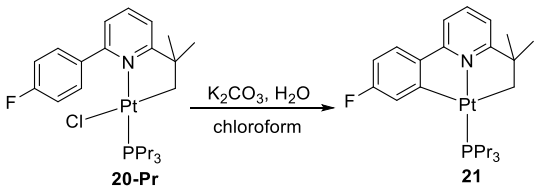

To a solution of **20-Pr** (46 mg, 7.43 x 10^{-5} mol) in chloroform (10 ml), was added a 2M solution of K_2CO_3 (2 ml). The mixture was then stirred (3 days). The solvent was removed and the crude product purified by chromatography on silica, eluting with chloroform (39 mg, 6.76 x 10^{-5} mol, 91 %).

Complex – **21-Pr**

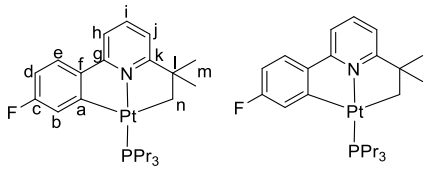

δ_H = 7.63 (1H, t, $^{3}J_{H\text{-}H}$ = 8 Hz, H_i), 7.43 (1H, dd, $^{3}J_{H\text{-}H}$ = 8 Hz, $^{4}J_{H\text{-}F}$ = 5 Hz, H_e), 7.36 (1H, d, $^{3}J_{H\text{-}H}$ = 8 Hz, H_h), 7.25 (1H, dd, $^{3}J_{H\text{-}F}$ = 9.5, $^{4}J_{H\text{-}H}$ = 2.5 Hz, $^{3}J_{H\text{-}Pt}$ = 29 Hz, H_b), 6.93 (1H, d, $^{3}J_{H\text{-}H}$ = 8 Hz, H_j), 6.67 (1H, td, $^{3}J_{H\text{-}H}$ = $^{3}J_{H\text{-}F}$ = 9.5, $^{4}J_{H\text{-}H}$ = 2.5 Hz, H_d), 1.86 (6H, m, P*CH*$_2$), 1.78 (2H, s, $^{2}J_{H\text{-}H}$ = 39 Hz, H_n), 1.56 (6H, m, PCH$_2$*CH*$_2$), 1.30 (6H, s H_m), 0.97 (9H, t, $^{3}J_{H\text{-}H}$ = 7.5, PCH$_2$CH$_2$*Me*) ppm.

δ_C = 14.79 (d, $^{3}J_{C\text{-}P}$ = 15.5 Hz, PCH$_2$CH$_2$*Me*), 15.63 (s, $^{3}J_{C\text{-}Pt}$ = 32.5 Hz, PCH$_2$*CH*$_2$), 26.14 (d, $^{1}J_{C\text{-}P}$ = 35.5, $^{2}J_{C\text{-}Pt}$ = 37.5 Hz, P*CH*$_2$), 33.11 (s, $^{3}J_{C\text{-}Pt}$ = 18.5 Hz, C_m), 34.79 (d, $^{2}J_{C\text{-}P}$ = 6 Hz, $^{1}J_{C\text{-}Pt}$ = 466 Hz, C_n), 51.52, (d, $^{3}J_{C\text{-}P}$ = 3.5 Hz, $^{2}J_{C\text{-}Pt}$ = 21 Hz, C_l), 108.05 (d, $^{2}J_{C\text{-}F}$ = 22 Hz, C_d), 114.28 (d, $^{4}J_{C\text{-}P}$ = 3 Hz, $^{3}J_{C\text{-}Pt}$ = 25.5 Hz, C_h), 117.50 (d, $^{4}J_{C\text{-}P}$ = 2.5 Hz, $^{3}J_{C\text{-}Pt}$ = 33

Hz, C_j), 122.31 (d, $^2J_{C\text{-}F}$ = 15 Hz, $^2J_{C\text{-}Pt}$ = 64.5 Hz, C_b), 124.77 (d, $^3J_{C\text{-}F}$ = 9 Hz, $^3J_{C\text{-}Pt}$ = 30 Hz, C_e), 136.76 (s, C_i), 145.20 (m, $^2J_{C\text{-}Pt}$ = 26 Hz, C_f), 163.22 (s, $^2J_{C\text{-}Pt}$ = 52 Hz, H_g), 163.72 (d, $^2J_{C\text{-}F}$ = 254.5 Hz, $^3J_{C\text{-}Pt}$ = 52 Hz, C_c), 173.95 (m, $^1J_{C\text{-}Pt}$ = 686 Hz, C_a), 176.22 (s, $^2J_{C\text{-}Pt}$ = 19 Hz, H_k) ppm.

δ_F = -111.69 ($^4J_{F\text{-}Pt}$ = 26.5 Hz) ppm.

δ_P = 0.44 ($^1J_{P\text{-}Pt}$ = 3813 Hz) ppm.

δ_{Pt} = -4026 (d, $^1J_{Pt\text{-}P}$ = ~3800 Hz) ppm.

HR-MS (ESI): found 582.2186 m/z, calculated 582.2191 m/z = $C_{24}H_{35}FNP^{194}Pt = [M]^+$.

Elemental analysis expected (result): C 49.48 (49.54), H 6.06 (6.07), N 2.40 (2.26).

6.4. Synthesis of the Complexes from Chapter 2

6.4.1. Synthesis of **4-Ph(c)**

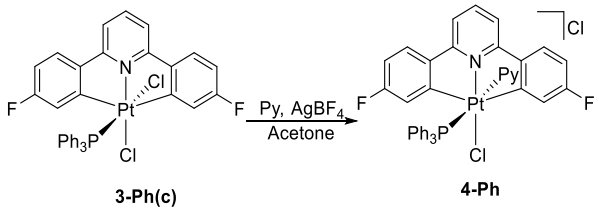

3-Ph(c) was characterised by a previous member of the Rourke group.[151] To a solution of **3-Ph(c)** (5 mg, 6.30 x 10^{-6} mol) in acetone (1 ml) was added pyridine (0.05 ml, excess) followed by $AgBF_4$ (about 2-5 mg, excess) at room temperature. The product was immediately seen in solution, and was separated from the waste AgCl by filtration. The product could not be purified as it degraded on silica.

Complex - **4-Ph(c)**

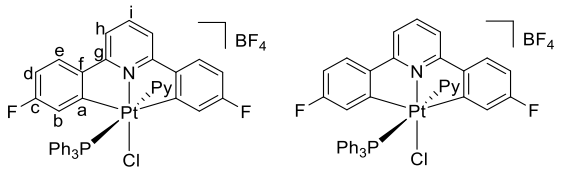

δ_H (Acetone-d_6) = 8.41 (2H, ddd, $^3J_{H-H}$ = 7 Hz, $^4J_{H-P}$ = 5.5 Hz, $^4J_{H-H}$ = 1 Hz, $^3J_{H-Pt}$ = 23.5 Hz, Py-*o*), 7.98 (2H, m, H_i, Py-*p*), 7.94 (2H, $^3J_{H-H}$ = 8.5 Hz, $^4J_{H-F}$ = 5 Hz, H_e), 7.75 (2H, $^3J_{H-H}$ = 8 Hz, $^4J_{H-Pt}$ = 8 Hz, H_h), 7.64 (2H, $^3J_{H-F}$ = 7.5 Hz, $^4J_{H-H}$ =2.5 Hz, $^3J_{H-Pt}$ = 12 Hz, H_b), 7.59 (3H, t, $^3J_{H-H}$ = 7.5 Hz, Ph-*p*), 7.55 (6H, dd, $^3J_{H-P}$ = 12.5, $^3J_{H-H}$ = 7.5 Hz, Ph-*o*), 7.45 (2H, td, $^3J_{H-H}$ = $^3J_{H-H}$ = 7 Hz, $^5J_{H-P}$ = 1 Hz, Py-*m*), 7.40 (6H, td, $^3J_{H-H}$ = $^3J_{H-H}$ = 7.7 Hz, $^4J_{H-P}$ = 3.5 Hz, Ph-*m*), 7.08 (2H, $^3J_{H-H}$ = $^3J_{H-F}$ = 8.5, $^4J_{H-H}$ = 2.5 Hz, H_d) ppm.

δ_F (Acetone-d_6) = -106.26 ($^4J_{F-Pt}$ = 14 Hz) ppm.

δ_P (Acetone-d_6) = -11.23 ($^1J_{P-Pt}$ = 2395 Hz) ppm.

δ_{Pt} (Acetone-d_6) = -2362 (d, $^1J_{Pt-P}$ = ~2500 Hz) ppm.

HR-MS (ESI): found 756.0935 m/z, calculated 756.0924 m/z = $C_{35}H_{24}ClF_2NP^{194}Pt$ = $[M\text{-}Py]^+$.

HR-MS (ESI): found 836.1350 m/z, calculated 835.1346 m/z = $C_{40}H_{29}ClF_2N_2P^{194}Pt$ = $[M]^+$.

6.4.2. Synthesis of **3-Bu(t)** and **3-Bu(c)**

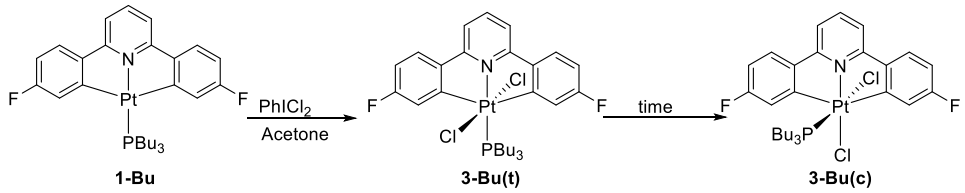

To an acetone (1 ml) solution of **1-Bu** (10 mg, 1.48 x 10^{-5} mol) was added $PhICl_2$ (5 mg, 1.78 x 10^{-5} mol, 1.2 eq) at room temperature. The reaction initially gives clean conversion to **3-Bu(t)**, but converts to **3-Bu(c)** when left in solution for up to a month. **3-Bu(c)** was purified by column chromatography, loading with chloroform and eluting with EtOAc to give clean product as a yellow solid (11 mg, 1.48 x 10^{-5} mol, quantitative yield).

Complex - **3-Bu(t)**

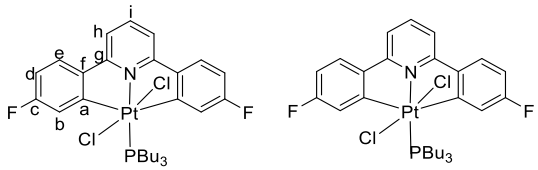

δ_H = 7.86 (1H, t, $^3J_{H\text{-}H}$ = 8 Hz, H_i), 7.77 (2H, dd, $^3J_{H\text{-}H}$ = 8.5, $^4J_{H\text{-}F}$ = 5.5 Hz, H_e), 7.57 (2H, dd, $^3J_{H\text{-}H}$ = 8 Hz, H_h), 7.30 (2H, dd, $^3J_{H\text{-}F}$ = 6.5 Hz, $^4J_{H\text{-}H}$ = 2.5 Hz, $^3J_{H\text{-}Pt}$ = ~17 Hz, H_b), 6.91 (2H, td, $^3J_{H\text{-}H}$ = $^3J_{H\text{-}F}$ = 8.5, $^4J_{H\text{-}H}$ = 2.5 Hz, H_d), 1.77 (6H, m, P*CH*$_2$), 1.14 (6H, m, PCH$_2$*CH*$_2$), 1.02 (6H, m, PCH$_2$*CH*$_2$*CH*$_2$), 0.78 (9H, t, $^3J_{H\text{-}H}$ = 7.5 Hz, PCH$_2$CH$_2$CH$_2$*Me*) ppm.

δ_C = 12.60 (s, PCH$_2$CH$_2$CH$_2$*Me*), 20.77 (d, $^1J_{C\text{-}P}$ = 35.5 Hz, $^2J_{C\text{-}Pt}$ = 14 Hz, P*CH*$_2$), 22.94 (d, $^3J_{C\text{-}P}$ = 15 Hz, PCH$_2$*CH*$_2$*CH*$_2$), 24.99 (d, $^2J_{C\text{-}P}$ = 5 Hz, PCH$_2$*CH*$_2$), 111.09 (d, $^2J_{C\text{-}F}$ = 22 Hz, C_d), 115.84 (d, $^3J_{C\text{-}Pt}$ = 4 Hz, C_h), 120.79 (d, $^2J_{C\text{-}F}$ = 19 Hz, $^2J_{C\text{-}Pt}$ = 19 Hz, C_b), 126.99 (d, $^3J_{C\text{-}F}$ = 8.5 Hz, $^3J_{C\text{-}Pt}$ = 17 Hz, C_e), 139.35 (s, C_i), 143.12 (s, C_f), 158.68 (m, $^1J_{C\text{-}Pt}$ = 519 Hz, C_a), 160.56 (s, $^2J_{C\text{-}Pt}$ = 32.5 Hz, C_g), 162.16 (d, $^1J_{C\text{-}F}$ = 256 Hz, $^3J_{C\text{-}Pt}$ = 31 Hz, C_c) ppm.

δ_F = -108.14 ($^4J_{F\text{-}Pt}$ = 16 Hz) ppm.

δ_P = -13.74 ($^1J_{P\text{-}Pt}$ = 2303 Hz) ppm.

δ_{Pt} = -2275 (d, $^1J_{Pt\text{-}P}$ = ~2400 Hz) ppm.

HR-MS (ESI): found 732.1648 m/z, calculated 732.1630m/z = $C_{29}H_{36}F_2Cl_2NP^{194}Pt$ = $[M]^+$.

Crystals suitable for X-ray analysis were grown by the slow evaporation of solvent from a chloroform solution – ps1.

Complex - **3-Bu(c)**

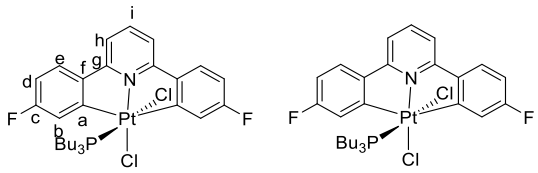

δ_H = 7.82 (2H, dd, $^3J_{H\text{-}F}$ = 8 Hz, $^4J_{H\text{-}H}$ = 2.5 Hz, $^3J_{H\text{-}Pt}$ = ~20 Hz, H_b), 7.67 (3H, m, $H_{e,i}$), 7.44 (2H, d, $^3J_{H\text{-}H}$ = 8.5 Hz, H_h), 6.80 (2H, dt, $^3J_{H\text{-}H}$ = $^3J_{H\text{-}F}$ = 8.5, $^4J_{H\text{-}H}$ = 2.5 Hz, H_d), 2.73 (6H, m, P*CH*$_2$), 1.11 (6H, m, PCH$_2$CH$_2$*CH*$_2$), 0.98 (6H, m, PCH$_2$*CH*$_2$), 0.75 (9H, t, $^3J_{H\text{-}H}$ = 7.5 Hz, PCH$_2$CH$_2$CH$_2$*Me*) ppm.

δ_C = 13.27 (s, PCH$_2$CH$_2$CH$_2$*Me*), 22.12 (d, $^1J_{C\text{-}P}$ = 38 Hz, $^2J_{C\text{-}Pt}$ = 25 Hz, P*CH*$_2$), 24.07 (d, $^3J_{C\text{-}P}$ = 14.5 Hz, PCH$_2$CH$_2$*CH*$_2$), 24.87 (d, $^2J_{C\text{-}P}$ = 5.5 Hz, PCH$_2$*CH*$_2$), 112.89 (d, $^2J_{C\text{-}F}$ = 25 Hz, C_d), 116.60 (s, $^3J_{C\text{-}Pt}$ = 30 Hz, C_h), 120.95 (d, $^2J_{C\text{-}F}$ = 19 Hz, $^2J_{C\text{-}Pt}$ = 19 Hz, C_b), 127.76 (d, $^3J_{C\text{-}F}$ = 7.5 Hz, $^3J_{C\text{-}Pt}$ = 20 Hz, C_e), 141.37 (s, C_i), 141.90 (d, $^4J_{C\text{-}F}$ = 2.5 Hz, $^2J_{C\text{-}Pt}$ = 25 Hz, C_f), 162.50 (s, $^2J_{C\text{-}Pt}$ = 37 Hz, C_g), 163.58 (m, $^1J_{C\text{-}Pt}$ = 514 Hz, C_a), 164.80 (d, $^1J_{C\text{-}F}$ = 261 Hz, $^3J_{C\text{-}Pt}$ = 28 Hz, C_c) ppm.

δ_F = -108.77 ($^4J_{F\text{-}Pt}$ = 15 Hz) ppm.

δ_P = -0.68 ($^1J_{P\text{-}Pt}$ = 2325 Hz) ppm.

δ_{Pt} = -2640 (d, $^1J_{Pt\text{-}P}$ = ~2400 Hz) ppm.

HR-MS (ESI): found = 732.1648 m/z, calculated = 732.1630 m/z = $C_{29}H_{37}F_2Cl_2NP^{194}Pt$ $[MH]^+$.

Elemental analysis found (calculated): C 46.47 (47.48), H 4.76 (4.95), N 1.80 (1.91).

Crystals suitable for X-ray analysis were grown by the slow evaporation of solvent from a chloroform solution – ps2.

6.4.3. Synthesis of **7-Bu(c)** via **5-Bu** and **6-Bu(t)**

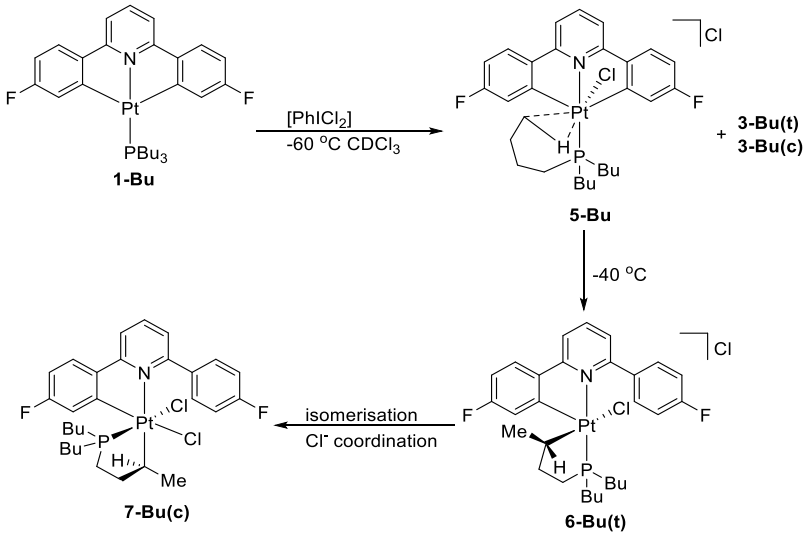

To a chloroform (10 ml) solution of **1-Bu** (20 mg, 2.95 x 10^{-5} mol) was added $PhICl_2$ (10 mg, 3.56 x 10^{-5} mol 1.2 eq) at -60 °C. The previously mentioned **3-Bu(t/c)** made up roughly 30% of the reaction mixture. The other 70% was made up by the agostic complex **5-Bu**. Allowing to warm to room temperature, **5-Bu** disappeared with the appearance of **6-Bu(t)**. Although **6-Bu(t)** could not be purified, if it was left for a day at room temperature **6-Bu(t)** converted fully into the final product **7-Bu(c)**. The product was then purified by column chromatography, loading and eluting with chloroform (11 mg, 1.48 x 10^{-5} mol, 50%).

Complex - **5-Bu**

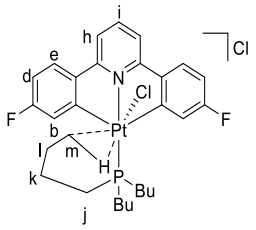

δ_H = 8.01 (2H, d, $^3J_{H\text{-}H}$ = 8Hz, H_h), 7.33 (1H, t, $^3J_{H\text{-}H}$ = 7Hz, H_i), 6.68 (1H, d, $^3J_{H\text{-}H}$ = 9Hz, $^3J_{H\text{-}Pt}$ = 60 Hz, H_b), 2.78 (m, Bu), 2.49 (m, Bu), 2.19 (m, Bu), 1.92 (m, Bu), 1.78 (m, Bu), 1.43 (m, Bu), 2.49 (2H, m, H_k), 2.18 (2H, m, H_l), 0.75 (3H, t, $^3J_{H\text{-}H}$ = 6 Hz, $J_{H\text{-}Pt}$ ~20 Hz, H_m) ppm.

δ_F = -108.7 ($^4J_{F\text{-}Pt}$ = 15 Hz) ppm.

δ_P = 49.55 ($^1J_{P\text{-}Pt}$ = 3064 Hz) ppm.

δ_{Pt} = -2341 (d, $^1J_{Pt\text{-}P}$ = ~3100 Hz) ppm.

Complex - **6-Bu(t)**

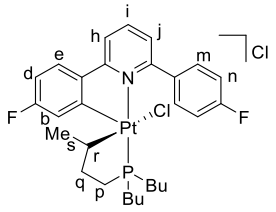

δ_H = 7.80 (2H, dd, $^3J_{H\text{-}F}$ = 4 Hz, $^3J_{H\text{-}H}$ = 8 Hz, H_m) 7.26 (1H, m, H_i),7.04 (1H, dt, $^3J_{H\text{-}F}$ = 10 Hz, $^4J_{H\text{-}H}$ = $^4J_{P\text{-}H}$ = 2.5 Hz, $^3J_{H\text{-}Pt}$ ~ 40 Hz, H_b), 2.45 (1H, m, $^2J_{H\text{-}Pt}$ ~ 100 Hz, H_r), 2.97 (m, H_p), 2.52 (m, H_q), 2.42 (m, P*CH*$_2$), 1.82 (m, PCH$_2$*CH*$_2$), 0.99 (6H, m, PCH$_2$CH$_2$CH$_2$*Me*), 0.42 (3H, d, $^3J_{H\text{-}H}$ = 7 Hz, $^3J_{H\text{-}Pt}$ = 38 Hz, H_s) ppm.

Note, strong correlation of Pt to H_m, H_h and H_l when HMBC Pt-H coupling parameter set to 100 Hz, but no correlation of Pt to H_l when this parameter is set to 50 Hz or less. When same parameter set to 10 Hz, we see an additional correlation to signal for H_o.

δ_F = -107.49 ($^4J_{F\text{-}Pt}$ = 39 Hz), -112.36 ppm.

δ_P = 39.36 ($^1J_{P\text{-}Pt}$ = 3122 Hz) ppm.

δ_{Pt} = -2570 (d, $^1J_{Pt\text{-}P}$ = ~3100 Hz) ppm.

HR-MS (ESI): found 660.2104 m/z, calculated 660.2096 m/z = $C_{29}H_{36}F2N_{35}ClP^{194}Pt$ = $[M\text{-}HCl]^+$.

HR-MS (ESI): found 696.1868 m/z, calculated 696.1863 m/z = $C_{27}H_{33}F_2PN^{194}Pt$ = $[M]^+$.

Complex - **7-Bu(c)**

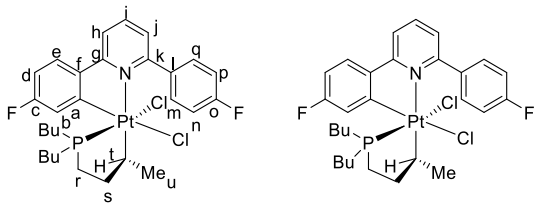

δ_H = 7.86 (2H, d, $^3J_{H\text{-}H}$ = 4.5 Hz, $H_{h,j}$), 7.84 (2H, m, $H_{m,q}$)**, 7.73 (1H, dd, $^3J_{H\text{-}H}$ = 8.5, $^4J_{H\text{-}F}$ = 5.5 Hz, H_e), 7.32 (3H, m, $H_{b,i}$), 7.14 (2H, t, $^3J_{H\text{-}H}$ = $^3J_{H\text{-}F}$ = 9Hz, $H_{n,p}$)*, 6.95 (1H, dt, $^3J_{H\text{-}H}$ = $^3J_{H\text{-}F}$ = 8.5, $^4J_{H\text{-}H}$ = 2 Hz, H_d), 3.59 (1H, tq,$^3J_{H\text{-}H}$ = 7Hz, 75 Hz, $^2J_{H\text{-}Pt,}$ H_c), 1.98 (1H, m, H_r), 1.84 (1H, m, H_s), 1.61 (2H, m, H_r), 1.44 (3H, d,$^3J_{H\text{-}H}$ = 6.5 Hz, 36 Hz $^3J_{H\text{-}Pt,}$ H_u), 1.32 (2H, m, Bu), 1.20 (1H, m, H_s), 1.00 (4H, m, Bu), 0.93 (2H, m, Bu), 0.89 (3H, t, $^3J_{H\text{-}H}$ = 7 Hz, PCH$_2$CH$_2$CH$_2$*Me*), 0.87 (2H, m, Bu), 0.68 (3H, t, $^3J_{H\text{-}H}$ = 7 Hz, PCH$_2$CH$_2$CH$_2$*Me*), ppm.

*At 298 K, at 400 MHz, $H_{n,p}$ is a triplet. At 253 K the triplet loses shape, becoming a broad lump (28 Hz FWHM). At 233 K the broad lump has now separated into two, about 44 Hz apart (7.19 ppm 32 Hz, 7.08 22 Hz FWHM).

**At 298 K, at 400 MHz, both H_m and H_q form a single peak (28Hz FWHM). This peak does not correlate to anything in a COSY spectrum. At 253 K the multiplet has separated into two. Due to the broadness of the peaks, only the position of one of the peaks can be assigned at around 8.25 ppm. At 233 K the peak at 8.25 has moved further downfield to 8.31, and narrowed (21 Hz FWHM). The corresponding peak lies around 7.31 shown by integration, giving a separation of 400 Hz. Constraints of the solvent prevent lowering the temperature further. Heating the sample to 328 K narrows the peak (9 Hz FWHM), and the peak now correlates to $H_{n,p}$ in a COSY spectrum.

δ_C = 13.12 (s, $PCH_2CH_2CH_2$*Me*), 13.43 (s, $PCH_2CH_2CH_2$*Me*), 20.95 (d, $^1J_{C\text{-}P}$ = 33Hz, $^2J_{C\text{-}Pt}$ = 45.5 Hz, Bu), 20.62 (d, $^1J_{C\text{-}P}$ = 35 Hz, $^2J_{C\text{-}Pt}$ = 15.5 Hz, Bu), 23.93 (d, $^1J_{C\text{-}P}$ = 39 Hz, $^2J_{C\text{-}Pt}$ = 70 Hz, C_r), 24.26 (m, Bu), 26.11 (s, $^2J_{C\text{-}Pt}$ = 26 Hz, C_u), 37.47 (d, $^2J_{C\text{-}P}$ = 2.5 Hz, $^2J_{C\text{-}Pt}$ = 16.9 Hz, C_s), 53.79 (d, $^2J_{C\text{-}P}$ = 3.5 Hz, $^1J_{C\text{-}Pt}$ = 572 Hz, C_t), 112.87 (d, $^2J_{C\text{-}F}$ = 23 Hz, C_d), 114.84 (d, $^2J_{C\text{-}F}$ = 22 Hz, $C_{n,p}$), 116.53 (d, $^2J_{C\text{-}F}$ = 21 Hz, $^2J_{C\text{-}Pt}$ = 30 Hz, C_b), 118.21 (s, $^2J_{C\text{-}Pt}$ = 9 Hz, C_j), 126.06 (s, C_i), 128.22 (d, $^3J_{C\text{-}F}$ = 9 Hz, $^3J_{C\text{-}Pt}$ = 39.5 Hz, C_e), 135.64 (d, $^4J_{C\text{-}F}$ = 3.5 Hz, C_h), 138.71 (s, C_l), 139.07 (d, $^4J_{C\text{-}F}$ = 2.5 Hz, C_f), 141.71 (d, $^3J_{C\text{-}F}$ = 6 Hz, $^1J_{C\text{-}Pt}$ = 844 Hz, C_a), 162.45 (s, $^2J_{C\text{-}Pt}$ = 48 Hz, $C_{g/k}$), 163 (d, $^1J_{C\text{-}F}$ = 255 Hz, $^3J_{C\text{-}Pt}$ = 70 Hz, C_c), 163.74 (d, $^1J_{C\text{-}Pt}$ = 248 Hz, C_o), 164.02 (m, $C_{g/k}$) ppm.

δ_F = -108.28 ($^4J_{F\text{-}Pt}$ = 43.5 Hz), -112.88 ppm.

δ_P = 40.02 ($^1J_{P\text{-}Pt}$ = 2945 Hz) ppm.

δ_{Pt} = -2721 (d, $^1J_{Pt\text{-}P}$ = ~3000 Hz) ppm.

HR-MS (ESI): found 660.2092 m/z, calculated 660.2096 m/z = $C_{29}H_{35}F_2NP^{194}Pt$ = $[M\text{-}HCl]^+$.

HR-MS (ESI): found 696.1863 m/z, calculated 696.1868 m/z = $C_{29}H_{36}F_2N^{35}ClP^{194}Pt$ = $[M\text{-}Cl]^+$.

Elemental analysis found (calculated): 48.09 (47.48), H 5.09 (4.95), N 1.50 (1.91).

Crystals suitable for X-ray analysis were grown by the slow evaporation of solvent from a chloroform solution – ps8.

6.4.4. Synthesis of **3-Pr(t)** and **3-Pr(c)**

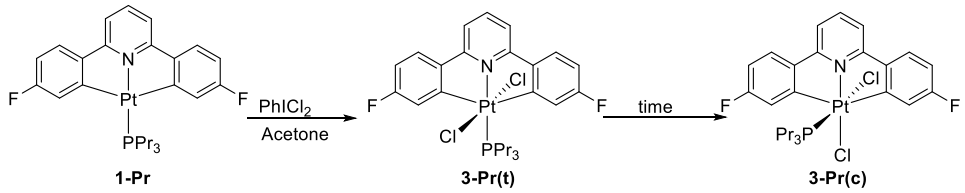

To an acetone (1 ml) solution of **1-Pr** (10 mg, 1.48 x 10^{-5} mol) was added $PhICl_2$ (5 mg, 1.67 x 10^{-5} mol, 1.1 eq) at room temperature. The reaction initially gives clean conversion to **3-Pr(t)**, but converts to a mixture of **4-Pr(t)** and **3-Pr(c)** (roughly 5:3). The mixture was purified to remove PhI by column chromatography (loading and eluting with chloroform) giving a yellow solid (11 mg, 1.48 x 10^{-5} mol) quantitative yield of Pt^{IV} dichloro-complexes).

Complex - **3-Pr(t)**

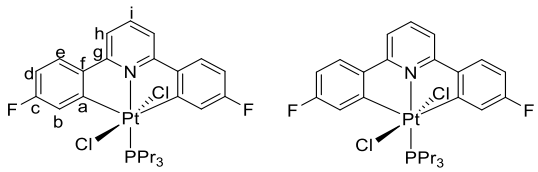

δ_H = 7.81 (1H, t, $^3J_{H\text{-}H}$ = 8 Hz, H_i), 7.73 (2H, dd, $^3J_{H\text{-}H}$ = 8 Hz, $^4J_{H\text{-}F}$ = 5 Hz, H_e), 7.53 (2H, dd, $^3J_{H\text{-}H}$ = 8 Hz, $^5J_{H\text{-}P}$ = 2 Hz, H_b), 7.26 (2H, dd, $^3J_{H\text{-}F}$ = 9 Hz, $^4J_{H\text{-}H}$ = 2 Hz, $^3J_{H\text{-}Pt}$ = 20 Hz, H_h), 6.88 (2H, td, $^3J_{H\text{-}H}$ = $^3J_{H\text{-}F}$ = 8 Hz, $^4J_{H\text{-}H}$ = 2 Hz, H_d), 2.47 (6H, m, P*CH₂*), 1.81 (6H, m, PCH_2*CH₂*), 1.12 (9H, td, $^3J_{H\text{-}H}$ = 7 Hz, $^4J_{H\text{-}P}$ = 1.5 Hz, PCH_2CH_2*Me*) ppm.

δ_C = 15.26 (s, PCH_2CH_2*Me*), 17.85 (d, $^2J_{C\text{-}P}$ = 5 Hz, PCH_2*CH₂*), 24.10 (d, $^1J_{C\text{-}P}$ = 36 Hz, $^2J_{C\text{-}Pt}$ = 18 Hz, P*CH₂*), 112.09 (d, $^3J_{C\text{-}F}$ = 22 Hz, C_d), 116.86 (d, $^4J_{C\text{-}P}$ = 4 Hz, C_h), 121.71 (d, $^2J_{C\text{-}F}$ = 19 Hz, $^2J_{C\text{-}Pt}$ = 21 Hz, C_b), 128.01 (d, $^3J_{C\text{-}F}$ = 8 Hz, C_e), 140.42 (s, C_i), 144.15 (t, $^4J_{C\text{-}F}$ = $^3J_{C\text{-}P}$ = 3 Hz, C_f), 159.63 (m, $^1J_{C\text{-}Pt}$ = 512 Hz, C_a), 161.58 (m, $^3J_{C\text{-}Pt}$ = 30 Hz, C_g), 163.20 (d, $^1J_{C\text{-}F}$ = 258 Hz, $^3J_{C\text{-}Pt}$ = 28 Hz, C_c) ppm.

δ_F = -108.06 ($^4J_{F\text{-}Pt}$ = 14 Hz) ppm.

δ_P = -13.96 ($^1J_{P\text{-}Pt}$ = 2310 Hz) ppm.

δ_{Pt} (Acetone-d_6) = -2282 (d, $^1J_{Pt\text{-}P}$ = ~2500 Hz) ppm.

Complex - **3-Pt(c)**

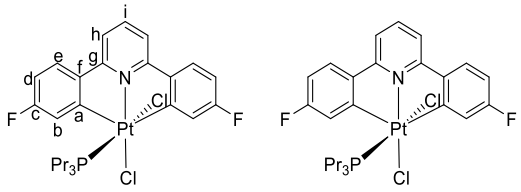

δ_H = 7.83 (3H, m, $H_{b,i}$), 7.71 (2H, dd, $^3J_{H\text{-}H}$ = 8 Hz, $^4J_{H\text{-}F}$ = 4 Hz, H_e), 7.51 (2H, d, $^3J_{H\text{-}H}$ = 8 Hz, H_h), 6.94 (2H, td, $^3J_{H\text{-}H}$ = $^3J_{H\text{-}F}$ = 8 Hz, $^4J_{H\text{-}H}$ = 2 Hz, H_d), 1.71 (6H, m, P*CH*$_2$), 1.10 (6H, m, PCH$_2$*CH*$_2$), 0.76 (9H, td, $^3J_{H\text{-}H}$ = 7 Hz, PCH$_2$CH$_2$*Me*) ppm.

δ_C = 15.40 (s, PCH$_2$CH$_2$*Me*), 16.72 (d, $^2J_{C\text{-}P}$ = 6 Hz, PCH$_2$*CH*$_2$), 24.30 (d, $^1J_{C\text{-}P}$ = 37 Hz, $^2J_{C\text{-}Pt}$ = 24 Hz, P*CH*$_2$), 112.88 (d, $^3J_{C\text{-}F}$ = 24 Hz, C_d), 116.35 (d, $^4J_{C\text{-}Pt}$ = 31.5 Hz, C_h), 120.98 (d, $^2J_{C\text{-}F}$ = 19 Hz, $^2J_{C\text{-}Pt}$ = 19 Hz, C_b), 127.63 (d, $^3J_{C\text{-}F}$ = 8 Hz, $^3J_{C\text{-}Pt}$ = 22 Hz, C_e), 141.10 (s, C_i), 141.70 (d, $^4J_{C\text{-}F}$ = 2 Hz, $^2J_{C\text{-}Pt}$ = 28 Hz C_f), 162.67 (m, $^3J_{C\text{-}Pt}$ = 35 Hz, C_g), 163.78 (m, $^1J_{C\text{-}Pt}$ = 512 Hz, C_a),164.90 (d, $^1J_{C\text{-}F}$ = 260 Hz, $^3J_{C\text{-}Pt}$ = 28 Hz, C_c) ppm.

δ_F = -105.57 ($^4J_{F\text{-}Pt}$ = 15 Hz) ppm.

δ_P= -1.42 ($^1J_{P\text{-}Pt}$ = 2342 Hz) ppm.

δ_{Pt} (Acetone-d_6) = -2625 (d, $^1J_{Pt\text{-}P}$ = ~3300 Hz) ppm.

Note: following data taken from a trans/cis mixture:

HR-MS (ESI): found 654.1382 m/z, calculated 654.1393 m/z = $C_{26}H_{30}F_2PN^{194}Pt$ = $[M\text{-}Cl]^+$.

HR-MS (ESI): found 712.0978 m/z, calculated 712.0979 m/z = $C_{26}H_{30}F_2PNNa^{194}Pt$ t = $[M+Na]^+$.

Elemental analysis found (calculated): C 45.16 (44.32), H 4.37 (4.12), N 2.03 (1.93).

Crystals suitable for X-ray analysis were grown by the slow evaporation of solvent from a chloroform solution – ps10.

6.4.5. Synthesis of **7-Pr(c)** via **5-Pr** and **7-Pr(c)**

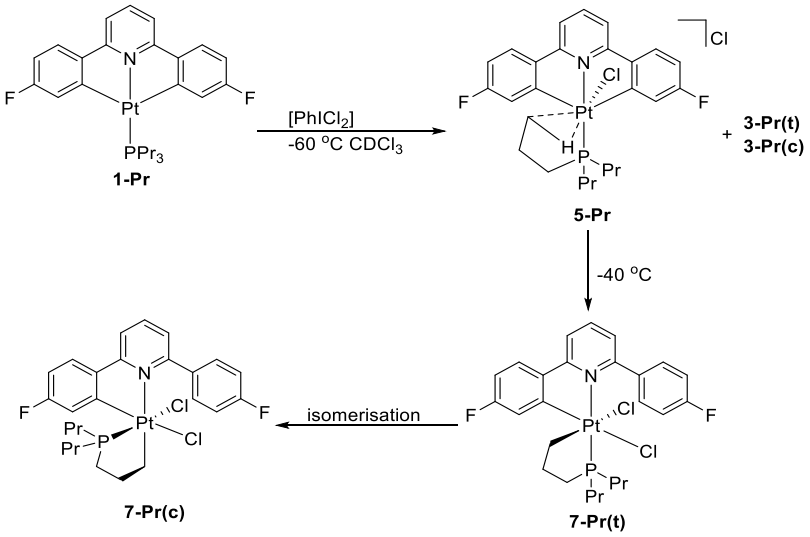

To a chloroform (10 ml) solution of **1-Pr** (20 mg, 3.22 x 10^{-5} mol) was added $PhICl_2$ (10 mg, 3.34 x 10^{-5} mol, 1.1 eq) at -60 °C. The previously mentioned **3-Pr(t/c)** made up 60% of the reaction mixture. The other 40% was made up by the agostic complex **5-Pr**. Allowing to warm to room temperature, **5-Pr** disappeared with the appearance of **7-Pr(t)**. Although **7-Pr(t)** could not be purified, if it was left for a week at room temperature **7-Pr(t)** converted fully into the final product **7-Pr(c)**. The product was then purified by column chromatography, loading and eluting with chloroform (8 mg, 1.13 x 10^{-5} mol, 35 %).

Complex - **5-Pr**

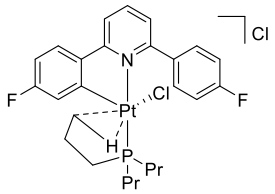

δ_P (213 K) = 51.00 ($^1J_{P\text{-}Pt}$ = 3080 Hz) ppm.

This product is short lived (even at -60 °C) only $^{31}P\{^1H\}$ data were collected.

Complex - **7-Pr(t)**

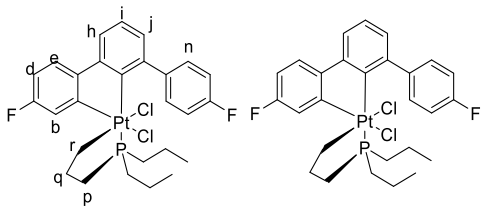

δ_H = 7.93 (1H, t, $^3J_{H\text{-}H}$ = 8Hz, H_i) 7.84 (1H, d, $^3J_{H\text{-}H}$ = 8 Hz, $H_{h/j}$), 7.31 (1H, d, $^3J_{H\text{-}H}$ = 8 Hz, $H_{h/j}$), 7.07 (1H, dt, $^3J_{H\text{-}F}$, 10 Hz, $^4J_{H\text{-}H}$ = $^4J_{H\text{-}P}$ = 2 Hz, H_b), 3.09 (1H, dt, $^2J_{H\text{-}H}$ = $^3J_{H\text{-}H}$ = 6.5 Hz, $^2J_{H\text{-}H}$ = 102 Hz, H_r), 2.37 (1H, m, $^2J_{H\text{-}Pt}$ = 56 Hz, H_r), 1.09 (3H, td, $^3J_{H\text{-}H}$ = 7.5 Hz, $^4J_{H\text{-}P}$ = 1 Hz, H_{Me}), 0.98 (3H, td, $^3J_{H\text{-}H}$ = 8 Hz, $^4J_{H\text{-}P}$ = 1.5 Hz, H_{Me}) ppm.

δ_F = = -109.54 ($^4J_{F\text{-}Pt}$ = 45 Hz), -111.90 ppm.

δ_P = = 47.86 ($^1J_{P\text{-}Pt}$ = 3129 Hz) ppm.

δ_{Pt} = = -2667 (d, $^1J_{Pt\text{-}P}$ = ~3300 Hz) ppm.

Complex - **7-Pr(c)**

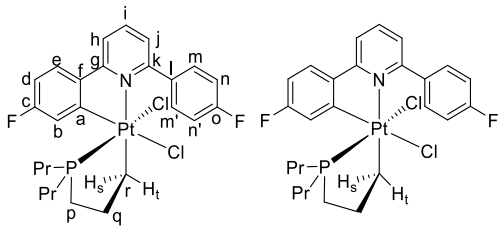

δ_H = 7.94 (2H, m, $H_{h,j}$), 7.87 (2H, m, H_m)*, 7.79 (1H, dd, $^3J_{H\text{-}H}$ = 9 Hz, $^4J_{H\text{-}F}$ = 6 Hz, H_e), 7.63 (1H, dd, $^3J_{H\text{-}H}$ = 5.5, 3 Hz, H_i), 7.30 (1H, $^3J_{H\text{-}F}$ = 10 Hz, $^4J_{H\text{-}H}$ = 3 Hz, $^3J_{H\text{-}Pt}$ = 47 Hz, H_b), 7.19 (2H, dd, $^3J_{H\text{-}F}$ = $^3J_{H\text{-}H}$ = 8.5 Hz, H_n)**, 7.01 (1H, td, $^3J_{H\text{-}H}$ = $^3J_{H\text{-}F}$ = 8.5 Hz, $^4J_{H\text{-}H}$ = 2.5 Hz, H_d), 3.70 (1H, m, $^2J_{H\text{-}Pt}$ = 95 Hz, H_t), 3.10 (1H, m, $^2J_{H\text{-}Pt}$ = 65 Hz, H_s)***, 2.06 (2H, m, Alkyl), 1.64 (2H, m, H_q), 1.36 – 1.17 (2H, m, H_p), 0.99 (4H, m, Alkyl), 0.94 – 0.79 (5H, m, Alkyl, PCH_2CH_2*Me*), 0.64 (3H, t, $^3J_{H\text{-}H}$ = 7 Hz, PCH_2CH_2*Me*) ppm.

*very broad resonance at 298 K. By 208 K H_m has become two separate proton environments. Coupling to the adjacent proton, H_n, can be seen by COSY at 218 K. At 208 K a broad triplet is seen ($^3J_{H\text{-}H}$ = 5.3 Hz, separation of peaks = 505 Hz, centre = 7.86 ppm. Even by 328 K, the peak has not coalesced to form a single peak, instead a broad peak remains (width at half height = 21 Hz). COSY at 328 K shows Coupling to H_n.

**At room temperature, and even down to 268 K, this peak is a triplet. The peak moves slightly to greater ppm with a decrease in temperature. By 208 K the triplet has

decoalesced into two peaks. It difficult to work out the width at half height due to overlapping peaks, but the peaks are separated by around 25 Hz.

***irradiation of this peak shows enhancement of H_b.

Proton H_d moves to lower ppm with decreasing temperature.

δ_C = 15.52 (d, $^3J_{C\text{-}Pt}$ = 8 Hz, PCH_2CH_2*Me*), 15.65 (d, $^3J_{C\text{-}P}$ = 6 Hz, PCH_2CH_2*Me*), 16.29 (d, $^2J_{C\text{-}P}$ = 6 Hz, $^3J_{C\text{-}Pt}$ = 24 Hz, PCH_2*CH₂*), 16.53 (d,$^2J_{C\text{-}P}$ = 5 Hz, $^3J_{C\text{-}Pt}$ = 11 Hz, PCH_2*CH₂*), 21.88 (d, $^1J_{C\text{-}P}$ = 33 Hz, $^2J_{C\text{-}Pt}$ = 42 Hz, P*CH₂*), (d, $^1J_{C\text{-}P}$ = 35 Hz, $^2J_{C\text{-}Pt}$ = 20 Hz, P*CH₂*), 26.45 (d, $^1J_{C\text{-}P}$ = 40 Hz, $^2J_{C\text{-}Pt}$ = 86 Hz, C_p), 28.56 (d, $^2J_{C\text{-}P}$ = 3 Hz, C_q), 37.82 (s, $^1J_{C\text{-}Pt}$ = 554 Hz, C_r), 122.89 (d, $^2J_{C\text{-}F}$ = 23 Hz, C_d), 115.05 (d, $^2J_{C\text{-}F}$ = 21 Hz, $C_{b,b'}$), 116.51 (d, $^2J_{C\text{-}F}$ = 21 Hz, $^2J_{C\text{-}Pt}$ = 42 Hz, C_b), 118.12 (s, $^3J_{C\text{-}Pt}$ = 11 Hz, C_h), 125.90 (s, C_i), 128.00 (d, $^3J_{C\text{-}F}$ = 9 Hz, $^3J_{C\text{-}Pt}$ = 40 Hz, C_e), 135.54 (d, $^4J_{C\text{-}F}$ = 3 Hz, C_l), 138.60 (d, $^4J_{C\text{-}F}$ = 2 Hz, C_f), 139.09 (s, C_j), 140.51 (dd, $^3J_{C\text{-}F}$ = 7 Hz, $^2J_{C\text{-}P}$ = 2 Hz, $^1J_{C\text{-}Pt}$ = 841 Hz, C_a), 162.10 (s, $^3J_{C\text{-}Pt}$ = 50 Hz, C_g), 163.81 (d, $^1J_{C\text{-}F}$ = 249 Hz, C_o), 163.88 ($^1J_{C\text{-}F}$ = 256 Hz, $^3J_{C\text{-}Pt}$ = 75 Hz, C_c), 163.97 (s, C_k) ppm.

δ_F = -107.23 ($^4J_{F\text{-}Pt}$ = 45 Hz), -112.12 ppm.

δ_P = 42.68, ($^1J_{P\text{-}Pt}$ = 2938 Hz) ppm.

δ_{Pt} = -2780 (d, $^1J_{Pt\text{-}P}$ = ~3300 Hz) ppm.

HR-MS (ESI): found 654.1390 m/z, calculated 654.1393 m/z = $C_{26}H_{30}ClF_2PN^{194}Pt$ = $[M\text{-}Cl]^+$.

Elemental analysis found (calculated): C 44.73 (45.16), H 4.23 (4.67), N 1.98 (1.97).

Crystals suitable for X-ray analysis were grown by the slow evaporation of solvent from a chloroform solution – ps17.

6.4.6. Synthesis of **2-Pr(t)** and **2-Pr(c)**

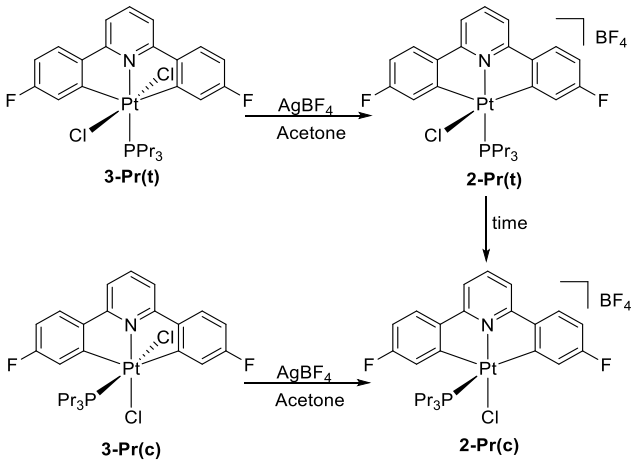

To a slurry of a mixture of **3-Pr(t)** and **3-Pr(c)** (5 mg, 8.06 x 10^{-6} mol) in acetone (1 ml) was added $AgBF_4$ (about 2-5 mg, excess) at room temperature. The products were immediately seen in solution in a ratio equal to the starting mixture, and were separated from the waste AgCl by filtration. The products could not be purified as they degraded on silica. Within a day **2-Pr(t)** fully converted into **2-Pr(c)**.

Complex - **2-Pr(t)**

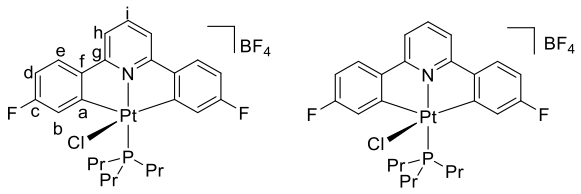

δ_H (Acetone-d_6) = 8.01 (1H, t, $^3J_{H\text{-}H}$ = 8 Hz, H_i), 7.96 (2H, dd, $^3J_{H\text{-}H}$ = 8.5 Hz, $^4J_{H\text{-}F}$ = 5.5 Hz, H_e), 7.86 (2H, d, $^3J_{H\text{-}H}$ = 8 Hz, $^5J_{H\text{-}P}$ = 2.5 Hz, H_h), 7.31 (2H, dd, $^3J_{H\text{-}F}$ = 8.5 Hz, $^4J_{H\text{-}H}$ = 2.5 Hz, $^3J_{H\text{-}Pt}$ = 13 Hz, H_b) 7.06 (2H, td, $^3J_{H\text{-}H}$ = $^3J_{H\text{-}F}$ = 8 Hz, $^4J_{H\text{-}H}$ = 2.5 Hz, H_d), 2.49 (6H, m, PCH_2), 1.77 (6H, m, PCH_2CH_2), 0.98 (9H, td, $^3J_{H\text{-}H}$ = 7 Hz, PCH_2CH_2Me) ppm.

δ_F (Acetone-d_6) = -109.19 ($^4J_{F\text{-}Pt}$ = 15.5 Hz) ppm.

δ_P (Acetone-d_6) = -12.10 ($^1J_{P\text{-}Pt}$ = 2261 Hz) ppm.

δ_{Pt} (Acetone-d_6) = -2196 (d, $^1J_{Pt\text{-}P}$ = ~2250 Hz) ppm.

Complex - **2-Pr(c)**

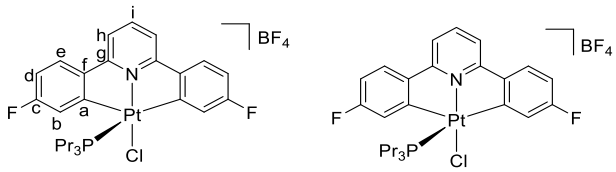

δ_H (Acetone-d_6) = 8.41 (1H, t, $^3J_{H\text{-}H}$ = 8 Hz, H_i), 8.04 (2H, dd, $^3J_{H\text{-}H}$ = 9 Hz, $^4J_{H\text{-}F}$ = 5 Hz, H_e), 7.98 (2H, d, $^3J_{H\text{-}H}$ = 8 Hz, $^4J_{H\text{-}Pt}$ = 16 Hz, H_h), 7.58 (2H, dd, $^3J_{H\text{-}F}$ = 7 Hz, $^4J_{H\text{-}H}$ = 2.5 Hz, $^3J_{H\text{-}Pt}$ = 13 Hz, H_i) 7.06 (2H, td, $^3J_{H\text{-}H}$ = $^3J_{H\text{-}F}$ = 9.5 Hz, $^4J_{H\text{-}H}$ = 2.5 Hz, H_d), 1.83 (6H, m, P*CH₂*), 1.17 (6H, m, PCH_2*CH₂*), 0.64 (9H, td, $^3J_{H\text{-}H}$ = 7 Hz, PCH_2CH_2*Me*) ppm.

δ_F (Acetone-d_6) = -107.61 ($^4J_{F\text{-}Pt}$ = 13 Hz) ppm.

δ_P (Acetone-d_6) = 13.74 ($^1J_{P\text{-}Pt}$ = 2622 Hz) ppm.

δ_{Pt} (Acetone-d_6) = -2245 (d, $^1J_{Pt\text{-}P}$ = ~2600 Hz) ppm.

6.4.7. Synthesis of **4-Pr(t)** and **4-Pr(c)**

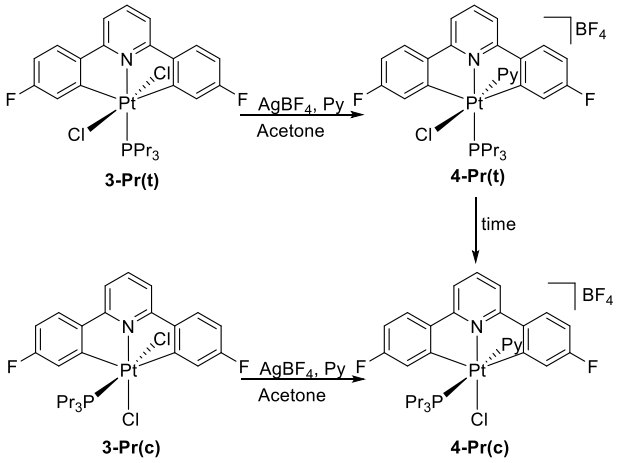

To a slurry of a mixture of **3-Pr(t)** and **3-Pr(c)** (5 mg, 8.06 x 10^{-6} mol) in acetone (1 ml) was added $AgBF_4$ (about 2-5 mg, excess) and pyridine (0.05 ml, excess) at room temperature. The products were immediately seen in solution in a ratio equal to the starting mixture, and were separated from the waste AgCl by filtration. The products could not be purified as they degraded on silica. Within a week **4-Pr(t)** fully converted into **4-Pr(c)**.

Complex - **4-Pr(t)**

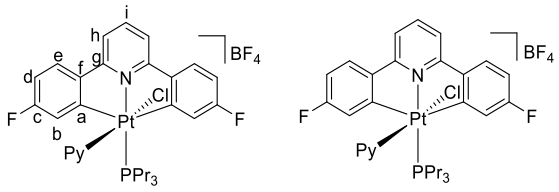

δ_H = 8.65 (2H, d, $^3J_{H\text{-}H}$ = 8.5 Hz, $^3J_{H\text{-}Pt}$ = 22 Hz, Py-*o*), 8.01 (2H, m, H_i, Py-*p*), 7.87 (2H, dd, $^3J_{H\text{-}H}$ = 8.5 Hz, $^4J_{H\text{-}F}$ = 5 Hz, H_e), 7.72 (2H, dd, $^3J_{H\text{-}F}$ = 8 Hz, $^5J_{H\text{-}P}$ = 1 Hz, H_h), 7.60 (4H, m, H_b, Py-*m*), 7.05 (2H, td, $^3J_{H\text{-}H}$ = $^3J_{H\text{-}F}$ = 8 Hz, $^4J_{H\text{-}H}$ = 2.5 Hz, H_d), 2.57 (6H, m, P*CH₂*), 1.62 (6H, m , PCH_2CH_2), 1.04 (9H, t, $^3J_{H\text{-}H}$ = 7 Hz, PCH_2CH_2Me) ppm.

δ_C = 15.48 (d, $^3J_{C\text{-}P}$ = 16 Hz, PCH_2CH_2Me), 18.05 (d, $^2J_{C\text{-}P}$ = 4.5 Hz, PCH_2CH_2), 24.73 (d, $^1J_{C\text{-}P}$ = 34.5 Hz, P*CH₂*), 114.00 (d, $^2J_{C\text{-}F}$ = 20 Hz, C_d), 118.25 (d, $^4J_{C\text{-}P}$ = 3.5 Hz, C_h), 122.41 (d, $^2J_{C\text{-}F}$ = 20 Hz, C_b), 128.73 (s, Py-*m*), 129.38 (d, $^3J_{C\text{-}F}$ = 10 Hz, C_e), 141.84 (s, C_i/Py-*p*), 142.30 (s, C_i/Py-*p*), 143.50 (t, $^3J_{C\text{-}P}$ = $^4J_{C\text{-}F}$ = 5 Hz, C_f), 152.88 (s, Py-*m*), 160.33 (m, $^1J_{C\text{-}Pt}$ = 523 Hz, C_a), 161.20 (s, C_g), 163.87 (d, $^1J_{C\text{-}F}$ = 260 Hz, H_c) ppm.

δ_F = -103.75 ($^4J_{F\text{-}Pt}$ = 11.5 Hz) ppm.

δ_P = -9.03 ($^1J_{P\text{-}Pt}$ = 2242 Hz) ppm.

δ_{Pt} = -1966 (d, $^1J_{Pt\text{-}P}$ = ~2800 Hz) ppm.

HR-MS (ESI): found 733.1815 m/z, calculated 733.1815 m/z = $C_{31}H_{35}ClF_2N_2P^{194}Pt$ = $[M]^+$.

Complex - **4-Pr(c)**

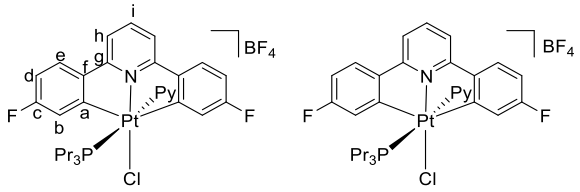

δ_H (Acetone-d_6) = 8.42 (2H, m, $^3J_{H\text{-}Pt}$ = 20 Hz, Py-*o*), 8.39 (1H, t, $^3J_{H\text{-}H}$ = 8 Hz, H_i), 8.24 (3H, m, $H_{e,h}$), 8.26 (1H, t, $^3J_{H\text{-}H}$ = 7.5 Hz, Py-*p*), 7.76 (2H, dd, $^3J_{H\text{-}F}$ = 7.5 Hz, $^4J_{H\text{-}H}$ = 2.5 Hz, $^3J_{H\text{-}Pt}$ = 14 Hz, H_b), 7.50 (2H, t, $^3J_{H\text{-}H}$ = 7.5 Hz, Py-*m*), 7.27 (2H, td, $^3J_{H\text{-}H}$ = $^3J_{H\text{-}F}$ = 8.5 Hz, $^4J_{H\text{-}H}$ = 2.5 Hz, H_d), 1.92 (6H, m, P*CH₂*), 1.31 (6H, m, PCH_2CH_2), 0.83 (9H, td, $^3J_{H\text{-}H}$ = 7 Hz, $^4J_{H\text{-}H}$ = 2 Hz, PCH_2CH_2Me) ppm.

δ_H = 8.21 (1H, t, $^3J_{H\text{-}H}$ = 7.5 Hz, H_i), 8.08 (2H, m, $^3J_{H\text{-}Pt}$ = 20 Hz, Py-*o*), 7.92 (4H, m, $H_{e,h}$), 7.70 (1H, t, $^3J_{H\text{-}H}$ = 7.5 Hz, Py-*p*), 7.58 (2H, d, $^3J_{H\text{-}F}$ = 7.5 Hz, $^3J_{H\text{-}Pt}$ = 12 Hz, H_b), 7.21 (2H,

m, Py-*m*), 7.04 (2H, t, $^{3}J_{H\text{-}H}$ = $^{3}J_{H\text{-}F}$ = 8.5 Hz, H_d), 1.66 (6H, m, PCH_2), 1.06 (6H, m, PCH_2CH_2), 0.74 (9H, t, $^{3}J_{H\text{-}H}$ = 7 Hz, PCH_2CH_2Me) ppm.

δ_C (Acetone-d_6) = 14.62 (d, $^{3}J_{C\text{-}P}$ = 16 Hz, PCH_2CH_2Me), 16.48 (d, $^{2}J_{C\text{-}P}$ = 5 Hz, $^{3}J_{C\text{-}Pt}$ = 9 Hz, PCH_2CH_2), 25.06 (d, $^{1}J_{C\text{-}P}$ = 38 Hz, $^{2}J_{C\text{-}Pt}$ = 23 Hz, PCH_2), 114.27 (d, $^{2}J_{C\text{-}F}$ = 23.5 Hz, C_d), 119.41 (s, $^{3}J_{C\text{-}Pt}$ = 30 Hz, C_h), 120.03 (d, $^{2}J_{C\text{-}F}$ = 19 Hz, $^{2}J_{C\text{-}Pt}$ = 16 Hz, C_b), 126.82 (d, $^{4}J_{C\text{-}P}$ = 2.5 Hz, $^{3}J_{C\text{-}Pt}$ = 16.5 Hz, Py-*m*), 129.83 (d, $^{3}J_{C\text{-}F}$ = 18 Hz, $^{3}J_{C\text{-}Pt}$ = 16 Hz, C_e), 140.95 (s, Py-*p*), 142.59 (s, $^{2}J_{C\text{-}Pt}$ = 23.5 Hz, C_f), 144.19 (s, C_a), 148.77 (s, Py-*o*), 162.15 (s, $^{2}J_{C\text{-}Pt}$ = 33 Hz, C_g), 162.46 (s, $^{1}J_{C\text{-}Pt}$ = 520 Hz, C_a), 165.10 (d, $^{1}J_{C\text{-}F}$ = 260 Hz, $^{3}J_{C\text{-}Pt}$ = 28.5 Hz, C_c) ppm.

δ_F (Acetone-d_6) = -106.15 ($^{4}J_{F\text{-}Pt}$ = 14.5 Hz) ppm.

δ_F = -103.55 ($^{4}J_{F\text{-}Pt}$ = 13.5 Hz) ppm.

δ_P (Acetone-d_6) = 0.66 ($^{1}J_{P\text{-}Pt}$ = 2213 Hz) ppm.

δ_P = 2.20 ($^{1}J_{P\text{-}Pt}$ = 2257 Hz) ppm.

δ_{Pt} (Acetone-d_6) = -2240 (d, $^{1}J_{Pt\text{-}P}$ = ~2550 Hz) ppm.

HR-MS (ESI): found 733.1826 m/z, calculated 733.1815 m/z = $C_{31}H_{35}F_2N_2P^{194}Pt$ = $[M]^+$.

6.4.8. Synthesis of **3-Tol(c)**, **7-Tol(t)** and **8**

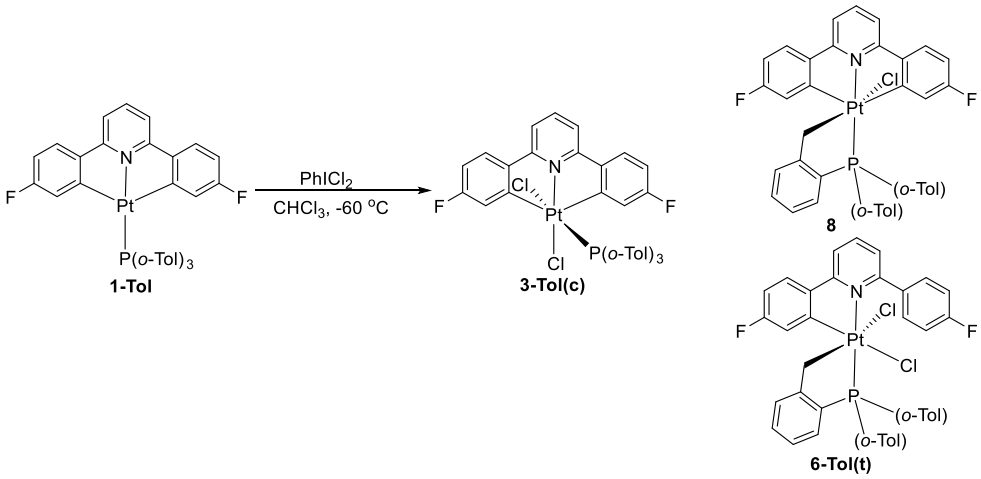

To a chloroform (10 ml) solution of **1-Tol** (20 mg, 2.62 x 10^{-5} mol) was added $PhICl_2$ (10 mg, 3.64 x 10^{-5} mol, 1.4 eq) at -60 °C giving full conversion to products. Allowing the reaction mixture to warm to room temperature led to irreversible precipitation of **6-Tol(t)** and **8**. **3-Tol(c)** was therefore easily recovered by removing the precipitate by filtration. **3-Tol(c)** was then purified by column chromatography, loading with chloroform and eluting with ethyl acetate giving the pure product as a yellow solid (3 mg, 3.66 x 10^{-6} mol, 14%).

Complex - **3-Tol(c)**

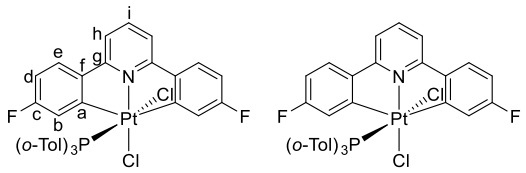

δ_H = 7.69 (2H, dd, $^3J_{H\text{-}F}$ = 8 Hz, $^4J_{H\text{-}H}$ = 2.5 Hz, $^3J_{H\text{-}Pt}$ = 19 Hz, H_b), 7.42 (1H, t, $^3J_{H\text{-}H}$ = 8 Hz, H_i), 7.31 (2H, dd, $^3J_{H\text{-}H}$ = 8.5 Hz, $^4J_{H\text{-}F}$ = 5 Hz, H_e), 7.18 (3H, m, H_l), 7.10 (3H, m, H_m), 7.01 (2H, d, $^3J_{H\text{-}H}$ = 8 Hz, H_h), 6.96 (3H, m, H_k), 6.85 (3H, m, H_n), 6.64 (2H, td, $^3J_{H\text{-}F}$ = $^3J_{H\text{-}F}$ = 8.5 Hz, $^4J_{H\text{-}H}$ = 2.5 Hz, H_d), 1.37 (9H, s, H_{Me}) ppm.

δ_C = 22.76 (d, $^3J_{C\text{-}P}$ = 4 Hz, C_{Me}), 122.32 (d, $^2J_{C\text{-}F}$ = 24 Hz, C_d), 116.19 (s, $^3J_{C\text{-}Pt}$ = 30 Hz, C_h), 121.85 (d, $^2J_{C\text{-}F}$ = 20 Hz, C_b), 124.78 (d, $^2J_{C\text{-}P}$ = 12 Hz, C_k), 127.03 (d, $^3J_{C\text{-}F}$ = 9 Hz, C_e), 129.05 (s, C_l), 131.54 (s, C_m), 132.86 (d, $^3J_{C\text{-}P}$ = 10 Hz, C_n), 140.37 (s, C_i), 121.94 (d, $^4J_{C\text{-}F}$ = 2 Hz, C_f), 143.28 (m, C_j), 162.08 (s, C_g), 163.93 (m, C_a), 164.13 (d, $^1J_{C\text{-}F}$ = 260 Hz, C_c) ppm.

δ_F = -106.5 ($^4J_{F\text{-}Pt}$ = 14 Hz) ppm.

δ_P = -13.96 ($^1J_{P\text{-}Pt}$ = 2470 Hz) ppm.

δ_{Pt} = -2403 (d, $^1J_{Pt\text{-}P}$ = ~2500 Hz) ppm.

HR-MS (ESI): found 798.1397 m/z, calculated 798.1394 m/z = $C_{38}H_{30}F_2PN^{194}Pt$ = $[M\text{-}Cl]^+$.

Crystals suitable for X-ray analysis were grown by the slow evaporation of solvent from a chloroform solution – ps27.

Complex - **8**

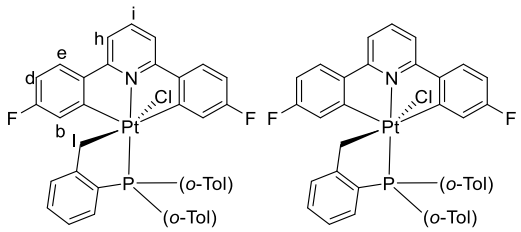

δ_H = 9.08 (dd, $^3J_{H\text{-}P}$ = 16 Hz, $^3J_{H\text{-}H}$ = 9 Hz, H_{Ar}), 6.18 (d, $^3J_{H\text{-}F}$ =11 Hz, $^3J_{H\text{-}Pt}$ = ~30 Hz, H_b), 5.18 (d, $^3J_{H\text{-}F}$ =10 Hz, $^3J_{H\text{-}Pt}$ = ~25 Hz, H_b), 2.75 (d, $^2J_{H\text{-}H}$ = 13 Hz, $^2J_{H\text{-}Pt}$ = 74 Hz, H_l), 3.77 (d, $^2J_{H\text{-}H}$ = 13 Hz, $^2J_{H\text{-}Pt}$ = 90 Hz, H_l) ppm.

δ_F = -107.52 ($^4J_{F\text{-}Pt}$ = 28 Hz), -110.29 ($^4J_{F\text{-}Pt}$ = 23 Hz) ppm.

δ_P = 20.26 ($^1J_{P\text{-}Pt}$ = 2818 Hz) ppm.

δ_{Pt} = -3028 (d, $^1J_{Pt\text{-}P}$ = ~2800 Hz) ppm.

Complex - **7-Tol(t)**

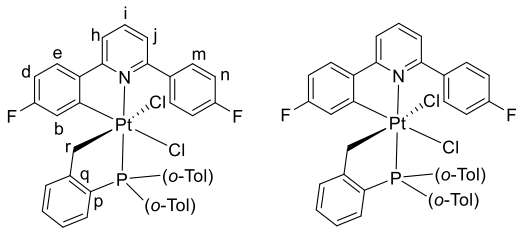

δ_H = 8.55 (dd, $^3J_{H\text{-}P}$ = 17 Hz, $^3J_{H\text{-}H}$ = 8 Hz, H_{Ar}), 5.92 (d, $^3J_{H\text{-}F}$ =11 Hz, $^3J_{H\text{-}Pt}$ = 39 Hz, H_b), 4.07 (d, $^2J_{H\text{-}H}$ = 12 Hz, $^2J_{H\text{-}Pt}$ = 76 Hz, H_r), 4.66 (d, $^2J_{H\text{-}H}$ = 12 Hz, $^2J_{H\text{-}Pt}$ = 102 Hz, H_r) ppm.

δ_F = -109.62 ($^4J_{F\text{-}Pt}$ = 43 Hz) -112.68 ppm.

δ_P = 33.21 ($^1J_{P\text{-}Pt}$ = 3199 Hz) ppm.

δ_{Pt} = -2527 (d, $^1J_{Pt\text{-}P}$ = ~2900 Hz) ppm.

Crystal suitable for X-ray analysis found by chance after a reaction – ps23.

6.4.9. Synthesis of **6-Tol(c)**

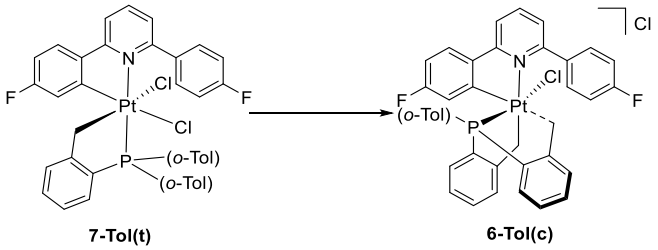

Crystals of **6-Tol(t)** were left in acetone solution for a month, after which time new peaks appeared in the NMR.

Complex - **6-Tol(c)**

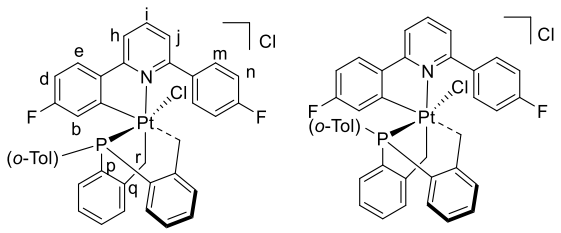

δ_H (Acetone-d_6) = 6.20 (1H, d, $^3J_{H\text{-}F}$ = 7 Hz, $^3J_{H\text{-}Pt}$ = 52 Hz, H_b), 5.12 (d, $^2J_{H\text{-}H}$ = 13.5 Hz, $^2J_{H\text{-}Pt}$ = 95 Hz, H_r), 4.25 (d, $^2J_{H\text{-}H}$ = 13.5 Hz, $^2J_{H\text{-}Pt}$ = 45 Hz, H_r) 1.86 (3H, s, Me), 1.22 (3H, s, Me)* ppm.

*When Pt-H coupling constant is set to 10 Hz a correlation to platinum is seen

δ_F (Acetone-d_6) = -109.33 ($^4J_{F\text{-}Pt}$ = 45 Hz) -115.18 ppm.

δ_P (Acetone-d_6) = 23.69 ($^1J_{P\text{-}Pt}$ = 2969 Hz) ppm.

δ_{Pt} (Acetone-d_6) = -2583 (d, $^1J_{Pt\text{-}P}$ = ~3000 Hz) ppm.

6.5. Synthesis of the Complexes from Chapter 3

6.5.1. Synthesis of **9**

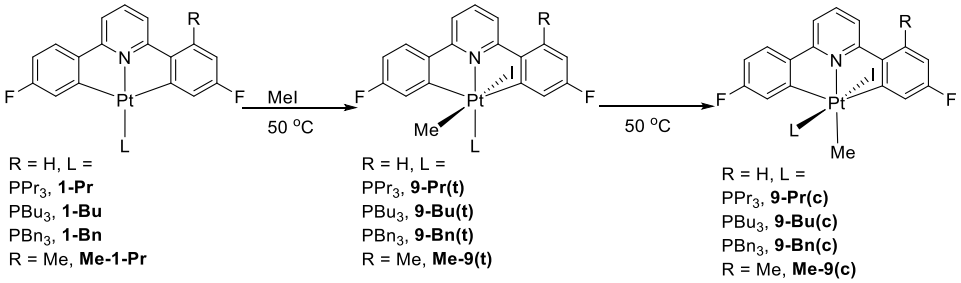

Samples of **1** (100 mg, **1-Pr**: 1.61 x 10^{-4} mol, **1-Bu**: 1.51 x 10^{-4} mol, **1-Bn**: 1.31 x 10^{-4} mol, **Me-1-Pr**: 1.58 x 10^{-4} mol) were dissolved in MeI (3 ml) and heated to reflux until full consumption of starting material was observed (**1-Pr**, **1-Bu** and **Me-1-Pr**: 1 hour, **1-Bn**: 2 days). The MeI was then removed under vacuum. The poorly soluble product was then washed with acetone to give a pure mixture of **9-L(t)** and **9-L(c)**. Longer reaction times (**1-Pr**, **1-Bu** and **Me-1-Pr**: 3 days, **1-Bn**: 2 weeks) gave only **9-L(c)** as desired products. Combined yields (**9-L(t)** and **9-L(c)** mixture): **9-Pr**: 116 mg, 1.70 x 10^{-4} mol, 95%, **9-Bu**: 112 mg, 1.40 x 10^{-4} mol, 93%, **9-Bn**: 101 mg, 1.11 x 10^{-4} mol, 85%, **Me-9-Pr**: 98 mg, 1.26 x 10^{-4} mol, 80%.

Complex - **9-Pr(t)**

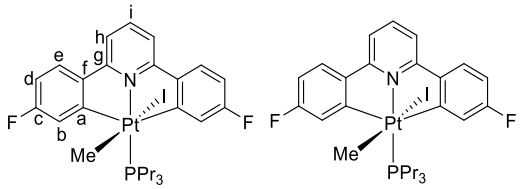

δ_H = 7.79 (1H, t, $^3J_{H\text{-}H}$ = 8.5 Hz, H_i), 7.71 (2H, dd, $^3J_{H\text{-}H}$ = 8.5 Hz, $^4J_{H\text{-}F}$ = 5.5 Hz, H_e), 7.48 (2H, dd, $^3J_{H\text{-}H}$ = 8.5 Hz, $^4J_{H\text{-}H}$ = 2 Hz, C_h), 7.22 (2H, dd, $^3J_{H\text{-}F}$ 10 Hz, $^4J_{H\text{-}H}$ = 2.5 Hz, $^3J_{H\text{-}Pt}$ = 23 Hz, H_b), 6.81 (2H, td, $^3J_{H\text{-}H}$ = $^3J_{H\text{-}F}$ = 8.5 Hz, $^4J_{H\text{-}H}$ = 2.5 Hz, H_d), 1.73 (6H, m, PCH_2CH_2), 2.45 (6H, m, PCH_2), 1.11 (9H, t, $^3J_{H\text{-}H}$ = 7 Hz, PCH_2CH_2Me), 1.02 (3H, d, $^3J_{H\text{-}P}$ = 3 Hz, $^1J_{H\text{-}Pt}$ = 67 Hz, PtMe) ppm.

δ_C = 3.55 (d, $^2J_{C\text{-}P}$ = 3Hz, $^1J_{C\text{-}Pt}$ = 516 Hz, PtMe), 14.40 (d, $^3J_{C\text{-}P}$ = 14Hz, PCH_2CH_2Me), 17.58 (d, $^2J_{C\text{-}P}$ = 5 Hz, $^3J_{C\text{-}Pt}$ = 11 Hz, PCH_2CH_2), 25.31 (d, $^1J_{C\text{-}P}$ = 36 Hz, $^2J_{C\text{-}Pt}$ = 23 Hz, PCH_2), 110.05 (d, $^2J_{C\text{-}F}$ = 22 Hz, C_d), 115.06 (d, $^6J_{C\text{-}F}$ = 4 Hz, $^3J_{C\text{-}Pt}$ = 21.5 Hz, C_h), 121.10 (d, $^2J_{C\text{-}F}$ = 18 Hz, $^2J_{C\text{-}Pt}$ = 36 Hz, C_b), 126.62 (d, $^3J_{C\text{-}F}$ = 9 Hz, $^3J_{C\text{-}Pt}$ = 24.5 Hz, C_e), 138.45

(s, C_i), 143.23 (m, C_f), 160.87 (s, $^2J_{C\text{-}Pt}$ = 39 Hz, C_g), 161.48 (m, $^1J_{C\text{-}Pt}$ = 569 Hz, C_a), 161.97 (d, $^1J_{C\text{-}F}$ = 254 Hz, $^3J_{C\text{-}Pt}$ = 40 Hz, C_c) ppm.

δ_F = -110.00 ($^4J_{F\text{-}Pt}$ = 23 Hz) ppm.

δ_P = -22.45 ($^1J_{P\text{-}Pt}$ = 2650 Hz) ppm.

δ_{Pt} = -3520 (d, $^1J_{Pt\text{-}P}$ = ~2900 Hz) ppm.

HR-MS (ESI): found 634.1934 m/z, calculated 634.1940 m/z = $C_{27}H_{33}F_2PN^{194}Pt$ = $[M\text{-}I]^+$.

Elemental analysis found (calculated): C 42.31 (42.53), H 4.27 (4.36), N 1.78 (1.84).

Crystals suitable for X-ray analysis were grown by the slow evaporation of solvent from a chloroform solution – ps20.

Complex - **9-Bu(t)**

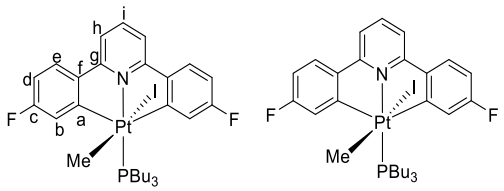

δ_H = 7.71 (1H, t, $^3J_{H\text{-}H}$ = 8 Hz, H_i), 7.65 (2H, dd, $^3J_{H\text{-}H}$ = 8.5 Hz, $^4J_{H\text{-}F}$ = 5.5 Hz, H_e), 7.41 (2H, dd, $^3J_{H\text{-}H}$ = 8 Hz, $^5J_{H\text{-}P}$ = 2 Hz, H_h), 7.18 (2H, dd, $^3J_{H\text{-}F}$ = 9.5 Hz, $^4J_{H\text{-}H}$ = 2.5 Hz, $^3J_{H\text{-}Pt}$ = 22 Hz, H_b), 6.74 (2H, td, $^3J_{H\text{-}H}$ = $^3J_{H\text{-}F}$ = 8.5 Hz, $^4J_{H\text{-}H}$ = 2.5 Hz, H_d), 2.43 (6H, m, P*CH₂*), 1.63 (6H, m, PCH_2*CH₂*), 1.46 (6H, m, PCH_2CH_2*CH₂*), 0.97 (3H, d, $^3J_{H\text{-}P}$ = 3 Hz, $^2J_{H\text{-}Pt}$ = 67 Hz, PtMe), 0.93 (9H, t, $^3J_{H\text{-}H}$ = 7 Hz, $PCH_2CH_2CH_2$*Me*) ppm.

δ_C = 3.59 (d, $^2J_{C\text{-}P}$ = 3 Hz, $^1J_{C\text{-}Pt}$ = 515 Hz, PtMe), 12.69 (s, $PCH_2CH_2CH_2$*Me*), 22.93 (m, PCH_2,PCH_2CH_2*CH₂*), 25.80 (d, $^2J_{C\text{-}P}$ = 5 Hz, $^3J_{C\text{-}Pt}$ = 10 Hz, C PCH_2*CH₂*), 110.06 (d, $^2J_{C\text{-}F}$ = 22 Hz, C_d), 115.07 (d, $^4J_{C\text{-}P}$ = 4 Hz, $^3J_{C\text{-}Pt}$ = 20 Hz, C_h), 121.18 (d, $^2J_{C\text{-}F}$ = 19 Hz, $^2J_{C\text{-}Pt}$ = 34 Hz, C_b),126.64 (d, $^3J_{C\text{-}P}$ = 9 Hz, $^3J_{C\text{-}Pt}$ = 24 Hz, C_e), 138.49 (s, C_i), 143.24 (t, $^3J_{C\text{-}P}$ = $^4J_{C\text{-}F}$ = 2 Hz, $^2J_{C\text{-}Pt}$ = 13 Hz, C_f), 160.85 (s, $^2J_{C\text{-}Pt}$ = 38 Hz, H_g), 161.54 (m, $^1J_{C\text{-}Pt}$ = 572 Hz, H_a), 161.95 (d, $^1J_{C\text{-}F}$ = 253 Hz, $^3J_{C\text{-}Pt}$ = 38 Hz, C_c) ppm.

δ_F = -109.50 ($^4J_{F\text{-}Pt}$ = 22 Hz) ppm.

δ_P = -21.77 ($^1J_{P\text{-}Pt}$ = 2644 Hz) ppm.

δ_{Pt} = -3517 (d, $^1J_{Pt\text{-}P}$ = ~2650 Hz) ppm.

HR-MS (ESI): found 676.2406 m/z, calculated 676.2410 m/z = $C_{30}H_{39}F_2NP^{194}Pt$ = $[M\text{-}I]^+$.

HR-MS (ESI): found 826.1352 m/z, calculated 826.1352 m/z = $C_{30}H_{39}F_2INP^{194}PtNa$ = $[M+Na]^+$.

Complex - **9-Bn(t)**

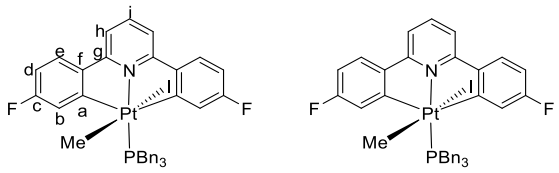

δ_H = 7.89 (1H, t, $^3J_{H\text{-}H}$ = 8 Hz, H_i), 7.80 (2H, dd, $^3J_{H\text{-}H}$ = 8.5 Hz, $^4J_{H\text{-}F}$ = 5.5 Hz, H_e), 7.59 (2H, dd, $^3J_{H\text{-}H}$ = 8 Hz, $^5J_{H\text{-}P}$ = 2 Hz, $^4J_{H\text{-}Pt}$ = 2 Hz, H_h), 7.46 (2H, dd, $^3J_{H\text{-}F}$ = 9.5 Hz, $^4J_{H\text{-}H}$ = 2 Hz, $^3J_{H\text{-}Pt}$ = 25 Hz, H_b), 7.29 (9H, m, Bn-*m,p*), 6.89 (2H, td, $^3J_{H\text{-}F}$ = $^3J_{H\text{-}H}$ = 8.5 Hz, $^4J_{H\text{-}H}$ = 2 Hz, H_d), 6.83 (6H, d, $^3J_{H\text{-}H}$ = 7.5 Hz, Bn-*o*), 4.09 (6H, d, $^2J_{H\text{-}P}$ = 10 Hz, $^3J_{H\text{-}Pt}$ = 20 Hz, Ph*CH*$_2$), 1.31 (3H, d, $^3J_{H\text{-}P}$ = 3 Hz, $^2J_{H\text{-}Pt}$ = 66 Hz, PtMe) ppm.

δ_F = -109.13 ($^4J_{F\text{-}Pt}$ = 22.5 Hz) ppm.

δ_P = -23.16 ($^1J_{P\text{-}Pt}$ = 2648 Hz) ppm.

δ_{Pt} = -3436 (d, $^1J_{Pt\text{-}P}$ = ~2700 Hz) ppm.

Complex - **Me-9-Pr(t)**

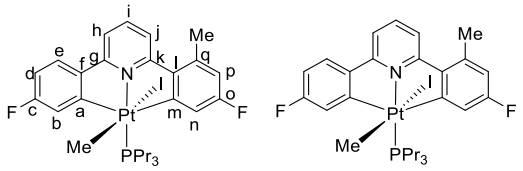

δ_H = 7.76 (1H, t, $^3J_{H\text{-}H}$ = 8 Hz, H_i), 7.73 (1H, m, H_j), 7.65 (1H, dd, $^3J_{H\text{-}H}$ = 8.5, $^4J_{H\text{-}F}$ = 5.5 Hz H_e), 7.46 (1H, dt, $^3J_{H\text{-}H}$ = 8Hz, $^4J_{H\text{-}H}$ = $^5J_{H\text{-}P}$ = 1.5 Hz, H_h), 7.17 (1H, dd, $^3J_{H\text{-}F}$ = 9.5 Hz, $^4J_{H\text{-}H}$ = 2.5, $^3J_{H\text{-}Pt}$ = 21.5 Hz, H_b), 7.07 (1H, dd, , $^3J_{H\text{-}F}$ = 9.5 Hz, $^4J_{H\text{-}H}$ = 2.5, $^3J_{H\text{-}Pt}$ = 24.5 Hz, H_n), 6.75 (1H, td, , $^3J_{H\text{-}F}$ = $^3J_{H\text{-}H}$ = 9 Hz, $^4J_{H\text{-}H}$ = 2.5, H_d), 6.58 (1H, dd, $^3J_{H\text{-}F}$ = 9.5 Hz, $^4J_{H\text{-}H}$ = 2.5, H_p), 2.64 (3H, s, Me), 2.40 (6H, m, P*CH*$_2$), 1.67 (6H, m, PCH$_2$*CH*$_2$), 1.05 (9H, dt, $^3J_{H\text{-}H}$ = 7 Hz, $^4J_{H\text{-}P}$ = 1 Hz, PCH$_2$CH$_2$*Me*), 0.98 (3H, d, $^3J_{H\text{-}P}$ = 3 Hz, $^2J_{H\text{-}Pt}$ = 67.5 Hz, PtMe) ppm.

δ_C = 4.30 (d, $^2J_{C\text{-}P}$ = 3 Hz, $^1J_{C\text{-}Pt}$ = 521.5 Hz, PtMe), 14.43 (d, $^3J_{C\text{-}P}$ = 15 Hz, PCH$_2$CH$_2$*Me*), 17.72 (d, $^2J_{C\text{-}P}$ = 5 Hz, $^3J_{C\text{-}Pt}$ = 10 Hz, PCH$_2$*CH*$_2$), 23.70 (s, Me), 25.36 (d, $^1J_{C\text{-}P}$ = 35 Hz, $^2J_{C\text{-}Pt}$ = 22 Hz, P*CH*$_2$), 110.03 (d, $^2J_{C\text{-}F}$ = 22.5 Hz, C_d), 114.26(d, $^2J_{C\text{-}F}$ = 20.5 Hz, C_p), 114.89 (d, $^4J_{C\text{-}P}$ = 4 Hz, $^3J_{C\text{-}Pt}$ = 21 Hz, C_h), 119.02 (m, $C_{n,j}$), 121.00 (d, $^2J_{C\text{-}F}$ = 18 Hz, $^2J_{C\text{-}Pt}$ = 33 Hz, C_b), 126.73 (d, $^3J_{C\text{-}F}$ = 7.5 Hz, $^2J_{C\text{-}Pt}$ = 23.5 Hz, C_e), 138.28 (s, C_i), 139.23 (d, $^3J_{C\text{-}F}$ = 8 Hz, $^3J_{C\text{-}Pt}$ = 25 Hz, C_q), 141.83 (m, C_l), 143.50 (m, C_f), 160.73 (d, $^1J_{C\text{-}F}$ = 255 Hz, $^3J_{C\text{-}Pt}$ = 43 Hz, C_o), 161.46 (s, $^2J_{C\text{-}Pt}$ = 39.5, $C_{g/k}$), 161.94 (s, $^2J_{C\text{-}Pt}$ = 37 Hz, $C_{g/k}$), 161.98 (d, $^2J_{C\text{-}F}$

= 254.5, $^{3}J_{C\text{-}Pt}$ = 40 Hz, C_c), 162.56 (m, $^{1}J_{C\text{-}Pt}$ = 561 Hz, C_a), 163.68 (m, $^{1}J_{C\text{-}Pt}$ = 563 Hz, C_m) ppm.

δ_F = -109.60 ($^{4}J_{F\text{-}Pt}$ = 24.5 Hz, F_o), -112.18 ($^{4}J_{F\text{-}Pt}$ = 23 Hz, F_c) ppm.

δ_P = -21.56 ($^{1}J_{P\text{-}Pt}$ = 2655 Hz) ppm.

δ_{Pt} = -3501 ($^{1}J_{Pt\text{-}P}$ = ~3000 Hz) ppm.

HR-MS (ESI): found 648.2094 m/z, calculated 648.2097 m/z = $C_{28}H_{35}F_2PN^{194}Pt$ = $[M\text{-}I]^+$.

HR-MS (ESI): found 798.1028 m/z, calculated 798.1039 m/z = $C_{28}H_{35}F_2PNI^{194}PtNa$ = $[M+Na]^+$.

Elemental Analysis calculated (found): C 43.31 (43.24), H 4.54 (4.47), N 1.80 (1.76).

Complex - **9-Pr(c)**

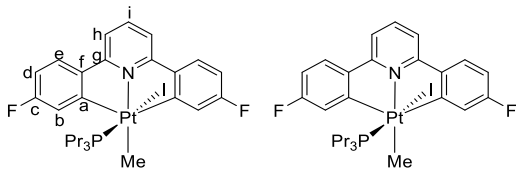

δ_H = 7.80 (1H, t, $^{3}J_{H\text{-}H}$ = 8 Hz, H_i), 7.74 (2H, dd, $^{3}J_{H\text{-}H}$ = 8 Hz, $^{4}J_{H\text{-}F}$ = 5.5 Hz, H_e), 7.53 (2H, d, $^{3}J_{H\text{-}H}$ = 8 Hz, H_h), 7.39 (2H, d, $^{3}J_{H\text{-}H}$ = 8.5 Hz, $^{3}J_{H\text{-}Pt}$ = 23 Hz, H_b), 6.82 (2H, t, $^{3}J_{H\text{-}H}$ = $^{3}J_{H\text{-}F}$ = 8 Hz, H_d), 1.57 (3H, d, $^{2}J_{H\text{-}P}$ = 3.5 Hz, $^{1}J_{H\text{-}Pt}$ = 62 Hz, PtMe), 1.41 (6H, m, P*CH₂*), 1.01 (6H, m, PCH_2*CH₂*), 0.71 (9H, t $^{3}J_{H\text{-}H}$ = 7 Hz, PCH_2CH_2*Me*) ppm.

δ_C = -15.16 (d, $^{2}J_{C\text{-}P}$ = 5 Hz, $^{1}J_{C\text{-}Pt}$ = 502.5 Hz, PtMe), 15.54 (d, $^{3}J_{C\text{-}P}$ = 15 Hz, PCH_2CH_2*Me*), 16.52 (d, $^{2}J_{C\text{-}P}$ = 6 Hz, $^{3}J_{C\text{-}Pt}$ = 13 Hz, PCH_2*CH₂*), 23.09 (d, $^{1}J_{C\text{-}P}$ = 35 Hz, $^{2}J_{C\text{-}Pt}$ = 29 Hz, P*CH₂*), 111.52 (d $^{2}J_{C\text{-}F}$ = 23.5 Hz, C_d), 115.85 (s, $^{3}J_{C\text{-}Pt}$ = 16 Hz, C_h), 121.15 (d, $^{2}J_{C\text{-}F}$ = 17.5 Hz, $^{2}J_{C\text{-}Pt}$ = 25.5 Hz, C_b), 127.47 (d, ^{3} $J_{C\text{-}F}$ = 8 Hz, $^{3}J_{C\text{-}Pt}$ = 23 Hz, C_e), 139.33 (s, C_i), 144.57 (m, C_f), 158.46 (m, $^{1}J_{C\text{-}Pt}$ = 540 Hz, C_a), 161.83 (s, $^{2}J_{C\text{-}Pt}$ = 33.5 Hz, C_g), 163.69 (d, $^{1}J_{C\text{-}F}$ = 256 Hz, $^{3}J_{C\text{-}Pt}$ = 39 Hz, C_c) ppm.

δ_F = -109.00 ($^{4}J_{F\text{-}Pt}$ = 23 Hz) ppm.

δ_P = -18.35 ($^{1}J_{P\text{-}Pt}$ = 2482 Hz) ppm.

δ_{Pt} = -3901 (d, $^{1}J_{Pt\text{-}P}$ = ~2730 Hz) ppm.

HR-MS (ESI): found 634.1941 m/z, calculated 634.1940 m/z = $C_{27}H_{33}F_2PN^{194}Pt$ = $[M\text{-}I]^+$.

Elemental analysis found (calculated): C 42.00 (42.53), H 4.10 (4.36), N 1.74 (1.84).

Complex - **9-Bu(c)**

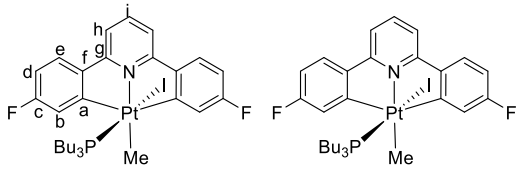

δ_H = 7.83 (1H, t, $^3J_{H\text{-}H}$ = 8 Hz H_i), 7.76 (2H, dd, $^3J_{H\text{-}H}$ = 9 Hz, $^4J_{H\text{-}F}$ = 5 Hz, H_e), 7.56 (2H, d, $^3J_{H\text{-}H}$ = 8 Hz, H_h), 7.40 (2H, dd, $^3J_{H\text{-}F}$ = 8 Hz, $^4J_{H\text{-}H}$ = 2 Hz, $^3J_{H\text{-}Pt}$ = 23 Hz, H_b), 6.85 (2H, dt, $^3J_{H\text{-}F}$ = $^3J_{H\text{-}H}$ = 9 Hz, $^4J_{H\text{-}H}$ = 2 Hz, H_d), 1.59 (3H, d, $^3J_{H\text{-}P}$ = 4 Hz, $^3J_{H\text{-}Pt}$ = 62 Hz, PtMe), 1.47 (6H, m, P*CH2*), 1.10 (6H, m, PCH_2CH_2*CH_2*), 0.95 (6H, m, PCH_2*CH_2*), 0.76 (9H, t, $^3J_{H\text{-}H}$ = 7 Hz, $PCH_2CH_2CH_2$*Me*) ppm.

δ_C = -16.06 (d, $^2J_{C\text{-}P}$ = 6 Hz, $^1J_{C\text{-}Pt}$ = 503 Hz, PtMe), 12.29 (s, $PCH_2CH_2CH_2$*Me*), 19.78 (d, $^1J_{C\text{-}P}$ = 35 Hz, $^2J_{C\text{-}Pt}$ = 29 Hz, P*CH2*), 23.13 (d, $^3J_{C\text{-}P}$ = 13 Hz, PCH_2CH_2*CH_2*), 23.68 (d, $^2J_{C\text{-}P}$ = 5.5 Hz, $^3J_{C\text{-}Pt}$ = 11 Hz, PCH_2*CH_2*), 110.51 (d, $^2J_{C\text{-}F}$ = 22 Hz, C_d), 114.87 (s, $^3J_{C\text{-}Pt}$ = 16 Hz, C_h), 120.18 (d, $^2J_{C\text{-}F}$ = 17 Hz, $^2J_{C\text{-}Pt}$ = 25 Hz, C_b),126.45 (d, $^3J_{C\text{-}P}$ = 8.5 Hz, $^3J_{C\text{-}Pt}$ = 22 Hz, C_e), 138.37 (s, C_i), 143.24 (m, C_f), 157.34 (m, $^1J_{C\text{-}Pt}$ = 541 Hz, H_a), 160.80 (s, $^2J_{C\text{-}Pt}$ = 29 Hz, H_g), 162.64 (d, $^1J_{C\text{-}F}$ = 259 Hz, $^3J_{C\text{-}Pt}$ = 39.5 Hz, C_c) ppm.

δ_F = -109.13 ppm ($^4J_{F\text{-}Pt}$ = 23 Hz) ppm.

δ_P = -18.13 ppm ($^1J_{P\text{-}Pt}$ = 2456 Hz) ppm.

δ_{Pt} = -3896 ppm (d, $^1J_{Pt\text{-}P}$ = ~3800 Hz) ppm.

HR-MS (ESI): found 676.2398 m/z, calculated 676.2410 m/z = $C_{30}H_{39}F_2NP^{194}Pt$ = $[M\text{-}I]^+$.

HR-MS (ESI): found 826.1340 m/z, calculated 826.1352 m/z = $C_{30}H_{39}F_2INNaP^{194}Pt$ = $[M+Na]^+$.

Elemental analysis found (calculated): 45.96 (44.78), H 5.02 (4.89), N 1.70 (1.74).

Crystals suitable for X-ray analysis were grown by the slow evaporation of solvent from a chloroform solution – ps5.

Complex - **9-Bn(c)**

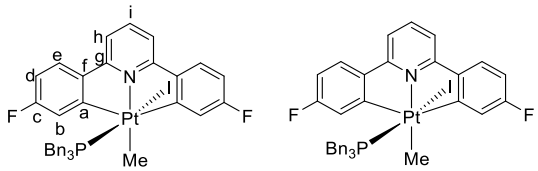

δ_H = 7.76 (2H, dd, $^3J_{H\text{-}H}$ = 9 Hz, $^4J_{H\text{-}F}$ = 5.5 Hz, H_e), 7.67 (1H, t, $^3J_{H\text{-}H}$ = 7.5 Hz, H_i), 7.48 (2H, dd, $^3J_{H\text{-}F}$ = 8 Hz, $^4J_{H\text{-}H}$ = 2 Hz, $^3J_{H\text{-}Pt}$ = 21 Hz, H_b), 7.41 (2H, d, $^3J_{H\text{-}H}$ = 7.5 Hz, H_h), 7.11 (3H, t, $^3J_{H\text{-}H}$ = 7.5 Hz, Bn-*p*), 6.98 (6H, t, $^3J_{H\text{-}H}$ = 7.5 Hz, Bn-*m*), 6.92 (2H, td, $^3J_{H\text{-}H}$ = $^3J_{H\text{-}F}$ = 9 Hz, $^4J_{H\text{-}H}$ = 2 Hz, H_d), 5.84 (6H, d, $^3J_{H\text{-}H}$ = 7.5 Hz, Bn-*o*), 3.03 (6H, d, $^2J_{H\text{-}P}$ = 11 Hz, $^3J_{H\text{-}Pt}$ = 23 Hz, Ph*CH*$_2$), 1.71 (3H, d, $^3J_{H\text{-}P}$ = 5 Hz, $^2J_{H\text{-}Pt}$ = 61 Hz, PtMe) ppm.

δ_C = -14.02 (d, $^2J_{C\text{-}P}$ = 5 Hz, $^1J_{C\text{-}Pt}$ = 503 Hz, PtMe), 28.13 (d, $^1J_{C\text{-}P}$ = 29 Hz, $^2J_{C\text{-}Pt}$ = 29 Hz, Ph*CH*$_2$), 111.82 (d, $^2J_{C\text{-}F}$ = 25 Hz, C_d), 116.26 (s, $^3J_{C\text{-}Pt}$ = 16 Hz, C_h), 121.34 (d, $^2J_{C\text{-}F}$ = 17.5 Hz, $^2J_{C\text{-}Pt}$ = 22 Hz, C_b), 127.24 (d, $^5J_{C\text{-}P}$ = 5 Hz, Bn-*p*), 127.61 (d, $^3J_{C\text{-}F}$ = 8 Hz, $^3J_{C\text{-}Pt}$ = 23 Hz, C_e), 128.83, (d, $^4J_{C\text{-}P}$ = 1.5 Hz, Bn-*m*), 130.08 (d, $^3J_{C\text{-}P}$ = 5 Hz, Bn-*o*), 131.73 (d, $^2J_{C\text{-}P}$ = 10 Hz, $^3J_{C\text{-}Pt}$ = 20 Hz, Bn-*i*), 139.45 (s, C_i), 144.83 (s, $^2J_{C\text{-}Pt}$ = 42 Hz, C_f), 158.44 (m, $^1J_{C\text{-}Pt}$ = 540 Hz, C_a), 161.35 (s, $^2J_{C\text{-}Pt}$ = 30 Hz, C_g), 163.96 (d, $^1J_{C\text{-}F}$ = 259 Hz, $^3J_{C\text{-}F}$ = 39 Hz, C_c) ppm.

δ_F = -108.00 ($^4J_{F\text{-}Pt}$ = 22.5 Hz) ppm.

δ_P = -23.19 ($^1J_{P\text{-}Pt}$ = 2403 Hz) ppm.

δ_{Pt} = -3898 (d, $^1J_{Pt\text{-}P}$ = ~2450 Hz) ppm.

HR-MS (ESI): found 779.1920 m/z, calculated 778.1940 m/z = $C_{39}H_{33}F_2NP^{194}Pt$ = $[M\text{-}I]^+$.

HR-MS (ESI): found 928.0864 m/z, calculated 928.0883 m/z = $C_{39}H_{33}F_2NP^{194}PtNa$ = $[M+Na]^+$.

Elemental analysis found (calculated): C 49.98 (51.67), H 3.42 (3.67), N 1.41 (1.54).

Complex - **Me-9-Pr(c)**

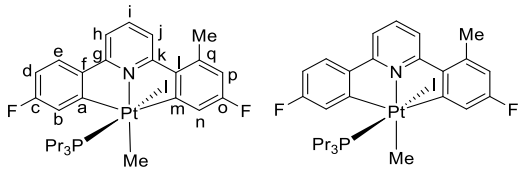

δ_H = 7.84 (2H, m, $H_{i,j}$), 7.76 (1H, dd, $^3J_{H\text{-}H}$ = 8.5 Hz, $^4J_{H\text{-}F}$ = 5 Hz, H_e), 7.58 (1H, dd, $^3J_{H\text{-}H}$ = 5.5 Hz, $^4J_{H\text{-}H}$ = 3 Hz, H_h), 7.40 (1H, dd, $^3J_{H\text{-}F}$ = 8.5 Hz, $^4J_{H\text{-}H}$ = 3 Hz, $^3J_{H\text{-}Pt}$ = 22 Hz, H_b), 7.32 (1H, dd, $^3J_{H\text{-}F}$ = 7.5 Hz, $^4J_{H\text{-}H}$ = 2.5 Hz, $^3J_{H\text{-}Pt}$ = 25 Hz, H_n), 6.84 (1H, td, $^3J_{H\text{-}H}$ = $^3J_{H\text{-}F}$ = 9 Hz, $^4J_{H\text{-}H}$ = 2.5 Hz, H_d), 6.67 (1H, dd, $^3J_{H\text{-}F}$ = 9.5 Hz, $^4J_{H\text{-}H}$ = 2.5 Hz, H_p), 2.74 (3H, s, Me), 1.55 (3H, d, $^3J_{H\text{-}P}$ = 4 Hz, $^2J_{H\text{-}Pt}$ = 62 Hz, PtMe), 1.41 (6H, m, PCH_2), 1.02 (6H, m, PCH_2CH_2), 0.73 (9H, t, $^3J_{H\text{-}H}$ = 7 Hz, PCH_2CH_2Me) ppm.

δ_C = -14.22 (d, $^2J_{C\text{-}P}$ = 5 Hz, $^1J_{C\text{-}Pt}$ = 506 Hz, PtMe), 15.61 (d, $^3J_{C\text{-}P}$ = 15 Hz, PCH_2CH_2Me), 16.52 (d, $^2J_{C\text{-}P}$ = 5.5 Hz, $^3J_{C\text{-}Pt}$ = 12 Hz, PCH_2CH_2), 22.98 (d, $^1J_{C\text{-}P}$ = 35 Hz, $^2J_{C\text{-}Pt}$ = 29 Hz, PCH_2), 24.42 (s, Me), 111.50 (d, $^2J_{C\text{-}F}$ = 23.5 Hz, C_d), 115.62 (m, $C_{h,p}$), 118.67 (d, $^2J_{C\text{-}F}$ = 16 Hz, $^2J_{C\text{-}Pt}$ = 22 Hz, C_n), 119.87 (s, $^3J_{C\text{-}Pt}$ = 15 Hz, C_j), 120.96 (d, $^2J_{C\text{-}F}$ = 16 Hz, $^2J_{C\text{-}Pt}$ = 25 Hz, C_b), 125.52 (d, $^3J_{C\text{-}F}$ = 8.5 Hz, $^3J_{C\text{-}Pt}$ = 21 Hz, C_e), 139.09 (s, C_i), 140.35 (d, $^3J_{C\text{-}F}$ = 8.5 Hz, C_q), 143.28 (s, C_l), 144.71 (s, C_f), 159.33 (m, $^1J_{C\text{-}Pt}$ = 596 Hz, C_a), 160.14 (m, $^1J_{C\text{-}Pt}$ = 486 Hz, C_m), 162.31 (d, $^1J_{C\text{-}F}$ = 258 Hz, $^3J_{C\text{-}Pt}$ = 41 Hz, C_o), 162.36 (s, $^2J_{C\text{-}Pt}$ = 29 Hz, C_k), 162.72 (s, $^2J_{C\text{-}Pt}$ = 29 Hz, C_g), 163.58 (d, $^1J_{C\text{-}F}$ = 255 Hz, $^3J_{C\text{-}Pt}$ = 41 Hz, C_c) ppm.

δ_F = -109.10 (s, $^4J_{F\text{-}Pt}$ = 22 Hz, F_c), -111.63 (s, $^4J_{F\text{-}Pt}$ = 23 Hz, F_o) ppm.

δ_P = -18.22 ($^1J_{P\text{-}Pt}$ = 2520 Hz) ppm.

δ_{Pt} = -3910 (d, $^1J_{Pt\text{-}P}$ = ~2550 Hz) ppm.

HR-MS (ESI): found 648.2082 m/z, calculated 648.2097 m/z = $C_{28}H_{35}F_2NP^{194}Pt$ = $[M\text{-}I]^+$.

HR-MS (ESI): found 798.1030 m/z, calculated 798.1039 m/z = $C_{28}H_{35}F_2INP^{194}PtNa$ = $[M+Na]^+$.

6.5.2. Synthesis of **11** via **10**

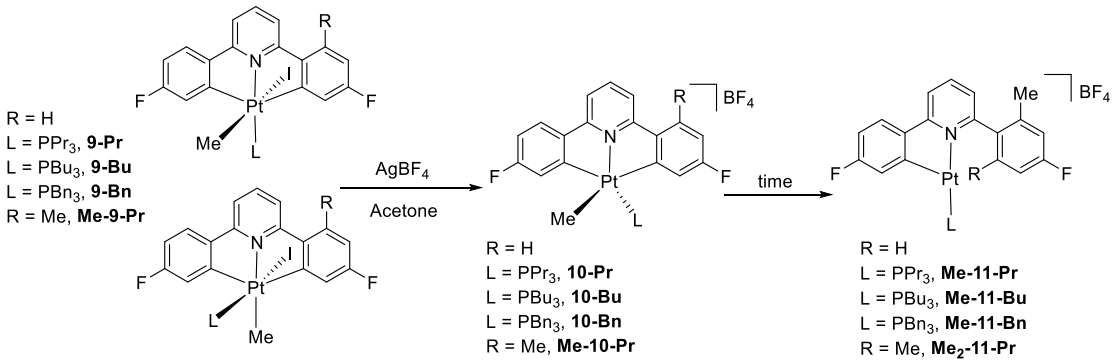

To an acetone (10 ml) suspension of either isomer of **9** (90 mg, **9-Pr**: 1.18 x 10^{-4} mol, **9-Bu**: 1.28 x 10^{-4} mol, **9-Bn**: 9.93 x 10^{-5} mol, **Me-9-Pr**: 1.16 x 10^{-4} mol), was added $AgBF_4$ (30-40 mg, excess). **9-Pr** and **9-Bu**, **10-L** were seen in solution, but converts over time to **Me-11-L**. In the case of **9-Bn** and **Me-9-Pr**, only see the corresponding **Me-11-Bn** or **Me2-11-Pr** were observed. The reaction mixture was then filtered to remove AgI, followed by the removal of solvent by evaporation. The products could not be purified as they degraded on silica. The ^{1}H NMR spectra of the products were clean enough to be carried forward to later stages.

Complex - **10-Pr**

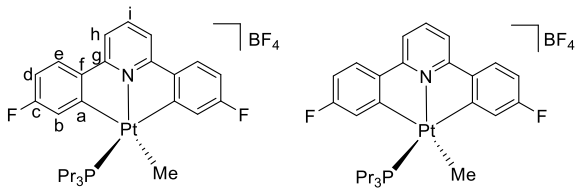

δ_H (Acetone-d_6) = 8.20 (1H, t, $^3J_{H\text{-}H}$ = 8 Hz, H_i), 8.10 (2H, dd, $^3J_{H\text{-}H}$ = 8.5 Hz, $^4J_{H\text{-}F}$ = 5.5 Hz, H_e), 8.05 (2H, d, $^3J_{H\text{-}H}$ = 8 Hz, H_h), 7.47 (2H, dd, $^3J_{H\text{-}F}$ = 8 Hz, $^4J_{H\text{-}H}$ = 2.5 Hz, $^3J_{H\text{-}Pt}$ = 21 Hz, H_b), 7.09 (2H, td, $^3J_{H\text{-}H}$ = $^3J_{H\text{-}F}$ = 8 Hz, $^4J_{H\text{-}H}$ = 2.5 Hz, H_d), 1.86 (6H, m, P*CH*$_2$), 1.60 (3H, s, $^2J_{H\text{-}Pt}$ = 55 Hz, PtMe), 1.20 (6H, m, PCH$_2$*CH*$_2$), 0.75 (9H, t, $^3J_{H\text{-}H}$ = 7 Hz, PCH$_2$CH$_2$*Me*) ppm.

δ_C (Acetone-d_6) = -4.37 (d, $^2J_{C\text{-}P}$ = 6 Hz, $^1J_{C\text{-}Pt}$ = 508 Hz, PtMe), 14.51 (d, $^3J_{C\text{-}P}$ = 15 Hz, PCH$_2$CH$_2$*Me*), 16.30 (d, $^2J_{C\text{-}P}$ = 5 Hz, $^3J_{C\text{-}Pt}$ = 15 Hz, PCH$_2$*CH*$_2$), 23.09 (d, $^1J_{C\text{-}P}$ = 42 Hz, $^2J_{C\text{-}Pt}$ = 34.5 Hz, P*CH*$_2$), 113.02 (d, $^2J_{C\text{-}F}$ = 23.5 Hz, C_d), 117.81 (s, $^3J_{C\text{-}Pt}$ = 14 Hz, C_h), 120.45 (d, $^2J_{C\text{-}F}$ = 18 Hz, $^2J_{C\text{-}Pt}$ = 27 Hz, C_b), 128.73 (d, $^3J_{C\text{-}F}$ = 8.5 Hz, $^3J_{C\text{-}Pt}$ = 21 Hz, C_e), 142.26 (s, C_i), 146.11 (m, C_f), 160.40 (m, C_a), 161.50 (s, $^2J_{C\text{-}Pt}$ = 29 Hz, C_g), 164.02 (d, $^1J_{C\text{-}F}$ = 256 Hz, $^3J_{C\text{-}Pt}$ = 39 Hz, C_c) ppm.

δ_F (Acetone-d_6) = -110.00 ($^4J_{F\text{-}Pt}$ = 19 Hz) ppm.

δ_P (Acetone-d_6) = 1.89 ($^1J_{P\text{-}Pt}$ = 3076 Hz) ppm.

δ_{Pt} (Acetone-d_6) = -2930 (d, $^1J_{Pt\text{-}P}$ = ~3300 Hz) ppm.

HR-MS (ESI): found 634.1938 m/z, calculated 634.1940 m/z = $C_{27}H_{33}F_2PN^{194}Pt$ = $[M]^+$.

Complex - **10-Bu**

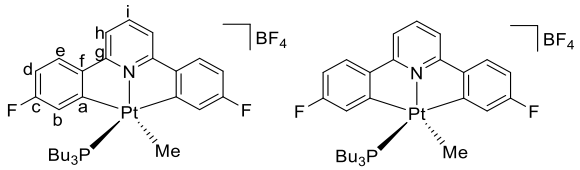

δ_H (Acetone-d_6) = 8.08 (1H, t, $^3J_{H\text{-}H}$ = 8 Hz, H_i), 7.99 (2H, dd, $^3J_{H\text{-}H}$ = 8.5 Hz, $^4J_{H\text{-}F}$ = 5 Hz, H_e), 7.94 (2H, $^3J_{H\text{-}H}$ = 8 Hz, H_h), 7.35 (2H, dd, $^3J_{H\text{-}H}$ = 8.5 Hz, $^4J_{H\text{-}F}$ = 3 Hz, $^3J_{H\text{-}Pt}$ = 21 Hz, H_b), 6.97 (2H, td, $^3J_{H\text{-}H}$ = $^3J_{H\text{-}F}$ = 8.5 Hz, $^4J_{H\text{-}H}$ = 3 Hz, H_d), 1.71 (6H, m, PCH_2), 1.48 (3H, s, $^2J_{H\text{-}H}$ = 55 Hz, PtMe), 1.01 (6H, m, PCH_2CH_2), 0.77 (6H, m, $PCH_2CH_2CH_2$), 0.61 (9H, t, $^3J_{H\text{-}H}$ = 6.5 Hz, $PCH_2CH_2CH_2Me$) ppm.

δ_F (Acetone-d_6) = -110.05 ($^4J_{F\text{-}Pt}$ = 19 Hz) ppm.

δ_P (Acetone-d_6) = 2.54 ($^1J_{P\text{-}Pt}$ = 3115 Hz) ppm.

δ_{Pt} (Acetone-d_6) = -2925 (d, $^1J_{Pt\text{-}P}$ = ~3150 Hz) ppm.

Complex - **Me-10-Pr**

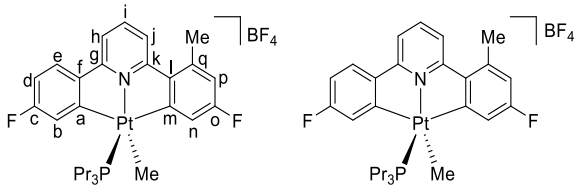

δ_H (233 K, Acetone-d_6) = 8.23 (2H, m, $H_{i,j}$), 8.16 (2H, m, $H_{e,h}$), 7.47 (1H, dd, $^3J_{H\text{-}F}$ = 8 Hz, $^4J_{H\text{-}H}$ = 2 Hz, $^3J_{H\text{-}Pt}$ = ~20 Hz, H_b), 7.36 (1H, dd, $^3J_{H\text{-}F}$ = 7 Hz, $^4J_{H\text{-}H}$ = 2 Hz, $^3J_{H\text{-}Pt}$ = ~20 Hz, H_n), 7.13 (1H, td, $^3J_{H\text{-}F}$ = 8.5 Hz, $^4J_{H\text{-}H}$ = 2 Hz, H_d), 7.01 (1H, dd, $^3J_{H\text{-}F}$ = 10 Hz, $^4J_{H\text{-}H}$ = 2 Hz, H_p), 2.82 (3H s, Me), 1.81 (6H, m, PCH_2), 1.52 (3H, s, $^2J_{H\text{-}Pt}$ = 53 Hz, PtMe), 1.12 (6H, m, PCH_2CH_2), 0.70 (9H, t, $^3J_{H\text{-}H}$ = 7 Hz, PCH_2CH_2Me) ppm.

δ_C (233 K, Acetone-d_6) = -3.78 (s, $^1J_{C\text{-}Pt}$ = 521 Hz, PtMe), 14.80 (d, $^3J_{C\text{-}P}$ = 18 Hz, PCH_2CH_2Me), 16.30 (s, PCH_2CH_2), 23.55 (s, Me), 24.42 (d, $^1J_{C\text{-}P}$ = 42 Hz, $^2J_{C\text{-}Pt}$ = 36 Hz, PCH_2), 113.09 (d, $^2J_{C\text{-}F}$ = 23 Hz, C_d), 116.75 (d, $^2J_{C\text{-}F}$ = 23 Hz, C_p), 117.84 (m, $C_{h,n}$),

120.36 (d, $^{2}J_{C\text{-}F}$ = 18 Hz, C_b), 121.92 (s, C_j), 128.93 (d, $^{3}J_{C\text{-}F}$ = 7 Hz, C_e), 141.83 (d, $^{3}J_{C\text{-}F}$ = Hz, C_q), 142.19 (s, C_i), 144.52 (s, C_l), 146.18 (C_f), 161.33 (m, $^{1}J_{C\text{-}Pt}$ = 530 Hz, C_m), 161.55 (s, C_g), 161.71 (m, $^{1}J_{C\text{-}Pt}$ = 526 Hz, C_a), 162.31 (s, $^{2}J_{C\text{-}Pt}$ = Hz, C_k), 162.48 (d, $^{1}J_{C\text{-}F}$ = 256 Hz, $^{3}J_{C\text{-}Pt}$ = 34 Hz, C_o), 163.91 (d, $^{1}J_{C\text{-}F}$ = 255 Hz, $^{3}J_{C\text{-}Pt}$ = 30 Hz, C_c) ppm.

δ_F (Acetone-d_6) = -110.00 ($^{4}J_{F\text{-}Pt}$ = 18 Hz), -112.33 ($^{4}J_{F\text{-}Pt}$ = 21 Hz) ppm.

δ_P (233 K, Acetone-d_6) = 1.36 ($^{1}J_{P\text{-}Pt}$ = 3109 Hz) ppm.

δ_{Pt} (233 K, Acetone-d_6) = -2971 (d, $^{1}J_{Pt\text{-}P}$ = ~3150 Hz) ppm.

Complex - **Me-11-Pr**

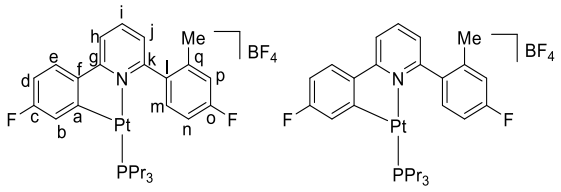

δ_H (Acetone-d_6) = 8.31 – 8.24 (2H, m, $H_{h,i}$), 7.99 (1H, dd, $^{3}J_{H\text{-}H}$ = 8.5 Hz, $^{4}J_{H\text{-}F}$ = 6 Hz, H_e), 7.77 (1H, dd, $^{3}J_{H\text{-}H}$ = 8.5 Hz, $^{4}J_{H\text{-}F}$ = 6 Hz, H_m), 7.61 (1H, dt, $^{3}J_{H\text{-}H}$ = 7 Hz, $^{4}J_{H\text{-}H}$ = $^{5}J_{H\text{-}P}$ = 1.5 Hz, H_j), 7.27 – 7.20 (2H, m, $H_{p,n}$), 7.05 (1H, td, $^{3}J_{H\text{-}H}$ = $^{3}J_{H\text{-}F}$ = 8.5 Hz, $^{4}J_{H\text{-}H}$ = 2.5 Hz, H_d), 7.01 (1H, dt, $^{3}J_{H\text{-}F}$ = 10 Hz, $^{4}J_{H\text{-}H}$ = $^{4}J_{H\text{-}P}$ = 2.5 Hz, H_b), 2.64 (3H, s, Me), 1.92 (6H, m, P*CH₂*), 1.66 (6H, m, PCH₂*CH₂*), 1.02 (9H, t, $^{3}J_{H\text{-}H}$ = 7.5 Hz, PCH₂CH₂*Me*) ppm.

δ_C (Acetone-d_6) = 14.78 (d, $^{3}J_{C\text{-}P}$ = 15 Hz, PCH₂CH₂*Me*), 18.12 (s, $^{3}J_{C\text{-}Pt}$ = 28 Hz, PCH₂*CH₂*), 20.38 (s, Me), 24.60 (d, $^{1}J_{C\text{-}P}$ = 36 Hz, $^{2}J_{C\text{-}Pt}$ = 36 Hz, P*CH₂*), 112.05 (d, $^{2}J_{C\text{-}F}$ = 22 Hz, C_d), 113.63 (d, $^{2}J_{C\text{-}F}$ = 22 Hz, C_p), 117.73 (d, $^{2}J_{C\text{-}F}$ = 22 Hz, C_n), 118.33 (s, $^{3}J_{C\text{-}Pt}$ = 20 Hz, C_h), 121.47 (dd, $^{2}J_{C\text{-}F}$ = 21 Hz, $^{3}J_{C\text{-}P}$ = 6 Hz, C_b), 125.96 (d, $^{4}J_{C\text{-}P}$ = 3 Hz, $^{3}J_{C\text{-}Pt}$ = 14 Hz, C_j), 127.22 $^{2}J_{C\text{-}F}$ = 10 Hz, C_e), 128.91 (t, $^{2}J_{C\text{-}P}$ = $^{3}J_{C\text{-}F}$ = 7 Hz, C_a), 132.46 (d, $^{3}J_{C\text{-}F}$ = 9 Hz, C_m), 134.06 (d, $^{4}J_{C\text{-}F}$ = 3 Hz, C_f), 139.13 (d, $^{3}J_{C\text{-}F}$ = 9 Hz, C_q), 141.27 (s, C_i), 142.47 (d, $^{4}J_{C\text{-}F}$ = 2 Hz, C_l), 158.83 (s, C_k), 162.10 (dd, $^{1}J_{C\text{-}F}$ = 253 Hz, $^{4}J_{C\text{-}P}$ = 3 Hz, C_c), 162.51 (d, $^{4}J_{C\text{-}P}$ = 4 Hz, C_g), 163.27 (d, $^{1}J_{C\text{-}F}$ = 248 Hz, C_o) ppm.

δ_F (Acetone-d_6) = -110.54 ($^{4}J_{F\text{-}Pt}$ = 61 Hz), -113.18 ppm.

δ_P (Acetone-d_6) = 4.43 ($^{1}J_{P\text{-}Pt}$ = 4018 Hz) ppm.

δ_{Pt} (Acetone-d_6) = -3829 (d, $^{1}J_{Pt\text{-}P}$ = ~4100 Hz) ppm.

HR-MS (ESI): found 634.1940 m/z, calculated 634.1940 m/z = $C_{27}H_{33}F_2PN^{194}Pt = [M]^+$.

Complex - **Me-11-Bu**

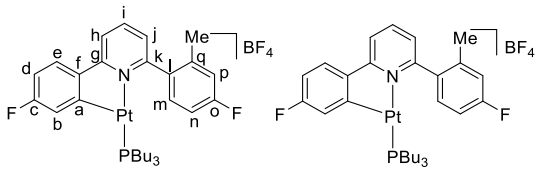

δ_H (Acetone-d_6) = 8.14 (2H, m, $H_{h,i}$), 7.85 (1H, dd, $^3J_{H\text{-}H}$ = 8.5 Hz, $^4J_{H\text{-}J}$ = 6 Hz, H_e), 7.66 (1H, dd, $^3J_{H\text{-}H}$ = 8.5 Hz, $^4J_{H\text{-}F}$ = 6 Hz, H_m), 7.49 (1H, d, $^3J_{H\text{-}H}$ = 7.5 Hz, H_j), 7.11 (2H, m, $H_{n,p}$), 6.91 (2H, m, $H_{b,d}$), 2.53 (3H, s, Me), 1.83 (6H, m, P*CH₂*), 1.50 (6H, m, PCH_2*CH₂*), 1.30 (6H, m, PCH_2CH_2*CH₂*), 0.77 (9H, t, $^3J_{H\text{-}H}$ = 7 Hz, $PCH_2CH_2CH_2$*Me*) ppm.

δ_C (Acetone-d_6) = 12.95 (s, $PCH_2CH_2CH_2$*Me*), 20.47 (s, Me), 22.08 (d, $^1J_{C\text{-}P}$ = 38 Hz, $^2J_{C\text{-}Pt}$ = 38 Hz, P*CH₂*), 23.63 (d, $^3J_{C\text{-}P}$ = 14 Hz, PCH_2CH_2*CH₂*), 26.50 (d, $^2J_{C\text{-}P}$ = 2.5 Hz, $^3J_{C\text{-}Pt}$ = 21 Hz, PCH_2*CH₂*), 111.98 (d, $^2J_{C\text{-}F}$ = 23 Hz, C_d), 113.62 (d, $^2J_{C\text{-}F}$ = 23 Hz, C_n), 117.82 (d, $^2J_{C\text{-}F}$ = 22 Hz, C_p), 118.27 (s, C_h), 121.42 (dd, $^2J_{C\text{-}F}$ = 21.5 Hz, $^3J_{C\text{-}P}$ = 7 Hz, $^2J_{C\text{-}Pt}$ = ~120 Hz, C_b), 125.90 (d, $^4J_{C\text{-}P}$ = 3 Hz, C_j), 127.14 (d, $^3J_{C\text{-}F}$ = 8.5 Hz, C_e), 129.35 (m, C_a), 132.43 (d, $^3J_{C\text{-}F}$ = 8 Hz, C_m), 134.08 (s, C_l), 139.16 (d, $^3J_{C\text{-}F}$ = 8 Hz, C_q), 141.16 (s, C_i), 142.36 (s, C_g), 158.79 (s, C_k), 162.11 (dd, $^1J_{C\text{-}F}$ = 253 Hz, $^4J_{C\text{-}P}$ = 3 Hz, C_c), 162.58 (d, $^3J_{C\text{-}P}$ = 2.5 Hz, C_g), 163.33 (d, $^1J_{C\text{-}F}$ = 249 Hz, C_o) ppm.

δ_F (Acetone-d_6) = -110.62 ($^4J_{F\text{-}Pt}$ = 63 Hz), -113.04 ppm.

δ_P (Acetone-d_6) = 5.69 ($^1J_{P\text{-}Pt}$ = 4042 Hz) ppm.

δ_{Pt} (Acetone-d_6) = -3830 (d, $^1J_{Pt\text{-}P}$ = ~3950 Hz) ppm.

HR-MS (ESI): found 676.2409 m/z, calculated 676.2410 m/z = $C_{30}H_{39}F_2NP^{194}Pt = [M]^+$.

Complex - **Me-11-Bn**

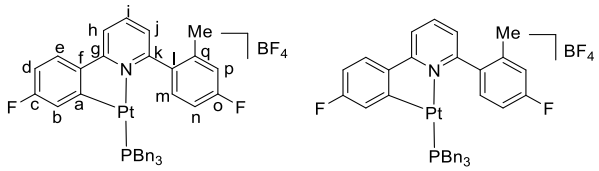

δ_H (Acetone-d_6) = 8.27 (2H, d, $^3J_{H\text{-}H}$ = 8 Hz, $H_{h,j}$), 8.01 (1H, dd, $^3J_{H\text{-}H}$ = 8.5 Hz, $^4J_{H\text{-}F}$ = 6 Hz, H_e), 7.67 (1H, dd, $^3J_{H\text{-}H}$ = 8.5 Hz, $^4J_{H\text{-}F}$ = 6 Hz, H_m), 7.58 (1H, t, $^3J_{H\text{-}H}$ = 8 Hz, H_i) 7.31 (15H, m, Bn-*o,m,p*), 7.23 (1H, dd, $^3J_{H\text{-}F}$ = 10 Hz, $^4J_{H\text{-}H}$ = 2 Hz, H_p), 7.14 (1H, dt, $^3J_{H\text{-}F}$ = 10 Hz, $^4J_{H\text{-}H}$ = $^4J_{H\text{-}P}$ = 2.5 Hz, H_b), 7.07 (2H, m, $H_{d,n}$), 3.51 (6H, t, $^2J_{H\text{-}H}$ = $^2J_{H\text{-}P}$ = 12.5 Hz, $^3J_{H\text{-}Pt}$ = ~45 Hz, Ph*CH₂*), 2.49 (3H, s, Me) ppm.

δ_C (Acetone-d_6) = 20.55 (s, Me), 29.40 (m, PhCH_2), 112.38 (d, $^2J_{C\text{-}F}$ = 22 Hz, C_d), 113.63 (d, $^2J_{C\text{-}F}$ = 19 Hz, C_n), 117.79 (d, $^2J_{C\text{-}F}$ = 25 Hz, C_p), 118.50 (s, C_h) 122.43 (dd, $^2J_{C\text{-}F}$ = 21 Hz, $^3J_{C\text{-}P}$ = 5 Hz, $^2J_{C\text{-}Pt}$ = ~90 Hz, C_b), 125.97 (d, $^5J_{C\text{-}P}$ = 3 Hz, C_i), 127.13 (d, $^5J_{C\text{-}P}$ = 3 Hz, Bn-*p*), 127.40 (d, $^3J_{C\text{-}F}$ = 9 Hz, C_e), 128.69 (s, Bn-*m*), 130.41 (d, $^3J_{C\text{-}P}$ = 6 Hz, Bn-*o*), 132.63 (d, $^3J_{C\text{-}F}$ = 8 Hz, C_m), 133.29 (d, $^2J_{C\text{-}P}$ = 5 Hz, Bn-*i*), 133.71 (d, $^4J_{C\text{-}F}$ = 2 Hz, C_l), 139.01 (d, $^3J_{C\text{-}F}$ = 8.5 Hz, C_q), 141.40 (s, C_j), 142.32 (d, $^4J_{C\text{-}F}$ = 2 Hz, C_f), 158.46 (s, H_k), 162.02 (dd, $^1J_{C\text{-}F}$ = 253 Hz, $^4J_{C\text{-}P}$ = 2 Hz, C_c), 162.55 (d, $^3J_{C\text{-}P}$ = 2.5 Hz, C_g), 163.04 (d, $^1J_{C\text{-}F}$ = 248 Hz, C_o) ppm.

δ_F (Acetone-d_6) = -109.44 ($^4J_{F\text{-}Pt}$ = 64 Hz), -112.64 ppm.

δ_P (Acetone-d_6) = 9.40 ($^1J_{P\text{-}Pt}$ = 4200 Hz) ppm.

δ_{Pt} (Acetone-d_6) = -3796 (d, $^1J_{Pt\text{-}P}$ = ~4250 Hz) ppm.

HR-MS (ESI): found 778.1946 m/z, calculated 778.1940 m/z = $C_{39}H_{33}F_2NP^{194}Pt$ = $[M]^+$.

Complex - **Me_2-11-Pr**

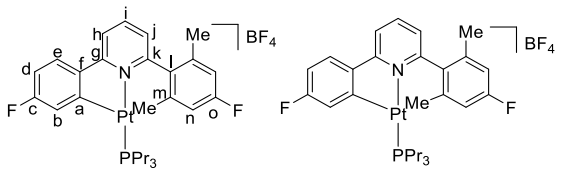

δ_H = 7.96 (1H, t, $^3J_{H\text{-}H}$ = 8 Hz, H_i), 7.79 (1H, d, $^3J_{H\text{-}H}$ = 8 Hz, H_h), 7.54 (1H, dd, $^3J_{H\text{-}H}$ = 9 Hz, $^4J_{H\text{-}F}$ = 6.5 Hz, H_e), 7.06 (1H, d, $^3J_{H\text{-}H}$ = 8 Hz, H_j), 6.96 (2H, d, $^3J_{H\text{-}F}$ = 9 Hz, H_n), 6.93 (1H, td, $^3J_{H\text{-}F}$ = $^3J_{H\text{-}H}$ = 8.5 Hz, $^4J_{H\text{-}H}$ = 2 Hz, H_d), 6.72 (1H, dt, $^3J_{H\text{-}F}$ = 10 Hz, $^4J_{H\text{-}H}$ = $^4J_{H\text{-}P}$ = 2 Hz, H_b), 2.25 (6H, s, Me), 1.79 (6H, m, PCH_2), 1.49 (6H, m, PCH_2CH_2), 0.95 (9H, t, $^3J_{H\text{-}H}$ = 7.5 Hz, PCH_2CH_2Me) ppm.

δ_C = 23.63 (d, $^3J_{C\text{-}P}$ = 15.5 Hz, PCH_2CH_2Me), 18.16 (d, $^2J_{C\text{-}P}$ = 2 Hz, $^3J_{C\text{-}P}$ = 17 Hz, PCH_2CH_2), 20.84 (s, Me), 24.20 (d, $^1J_{C\text{-}P}$ = 36.5 Hz, $^2J_{C\text{-}Pt}$ = 48 Hz, PCH_2), 112.05 (d, $^2J_{C\text{-}F}$ = 22.5 Hz, C_d), 116.16 05 (d, $^2J_{C\text{-}F}$ = 20.5 Hz, C_n), 118.13 (s, H_h), 121.77 (dd, $^2J_{C\text{-}F}$ = 21 Hz, $^3J_{C\text{-}P}$ = 6 Hz, C_b), 126.18 (d, $^4J_{C\text{-}P}$ = 4.5 Hz, C_j), 126.42 (d, $^3J_{C\text{-}F}$ = 9 Hz, C_e), 129.46 (t, $^2J_{C\text{-}P}$ = $^3J_{C\text{-}F}$ = 8 Hz, $^1J_{C\text{-}Pt}$ = 686 Hz, C_a), 131.70 (d, $^4J_{C\text{-}F}$ = 2.5 Hz, C_l), 140.00 (d, $^3J_{C\text{-}F}$ = 8.5 Hz, C_m), 140.31 (s, C_i), 141.79 (d, $^4J_{C\text{-}F}$ = 2.5 Hz, C_f), 158.32 (s, C_k), 162.5 (dd, $^1J_{C\text{-}F}$ = 254 Hz, $^4J_{C\text{-}P}$ = 2 Hz, C_c), 163.10 (d, $^1J_{C\text{-}F}$ = 253 Hz, C_o), 163.65 (d, $^3J_{C\text{-}P}$ = 2.5 Hz, C_g) ppm.

δ_F = -108.56, -108.58 ($^4J_{F\text{-}Pt}$ = 57 Hz) ppm.

δ_P = 3.66 ($^1J_{P\text{-}Pt}$ = 4148 Hz) ppm.

δ_{Pt} = -3903 (d, $^{1}J_{Pt\text{-}P}$ = ~4300 Hz) ppm.

HR-MS (ESI): found 648.2091 m/z, calculated 648.2097 m/z = $C_{28}H_{35}F_2PN^{194}Pt = [M]^+$.

6.5.3. Synthesis of **12**

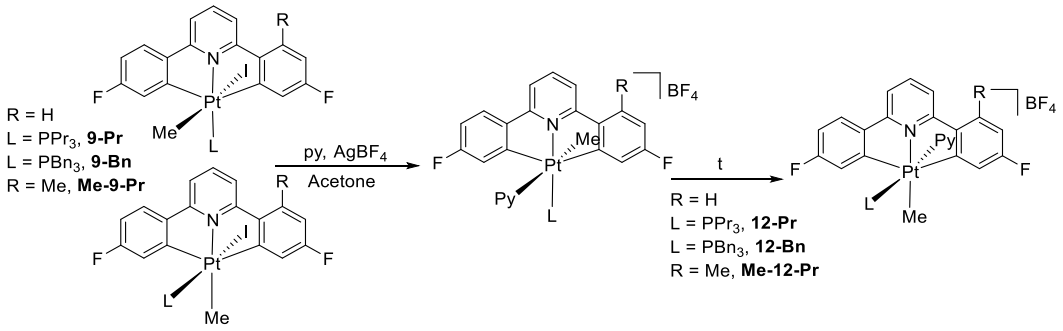

To an acetone (1 ml) suspension of either isomer of **9** (10 mg, **9-Pr**: 1.31 x 10^{-5} mol, **9-Bn**: 1.10 x 10^{-5} mol, **Me-9-Pr**: 1.29 x 10^{-5} mol), was added pyridine (~10 mg, excess). $AgBF_4$ (5-10 mg, excess) was added next, resulting in immediate precipitation of AgI. After 30 minutes, the product was then filtered and then diluted in a small amount of DCM. The excess pyridine was then removed by washing with water. The DCM layer was then dried with $MgSO_4$, and solvent removed by evaporation under vacuum to give **12-Pr(c), 12c-Bn(c)** and **Me-12-Pr(c)**. To observe **12-Pr(t)**, the reaction was done in an NMR tube, and the reaction monitored by NMR. The products could not be purified as they degraded on silica.

Complex - **12-Pr(t)**

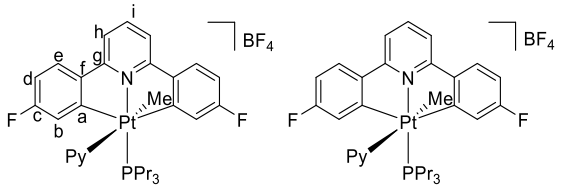

δ_H (Acetone-d_6) δ = 8.68 (m, $^{3}J_{H\text{-}Pt}$ = 40 Hz, Py-*o*), 7.61 (dd, $^{3}J_{H\text{-}F}$ = 9.5 Hz, $^{4}J_{H\text{-}H}$ = 2.5 Hz, H_b), 7.20 (td, $^{3}J_{H\text{-}F} = {}^{3}J_{H\text{-}H}$ = 8.5, $^{4}J_{H\text{-}H}$ = 2.5 Hz, H_d), 2.50 (m, P*CH*$_2$), 1.70 (m, PCH$_2$*CH*$_2$), 1.06 (d, $^{3}J_{H\text{-}P}$ = 3.5 Hz, $^{2}J_{H\text{-}Pt}$ = 66 Hz, PtMe), 1.02 (td, $^{3}J_{H\text{-}H}$ = 7 Hz, $^{4}J_{H\text{-}P}$ = 1 Hz, PCH$_2$CH$_2$*Me*) ppm.

δ_F (Acetone-d_6) δ = -107.87 ($^{4}J_{F\text{-}Pt}$ = 20.5 Hz) ppm.

δ_P (Acetone-d_6) δ = -16.74 ($^{1}J_{P\text{-}Pt}$ = 2600 Hz) ppm.

δ_{Pt} (Acetone-d_6) δ = -2838 (d, $^{1}J_{Pt\text{-}P}$ = ~3000 Hz) ppm.

Complex - **12-Pr(c)**

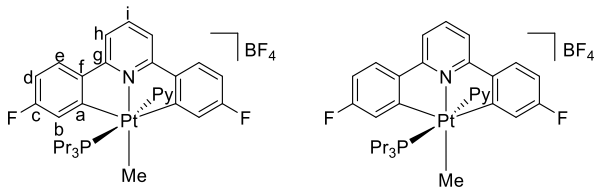

δ_H (Acetone-d_6) = 8.10 (1H, t, $^3J_{H-H}$ = 8 Hz, H_i), 7.90 (2H, dd, $^3J_{H-H}$ = 8.5 Hz, $^4J_{H-H}$ = 5 Hz, H_e), 7.87 (2H, m, $^3J_{H-Pt}$ = 26 Hz, Py-*o*), 7.80 (2H, d, $^3J_{H-H}$ = 8 Hz, H_h), 7.70 (1H, t, $^3J_{H-H}$ = 7 Hz, Py-*p*), 7.24 (2H, dd, $^3J_{H-F}$ = 8 Hz, $^4J_{H-H}$ = 2.5 Hz, $^3J_{H-Pt}$ = 20.5 Hz, H_b), 7.15 (2H, t, $^3J_{H-H}$ = 7 Hz, Py-*o*), 7.01 (2H, td, $^3J_{H-H}$ = $^3J_{H-F}$ = 8.5 Hz, $^4J_{H-H}$ = 2.5 Hz, H_d), 1.54 (6H, m, P*CH₂*), 1.16 (3H, d, $^3J_{H-P}$ = 2 Hz, $^2J_{H-Pt}$ = 56 Hz, PtMe), 0.99 (6H, m, PCH_2*CH₂*), 0.71 (9H, td, $^3J_{H-H}$ = 7 Hz, $^4J_{H-P}$ = 1.5 Hz, PCH_2CH_2*Me*) ppm.

δ_C (Acetone-d_6) = -5.18 (d, $^2J_{C-P}$ = 5.5 Hz, $^1J_{C-Pt}$ = 538 Hz, PtMe), 14.48 (d, $^3J_{C-P}$ = 16 Hz, PCH_2CH_2*Me*), 15.71 (d, $^2J_{C-P}$ = 5.5 Hz, $^3J_{C-Pt}$ = 11 Hz, PCH_2*CH₂*), 23.72 (d, $^1J_{C-P}$ = 39 Hz, $^2J_{C-Pt}$ = 28 Hz, P*CH₂*), 112.96 (d, $^2J_{C-F}$ = 22.5 Hz, C_d), 117.48 (s, $^3J_{C-Pt}$ = 14 Hz, C_h), 118.67 (d, $^2J_{C-F}$ = 18.5 Hz, $^2J_{C-Pt}$ = 18 Hz, C_b), 125.66 (d, $^4J_{C-P}$ = 3.5, $^3J_{C-Pt}$ = 18.5 Hz, Py-*m*), 128.67 (d, $^3J_{C-F}$ = 8.5 Hz, $^3J_{C-Pt}$ = 17 Hz, C_e), 138.84 (s, Py-*p*), 141.78 (s, C_a), 143.47 (d, $^4J_{C-F}$ = 2.5 Hz, C_d), 148.09 (s, $^2J_{C-Pt}$ = 8.5 Hz, Py-*o*), 159.40 (m, $^1J_{C-Pt}$ = 547 Hz, C_a), 159.49 (s, $^2J_{C-Pt}$ = 30 Hz, C_g), 163.39 (d, $^1J_{C-F}$ = 260 Hz, $^3J_{C-Pt}$ = 38 Hz, C_c) ppm.

δ_F (Acetone-d_6) = -106.06 ($^4J_{F-Pt}$ = 20 Hz) ppm.

δ_P (Acetone-d_6) = -9.05 ($^1J_{P-Pt}$ = 2645 Hz) ppm.

δ_{Pt} (Acetone-d_6) = -3111 (d, $^1J_{Pt-P}$ = ~2850 Hz) ppm.

HR-MS (ESI): found 713.2371 m/z, calculated 713.2362 m/z = $C_{32}H_{38}F_2PN_2{}^{194}Pt$ = $[M]^+$.

HR-MS (ESI): found 634.1940 m/z, calculated 634.1940 m/z = $C_{27}H_{33}F_2P{}^{194}Pt$ = $[M\text{-}Py]^+$.

Complex - **12-Bn(c)**

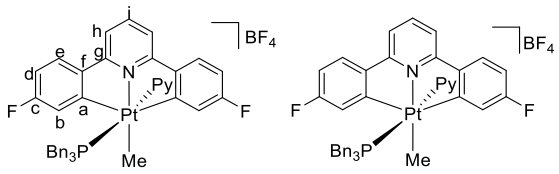

δ_H = 7.95 (5H, m, $H_{i,e,}$ Py-*o*), 7.79 (1H, t, $^3J_{H\text{-}H}$ = 8 Hz, Py-*p*), 7.66 (2H, d, $^3J_{H\text{-}H}$ = 8 Hz, H_h), 7.42 (2H, dd, $^3J_{H\text{-}F}$ = 8 Hz, $^4J_{H\text{-}H}$ = 2 Hz, $^3J_{H\text{-}Pt}$ = 16 Hz, H_b), 7.26 (2H, m, Py-*m*), 7.16 (5H, m, $H_{d,}$ Bn-*p*), 7.03 (6H, t, $^3J_{H\text{-}H}$ = 7.5 Hz, Bn-*m*), 5.97 (6H, d, $^3J_{H\text{-}H}$ = 7.5 Hz, Bn-*o*), 3.25 (6H, d, $^2J_{H\text{-}P}$ = 11.5 Hz, $^3J_{H\text{-}Pt}$ = 21 Hz, Ph*CH₂*), 1.43 (3H, d, $^3J_{H\text{-}P}$ = 2Hz, $^2J_{H\text{-}Pt}$ = 56 Hz, PtMe) ppm.

δ_C = -4.08 (d, $^2J_{C\text{-}P}$ = 6.5 Hz, PtMe), 29.19 (d. $^1J_{C\text{-}P}$ = 35 Hz, $^2J_{C\text{-}Pt}$ = 31 Hz, Ph*CH₂*), 113.15 (d, $^2J_{C\text{-}F}$ = 23 Hz, C_d), 117.81 (s, C_h), 118.89 (d, $^2J_{C\text{-}F}$ = 17.5 Hz, $^2J_{C\text{-}Pt}$ = 17.5 Hz, C_b), 125.84 (d, $^4J_{C\text{-}P}$ = 2.5 Hz, $^3J_{C\text{-}Pt}$ = 17.5 Hz, Py-*m*), 126.94 (d, $^4J_{C\text{-}P}$ = 2.5 Hz, Bn-*p*), 128.27 (d, $^3J_{C\text{-}P}$ = 7 Hz, Bn-*m*), 128.87 (m, $C_{e,}$ Bn-*o*), 129.71 (d, $^2J_{C\text{-}P}$ = 9 Hz, $^3J_{C\text{-}Pt}$ = 9 Hz, Bn-*i*), 139.10 (s, Py-*p*), 141.91 (s, Py-*o*), 144.05 (s, C_f), 148.17 (s, C_i), 158.91 (s, $^2J_{C\text{-}Pt}$ = 28 Hz, C_g), 159.24 (m, $^1J_{C\text{-}Pt}$ = 542 Hz, C_a), 163.57 (d, $^1J_{C\text{-}F}$ = 257 Hz, $^3J_{C\text{-}Pt}$ = 31 Hz, C_c) ppm.

δ_F = -105.29 ($^4J_{F\text{-}Pt}$ = 19 Hz) ppm.

δ_P = -13.24 ($^1J_{P\text{-}Pt}$ = 2639 Hz) ppm.

δ_{Pt} = -3086 (d, $^1J_{Pt\text{-}P}$ = ~2600 Hz) ppm.

HR-MS (ESI): found 857.2369 m/z, calculated 857.2362 m/z = $C_{44}H_{38}F_2N_2P^{194}Pt$ = $[M]^+$.

Complex - **Me-12-Pr(t)**

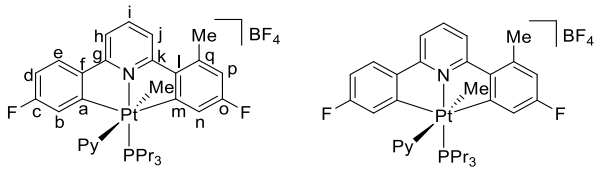

δ_H (Acetone-d_6) = 8.38 (2H, $^3J_{H\text{-}H}$ = 5.39 Hz, $^3J_{H\text{-}Pt}$ = ~16 Hz, Py-*o*), 7.59 (1H, m, H_b), 7.48 (1H, m, H_n), 7.18 (1H, td, $^3J_{H\text{-}F}$ = 8.5 Hz, $^4J_{H\text{-}H}$ = 2 Hz, H_d), 7.05 (1H, d, $^3J_{H\text{-}F}$ = 8.5 Hz, H_p), 2.81 (3H, s, Me), 2.47 (6H, m, P*CH₂*), 1.69 (6H, m, PCH_2*CH₂*), 1.40 (3H, s, $^2J_{H\text{-}Pt}$ = 57 Hz, PtMe) 1.01 (9H, t, $^3J_{H\text{-}H}$ = 7 Hz, PCH_2CH_2*Me*) ppm.

δ_F (Acetone-d_6) = -107.98 ($^4J_{F\text{-}Pt}$ = 21 Hz), -110.83 ($^4J_{F\text{-}Pt}$ = 21.5 Hz) ppm.

δ_P (Acetone-d_6) = -16.78 ($^1J_{P\text{-}Pt}$ = 2589 Hz) ppm.

δ_{Pt} (Acetone-d_6) = - 2824 (d, $^1J_{Pt\text{-}P}$ = ~2600 Hz) ppm.

Complex - **Me-12-Pr(c)**

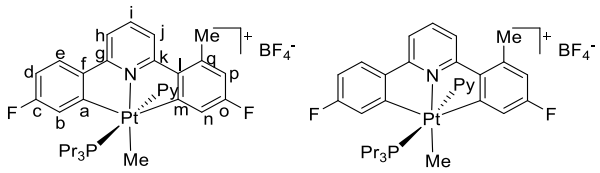

δ_H = 8.14 (1H, t, $^3J_{H\text{-}H}$ = 7.5 Hz, H_i), 8.04 (1H, d, $^3J_{H\text{-}H}$ = 7.5 Hz, H_j), 7.94 (3H, m, H_e, Py-*o*), 7.87 (1H, d, $^3J_{H\text{-}H}$ = 7.5 Hz, H_h), 7.79 (1 H, t, $^3J_{H\text{-}H}$ = 7.5 Hz, Py-*p*), 7.32 (1H, dd, $^3J_{H\text{-}F}$ = 8 Hz, $^4J_{H\text{-}H}$ = 2.5 Hz, $^3J_{H\text{-}Pt}$ = 16 Hz, H_b), 7.22 (3H, m, H_n, Py-*m*), 7.06 (1H, td, $^3J_{H\text{-}H}$ = $^3J_{H\text{-}F}$ = 9 Hz, $^4J_{H\text{-}H}$ = 2.5 Hz, H_d), 6.87 (1H, dd, $^3J_{H\text{-}F}$ = 9.5 Hz, $^4J_{H\text{-}H}$ = 2 Hz, H_p), 2.79 (3H, s, Me), 1.58 (6H, m, P*CH₂*), 1.20 (3H, s, $^2J_{H\text{-}Pt}$ = 55.71 Hz, PtMe), 1.05 (6H, m, PCH_2CH_2), 0.77 (9H, t, $^3J_{H\text{-}H}$ = 7 Hz, PCH_2CH_2Me) ppm.

δ_F = -105.85 ($^4J_{F\text{-}Pt}$ = 20 Hz, F_c), -108.45 ($^4J_{Pt\text{-}F}$ = 22.5 Hz, F_o) ppm.

δ_P = -9.03 ($^1J_{P\text{-}Pt}$ = 2666 Hz) ppm.

δ_{Pt} = -3122 (d, $^1J_{Pt\text{-}P}$ = ~2850 Hz) ppm.

HR-MS (ESI): found 648.2105 m/z, calculated 648.2096 m/z = $C_{28}H_{35}F_2NP^{194}Pt$ = $[M\text{-}Py]^+$.

HR-MS (ESI): found 727.2518 m/z, calculated 727.2532 m/z = $C_{33}H_{40}F_2N_2P^{194}Pt$ = $[M]^+$.

6.5.4. Synthesis of **Me-13-L**

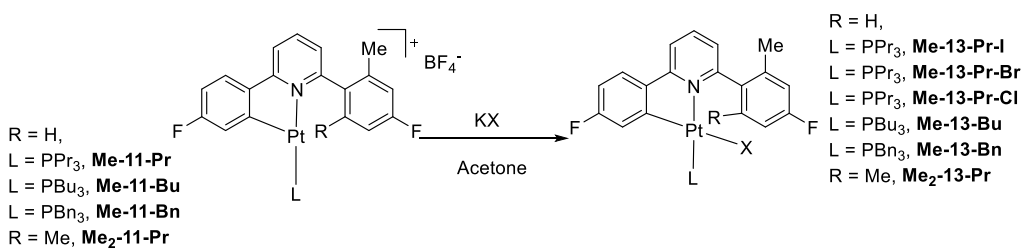

Yields of **Me-13-Pr** with I, Br and Cl counterions were not calculated, and only monitored for conversion. A sample of **Me-11-Pr** (~10 mg each) was dissolved in $CDCl_3$ (0.5 ml), the chosen NaX salt was added in excess, and the reaction monitored by NMR. Within 24 hours all showed complete conversion.

NaI (10 mg, excess) was added to an acetone solution (10 ml) of the crude **Me-11-L** or **Me2-13-Pr** from the synthesis of **11** step. Instantly the remaining $AgBF_4$ reacted to give a yellow precipitate. After a day, full conversion was seen. Solvent was removed, leaving an orange oil. Purification by column chromatography, loading and eluting with toluene gave the pure **Me-13-L** or **Me2-13-Pr** as yellow solids. Yields: **Me-13-Bu**: 115 mg, 1.24 x 10^{-4} mol, 97%, **Me-13-Bn**: 97 mg, 9.43 x 10^{-5} mol, 95%, **Me2-13-Pr**: 102 mg, 1.13 x 10^{-4} mol, 98%.

Complex - **Me-13-Pr-I**

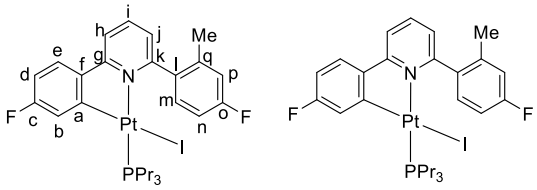

δ_H (Acetone-d_6) = 8.08 (2H, m, $H_{i,j}$), 7.92 (1H, dd, $^3J_{H\text{-}H}$ = 8.5 Hz, $^4J_{H\text{-}F}$ = 6 Hz, H_e), 7.74 (1H, dd, $^3J_{H\text{-}H}$ = 8 Hz, $^4J_{H\text{-}F}$ = 5.5 Hz, H_m), 7.54 (1H, d, $^3J_{H\text{-}H}$ = 6.5 Hz, H_h), 7.14 (1H, dt, $^3J_{H\text{-}F}$ = 10.5 Hz, $^4J_{H\text{-}H}$ = $^4J_{H\text{-}P}$ = 2.5 Hz, $^3J_{H\text{-}Pt}$ = 62 Hz, H_b), 7.05 (2H, m, $H_{p,n}$), 6.98 (1H, td, $^3J_{H\text{-}H}$ = $^3J_{H\text{-}F}$ =8.5 Hz, $^4J_{H\text{-}H}$ = 2.5 Hz, H_d), 2.60 (3H, s, Me), 2.15 (6H, m, PCH_2), 1.69 (6H, m, PCH_2CH_2), 0.99 (9H, t, $^3J_{H\text{-}H}$ = 7.5 Hz, PCH_2CH_2Me) ppm.

δ_C (Acetone-d_6) = 14.96 (d, $^3J_{C\text{-}P}$ = 15 Hz, PCH_2CH_2Me), 1.58 (s, $^3J_{C\text{-}Pt}$ = 30 Hz, PCH_2CH_2), 21.5 (s, Me), 29.32 (m, PCH_2), 110.02 (d, $^2J_{C\text{-}F}$ = 23 Hz, C_d), 111.71 (d, $^2J_{C\text{-}F}$ = 20 Hz, C_n), 117.09 (m, $C_{j,p}$), 119.42 (dd, $^2J_{C\text{-}F}$ = 19 Hz, $^3J_{C\text{-}P}$ = 5 Hz, $^2J_{C\text{-}Pt}$ = 107 Hz, C_b), 125.135 (d, $^4J_{C\text{-}P}$ = 2.5 Hz, C_h), 126.67 (d, $^3J_{C\text{-}F}$ = 8 Hz, $^3J_{C\text{-}Pt}$ = 48 Hz, C_e), 133.25 (d, $^3J_{C\text{-}F}$ = 9 Hz, C_m), 138.42 (s, C_i), 138.46 (s, C_l), 139.76 ($^3J_{C\text{-}F}$ = 8 Hz, C_q), 142.35 (d, $^4J_{C\text{-}F}$ = 2 Hz, C_l), 148.71 (t, $^3J_{C\text{-}P}$ = $^4J_{C\text{-}F}$ = 5 Hz, $^1J_{C\text{-}Pt}$ = 1139 Hz, C_a), 161.03 (s, C_g), 162.25 (dd,

$^{1}J_{C\text{-}F}$ = 252 Hz, $^{4}J_{C\text{-}P}$ = 2.5 Hz, $^{3}J_{C\text{-}Pt}$ = 36 Hz, C_c), 163.09 (d, $^{3}J_{C\text{-}P}$ = 3 Hz, $^{2}J_{C\text{-}Pt}$ = 72 Hz, C_g), 163.45 (d, $^{1}J_{C\text{-}P}$ = 246 Hz, C_o) ppm.

δ_F (Acetone-d_6) = -112.40 ($^{4}J_{F\text{-}Pt}$ = 64 Hz), -115.07 ppm.

δ_P (Acetone-d_6) = -1.20 ($^{1}J_{P\text{-}Pt}$ = 4000 Hz) ppm.

δ_{Pt} (Acetone-d_6) = -3946 (d, $^{1}J_{Pt\text{-}P}$ = ~4000 Hz) ppm.

HR-MS (ESI): found 634.1928 m/z, calculated 634.1940 m/z = $C_{27}H_{33}F_2NP^{194}Pt$ = $[M\text{-}I]^+$.

Elemental analysis found (calculated): C 43.20 (42.53), H 4.40 (4.36), N 1.76 (1.84).

Crystals suitable for X-ray analysis were grown by the slow evaporation of solvent from a chloroform solution – ps25.

Complex - **Me-13-Pr-Br**

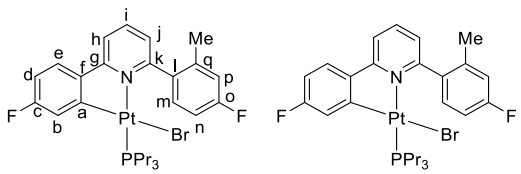

δ_H (Acetone-d_6) = 8.07 (2H, m, $H_{h,i}$), 7.88 (1H, t, $^{3}J_{H\text{-}H}$ = $^{4}J_{H\text{-}F}$ = 6 Hz, H_e), 7.57 (1H, t, $^{3}J_{H\text{-}H}$ = $^{4}J_{H\text{-}F}$ = 6 Hz, H_m), 7.51 (1H, d, $^{3}J_{H\text{-}H}$ = 7 Hz, H_j), 7.14 (1H, d, $^{3}J_{H\text{-}F}$ = 10 Hz, $^{3}J_{H\text{-}Pt}$ = 65 Hz, H_b), 6.97 (3H, m, $H_{d,n,p}$), 2.57 (3H, s, Me), 2.07 (6H, m, P*CH*$_2$), 1.65 (6H, m, PCH$_2$*CH*$_2$), 1.00 (9H, t, $^{3}J_{H\text{-}H}$ = 7 Hz, PCH$_2$CH$_2$*Me*) ppm.

δ_C (Acetone-d_6) = 14.95 (d, $^{3}J_{C\text{-}P}$ = 16 Hz, PCH$_2$CH$_2$*Me*), 18.38 (s, $^{3}J_{C\text{-}Pt}$ = 25 Hz, PCH$_2$*CH*$_2$), 21.13 (s, Me), 27.43 (d, $^{1}J_{C\text{-}P}$ = 38 Hz, $^{2}J_{C\text{-}Pt}$ = 38 Hz, P*CH*$_2$), 109.85 (d, $^{2}J_{C\text{-}F}$ = 23.5 Hz, C_d), 111.47 (d, $^{2}J_{C\text{-}F}$ = 21 Hz, C_n), 116.61 (m, $C_{p,h}$), 120.42 (d, $^{2}J_{C\text{-}F}$ = 20 Hz, $^{2}J_{C\text{-}Pt}$ = 102 Hz, C_b), 125.10 (s C_j), 126.71 (d, $^{3}J_{C\text{-}F}$ = 9.5 Hz, $^{3}J_{C\text{-}Pt}$ = 54 Hz, C_e), 133.31 (d, $^{3}J_{C\text{-}F}$ = 9 Hz, C_m), 137.75 (s, C_l), 138.76 (s, C_i), 139.58 (d, $^{3}J_{C\text{-}F}$ = 8.5 Hz, C_q), 143.10 (s, C_f), 147.19 (m, C_a), 160.99 (s, C_k), 162.21 (d, $^{1}J_{C\text{-}F}$ = 250 Hz, C_c), 163.02 (d, $^{1}J_{C\text{-}F}$ = 244 Hz, C_o), 163.74 (m, C_g) ppm.

δ_F (Acetone-d_6) = -112.83 ($^{4}J_{F\text{-}Pt}$ = 62 Hz), -115.68 ppm.

δ_P (Acetone-d_6) = -1.60 ($^{1}J_{P\text{-}Pt}$ = 4061 Hz) ppm.

δ_{Pt} (Acetone-d_6) = -3879 (d, $^{1}J_{Pt\text{-}P}$ = ~4100 Hz) ppm.

HR-MS (ESI): found 634.1941 m/z, calculated 634.1940 m/z = $C_{27}H_{33}F_2NP^{194}Pt$ = $[M\text{-}Br]^+$.

Complex - **Me-13-Pr-Cl**

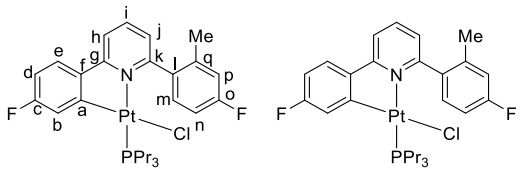

δ_H (Acetone-d_6) δ = 8.09 (1H, t, $^3J_{H-H}$ = 8 Hz, H_i), 8.03 (1H, d, $^3J_{H-H}$ = 8 Hz, H_h), 7.85 (1H, dd, $^3J_{H-H}$ = 8.5 Hz, $^4J_{H-F}$ = 6 Hz, H_e), 7.46 (2H, m, $H_{j,m}$), 7.13 (1H, dt, $^3J_{H-H}$ = 10.5 Hz, $^4J_{H-H}$ = $^4J_{H-P}$ = 5 Hz, $^3J_{H-Pt}$ = 65 Hz, H_b), 6.96 (2H, m, $H_{n,p}$), 6.91 (1H, td, $^3J_{H-H}$ = $^3J_{H-F}$ = 8.5 Hz, $^4J_{H-H}$ = 2.5 Hz, H_d), 2.54 (3H, s, Me), 1.99 (6H, m, P*CH₂*), 1.62 (6H, m, PCH₂*CH₂*), 0.99 (9H, t, $^3J_{H-H}$ = 7.5 Hz, PCH₂CH₂*Me*) ppm.

δ_C = (Acetone-d_6) = 14.92 (d, $^3J_{C-P}$ = 15.5 Hz, PCH₂CH₂*Me*), 18.17 (s, $^3J_{C-Pt}$ = 30.5 Hz, PCH₂*CH₂*), 20.81 (s, Me), 26.12 (d, $^1J_{C-P}$ = 37.5 Hz, $^2J_{C-Pt}$ = 37.5 Hz, P*CH₂*), 109.67 (d, $^2J_{C-F}$ = 23.5 Hz, C_d), 111.37 (d, $^2J_{C-F}$ = 21 Hz, C_n), 116.32 (d, $^2J_{C-F}$ = 21 Hz, C_p), 116.50 (s, $^4J_{C-Pt}$ = 20 Hz, C_h), 121.03 (dd, $^2J_{C-F}$ = 19 Hz, $^3J_{C-P}$ = 4 Hz, $^2J_{C-Pt}$ = 96 Hz, C_b), 125.08 (d, $^4J_{C-P}$ = 4.5 Hz, $^4J_{C-Pt}$ = 17 Hz, C_j), 126.73 (d, $^3J_{C-F}$ = 9.5 Hz, $^3J_{C-Pt}$ = 46 Hz, C_e), 133.00 (d, $^3J_{C-F}$ = 9 Hz, C_m), 137.23 (d, $^4J_{C-F}$ = 3 Hz, C_l), 138.95 (s, C_i), 139.25 (d, $^3J_{C-F}$ = 8.5 Hz, C_q), 143.50 (d, $^4J_{C-F}$ = 3 Hz, C_f), 146.79 (t, $^3J_{C-F}$ = $^2J_{C-P}$ = 7 Hz, $^1J_{C-Pt}$ = 1081 Hz, C_a), 160.84 (s, C_k), 162.40 (dd, $^1J_{C-F}$ = 251 Hz, $^4J_{C-P}$ = 2.5 Hz, C_c), 162.93 (d, $^1J_{C-F}$ = 244.5 Hz, C_o), 164.20 (d, $^3J_{C-P}$ = 3 Hz, C_g) ppm.

δ_F (Acetone-d_6) = -113.11 ($^4J_{F-Pt}$ = 64 Hz), -116.05 ppm.

δ_P (Acetone-d_6) = -1.10 ($^1J_{P-Pt}$ = 4083 Hz) ppm.

δ_{Pt} (Acetone-d_6) = -3847 (d, $^1J_{Pt-P}$ = ~4150 Hz) ppm.

HR-MS (ESI): found 634.1940 m/z, calculated 634.1940 m/z = $C_{23}H_{33}F_2NP^{194}Pt$ = $[M-Cl]^+$.

Complex - **Me-13-Bu**

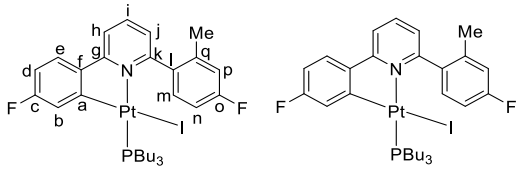

δ_H = 7.83 (1H, t, $^3J_{H-H}$ = 8 Hz, H_i), 7.70 (2H, m, $H_{h,m}$), 7.64 (1H, dd, $^3J_{H-H}$ = 8 Hz, $^4J_{H-F}$ = 5.5 Hz, H_e), 7.29 (d, $^3J_{H-H}$ = 8 Hz, H_j), 7.06 (1H, dt, $^3J_{H-F}$ = 10.5 Hz, $^4J_{H-H}$ = $^4J_{H-P}$ = 2.5 Hz, $^3J_{H-Pt}$ = 64 Hz, H_b), 6.98 (1H, dd, $^3J_{H-F}$ = 10 Hz, $^4J_{H-H}$ = 2.5 Hz, H_p), 6.90 (2H, m, $H_{d,n}$),

2.60 (3H, s, Me), 2.08 (6H, m, P*CH₂*), 1.57 (6H, m, PCH₂*CH₂*), 1.40 (6H, m, PCH₂CH₂*CH₂*), 0.90 (9H, t, $^{3}J_{H\text{-}H}$ = 7.5 Hz, PCH₂CH₂CH₂*Me*) ppm.

δ_C = 13.69 (s, PCH₂CH₂CH₂*Me*), 22.21 (s, Me), 24.00 (d, $^{3}J_{C\text{-}P}$ = 14 Hz, PCH₂CH₂*CH₂*), 26.76 (d, $^{1}J_{C\text{-}P}$ = 38 Hz, $^{2}J_{C\text{-}Pt}$ = 38 Hz, P*CH₂*), 27.06 (s, $^{3}J_{C\text{-}Pt}$ = 24 Hz, PCH₂*CH₂*), 110.31 (d, $^{2}J_{C\text{-}F}$ = 23 Hz, C_d), 111.91 (d, $^{2}J_{C\text{-}F}$ = 21 Hz, C_n), 116.48 (s, C_h), 117.55 (d, $^{2}J_{C\text{-}F}$ = 22 Hz, C_p), 119.62 (dd, $^{2}J_{C\text{-}F}$ = 19 Hz, $^{3}J_{C\text{-}P}$ = 5 Hz, $^{2}J_{C\text{-}Pt}$ = 104 Hz, C_b), 124.78 (d, $^{4}J_{C\text{-}P}$ = 4 Hz, C_j), 126.09 (d, $^{3}J_{C\text{-}F}$ = 9 Hz, C_p), 133.08 (d, $^{3}J_{C\text{-}F}$ = 9 Hz, C_m), 137.52 (s, H_i), 138.19 (s, C_l), 139.65 (d, $^{3}J_{C\text{-}F}$ = 8 Hz, C_q), 142.22 (s, C_f), 148.63 (t, $^{2}J_{C\text{-}P}$ = $^{3}J_{C\text{-}F}$ = 5 Hz, $^{1}J_{C\text{-}Pt}$ = 1128 Hz, H_a), 161.31 (s, C_k), 162.17 (dd, $^{1}J_{C\text{-}F}$ = 252 Hz, $^{4}J_{C\text{-}P}$ = 4 Hz, H_c), 163.31 (d, $^{3}J_{C\text{-}P}$ = 4 Hz, C_g), 163.46 (d, $^{1}J_{C\text{-}F}$ = 250 Hz, C_o) ppm.

δ_F = -111.05 ($^{4}J_{F\text{-}Pt}$ = 63 Hz), -112.65 ppm.

δ_P = -1.10 ($^{1}J_{P\text{-}Pt}$ = 4005 Hz) ppm.

δ_{Pt} = -3967 (d, $^{1}J_{Pt\text{-}P}$ = ~4050 Hz) ppm.

HR-MS (ESI): found 676.2415 m/z, calculated 676.2410 m/z = $C_{30}H_{39}F_2NP^{194}Pt$ = $[M\text{-}I]^+$.

Elemental analysis, expected (result): C 44.78 (44.99), H 4.89 (4.91), N 1.74 (1.65).

Crystals suitable for X-ray analysis were grown by the slow evaporation of solvent from a chloroform solution – ps35.

Complex - **Me-13-Bn**

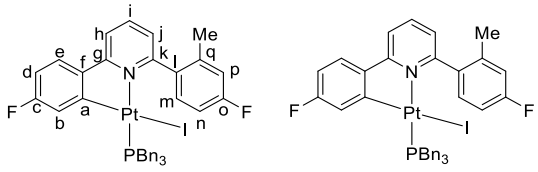

δ_H = 7.79 (1H, t, $^{3}J_{H\text{-}H}$ = 8 Hz, H_i), 7.67 (1H, dd, $^{3}J_{H\text{-}H}$ = 9 Hz, $^{4}J_{H\text{-}F}$ = 6 Hz, H_m), 7.61 (1H, d, $^{3}J_{H\text{-}H}$ = 9 Hz, H_h), 7.42 (1H, dd, $^{3}J_{H\text{-}H}$ = 9 Hz, $^{4}J_{H\text{-}F}$ = 6 Hz, H_e), 7.32 (6H, m, Bn-*o*), 7.24 (1H, d, $^{3}J_{H\text{-}H}$ = 9 Hz, H_j), 7.12 (9H, m, Bn-*m,p*), 6.92 (1H, dd, $^{3}J_{H\text{-}F}$ = Hz, $^{4}J_{H\text{-}H}$ = Hz, H_p), 6.67 (1H, td, $^{3}J_{H\text{-}H}$ = $^{3}J_{H\text{-}F}$ = 8.5 Hz, $^{4}J_{H\text{-}H}$ = 2.5 Hz, H_n), 6.59 (1H, td, $^{3}J_{H\text{-}H}$ = $^{3}J_{H\text{-}F}$ = 8.5 Hz, $^{4}J_{H\text{-}H}$ = 2.5 Hz, H_n), 6.15 (1H, dt, $^{3}J_{H\text{-}F}$ = 10.5 Hz, $^{4}J_{H\text{-}H}$ = $^{4}J_{H\text{-}P}$ = 2.5 Hz, $^{3}J_{H\text{-}Pt}$ = ~60 Hz, H_b), 3.45 (6H, m, Ph*CH₂*)*, 2.55 (2H, s, Me) ppm.

*At 298 K, this peak has separated into 2 broad peaks, separated by 320 Hz, and FWHH 55 Hz. At 278 the broad beaks have begun to show multiplicity as two triplets, now 423 Hz

apart. At 333 K there is a single broad peak at 3.60 FWHH ~100 Hz. Unable to increase temperature further in $CDCl_3$.

δ_C = 21.07 (s, Me), 31.15 (d, $^1J_{C\text{-}P}$ = 35 Hz, $^2J_{C\text{-}Pt}$ = 35 Hz, Ph*CH*$_2$), 109.18 (d, $^2J_{C\text{-}F}$ = 23.5 Hz, C_d), 110.80 (d, $^2J_{C\text{-}F}$ = 23.5 Hz, C_n), 115.62 (s, C_h), 116.71 (d, $^2J_{C\text{-}F}$ = 21.5 Hz, C_p), 119.16 (dd, $^2J_{C\text{-}F}$ = 20 Hz, $^3J_{C\text{-}P}$ = 4 Hz, $^2J_{C\text{-}Pt}$ = ~115 Hz, C_b), 123.39 (d, $^4J_{C\text{-}P}$ = 5.5 Hz, C_j), 124.05 (d, $^2J_{C\text{-}F}$ = 9 Hz, C_e), 125.86 (d, $^5J_{C\text{-}P}$ = 2 Hz, Bn-*p*), 127.32 (d, $^4J_{C\text{-}P}$ = 2.5 Hz, Bn-*m*), 129.28 (d, $^3J_{C\text{-}P}$ = 7 Hz, Bn-*o*), 131.60 (d, $^3J_{C\text{-}F}$ = 9 Hz, C_m), 132.60 (d, $^2J_{C\text{-}P}$ = 6.5 Hz, Bn-*i*), 136.56 (s, C_i), 136.69 (s, C_l), 138.68 (d, $^3J_{C\text{-}F}$ = 8 Hz, C_q), 139.82 (s, C_f), 147.25 (dd, $^2J_{C\text{-}F}$ = 5.5 Hz, $^3J_{C\text{-}P}$ = 3.5 Hz, $^2J_{H\text{-}Pt}$ = 1140 Hz, C_a), 159.83 (s, C_k), 160.66 (dd, $^1J_{C\text{-}F}$ = 254 Hz, $^4J_{C\text{-}P}$ = 3 Hz, C_c), 162.41 (d, $^3J_{C\text{-}P}$ = 3 Hz, C_g), 162.51 (d, $^1J_{C\text{-}F}$ = 248 Hz, C_o) ppm.

δ_F = -109.02 ($^4J_{F\text{-}Pt}$ = 63 Hz), -111.76 ppm.

δ_P = -0.30 ($^1J_{P\text{-}Pt}$ = 4180 Hz) ppm.

δ_{Pt} = -3857 (d, $^1J_{Pt\text{-}P}$ = ~4150 Hz) ppm.

HR-MS (ESI): found 778.1925 m/z, calculated 778.1940 m/z = $C_{39}H_{33}F_2NP^{194}Pt$ = $[M\text{-}I]^+$. Elemental analysis found (calculated): C 43.20 (51.67), H 4.40 (3.67) N 1.76 (1.54).

Complex - **Me$_2$-13-Pr**

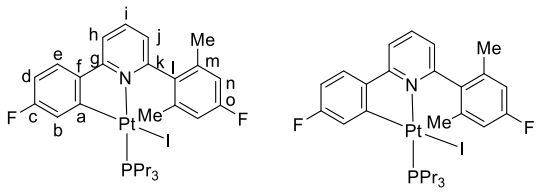

δ_H (Acetone-d_6) = 8.16 (2H, m, $H_{h,i}$), 7.94 (1H, dd, $^3J_{H\text{-}H}$ = 8.5 Hz, $^4J_{H\text{-}F}$ = 6 Hz, H_e), 7.30 (1H, d, $^3J_{H\text{-}H}$ = 8.1 Hz, H_j), 7.09 (1H, dt, $^3J_{H\text{-}F}$ = 11 Hz, $^4J_{H\text{-}H}$ = $^4J_{H\text{-}P}$ = 2.5 Hz, $^3J_{H\text{-}Pt}$ = 66 Hz, H_b), 6.96 (2H, td, $^3J_{H\text{-}H}$ = $^3J_{H\text{-}F}$ = 8.5 Hz, $^4J_{H\text{-}H}$ = 2.5 Hz, H_d), 6.79 (2H, d, $^3J_{H\text{-}F}$ = 8.5 Hz, H_n), 2.40 (6H, s, Me), 2.13 (6H, m, P*CH*$_2$), 1.64 (6H, m, PCH_2CH_2), 0.95 (9H, t, $^3J_{H\text{-}H}$ = 7 Hz, PCH_2CH_2*Me*) ppm.

δ_C (Acetone-d_6) = 15.09 (d, $^3J_{C\text{-}P}$ = 16 Hz, PCH_2CH_2*Me*), 18.58 (s, $^3J_{C\text{-}Pt}$ = 31 Hz, PCH_2*CH*$_2$), 22.00 (s, Me), 29.56 (m, P*CH*$_2$), 110.09 (d, $^2J_{C\text{-}F}$ = 21.5 Hz, C_c), 113.98 (d, $^2J_{C\text{-}F}$ = 21.5 Hz, C_o), 118.13 (s, C_h), 119.46 (dd, $^2J_{C\text{-}F}$ = 18.5 Hz, $^3J_{C\text{-}P}$ = 5 Hz, $^2J_{C\text{-}Pt}$ = 100 Hz, C_b), 126.41 (s, C_j), 126.93 (d, $^3J_{C\text{-}F}$ = 9.5 Hz, $^3J_{C\text{-}Pt}$ = 46 Hz, C_e), 137.43 (d, $^4J_{C\text{-}F}$ = 3 Hz, C_l), 139.03 (s, C_i), 140.25 (d, $^3J_{C\text{-}F}$ = 9 Hz, C_m), 142.21 (d, $^4J_{C\text{-}F}$ = 2 Hz, C_f), 149.84 (t, $^2J_{C\text{-}P}$ = $^3J_{C\text{-}F}$ = 5 Hz, $^1J_{C\text{-}Pt}$ = 1129 Hz, C_a), 160.37 (s, C_k), 162.50 (dd, $^1J_{C\text{-}F}$ = 3.5 Hz, $^4J_{C\text{-}P}$ = 253 Hz, C_c), 162.74 (d, $^1J_{C\text{-}F}$ = 244 Hz, C_o), 163.50 (m, C_g) ppm.

δ_F (Acetone-d_6) = -112.53 (broad peak FWHH 60Hz), -116.70 ppm.

δ_P (Acetone-d_6) = -0.10 ($^1J_{P\text{-}Pt}$ = 4052 Hz) ppm.

δ_{Pt} (Acetone-d_6) = -3957 (d, $^1J_{Pt\text{-}P}$ = ~4250 Hz) ppm.

HR-MS (ESI): found 648.2093 m/z, calculated 648.2096 m/z = $C_{28}H_{35}FNP^{194}Pt$ = $[M\text{-}I]^+$.

Elemental analysis result (expected): C 43.31 (42.29), H 4.54 (4.33), N 1.80 (1.69).

Crystals suitable for X-ray analysis were grown by the slow evaporation of solvent from a chloroform solution – ps37.

6.5.5. Synthesis of **Me-1-Pr** and **Me-1-Bn**

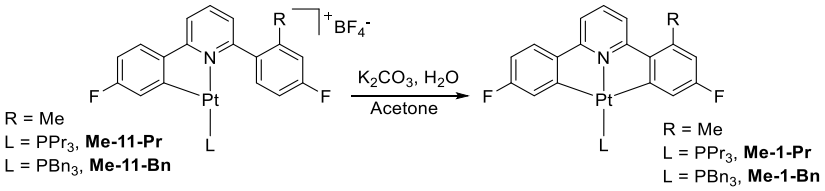

To separate solutions of **Me-11-L** (L = **Pr:** 100 mg, 1.16 x 10^{-4} mol L = **Bn:** 100 mg, 1.01 x 10^{-4} mol) in chloroform (10 ml), 2M K_2CO_3 (1 ml) was added, and left to stir at room temperature for 1 day. The chloroform layer was then separated from the aqueous layer, dried with $MgSO_4$ and solvent removed by evaporation. The crude product was then purified by column chromatography loading and eluting with toluene to give pure **Me-1-L** as a yellow solid (L = **Pr:** 83 mg, 1.07 x 10^{-4} mol, 93% L = **Bn:** 85 mg, 9.26 x 10^{-5} mol, 92%).

Complex – **Me-1-Pr**

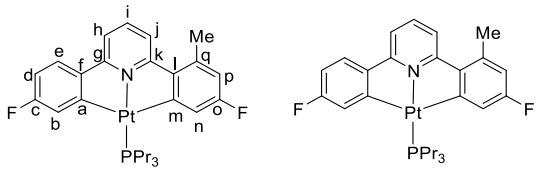

δ_H = 7.53 (1H, t, $^3J_{H-H}$ = 8 Hz, H_i), 7.41 (1H, d, $^3J_{H-H}$ = 8 Hz, H_j), 7.38 (1H, dd, $^3J_{H-H}$ = 8.5 Hz, $^4J_{H-F}$ = 5.5 Hz, H_e), 7.16 (1H, d, $^3J_{H-H}$ = 8 Hz, H_h), 7.14 (1H, dd, $^3J_{H-F}$ = 10 Hz, $^4J_{H-H}$ = 2.5 Hz, $^3J_{H-Pt}$ = 32 Hz, H_b), 7.07 (1H, dd, $^3J_{H-F}$ = 9 Hz, $^4J_{H-H}$ = 2 Hz, $^3J_{H-Pt}$ = 36 Hz, H_n), 6.65 (1H, td, $^3J_{H-H}$ = $^3J_{H-F}$ = 8.5 Hz, $^4J_{H-H}$ = 2.5 Hz, H_d), 6.47 (1H, dd, $^3J_{H-F}$ = 10 Hz, $^4J_{H-H}$ = 2 Hz, H_p), 2.51 (3H, s, Me), 2.00 (6H, m, P*CH₂*), 1.58 (6H, m, PCH₂*CH₂*), 0.96 (9H, t, $^3J_{H-H}$ = 7.5 Hz, PCH₂CH₂*Me*) ppm.

δ_C = 14.70 (d, $^3J_{C-P}$ = 15 Hz, PCH₂CH₂*Me*), 17.63 (s, $^3J_{C-Pt}$ = 34 Hz, PCH₂*CH₂*), 23.45 (s, Me), 25.93 (d, $^1J_{C-P}$ = 36 Hz, $^2J_{C-Pt}$ = 34 Hz, P*CH₂*), 109.24 (d, $^2J_{C-F}$ = 23 Hz, C_d), 113.37 (d, $^4J_{C-P}$ = 3 Hz, $^3J_{C-Pt}$ = 26 Hz, C_j), 113.51 (d, $^2J_{C-F}$ = 22 Hz, C_p), 117.80 (d, $^4J_{C-P}$ = 3 Hz, $^3J_{C-Pt}$ = 26 Hz, C_h), 120.91 (dd, $^2J_{C-F}$ = 16 Hz, $^3J_{C-P}$ = 2 Hz, $^2J_{C-Pt}$ = 58 Hz, C_n), 122.88 (d, $^2J_{C-F}$ = 16.5 Hz, $^2J_{C-Pt}$ = 64 Hz, C_b), 124.97 (d, $^3J_{C-F}$ = 8.5 Hz, $^3J_{C-Pt}$ = 30 Hz, C_e), 137.47 (d, $^3J_{C-F}$ = 8 Hz, C_q), 138.47 (s, C_i), 144.79 (t, $^3J_{C-P}$ = $^4J_{C-F}$ = 2.5 Hz, $^2J_{C-Pt}$ = 35 Hz, C_l), 146.12 (t, $^3J_{C-P}$ = $^4J_{C-F}$ = 2.5 Hz, $^2J_{C-Pt}$ = 26 Hz, C_f), 162.11 (d, $^1J_{C-F}$ = 254 Hz, $^3J_{C-Pt}$ = 57 Hz, C_o), 163.28 (d, $^1J_{C-F}$ = 253 Hz, $^3J_{C-Pt}$ = 50 Hz, C_c), 164.44 (s, $^2J_{C-Pt}$ = 70 Hz, $C_{k/g}$), 164.68 (s, $^2J_{C-Pt}$ = 60 Hz, $C_{k/g}$), 168.94 (m, $^1J_{C-Pt}$ = 704 Hz, $C_{a/m}$), 169.40 (m, $^1J_{C-Pt}$ = 704 Hz, $C_{a/n}$) ppm.

δ_F = -111.01 ($^4J_{F-Pt}$ = 24 Hz, F_c), -113.45 ($^4J_{F-Pt}$ = 27.5 Hz, F_o) ppm.

δ_P = 2.70 ($^1J_{P\text{-}Pt}$ = 3733 Hz) ppm.

δ_{Pt} = -4200 (d, $^1J_{Pt\text{-}P}$ = ~3800 Hz) ppm.

HR-MS (ESI): found 634.1940 m/z, calculated 634.1940 m/z = $C_{27}H_{32}F_2PN^{194}Pt = [M]^+$.

Elemental analysis found (calculated): C 51.07 (51.10), H 5.05 (5.08), N 2.03 (2.21).

Crystals suitable for X-ray analysis were grown by the slow evaporation of solvent from a chloroform solution – ps19.

Complex – **Me-1-Bn**

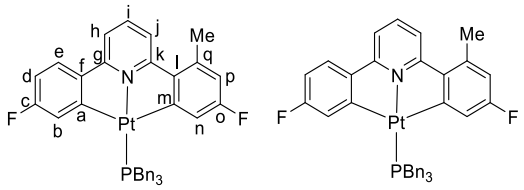

δ_H = 7.60 (1H, t, $^3J_{H\text{-}H}$ = 8 Hz, H_i), 7.45 (1H, d, $^3J_{H\text{-}H}$ = 8 Hz, H_j), 7.38 (1H, dd, $^3J_{H\text{-}H}$ = 8.5 Hz, $^4J_{H\text{-}F}$ = 5.5 Hz, H_e), 7.31 (6H, d, $^3J_{H\text{-}H}$ = 7 Hz, Bn-*o*), 7.21 (1H, d, $^3J_{H\text{-}H}$ = 8 Hz, H_h), 7.13 (9H, m, Bn-*m*,*p*), 6.80 (1H, dd, $^3J_{H\text{-}F}$ = 9 Hz, $^4J_{H\text{-}H}$ = 1.5 Hz, $^3J_{H\text{-}Pt}$ = ~30 Hz, H_n), 6.75 (1H, dd, $^3J_{H\text{-}F}$ = 10 Hz, $^4J_{H\text{-}H}$ = 2 Hz, $^3J_{H\text{-}Pt}$ = ~25 Hz, H_b), 6.58 (1H, td, $^3J_{H\text{-}F}$ = $^3J_{H\text{-}H}$ = 8.5 Hz, $^4J_{H\text{-}H}$ = 2 Hz, H_d), 6.42 (1H, dd, $^3J_{H\text{-}F}$ = 9.5 Hz, $^4J_{H\text{-}H}$ = 1.5 Hz, H_p), 3.43 (6H, d, $^2J_{H\text{-}P}$ = 9 Hz, $^3J_{H\text{-}Pt}$ = 32 Hz, Ph*CH*$_2$), 2.52 (3H, s, Me) ppm.

δ_C = 19.21 (s, Me), 25.52 (d, $^1J_{C\text{-}P}$ = 30 Hz, $^2J_{C\text{-}Pt}$ = 30 Hz, Ph*CH*$_2$), 105.11 (d, $^2J_{C\text{-}F}$ = 20 Hz, C_d), 109.32 (m, $C_{h,p}$), 113.77 (d, $^4J_{H\text{-}P}$ = 3 Hz, $^3J_{H\text{-}Pt}$ = 27 Hz, H_j), 117.03 (d, $^2J_{C\text{-}F}$ = 18 Hz, $^2J_{C\text{-}Pt}$ = 47 Hz, C_n), 118.86 (d, $^2J_{C\text{-}F}$ = 18 Hz, $^2J_{C\text{-}Pt}$ = 56 Hz, C_b), 120.81 (d, $^3J_{C\text{-}F}$ = 10 Hz, $^3J_{C\text{-}Pt}$ = 30 Hz, C_e), 121.60 (d, $^5J_{C\text{-}P}$ = 2 Hz, Bn-*p*), 123.33 (s, Bn-*m*), 125.18 (d, $^3J_{C\text{-}P}$ = 5.5 Hz, Bn-*o*), 128.61 (d, $^2J_{C\text{-}P}$ = 5 Hz, $^3J_{C\text{-}Pt}$ = 16 Hz, Bn-*q*), 113.32 (d, $^3J_{C\text{-}F}$ = 8 Hz, C_q), 134.43 (s, C_i), 140.42 (m, C_l), 141.66 (m, C_f), 157.81 (d, $^1J_{C\text{-}F}$ = 253 Hz, $^3J_{C\text{-}Pt}$ = 56 Hz, C_o), 159.02 (d, $^1J_{C\text{-}F}$ = 252 Hz, $^3J_{C\text{-}Pt}$ = 46 Hz, C_c) 160.37 (s, $^2J_{C\text{-}Pt}$ = 61 Hz, $C_{g/k}$), 160.67 (s, $^2J_{C\text{-}Pt}$ = 61 Hz, $C_{g/k}$), 165.78 (m, $^1J_{C\text{-}Pt}$ = 700 Hz, C_a), 166.15 (m, $^1J_{C\text{-}Pt}$ = 702 Hz, C_m) ppm.

δ_F = -110.69 ($^4J_{F\text{-}Pt}$ = 26.5 Hz, F_c), -113.14 ($^4J_{F\text{-}Pt}$ = 29 Hz, F_o) ppm.

δ_P = 1.18 ($^1J_{P\text{-}Pt}$ = 3893 Hz) ppm.

δ_{Pt} = -4097 (d, $^1J_{Pt\text{-}P}$ = ~3900 Hz) ppm.

HR-MS (ESI): found 778.1918 m/z, calculated 778.1940 m/z = $C_{39}H_{32}F_2NP^{194}Pt = [M]^+$.

Elemental analysis found (calculated): C 60.00 (60.15), H 4.07 (4.14) N 1.73 (1.80).

Crystals suitable for X-ray analysis were grown by the slow evaporation of solvent from a chloroform solution – ps32

6.5.6. Synthesis of **14(t)** and **15**

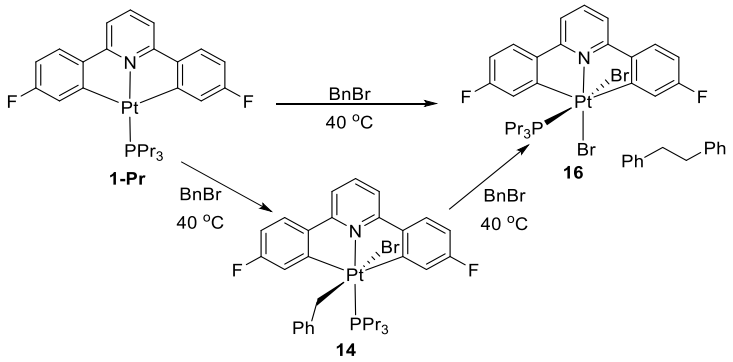

To a solution of **1-Pr** (70 mg, 1.13 x 10^{-4} mol) in chloroform (10 ml), was added BnBr (21 mg, 1.24 x 10^{-4} mol, 1.1 eq). The reaction mixture was then stirred for an hour at 50 °C. The solvent was then removed, followed by washing the crude mixture with petrol. The crude mixture was then purified by column chromatography loading with toluene, followed by eluting with **14:** DCM, and **16:** EtOAc, to give clean amounts of each product (**14**: 34.5 mg, 4.85 x 10^{-5} mol, 43 %, **16**: 10.5 mg, 1.34 x 10^{-5} mol, 12%). The yield of **16** can be increased to nearly quantitative by instead using 2.1 eq of BnBr.

Complex – **14(t)**

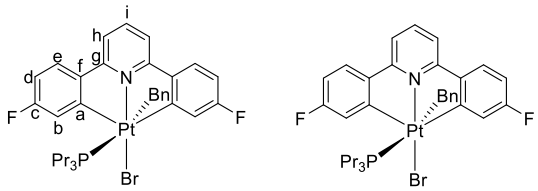

δ_H = 7.49 (2H, dd, $^3J_{H\text{-}H}$ = 9 Hz, $^4J_{H\text{-}F}$ = 5.5 Hz, H_e), 7.39 (1H, t, $^3J_{H\text{-}H}$ = 8 Hz, H_i), 7.31 (2H, $^3J_{H\text{-}F}$ = 9.5 Hz, $^4J_{H\text{-}H}$ = 2.5 Hz, $^3J_{H\text{-}Pt}$ = 31.5 Hz, H_b), 7.03 (2H, dd, $^3J_{H\text{-}H}$ = 8 Hz, $^4J_{H\text{-}H}$ = 2.5 Hz, H_h), 6.83 (2H, td, $^3J_{H\text{-}F}$ = $^3J_{H\text{-}H}$ = 8.5 Hz, $^4J_{H\text{-}H}$ = 2.5 Hz, H_d), 6.64 (1H, t, $^3J_{H\text{-}H}$ = 6.5 Hz, Bn-*p*), 6.40 (2H, dd, $^3J_{H\text{-}H}$ = 6.5 Hz, Bn-*m*), 5.78 (2H, d, $^3J_{H\text{-}H}$ = 6.5 Hz, Bn-*o*), 3.36 (2H, d, $^3J_{H\text{-}P}$ = 4 Hz, $^2J_{H\text{-}Pt}$ = 88 Hz, Pt*CH*$_2$), 2.43 (6H, m, P*CH*$_2$), 1.73 (6H, m, PCH$_2$*CH*$_2$), 1.06 (9H, t, $^3J_{H\text{-}H}$ = 7 Hz, PCH$_2$CH$_2$*Me*) ppm.

δ_C = 15.74 (s, PCH$_2$CH$_2$*Me*), 18.48 (d, $^2J_{C\text{-}P}$ = 5 Hz, PCH$_2$*CH*$_2$), 21.61 (d, $^2J_{C\text{-}P}$ = 2 Hz, $^1J_{C\text{-}Pt}$ = 506 Hz, Pt*CH*$_2$), 24.91 (d, $^1J_{C\text{-}P}$ = 35 Hz, $^2J_{C\text{-}Pt}$ = 21 Hz, P*CH*$_2$), 111.31 (d, $^2J_{C\text{-}F}$ = 23 Hz, H_t), 115.62 (s, $^3J_{C\text{-}Pt}$ = 23 Hz, C_h), 121.91 (d, $^2J_{C\text{-}F}$ = 18 Hz, $^2J_{C\text{-}Pt}$ = 35 Hz, C_b), 125.12 (s, $^5J_{C\text{-}Pt}$ = 15 Hz, Bn-*p*), 126.82 (s, $^4J_{C\text{-}Pt}$ = 15 Hz, Bn-*m*), 127.79 (d, $^3J_{C\text{-}F}$ = 8.5 Hz, $^3J_{C\text{-}Pt}$ =

24 Hz, C_e), 127.97 (s, $^3J_{C\text{-}Pt}$ = 22 Hz, Bn-*o*), 138.86 (s, C_i), 140.78 (s, $^2J_{C\text{-}Pt}$ = 47 Hz, Bn-*i*), 145.59 (m, C_f), 161.12 (s, $^2J_{C\text{-}Pt}$ = 35 Hz, C_g), 163.06 (d, $^1J_{C\text{-}F}$ = 255 Hz, $^3J_{H\text{-}H}$ = 44 Hz, C_c), 165.47 (m, $^1J_{C\text{-}Pt}$ = 591 Hz, C_a) ppm.

δ_F = -109.92 ($^4J_{F\text{-}Pt}$ = 24 Hz) ppm.

δ_P = -20.50 ($^1J_{P\text{-}Pt}$ = 2683Hz) ppm.

δ_{Pt} = -3056 (d, $^1J_{Pt\text{-}P}$ = ~2800 Hz) ppm.

HR-MS (ESI): found 710.2255 m/z, calculated 710.2253 m/z = $C_{33}H_{37}F_2NP^{194}Pt$ = $[M\text{-}Br]^+$.

Elemental Analysis found (calculated): C 49.49 (50.07), H 4.64 (4.71), N 1.75 (1.77).

Complex - **15**

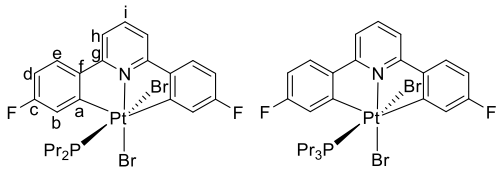

δ_H = 7.95 (2H, dd, $^3J_{H\text{-}F}$ = 8 Hz, $^4J_{H\text{-}H}$ = 2 Hz, $^3J_{H\text{-}Pt}$ = 16 Hz, H_b), 7.83 (1H, t, $^3J_{H\text{-}H}$ = 7.5 Hz, H_i), 7.73 (2H, dd, $^3J_{H\text{-}H}$ = 8.5 Hz, $^4J_{H\text{-}F}$ = 5 Hz, H_e), 7.51 (2H, d, $^3J_{H\text{-}H}$ = 7.5 Hz, H_h), 6.92 (2H, dt, $^3J_{H\text{-}H}$ = $^3J_{H\text{-}F}$ = 8.5 Hz, $^4J_{H\text{-}H}$ = 2 Hz, H_d), 1.73 (6H, m, P*CH₂*), 1.07 (6H, m, PCH_2*CH₂*), 0.76 (9H t, $^3J_{H\text{-}H}$ = 7 Hz, PCH_2CH_2*Me*) ppm.

δ_C = 15.49 (d, $^3J_{C\text{-}P}$ = 15.3 Hz, PCH_2CH_2*Me*), 16.98 (d, $^2J_{C\text{-}P}$ = 13.5 Hz, $^3J_{C\text{-}Pt}$ = 20.5 Hz, PCH_2*CH₂*), 24.76 (d, $^1J_{C\text{-}P}$ = 36 Hz $^2J_{C\text{-}Pt}$ = 25 Hz, P*CH₂*), 112.66 (d, $^2J_{C\text{-}F}$ = 24 Hz, H_d), 116.37 (s, $^3J_{C\text{-}Pt}$ = 30 Hz, C_h), 122.44 (d, $^2J_{C\text{-}F}$ = 19 Hz, $^2J_{C\text{-}Pt}$ = 19 Hz, C_b), 127.63 (d, $^3J_{C\text{-}F}$ = 8.5 Hz, $^3J_{C\text{-}Pt}$ = 24 Hz, C_e), 140.86 (s, C_i), 142.17 (m, C_f), 161.48 (m, C_a), 162.82 (s, $^2J_{C\text{-}Pt}$ = 37 Hz, C_g), 164.98 (d, $^1J_{C\text{-}F}$ = 259 Hz, $^3J_{C\text{-}Pt}$ = 32 Hz, C_c) ppm.

δ_F = -106.40 ($^4J_{F\text{-}Pt}$ = 16 Hz) ppm.

δ_P = -6.66 ($^1J_{P\text{-}Pt}$ = 2241 Hz) ppm.

δ_{Pt} = -3111 (d, $^1J_{Pt\text{-}P}$ = ~ 2650 Hz) ppm.

Crystals suitable for X-ray analysis were grown by the slow evaporation of solvent from a chloroform solution – ps18.

6.5.7. Synthesis of **17**

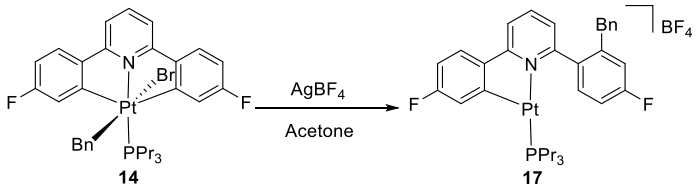

To solution of **14** (10 mg, 1.26 x 10^{-5} mol) in acetone (10 ml), was added $AgBF_4$ (2-5 mg, excess). The reaction mixture was filtered to remove AgI, followed by the removal of solvent by evaporation. The product could not be purified as it degraded on silica. The reaction gives clean conversion, to give adequately pure **17** without further purification.

Complex – **17**

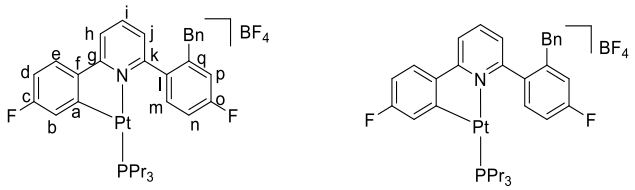

δ_H (Acetone-d_6) = 8.14 (1H, d, $^3J_{H\text{-}H}$ = 8 Hz, H_j), 8.04 (1H, t, $^3J_{H\text{-}H}$ = 8 Hz, H_i), 7.98 (1H, dd, $^3J_{H\text{-}H}$ = 9.5 Hz, $^4J_{H\text{-}F}$ = 6 Hz, H_e), 7.69 (1H, dd, $^3J_{H\text{-}H}$ = 8 Hz, $^4J_{H\text{-}F}$ = 6 Hz, H_m), 7.35 (1H, dd, $^3J_{H\text{-}F}$ = 10 Hz, $^4J_{H\text{-}H}$ = 2.5 Hz, H_p), 2.27 (1H, td, $^3J_{H\text{-}F}$ = $^3J_{H\text{-}H}$ = 8 Hz, $^4J_{H\text{-}H}$ = 2.5 Hz, H_n), 7.18 (1H, d, $^3J_{H\text{-}H}$ = 8Hz, H_J), 7.12-7.02 (5H, m, Bn-*m*,*p* $H_{b,d}$), 6.71 (2H, m, Bn-*o*), 5.21 (1H, d, $^3J_{H\text{-}H}$ = 15 Hz, PhCH_2), 4.40 (1H, d, $^3J_{H\text{-}H}$ = 15 Hz, PhCH_2), 2.00 (6H, m, PCH_2), 1.74 (6H, m, PCH_2CH_2), 1.07 (9H, t, $^3J_{H\text{-}H}$ = 7 Hz, PCH_2CH_2Me) ppm.

δ_C (Acetone-d_6) = 14.94 (s, PCH_2CH_2Me), 1.82 (s, $^3J_{C\text{-}Pt}$ = 30 Hz, PCH_2CH_2), 24.71 (d, $^1J_{C\text{-}P}$ = 37 Hz, $^2J_{C\text{-}Pt}$ = 34 Hz, PCH_2), 39.75 (s, PhCH_2), 112.20 (d, $^2J_{C\text{-}F}$ = 24 Hz, C_d), 114.36 (d, $^2J_{C\text{-}F}$ = 23 Hz, $C_{n,p}$), 118.22 (m, $C_{j,p}$), 121.57 (d, $^2J_{C\text{-}F}$ = 21 Hz, $^3J_{C\text{-}P}$ = 7 Hz C_b), 126.11 (s, Bn-*p*), 126.41 (d, $^3J_{C\text{-}P}$ = 4 Hz, H_h), 127.17 (d, $^3J_{C\text{-}F}$ = 10 Hz, C_e), 128.21-128.34 (m, Bn-*o*,*m*), 129.10 (t, $^3J_{C\text{-}F}$ = $^2J_{C\text{-}P}$ = 7 Hz, C_a), 132.05 (d, $^3J_{C\text{-}F}$ = 9 Hz, C_m), 134.17 (d, $^4J_{C\text{-}F}$ = 3 Hz, C_l), 139.32 (s, C_s), 141.25 (s, C_i), 142.38 (d, $^4J_{C\text{-}P}$ = 2 Hz, C_f), 143.26 (d, $^3J_{C\text{-}F}$ = 8 Hz, C_q), 159.24 (s, C_k), 162.22 (dd, $^1J_{C\text{-}F}$ = 253 Hz, $^4J_{C\text{-}P}$ = 3 Hz, C_c), 162.46 (d, $^4J_{C\text{-}P}$ = 3 Hz, C_g), 163.30 (d, $^1J_{C\text{-}F}$ = 249 Hz, C_o) ppm.

δ_F (Acetone-d_6) = -110.30 ($^4J_{F\text{-}Pt}$ = 65 Hz), -112.62 ppm.

δ_P (Acetone-d_6) = 4.69 ($^1J_{P\text{-}Pt}$ = 4030 Hz) ppm.

δ_{Pt} (Acetone-d_6) = -3851 (d, $^1J_{Pt\text{-}P}$ = ~4400 Hz) ppm.

HR-MS (ESI): found 710.2240 m/z, calculated 710.2253 m/z = $C_{33}H_{36}F_2PN^{194}Pt$ = $[M]^+$.

6.5.8. Synthesis of **18**

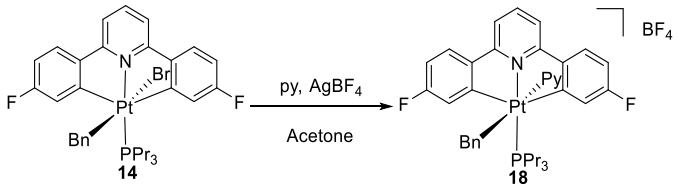

To a slurry of **14** (10 mg, 1.26 x 10^{-5} mol) in acetone (1 ml), a large excess of pyridine was added (~4 mg). An excess of $AgBF_4$ (5-10 mg, excess) was added, resulting in immediate precipitation of AgI. After 30 min, the waste AgI was filtered from the solution, followed by dilution of the solvent with DCM. Excess pyridine was then removed through repeated washings with water. The organic layer was then dried with $MgSO_4$, followed by removal of solvent by evaporation giving **18**. The product could not be purified as it degraded on silica.

Complex - **18**

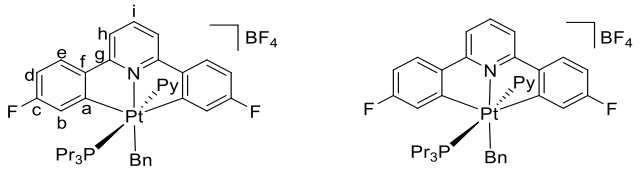

δ_H = 8.02 (1H, t, $^3J_{H\text{-}H}$ = 8 Hz, H_i), 7.96 (2H, dd, $^3J_{H\text{-}H}$ = 9 Hz, $^4J_{H\text{-}F}$ = 5 Hz, H_e), 7.87 (1H, t, $^3J_{H\text{-}H}$ = 7.5 Hz, Py-*p*), 7.78 (2H, d, $^3J_{H\text{-}H}$ = 8Hz, H_h), 7.57 (3H, m, Bn-*p*, Py-*o*), 7.47 (2H, t, $^3J_{H\text{-}H}$ = 6.5 Hz, Py-*m*), 7.34 (1H, dd, $^3J_{H\text{-}F}$ = 8 Hz, $^4J_{H\text{-}H}$ = 2.5 Hz, $^3J_{H\text{-}Pt}$ = 18 Hz, H_b), 7.13 (1H, td, $^3J_{H\text{-}H}$ = $^3J_{H\text{-}F}$ = 8.5 Hz, $^4J_{H\text{-}H}$ = 2.5 Hz, H_d), 6.85 (4H, m, Bn-*o*,*m*), 3.55 (2H, d, $^3J_{H\text{-}P}$ = 4 Hz, $^2J_{H\text{-}Pt}$ = 70 Hz, Pt*CH*$_2$), 1.70 (6H, m, P*CH*$_2$), 1.06 (6H, m, PCH$_2$*CH*$_2$), 0.79 (9H, t, $^3J_{H\text{-}H}$ = 6.5 Hz, PCH$_2$CH$_2$*Me*) ppm.

δ_F = -105.1 ($^4J_{F\text{-}Pt}$ = 21 Hz) ppm.

δ_P = -9.20 ($^1J_{P\text{-}Pt}$ = 2658 Hz) ppm.

δ_{Pt} = -2864 (d, $^1J_{Pt\text{-}P}$ = ~2850 Hz) ppm.

HR-MS (ESI): found 710.2256 m/z, calculated 710.2253 m/z = $C_{33}H_{37}F_2NP^{194}Pt$ = [M-Py]$^+$.

6.5.9. Synthesis of **19**

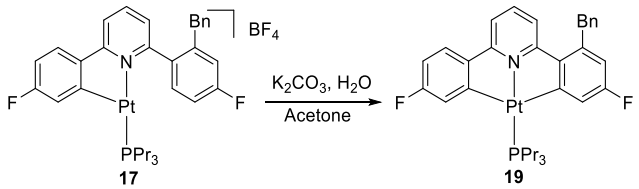

To a solution of complex **17** (12 mg, 1.50 x 10^{-5} mol) in chloroform (10 ml), K_2CO_3 (0.5 g) was added, and the mixture was stirred for 3 days. The solvent was removed and the crude product purified by chromatography on silica, eluting with chloroform (9 mg, 1.24 x 10^{-5} mol, 83%).

Complex - **19**

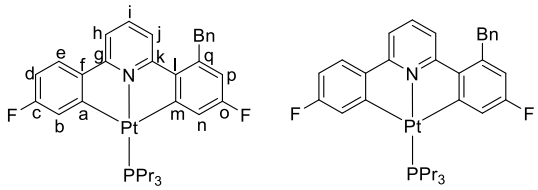

δ_H = 7.36 (2H, m, $H_{i,b}$), 7.24 (2H, t, $^3J_{H\text{-}H}$ = 7 Hz, Bn-*m*), 7.12 (7H, m, Bn-*o*,*p*, $H_{e,h,j,n}$), 6.64 (1H, td, $^3J_{H\text{-}H}$ = $^3J_{H\text{-}F}$ = 8.5 Hz, $^4J_{H\text{-}H}$ = 2.5 Hz, H_d), 6.41 (1H, dd, $^3J_{H\text{-}F}$ = 9.5 Hz, $^4J_{H\text{-}H}$ = 2.5 Hz, H_p), 4.20 (2H, s, Ph*CH*$_2$), 2.02 (6H, m, P*CH*$_2$), 1.60 (6H, m, PCH$_2$*CH*$_2$), 0.98 (9H, t, $^3J_{H\text{-}H}$ = 7 Hz, PCH$_2$CH$_2$*Me*) ppm.

δ_H (Acetone-d_6) = 7.69 (1H, t, $^3J_{H\text{-}H}$ = 8.5 Hz, H_i) 7.65 (1H, dd, $^3J_{H\text{-}H}$ = 8.5 Hz, $^4J_{H\text{-}F}$ = 6 Hz, H_e), 7.51 (1H, d, $^3J_{H\text{-}H}$ = 8.5 Hz, $H_{h/j}$), 7.45 (1H, d, $^3J_{H\text{-}H}$ = 8.5 Hz, $H_{h/j}$), 7.35 (2H, dd, $^3J_{H\text{-}H}$ = $^3J_{H\text{-}H}$ = 8 Hz, Bn-*m*), 7.30 (2H, dd, $^3J_{H\text{-}F}$ = 10 Hz, $^4J_{H\text{-}H}$ = 2.5 Hz, $^3J_{H\text{-}Pt}$ = 14 Hz, $H_{b,n}$), 7.25 (1H, d, $^3J_{H\text{-}H}$ = 7.5 Hz, Bn-*p*), 7.22 (2H, d, $^3J_{H\text{-}H}$ = 7.5 Hz, Bn-*o*), 6.75 (1H, td, $^3J_{H\text{-}H}$ = $^3J_{H\text{-}F}$ = 8.5 Hz, $^4J_{H\text{-}H}$= 2.5 Hz, H_d), 6.52 (1H, dd, $^3J_{H\text{-}F}$ = 10 Hz, $^4J_{H\text{-}H}$ = 2.5 Hz, H_p), 4.5 (2H, s, Ph*CH*$_2$), 2.20 (6H, m, P*CH*$_2$), 1.72 (6H, m, PCH$_2$*CH*$_2$), 1.05 (9H, t, $^3J_{H\text{-}H}$ = 7.5 Hz, PCH$_2$CH$_2$*Me*) ppm.

δ_C = 15.78 (d, $^3J_{C\text{-}P}$ = 13 Hz, PCH$_2$CH$_2$*Me*), 18.66 (s, $^3J_{C\text{-}C}$ = 33 Hz, PCH$_2$*CH*$_2$), 26.93 (d, $^1J_{C\text{-}P}$ = 35 Hz, P*CH*$_2$), 41.52 (s, Ph*CH*$_2$), 110.32 (d, $^2J_{C\text{-}F}$ = 28 Hz, C_d), 114.63 (m, $C_{p,h/j}$), 119.04 (d, $^4J_{C\text{-}P}$ = 3 Hz, $^3J_{C\text{-}Pt}$ = 26 Hz, $C_{h/j}$), 122.58 (dd, $^2J_{C\text{-}F}$ = 16 Hz, $^3J_{C\text{-}P}$ = 2 Hz, $^2J_{C\text{-}Pt}$ = 55 Hz, C_n), 123.88 (d, $J_{C\text{-}F}$ = 16.5 Hz, $^2J_{C\text{-}Pt}$ = 63 Hz, C_b), 125.98 (d, $^3J_{C\text{-}F}$ = 8.5 Hz, $^3J_{C\text{-}Pt}$ = 30 Hz, C_e), 126.37 (s, Bn-*p*), 128.61 (s, Bn-*o*/*p*), 128.76 (s, Bn-*o*/*p*), 139.44 (s, C_s), 139.51 (s, C_i), 139.89 (d, $^3J_{C\text{-}F}$ = 7.5 Hz, C_q), 146.37 (t, $^4J_{C\text{-}F}$ = $^3J_{C\text{-}P}$ = 2 Hz, $^2J_{C\text{-}Pt}$ = 30 Hz, C_l), 147.11 (t, $^4J_{C\text{-}F}$ = $^3J_{C\text{-}P}$ = 2 Hz, $^2J_{C\text{-}Pt}$ = 28 Hz, C_f), 163.45 (d, $^1J_{C\text{-}F}$ = 254 Hz, $^3J_{C\text{-}Pt}$ = 56 Hz,

C_o), 164.25 (d, $^1J_{C\text{-}F}$ = 253 Hz, $^3J_{C\text{-}Pt}$ = 52 Hz, C_c), 164.61 (s, $^2J_{C\text{-}Pt}$ = 60 Hz, C_g), 165.57 (s, $^2J_{C\text{-}Pt}$ = 62 Hz, C_k), 169.68 (m, $^1J_{C\text{-}Pt}$ = 701 Hz, C_a), 170.69 (m, $^1J_{C\text{-}Pt}$ = 701 Hz, C_m) ppm.

δ_F = -110.0 ($^4J_{F\text{-}Pt}$ = 27.5 Hz, F_c) -112.9 ($^4J_{F\text{-}Pt}$ = 29 Hz, F_o) ppm.

δ_F (Acetone-d_6) = -112.6 ($^4J_{F\text{-}Pt}$ = 27 Hz, F_c) -114.4 ($^4J_{F\text{-}Pt}$ = 28 Hz, F_o) ppm.

δ_P = 2.57 ($^1J_{P\text{-}Pt}$ = 3727 Hz) ppm.

δ_P (Acetone-d_6) = 2.70 ($^1J_{P\text{-}Pt}$ = 3762 Hz) ppm.

δ_{Pt} (Acetone-d_6) = -4170 (d, $^1J_{Pt\text{-}P}$ = ~4400 Hz) ppm.

HR-MS (ESI): found 710.2249 m/z, calculated 710.2253 m/z = $C_{33}H_{36}F_2PN^{194}Pt = [M]^+$.

Elemental Analysis found (Calculated): C 55.15 (55.77), H 5.12 (5.11), N 1.89 (1.97).

6.5.10. Synthesis of **22(RX)** and **R-23**

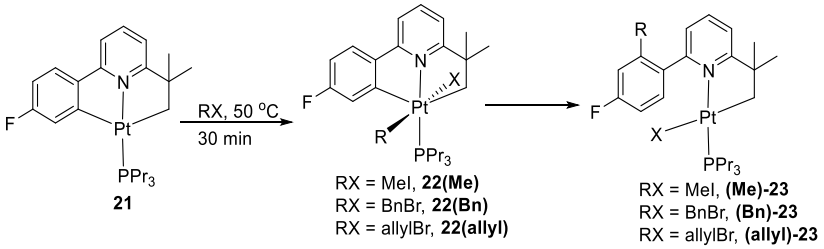

22(Me) and **Me-23** MeI (20 µl, excess), was added to a solution of **21** (46 mg, 7.90 x 10^{-5} mol) in chloroform and heated (50 °C, 1 hour) to give full conversion to **Me-23**. The solvent was removed to give pure **Me-23** (58 mg, 7.90 x 10^{-5} mol, quantitative yield). If the reaction time was reduced to 30 min, it was possible to identify **22(Me)** by NMR analysis, but it was not possible to purify the complex.

22(ally), **allyl-23**, **22(Bn)** and **Bn-23** were synthesised in a similar procedure, also giving quantitative yields (**allyl-23:** 49 mg **Bn-23:** 53 mg).

Complex - **22(Me)**

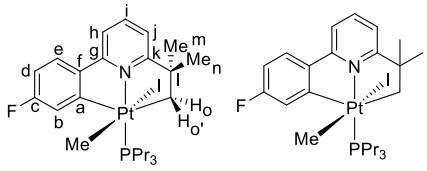

Not isolated

δ_H = 7.67 (2H, m, $H_{i,e}$), 7.50 (1H, d, $^3J_{H\text{-}H}$ = 7 Hz, H_h), 7.26 (1H, dd, $^3J_{H\text{-}F}$ = 9 Hz, $^4J_{H\text{-}H}$ = 2.5 Hz, $^3J_{H\text{-}Pt}$ = 25 Hz, H_b), 6.86 (1H, d, $^3J_{H\text{-}H}$ = 7 Hz, H_h), 6.70 (1H, td, $^3J_{H\text{-}H}$ = $^3J_{H\text{-}F}$ = 8.5

Hz, $^{4}J_{H\text{-}H}$ = 2.5 Hz, H_d), 3.13 (1H, d, $^{2}J_{H\text{-}H}$ = 10.5 Hz, $^{2}J_{H\text{-}Pt}$ = 60 Hz, $H_{o'}$), 2.17 (6H, m, P*CH₂*), 1.69 (1H, dd, $^{2}J_{H\text{-}H}$ = 10.5 Hz, $^{3}J_{H\text{-}P}$ = 2 Hz, $^{2}J_{H\text{-}Pt}$ = 20 Hz, H_o), 1.60 (6H, m, PCH_2*CH₂*), 1.56 (3H, s, H_n), 1.31 (3H, s, H_m), 1.01 (12H, m, PtMe, PCH_2CH_2*Me*) ppm.

δ_C = 5.03 (d, $^{2}J_{C\text{-}P}$ = 4 Hz, $^{1}J_{C\text{-}Pt}$ = 563 Hz, PtMe), 14.54 (d, $^{3}J_{C\text{-}P}$ = 14.5 Hz, PCH_2CH_2*Me*), 16.83 ($^{2}J_{C\text{-}P}$ = 3 Hz, PCH_2*CH₂*), 25.36 (d, $^{1}J_{C\text{-}P}$ = 37 Hz, $^{2}J_{C\text{-}Pt}$ = 24 Hz, P*CH₂*), 29.74 (d, $^{2}J_{C\text{-}P}$ = 3 Hz, $^{1}J_{C\text{-}Pt}$ = 388 Hz, C_o), 32.71 (s, C_n), 35.49 (s, C_m), 52.16 (s, C_l), 109.30 (d, $^{2}J_{C\text{-}F}$ = 25 Hz, C_d), 116.27 (s, C_h), 119.56 (s, $^{3}J_{C\text{-}Pt}$ = 28 Hz, C_j), 121.58 (d, $^{2}J_{C\text{-}F}$ = 17 Hz, $^{2}J_{C\text{-}Pt}$ = 34 Hz, C_b), 126.05 (d, $^{3}J_{C\text{-}F}$ = 9 Hz, $^{3}J_{C\text{-}Pt}$ = 22 Hz, C_e), 137.20 (s, C_i), 143.19 (s, C_f), 160.00 (s, $^{2}J_{C\text{-}Pt}$ = 31 Hz, C_g), 162.38 (d, $^{1}J_{C\text{-}F}$ = 255 Hz, $^{3}J_{C\text{-}Pt}$ = 39 Hz, C_c), 167.94 (m, $^{1}J_{C\text{-}Pt}$ = 536 Hz, C_a), 175.88 (s, $^{2}J_{C\text{-}Pt}$ = 48 Hz, C_k) ppm.

δ_F = -110.33 ($^{4}J_{F\text{-}Pt}$ = 22 Hz) ppm.

δ_P = -22.00 ($^{1}J_{P\text{-}Pt}$ = 2704 Hz) ppm.

δ_{Pt} = -3500 (d, $^{1}J_{Pt\text{-}P}$ = ~2750 Hz) ppm.

HR-MS (ESI): found 596.2348 m/z, calculated 596.2347 m/z = $C_{25}H_{38}FNP^{194}Pt$ = $[M\text{-}I]^+$.

Complex - **Me-23**

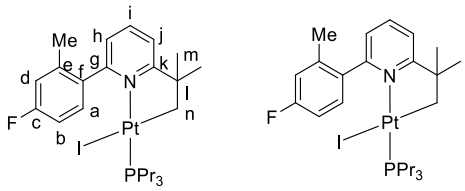

δ_H = 7.70 (1H, t, $^{3}J_{H\text{-}H}$ = $^{3}J_{H\text{-}H}$ = 8 Hz, H_i), 7.65 (1H, dd, $^{3}J_{H\text{-}H}$ = 8.5 Hz, $^{4}J_{H\text{-}F}$ = 6 Hz, H_a), 6.16 (2H, m, $H_{h,j}$), 6.86 (1H, dd, $^{3}J_{H\text{-}H}$ = 10 Hz, $^{4}J_{H\text{-}H}$ = 2.5 Hz, H_d), 6.80 (1H, td, $^{3}J_{H\text{-}H}$ = $^{3}J_{H\text{-}F}$ = 8 Hz, $^{4}J_{H\text{-}H}$ = 2.5 Hz, H_b), 2.45 (3H, s, Me), 1.77 (6H, m, P*CH₂*) 1.49 (14H, m, $H_{m,n}$, PCH_2*CH₂*), 0.95 (9H, t, $^{3}J_{H\text{-}H}$ = 7 Hz, PCH_2CH_2*Me*) ppm.

(600 MHz) Note that at 298 K P*CH₂* is broader than normal, without its characteristic shape. H_m is split into two broad peaks separated by 85 Hz. At 328 K, H_m has coalesced to form one broad resonance hidden under H_q, and P*CH₂* has regained its characteristic shape. Lowering the temperature to 268 K, H_m now comprises of two distinct peaks (1.44 and 1.66). Two new peaks also appear which correspond to H_n. These peaks are at 1.74 (1H, dd, $^{2}J_{H\text{-}H}$ = 10 Hz, $^{3}J_{H\text{-}P}$ = 3.5 Hz) and 2.21 74 (1H, d, $^{2}J_{H\text{-}H}$ = 10 Hz, $^{2}J_{H\text{-}Pt}$ = ~43 Hz) which were previously hidden under PCH_2*CH₂*. Lowering the temperature further to 238 K we see P*CH₂* beginning to separate into 2 peaks.

δ_C = 14.68 (d, $^3J_{C\text{-}P}$ = 15 Hz, $PCH_2CH_2\mathit{Me}$), 16.96 (s, $^3J_{C\text{-}Pt}$ = 35 Hz, $PCH_2\mathit{CH_2}$), 20.67 (s, Me), 26.49 (d, $^1J_{C\text{-}P}$ = 38 Hz, $^2J_{C\text{-}Pt}$ = 38 Hz, $P\mathit{CH_2}$), 31.58 (d, $^2J_{C\text{-}P}$ = 4 Hz, $^1J_{C\text{-}Pt}$ = 727 Hz, C_n), 48.83 (s, C_l), 110.64 (d, $^2J_{C\text{-}F}$ = 20 Hz, C_b), 116.18 (d, $^2J_{C\text{-}F}$ = 22 Hz, C_d), 118.35 (s, $^3J_{C\text{-}Pt}$ = 20 Hz, C_j), 124.57 (d, $^4J_{C\text{-}P}$ = 4 Hz, C_h), 134.56 (d, $^3J_{C\text{-}F}$ = 10 Hz, C_a), 135.9 (s, C_i), 136.91 (d, $^4J_{C\text{-}F}$ = 8 Hz, C_f), 138.31 (d, $^3J_{C\text{-}F}$ = 3 Hz, C_e), 159.57 (s, C_k), 162.22 (d, $^1J_{C\text{-}F}$ = 251 Hz, C_c), 173.30 (d, $^3J_{C\text{-}P}$ = 3 Hz, C_g) ppm.

Note that at 298 K C_m does not show a resonance. This is probably due to broadness of this peak at this temperature.

δ_F = -113.28 ppm.

δ_P = -2.05 ($^1J_{P\text{-}Pt}$ = 4303 Hz) ppm.

δ_{Pt} = -4339 ($^1J_{Pt\text{-}P}$ = ~4300 Hz) ppm.

HR-MS (ESI): found 596.2353 m/z, calculated 596.2347 m/z = $C_{25}H_{38}FNP^{194}Pt$ = $[M\text{-}I]^+$.

Elemental analysis expected (result): C 41.44 (41.54), H 5.29 (5.26), N 1.93 (1.78).

Complex - **allyl-22**

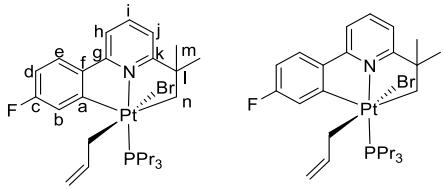

Not isolated

δ_H = 7.69 (2H, m, $H_{e,i}$), 7.52 (1H, d, $^3J_{H\text{-}H}$ = 8 Hz, $H_{h/j}$), 7.33 (1H, dd, $^3J_{H\text{-}F}$ = 9 Hz, $^4J_{H\text{-}H}$ = 2.5 Hz, $^3J_{H\text{-}Pt}$ = 20 Hz, H_b), 6.91 (1H, d, $^3J_{H\text{-}H}$ = 8 Hz, $H_{h/j}$), (1H, td, $^3J_{H\text{-}F}$ = $^3J_{H\text{-}H}$ = 9 Hz, $^4J_{H\text{-}H}$ = 2.5 Hz, H_d), 5.00 (1H, m, Allyl), 4.40 (2H, m, Allyl), 2.21 (6H, m, $P\mathit{CH_2}$), 1.67 (6H, m, $PCH_2\mathit{CH_2}$), 1.62 (3H, s, H_m), 1.36 (3H, s, H_m), 1.08 (9H, t, $^3J_{H\text{-}H}$ = 7 Hz, $PCH_2CH_2\mathit{Me}$) ppm.

δ_F = -110.59 ($^4J_{F\text{-}Pt}$ = 21 Hz) ppm.

δ_P = -20.90 ($^1J_{P\text{-}Pt}$ = 2775 Hz) ppm.

Complex - **allyl-23**

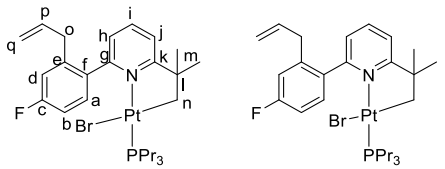

δ_H = 7.76 (1H, t, $^3J_{H\text{-}H}$ = 7.5 Hz, H_i), 7.63 (1H, dd, $^3J_{H\text{-}H}$ = 8 Hz, $^4J_{H\text{-}F}$ = 6 Hz, H_a), 7.26 (1H, d, $^3J_{H\text{-}H}$ = 7.5 Hz, H_j), 7.23 (1H, d, $^3J_{H\text{-}H}$ = 7.5 Hz, H_h), 6.98 (1H, dd, $^3J_{H\text{-}F}$ = 10 Hz, $^4J_{H\text{-}H}$ = 2 Hz, H_d), 6.90 (1H, td, $^3J_{H\text{-}H}$ = $^3J_{H\text{-}F}$ = 8 Hz, $^4J_{H\text{-}H}$ = 2 Hz, H_b), 5.99 (1H, ddt, $^3J_{H\text{-}Htrans}$ = 17 Hz, $^3J_{H\text{-}Hcis}$ = 10 Hz, $^3J_{H\text{-}H}$ = 6.5 Hz, H_p), 5.06 (1H, dd, $^3J_{H\text{-}H}$ = 10 Hz, $^3J_{H\text{-}H}$ = 1.5 Hz, H_q), 5.01 (1H, dd, $^3J_{H\text{-}H}$ = 17 Hz, $^3J_{H\text{-}H}$ = 1.5 Hz, H_q), 3.69 (1H, d, $^3J_{H\text{-}H}$ = 6.5 Hz, H_o), 2.046 (1H, d, $^2J_{H\text{-}H}$ = 9.5 Hz, $^2J_{H\text{-}Pt}$ = 60 Hz, H_n), 1.77 (6H, m, P*CH₂*), 1.68 (1H, d, $^2J_{H\text{-}H}$ = 9.5 Hz, H_n), 1.63 (3H, s, H_m), 1.58 (6H, m, PCH_2*CH₂*), 1.48 (3H, s, H_m), 1.01 (9H, t, $^3J_{H\text{-}H}$ = 6 Hz, PCH_2CH_2*Me*) ppm.

Note that at room temperature both H_m and H_n have separated into two peaks each, separated by 75 Hz and 183 Hz respectively.

δ_C = 15.73 (d, $^3J_{C\text{-}P}$ = 15 Hz, PCH_2CH_2*Me*), 17.91 (s, $^3J_{C\text{-}Pt}$ = 32 Hz, PCH_2*CH₂*), 26.27 (d, $^1J_{C\text{-}P}$ = 37 Hz, $^2J_{C\text{-}Pt}$ = 46 Hz, P*CH₂*), 27.39 (d, $^2J_{C\text{-}P}$ = 5 Hz, $^1J_{C\text{-}Pt}$ = 746 Hz, C_n), 32.58 (s, $^3J_{C\text{-}Pt}$ = 59 Hz, H_m), 34.07 (s, $^3J_{C\text{-}Pt}$ = 33 Hz, H_m), 38.49 (s, C_o), 49.72 (s, $^2J_{C\text{-}Pt}$ = 23.5 Hz, C_l), 112.08 (d, $^2J_{C\text{-}F}$ = Hz, C_b), 115.96 (d, $^2J_{C\text{-}F}$ = Hz, C_d), 116.37 (s, C_q), 119.62 (s, $^3J_{C\text{-}Pt}$ = 25 Hz, C_j), 125.67 (d, $^4J_{C\text{-}P}$ = 4 Hz, C_h), 132.71 (d, $^3J_{C\text{-}F}$ = 9.5 Hz, C_h), 136.95 (m, C_f), 137.05 (m, $C_{i,p}$), 141.01 (d, $^3J_{C\text{-}F}$ = 8.5 Hz, C_e), 159.90 (s, C_g), 163.21 (d, $^1J_{C\text{-}F}$ = 249 Hz, C_c), 174.60 (s, C_k) ppm.

δ_F = -113.00 ppm.

δ_P = -1.2 ($^1J_{P\text{-}Pt}$ = 4330 Hz) ppm.

δ_{Pt} = -4214 ($^1J_{Pt\text{-}P}$ = ~4350 Hz) ppm.

HR-MS (ESI): found 622.2493 m/z, calculated 622.2504 m/z = $C_{27}H_{40}FNP^{194}Pt$ = $[M\text{-}Br]^+$.

Complex - **22(Bn)**

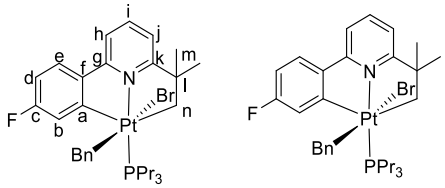

Not isolated

δ_F = - 110.79 ($^4J_{F\text{-}Pt}$ = 21.5 Hz) ppm.

δ_P = -21.10 ($^1J_{P\text{-}Pt}$ = 2767 Hz) ppm.

Complex - **Bn-23**

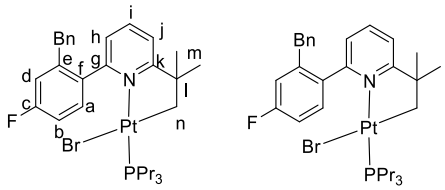

δ_H = 7.57 (2H, m, $H_{a,i}$), 7.14 (3H, m, H_j, Bn-*m*), 7.08 (1H, m, Bn-*p*), 7.05 (2H, d, $^3J_{H\text{-}H}$ = 7.5 Hz, Bn-*o*), 6.99 (2H, d, $^3J_{H\text{-}H}$ = 7.5 Hz, H_h), 6.85 (1H, td, $^3J_{H\text{-}H}$ = $^3J_{H\text{-}F}$ = 8.5 Hz, $^4J_{H\text{-}H}$ = 2.5 Hz, H_b), 6.70 (1H, td, $^3J_{H\text{-}F}$ = 10 Hz, $^4J_{H\text{-}H}$ = 2.5 Hz, H_b), 4.41 (1H, d, $^2J_{H\text{-}H}$ = 16.5 Hz, H_o), 2.41 (1H, d, $^2J_{H\text{-}H}$ = 16.5 Hz, Bn-*CH*$_2$), 1.93 (1H, d, $^2J_{H\text{-}H}$ = 10.5 Hz, $^2J_{H\text{-}Pt}$ = 51 Hz, H_n), 1.72 (7H, m, H_n, P*CH*$_2$), 1.53 (9H, m, H_m, PCH$_2$*CH*$_2$), 1.43 (3H, s, H_m), 0.96 (9H, t, $^3J_{H\text{-}H}$ = 7 Hz, PCH$_2$CH$_2$*Me*) ppm.

(600 MHz) Note that at 298 K Bn-CH$_2$, H_m and H_n have separated into 2 peaks each. They are separated by 103, 60 and 102 Hz respectively. By 328 K, multiplicity is lost in all cases due to broadening of the peaks.

δ_C = 15.70 (d, $^3J_{C\text{-}P}$ = 14.5 Hz, PCH$_2$CH$_2$*Me*), 17.89 (s, $^3J_{C\text{-}Pt}$ = 31 Hz, PCH$_2$*CH*$_2$), 26.22 (d, $^3J_{C\text{-}P}$ = 38 Hz, $^2J_{C\text{-}Pt}$ = 38 Hz, P*CH*$_2$), 27.57 (d, $^2J_{C\text{-}P}$ = 5 Hz, $^1J_{C\text{-}Pt}$ = 741 Hz, C_n), 32.83 (s, C_m), 33.81 (s, C_m), 40.05 (s, Bn-*CH*$_2$), 49.66 (s, C_l), 112.13 (d, $^2J_{C\text{-}F}$ = 20 Hz, C_b), 116.64 (d, $^2J_{C\text{-}F}$ = 21 Hz, C_d), 119.64 (s, $^3J_{C\text{-}Pt}$ = 24 Hz, C_j), 125.69 (d, $^4J_{C\text{-}P}$ = 3.5 Hz, C_h), 125.98 (s, Bn-*p*), 128.32 (s, Bn-*m*), 129.26 (s, Bn-*o*), 132.94 (d, $^3J_{C\text{-}F}$ = 8.5 Hz, C_a), 136.94 (d, $^3J_{C\text{-}F}$ = 3 Hz, C_f), 137.03 (s, C_i), 140.33 (s, Bn-*i*), 142.12 (d, $^3J_{C\text{-}F}$ = 8 Hz, C_b), 159.95 (s, C_g), 163.13 (d, $^1J_{C\text{-}F}$ = 247 Hz, C_c), 174.49 (d, $^2J_{C\text{-}P}$ = 3 Hz, C_k) ppm.

Note that at 298 K C_m is split into 2 peaks separated by 114 Hz.

δ_F = -112.82 ppm.

δ_P = -1.05 ($^1J_{P\text{-}Pt}$ = 4318 Hz) ppm.

δ_{Pt} = -4219 ($^1J_{Pt\text{-}P}$ = ~4300 Hz) ppm.

HR-MS (ESI): found 672.2657 m/z, calculated 672.2660 m/z = $C_{31}H_{42}FNP^{194}Pt$ = $[M\text{-}Br]^+$.

Elemental analysis found (calculated): C 46.75 (49.14), H 6.06 (5.62), N 1.49 (1.86).

6.5.11. Synthesis of **24**

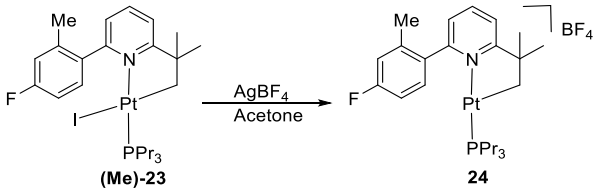

To solution of complex **Me-23** (10 mg, 1.38 x 10^{-5} mol) in acetone (0.6 ml) at room temperature, $AgBF_4$ was added (~5 mg, excess) giving full conversion. Complex **Me-24** was not isolated, and only characterised in solution.

Complex - **24**

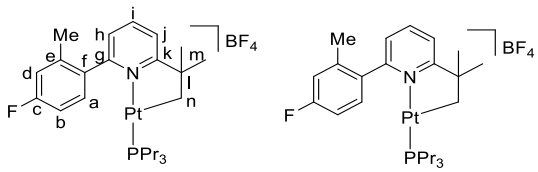

δ_H (Acetone-d_6) = 8.11 (1H, t, $^3J_{H\text{-}H}$ = 8 Hz, H_i), 7.59 (2H, m, $H_{j,a}$), 7.40 (1H, d, $^3J_{H\text{-}H}$ = 8 Hz, H_h), 7.04 (2H, m, $H_{b,d}$), 2.42 (3H, s, Me), 2.00 (2H, m, $^2J_{H\text{-}Pt}$ = ~32 Hz, H_n), 1.54 (12H, m, P*CH*$_2$, PCH$_2$*CH*$_2$), 0.91 (9H, t, $^3J_{H\text{-}H}$ = 7 Hz, PCH$_2$CH$_2$*Me*) ppm.

δ_C = 15.01 (d, $^3J_{C\text{-}P}$ = 15.5 Hz, PCH$_2$CH$_2$*Me*), 16.61 (d, $^2J_{C\text{-}P}$ = 5.5 Hz, $^1J_{C\text{-}Pt}$ = 765 Hz, C_n), 17.45 (s, $^3J_{C\text{-}Pt}$ = 30 Hz, PCH$_2$*CH*$_2$), 20.03 (s, Me), 24.77 (d, $^1J_{C\text{-}P}$ = 38 Hz, $^2J_{C\text{-}Pt}$ = 42 Hz, P*CH*$_2$), 31.21 (s, C_m), 49.68 (s, C_l), 113.04 (d, $^2J_{C\text{-}F}$ = 25 Hz, C_b), 117.25 (d, $^2J_{C\text{-}F}$ = 22 Hz, C_d), 121.13 (s, C_j), 125.93 (s, C_h), 131.83 (d, $^3J_{C\text{-}F}$ = 8.5 Hz, C_a), 134.63 (s, C_f), 139.07 (d, $^3J_{C\text{-}F}$ = 8.5 Hz, C_e), 140.10 (s, C_i), 158.35 (s, C_g), 163.02 (d, $^1J_{C\text{-}F}$ = 245 Hz, C_c), 173.43 (s, C_k) ppm.

δ_F (Acetone-d_6) = -114.13 ppm.

δ_P (Acetone-d_6) = 3.00 ($^1J_{P\text{-}Pt}$ = 4272 Hz) ppm.

δ_{Pt} (Acetone-d_6) = -4116 ($^1J_{Pt\text{-}P}$ = ~4400 Hz) ppm.

HR-MS (ESI): found 596.2349 m/z, calculated 596.2347 m/z = $C_{25}H_{38}FPN^{194}Pt$ = $[M]^+$.

6.5.12. Synthesis of **Me-21** and **Bn-21**

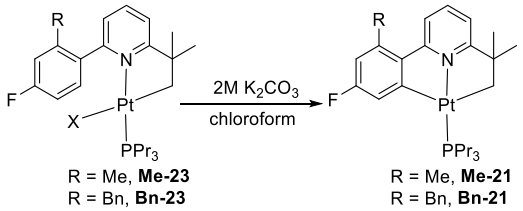

Me-21 To a solution of complex **Me-23** (58 mg, 8.00 x 10^{-5} mol) in chloroform (10 ml), was added a solution of K_2CO_3 (0.5 g) in water (2 ml); the mixture was then stirred (3 days). The solvent was removed and the crude product purified by chromatography on silica, eluting with chloroform (45 mg, 7.53 x 10^{-5} mol, 94%).

Bn-21 was prepared in a similar fashion.

Complex - **Me-21**

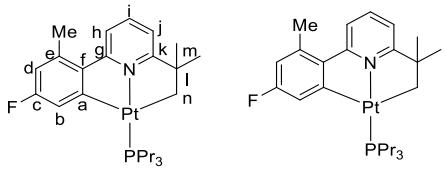

δ_H = 7.71 (2H, m, $H_{h,i}$), 7.25 (1H, m, H_b), 7.02 (1H, d, $^3J_{H\text{-}H}$ = 8.5 Hz, H_j), 6.56 (1H, dd, $^3J_{H\text{-}H}$ = 9.5 Hz, $^5J_{H\text{-}P}$ = 2 Hz, H_d), 2.63 (3H, s, Me), 1.92 (6H, m, P*CH*$_2$), 1.81 (2H, s, $^2J_{H\text{-}Pt}$ = 37 Hz, H_n), 1.62 (6H, m, PCH$_2$*CH*$_2$), 1.37 (6H, s, H_m), 1.04 (9H, t, $^3J_{H\text{-}H}$ = 7 Hz, PCH$_2$CH$_2$*Me*) ppm.

δ_C = 14.81 (d, $^3J_{C\text{-}P}$ = 14.5 Hz, PCH$_2$CH$_2$*Me*), 17.27 (s, $^3J_{C\text{-}Pt}$ = 32 Hz, PCH$_2$*CH*$_2$), 23.73 (s, Me), 26.01 (d, $^1J_{C\text{-}P}$ = 35 Hz, $^2J_{C\text{-}Pt}$ = 35 Hz, P*CH*$_2$), 33.36 (s, $^3J_{C\text{-}Pt}$ = 18 Hz, C_m), 35.18 (d, $^2J_{C\text{-}P}$ = 6.5 Hz, $^1J_{C\text{-}Pt}$ = 460 Hz, C_n), 51.43 (d, $^3J_{C\text{-}P}$ = 4 Hz, C_l), 112.42 (d, $^3J_{C\text{-}F}$ = 21.5 Hz, C_d), 117.06 (d, $^4J_{C\text{-}P}$ = 3 Hz, $^3J_{C\text{-}Pt}$ = 31 Hz, C_h), 118.36 (d, $^4J_{C\text{-}P}$ = 3 Hz, $^3J_{C\text{-}Pt}$ = 23 Hz, C_j), 120.13 (d, $^2J_{C\text{-}F}$ = 14 Hz, $^2J_{C\text{-}Pt}$ = 60 Hz, C_b), 136.42 (s, C_i), 137.37 (d, $^3J_{C\text{-}F}$ = 7.5 Hz, $^3J_{C\text{-}Pt}$ = 31 Hz, C_e), 143.77 (s, $^2J_{C\text{-}Pt}$ = 29 Hz, C_f), 162.55 (d, $^1J_{C\text{-}F}$ = 254 Hz, $^3J_{C\text{-}Pt}$ = 55 Hz, C_c), 163.69 (s, $^2J_{C\text{-}Pt}$ = 54 Hz, C_g), 175.35 (m, $^1J_{C\text{-}Pt}$ = 680 Hz, C_a), 177.22 (s, $^2J_{C\text{-}Pt}$ = 54.5 Hz, C_k) ppm.

δ_F = -114.13 ($^4J_{F\text{-}Pt}$ = 28 Hz) ppm.

δ_P = 0.96 ($^1J_{P\text{-}Pt}$ = 3820 Hz) ppm.

δ_{Pt} = -3995 (d, $^1J_{Pt\text{-}P}$ = ~3900 Hz) ppm.

HR-MS (ESI): found 604.2003 m/z, calculated 604.2010 m/z = $C_{25}H_{37}FNP^{194}Pt$ = $[M]^+$.

Elemental analysis found (calculated): C 50.83 (50.33), H 6.43 (6.25), N 2.19 (2.35).

Complex - **Bn-21**

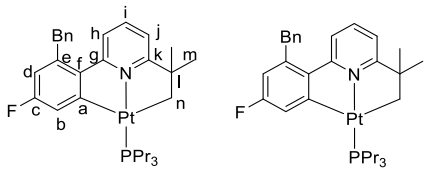

δ_H = 7.55 (1H, t, $^3J_{H-H}$ = 7.5 Hz, H_i), 7.41 (1H, d, $^3J_{H-H}$ = 7.5 Hz, H_h), 7.35 (d, 1H, $^3J_{H-F}$ = 8 Hz, $^4J_{H-H}$ = 2 Hz, $^3J_{H-Pt}$ = #20 Hz, H_b), 7.31 (3H, m, Bn-*m*,*p*), 7.20 (2H, d, $^3J_{H-H}$ = 8.5 Hz, Bn-*o*), 6.98 (1H, d, $^3J_{H-H}$ = 7.5 Hz, H_j), 6.51 (1H, dd, $^3J_{H-F}$ = 10 Hz, $^4J_{H-H}$ = 2 Hz, H_d), 4.34 (2H, s, Bn-*CH*$_2$), 1.95 (6H, m, P*CH*$_2$), 1.83 (2H, s, $^2J_{H-Pt}$ = 37 Hz, H_n), 1.66 (6H, m, PCH$_2$*CH*$_2$), 1.38 (6H, s, C_m), 1.07 (9H, t, $^3J_{H-H}$ = 7 Hz, PCH$_2$CH$_2$*Me*) ppm.

δ_C = 14.79 (d, $^3J_{C-P}$ = 14 Hz, PCH$_2$CH$_2$*Me*), 17.26 (s, $^3J_{C-Pt}$ = 30.5 Hz, PCH$_2$*CH*$_2$), 26.00 (d, $^1J_{C-P}$ = 36 Hz, $^2J_{C-Pt}$ = 36 Hz, P*CH*$_2$), 33.36 (s, $^3J_{C-Pt}$ = 17 Hz, C_m), 35.17 (s, C_n), 40.86 (s, Bn-*CH*$_2$), 51.44 (s, C_l), 112.69 (d, $^2J_{C-F}$ = 24 Hz, C_d), 117.35 (s, C_j), 118.52 (s, C_h), 120.83 (d, $^2J_{C-F}$ = 16 Hz, C_b), 125.29 (s, Bn-*p*), 127.69 (s, Bn-*o*,*m*), 136.46 (s, C_i), 138.82 (s, Bn-*i*), 144.28 (s, C_f), 162.82 (s, C_g), 162.85 (d, $^1J_{C-F}$ = 253 Hz, C_c), 175.66 (m, C_a), 177.07 (s, C_k) ppm.

δ_F = -113.66 ($^4J_{F-Pt}$ = 26.5 Hz) ppm.

δ_P = 0.86 ($^1J_{P-Pt}$ = 3813 Hz) ppm.

δ_{Pt} = -3987 (d, $^1J_{Pt-P}$ = ~3850 Hz) ppm.

HR-MS (ESI): found 672.2661 m/z, calculated 672.2660 m/z = $C_{31}H_{41}FNP^{194}Pt$ [M].

6.5.13. Synthesis of **Me-22(Me)** and **Me$_2$-23**

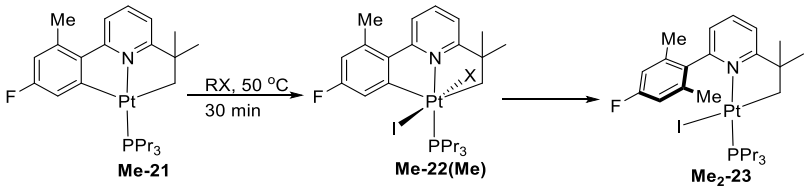

MeI (20 µl, excess), was added to a solution of **Me-21** (10 mg, 1.68 x 10^{-5} mol) in chloroform and heated (50 °C, 1 hour) to give full conversion to **Me$_2$-23**. The solvent was removed to give pure **Me$_2$-23** (12 mg, 1.68 x 10^{-5} mol, quantitative). If the reaction time was reduced to 30 min, it was possible to identify key NMR resonances for **Me-22(Me)**, but it was not possible to purify the complex.

Complex - **Me-22(Me)**

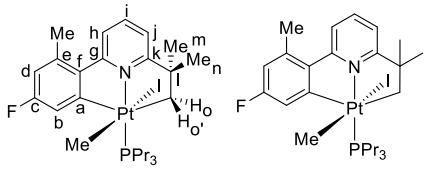

Not isolated

δ_F = -113.19 ppm.

δ_P = -19.77 ppm.

Complex - **Me$_2$-23**

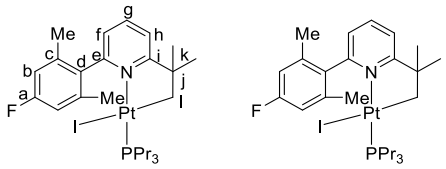

δ_H = 7.80 (1H, t, $^3J_{H\text{-}H}$ = 8 Hz, H_g), 7.27 (1H, d, $^3J_{H\text{-}H}$ = 8 Hz, H_h), 7.08 (1H, d, $^3J_{H\text{-}H}$ = 8 Hz, H_f), 6.73 (2H, d, $^3J_{H\text{-}F}$ = 9.5 Hz, H_b), 2.35 (6H, s, Me), 1.83 (8H, m, H_l, P*CH$_2$*), 1.56 (12H, m, H_k, PCH$_2$*CH$_2$*), 0.99 (9H, t, $^3J_{H\text{-}H}$ = 7 Hz, PCH$_2$CH$_2$*Me*) ppm.

δ_C = 15.76 (d, $^3J_{C\text{-}P}$ = 18 Hz, PCH$_2$CH$_2$*Me*), 18.00 (s, $^3J_{C\text{-}Pt}$ = 30 Hz, PCH$_2$*CH$_2$*) 22.24 (s, Me), 27.57 (d, $^1J_{C\text{-}P}$ = 35 Hz, $^2J_{C\text{-}Pt}$ = 48 Hz, P*CH$_2$*), 33.23 (s, $^3J_{C\text{-}Pt}$ = 44 Hz, C_k), 35.16 (s, $^1J_{C\text{-}Pt}$ = 727 Hz, C_l), 49.98 (s, C_j), 114.22 (d, $^2J_{C\text{-}F}$ = 23 Hz, C_b), 119.42 (s, C_h), 126.44 (s, C_f), 136.86 (s, C_d), 137.44 (s, C_g), 139.83 (d, $^3J_{C\text{-}F}$ = 10 Hz, C_c), 160.69 (s, C_e), 162.80 (d, $^1J_{C\text{-}F}$ = 254 Hz, C_a), 174.32 (s, C_i) ppm.

δ_F = -114.84 ppm.

δ_P = -1.80 ($^1J_{P\text{-}Pt}$ = 4292 Hz) ppm.

δ_{Pt} = -4382 (d, $^1J_{Pt\text{-}P}$ = ~4300 Hz) ppm.

HR-MS (ESI): found 610.2508, calculated 610.2504 m/z = $C_{26}H_{40}FNP^{194}Pt = [M\text{-}I]^+$.

Elemental analysis found (calculated): C 43.85 (42.28), H 5.73 (5.46), N 1.85 (1.90).

6.5.14. Synthesis of **Me_2-23** and **Bn_2-23** by 1-pot

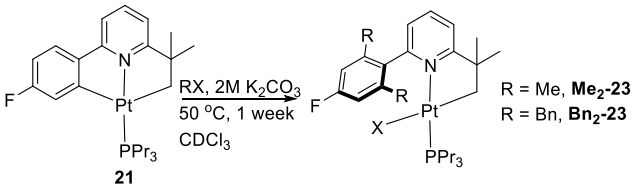

Me_2-23 To solution of **21** (25 mg, 4.29 x 10^{-5} mol) in chloroform (0.6 ml) was added MeI (20 µl, excess) and 2M aqueous K_2CO_3 (0.08 ml). The reaction mixture was then heated with stirring (50 °C, 1 week). The water layer was decanted off, and the solvent and excess MeI removed. The product was purified by column chromatography on silica, elution was with toluene, giving pure Me_2-23 (29 mg, 3.95 x 10^{-5} mol, 92%).

Bn_2-3 was prepared in a similar fashion, also starting with **21** (25 mg, 4.29 x 10^{-5} mol). Attempts to improve the purity of **Bn_2-23** after the one-pot method were unsuccessful, but the crude was relatively clean.

Complex - **Bn_2-23**

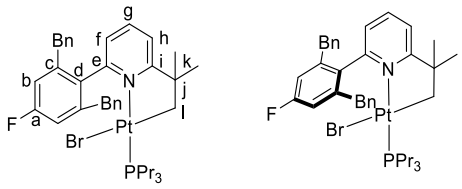

δ_H = 7.32 (1H, t, $^3J_{H\text{-}H}$ = 8.5 Hz, H_g), 7.07 (7H, m, H_h, Bn-*m*,*p*), 6.91 (4H, d, $^3J_{H\text{-}H}$ = 8 Hz, Bn-*o*), 6.61 (2H, d, $^3J_{H\text{-}F}$ = 10 Hz, H_b), 6.53 (2H, d, $^3J_{H\text{-}H}$ = 8.5 Hz, H_f), 4.16 (2H, d, $^2J_{H\text{-}H}$ = 16 Hz, Bn-*CH_2*), 4.09 (2H, d, $^2J_{H\text{-}H}$ = 16 Hz, Bn-*CH_2*), 1.75 (8H, m, H_l, P*CH_2*), 1.55 (6H, m, PCH_2CH_2), 1.52 (6H, m, H_k), 0.96 (9H, t, $^3J_{H\text{-}H}$ = 7 Hz, PCH_2CH_2*Me*) ppm.

δ_C = 15.80 (d, $^3J_{C\text{-}P}$ = 16 Hz, PCH_2CH_2*Me*), 18.02 (s, $^3J_{C\text{-}Pt}$ = 27 Hz, PCH_2*CH_2*), 26.35 (d, $^1J_{C\text{-}P}$ = 37 Hz, $^2J_{C\text{-}Pt}$ = 34 Hz, P*CH_2*), 29.50 (d, $^2J_{C\text{-}P}$ = 4 Hz, C_l), 33.40 (s, C_k), 40.69 (s, C_m), 49.60 (s, C_j), 114.56 (d, $^2J_{C\text{-}F}$ = 22 Hz, C_b), 119.66 (s, C_f), 125.88 (s, Bn-*p*), 127.26 (s, C_h), 128.18 (s, Bn-*m*), 129.09 (s, Bn-*o*), 135.83 (s, C_d), 136.81 (s, C_g), 140.44 (s, C_n), 143.01 (d, $^3J_{C\text{-}F}$ = 8 Hz, C_c), 159.11 (s, C_e), 162.85 (d, $^1J_{C\text{-}F}$ = 247 Hz, C_a), 174.50 (s, C_i) ppm.

δ_F = -113.65 ppm.

δ_P = -0.93 (d, $^1J_{P\text{-}Pt}$ = 4298 Hz) ppm.

δ_{Pt} = -4250 ($^1J_{Pt\text{-}P}$ = ~4300 Hz) ppm.

HR-MS (ESI): found 762.3137 m/z, calculated 762.3130 m/z = $C_{38}H_{48}FNP^{194}Pt$ $[M\text{-}Br]^+$

6.6. Synthesis of the Complexes from Chapter 4

6.6.1. Synthesis of **27(t)**

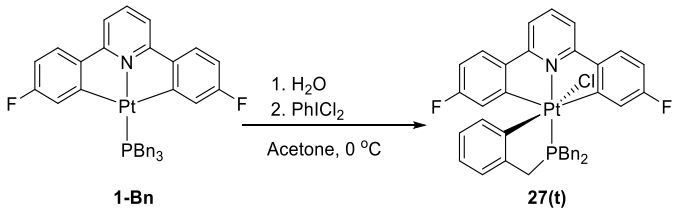

Complex **1-Bn** (80 mg, 1.04 x 10^{-4} mol) was dissolved in acetone (40 ml), and water (10 ml) added. To this solution, an acetone solution of $PhICl_2$ (34 mg, 1.26 x 10^{-4} mol, 1.2 eq) was added dropwise with stirring at room temperature, resulting in the disappearance of the yellow colour. The solvent was removed, the crude product washed with acetone and collected by filtration as a light cream solid (75 mg, 9.39 x 10^{-5} mol, 90%).

Complex - **27(t)**

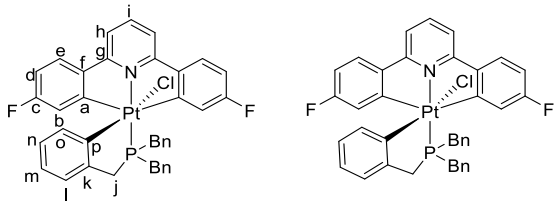

δ_H = 7.95 (1H, t, $^3J_{H\text{-}H}$ = 8.5 Hz, H_i), 7.76 (2H, dd, $^3J_{H\text{-}H}$ = 8.5 Hz, $^4J_{H\text{-}F}$ = 6 Hz, H_e), 7.64 (2H, dd, $^3J_{H\text{-}H}$ = 8 Hz, $^5J_{H\text{-}P}$ = 1.5 Hz, H_h), 6.37 (6H, m, Bn-*m,p*), 7.34 (2H, dd, $^3J_{H\text{-}F}$ = 9.5 Hz, $^4J_{H\text{-}H}$ = 2 Hz, $^3J_{H\text{-}Pt}$ = 43 Hz, H_b), 7.21 (4H, d, $^3J_{H\text{-}H}$ = 7 Hz, Bn-*o*), 6.93 (1H, d, $^3J_{H\text{-}H}$ = 7 Hz, H_l), 6.83 (2H, td, $^3J_{H\text{-}H}$ = $^3J_{H\text{-}F}$ = 8.5 Hz, $^4J_{H\text{-}H}$ = 2 Hz, H_d), 6.91 (1H, t, $^3J_{H\text{-}H}$ = 7 Hz, H_m), 6.57 (1H, t, $^3J_{H\text{-}H}$ = 7 Hz, H_n), 6.19 (1H, d, $^3J_{H\text{-}H}$ = Hz, $^3J_{H\text{-}Pt}$ = 47 Hz, H_o), 4.20 (2H, dd, $^2J_{H\text{-}H}$ = 15 Hz, $^2J_{H\text{-}P}$ = 12 Hz, Ph*CH₂*), 4.06 (2H, dd, $^2J_{H\text{-}H}$ = 15 Hz, $^2J_{H\text{-}P}$ = 12 Hz, $^3J_{H\text{-}Pt}$ = 18 Hz, Ph*CH₂*), 3.61 (2H, d, $^2J_{H\text{-}P}$ = 11 Hz, $^3J_{H\text{-}Pt}$ = 16 Hz, H_j) ppm.

δ_C = 29.28 (d, $^1J_{C\text{-}P}$ = 30 Hz, $^2J_{C\text{-}Pt}$ = 25 Hz, Ph*CH₂*), 34.76 (d, $^1J_{C\text{-}P}$ = 40 Hz, $^2J_{C\text{-}Pt}$ = 62 Hz, C_j), 111.68 (d, $^2J_{C\text{-}F}$ = 25.5 Hz, C_d), 116.59 (s, C_h), 122.49 (d, $^2J_{C\text{-}F}$ = 19 Hz, $^2J_{C\text{-}Pt}$ = 32 Hz, C_b), 125.17 (s, C_m), 125.61 (d, $^3J_{C\text{-}P}$ = 18 Hz, C_l), 126.89 (s, $^3J_{C\text{-}Pt}$ = 45 Hz, C_n), 129.79 (s, Bn-*p*), 128.02 (d, $^3J_{C\text{-}F}$ = 8 Hz, $^3J_{C\text{-}Pt}$ = 16 Hz, C_e), 128.84(s, $^2J_{C\text{-}Pt}$ = 13.5 Hz, C_o), 129.21 (s, Bn-*m*), 130.39 (d, $^3J_{C\text{-}P}$ = Hz, Bn-*o*), 131.19 (s, $^1J_{C\text{-}Pt}$ = 449 Hz, C_p), 131.93 (d, $^2J_{C\text{-}P}$ = 8 Hz, $^3J_{C\text{-}Pt}$ = 16 Hz, Bn-*i*), 140.23 (s, C_i), 140.53 (d, $^2J_{C\text{-}P}$ = 9 Hz, C_k), 143.47 (m, C_f), 161.91 (s, $^2J_{C\text{-}Pt}$ = 33 Hz, C_g), 162.49 (m, $^1J_{C\text{-}Pt}$ = 468 Hz, C_a), 163.10 (d, $^1J_{C\text{-}Pt}$ = 256 Hz, $^3J_{C\text{-}F}$ = 40 Hz, C_c) ppm.

δ_F = -108.450 ($^4J_{F\text{-}Pt}$ = 20 Hz) ppm.

δ_P = 19.37 ($^1J_{P\text{-}Pt}$ = 2649 Hz) ppm.

δ_{Pt} = -2911 (d, $^1J_{Pt\text{-}P}$ = ~2700 Hz) ppm.

HR-MS (ESI): found 762.1628 m/z, calculated 762.1627 m/z = $C_{38}H_{29}F_2NP^{194}Pt$ = $[M\text{-}Cl]^+$.

Crystals suitable for X-ray analysis were grown by the slow evaporation of solvent from a chloroform solution – ps29.

6.6.2. Synthesis of **Me-27(t)**

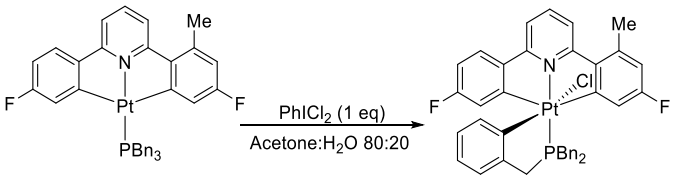

Me-1-Bn **Me-27(t)**

Complex **Me-1-Bn** (50 mg, 6.43 x 10^{-5} mol) was dissolved in acetone (40 ml), and water (10 ml) added. To this solution, an acetone solution of $PhICl_2$ (21 mg, 7.71 x 10^{-5} mol, 1.2 eq) was added dropwise with stirring at room temperature, resulting in the disappearance of the yellow colour. The solvent was removed, and the crude product washed with acetone and collected by filtration as a light cream solid. (43 mg, 5.27 x 10^{-5} mol, 82%).

Complex - **Me-27(t)**

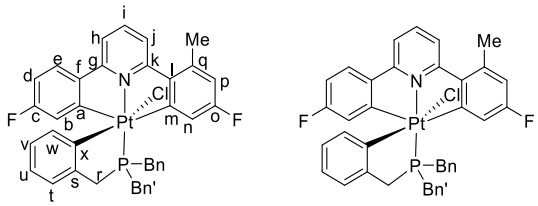

δ_H = 7.93 (2H, m, $H_{i,j}$), 7.76 (1H, dd, $^3J_{H\text{-}H}$ = 8.5 Hz, $^4J_{H\text{-}F}$ = 5.5 Hz, H_e), 7.65 (1H, d, $^3J_{H\text{-}H}$ = 7 Hz, H_h), 7.37 (7H, m, H_b, Bn), 7.31 (1H, d, $^3J_{H\text{-}F}$ = Hz, H_n), 7.24 (2H, d, $^3J_{H\text{-}H}$ = 6.5 Hz, Bn), 7.17 (2H, d, $^3J_{H\text{-}H}$ = 6.5 Hz, Bn), 6.91 (1H, d, $^3J_{H\text{-}H}$ = 7.5 Hz, $^4J_{H\text{-}Pt}$ = 12 Hz, H_t), 6.83 (1H, td, $^3J_{H\text{-}H}$ = $^3J_{H\text{-}F}$ = 8 Hz, $^4J_{H\text{-}H}$ = 2.5 Hz, H_d), 6.79 (1H, t, $^3J_{H\text{-}H}$ = 7.5 Hz, H_u), 6.65 (1H, dd, $^3J_{H\text{-}F}$ = Hz, $^4J_{H\text{-}H}$ = Hz, H_p), 6.58 (1H, t, $^3J_{H\text{-}H}$ = 7.5 Hz, H_v), 6.18 (1H, d, $^3J_{H\text{-}H}$ = 7.5 Hz, $^3J_{H\text{-}Pt}$ = 47 Hz, H_w), 4.21 (2H, m, Ph*CH*$_2$), 4.06 (2H, m, Ph*CH*$_2$), 3.60 (2H, d, $^2J_{H\text{-}P}$ = 11.5 Hz, $^3J_{H\text{-}Pt}$ = 15 Hz, H_r), 2.75 (3H, s, Me) ppm.

δ_C = 24.95 (s, Me), 28.90 (d, $^1J_{C\text{-}P}$ = 29 Hz, $^2J_{C\text{-}Pt}$ = 28 Hz, Ph*CH*$_2$), 29.70 (d, $^1J_{C\text{-}Pt}$ = 29 Hz, $^2J_{C\text{-}P}$ = 22 Hz, Ph*CH*$_2$), 34.77 (d, $^1J_{C\text{-}P}$ = 40 Hz, $^2J_{C\text{-}Pt}$ = 68 Hz, C_r), 111.65 (d, $^2J_{C\text{-}F}$ =

24 Hz, C_d), 115.96 (d, $^2J_{C-F}$ = 20 Hz, C_p), 116.45 (d, $^4J_{C-P}$ = 3.5 Hz, $^3J_{C-Pt}$ = 18 Hz, C_h), 120.43 (m, $C_{j,n}$), 122.35 (d, $^2J_{C-F}$ = 18 Hz, $^2J_{C-Pt}$ = 18 Hz, C_b), 125.11 (s, C_u), 125.62 (d, $^3J_{C-P}$ = 17.5 Hz, $^3J_{C-Pt}$ = 39 Hz, C_t), 126.86 (s, $^3J_{C-Pt}$ = 46 Hz, C_v), 127.76 (m, Bn), (d, $^3J_{C-F}$ = 8.5 Hz, $^3J_{C-Pt}$ = 23 Hz, C_e), 128.74 (s, $^2J_{C-Pt}$ = 14 Hz, C_w), 127.17 (m, Bn), 130.42 (m, Bn), 131.52 (s, C_s), 132.04 (m, Bn), 139.97 (s, C_i), 140.62 (d, $^3J_{C-F}$ = 7.5 Hz, C_q), 140.65 (d, $^2J_{C-P}$ = 10.5 Hz, $^1J_{C-Pt}$ = 53 Hz, C_x), 142.01 (t, $^3J_{C-P}$ = $^4J_{C-F}$ = 2.5 Hz, $^2J_{C-Pt}$ = 13.5 Hz, C_l), 143.65 (t, $^3J_{C-P}$ = $^4J_{C-F}$ = 2.5 Hz, $^2J_{C-Pt}$ = ~13 Hz, C_f), 161.84 (d, $^1J_{C-F}$ = 254 Hz, $^3J_{C-Pt}$ = 53 Hz, C_c), 162.40 (s, $^2J_{C-Pt}$ = 32 Hz, C_k), 162.91 (s, $^2J_{C-Pt}$ = 31 Hz, C_g), 163.07 (d, $^1J_{C-F}$ = 256 Hz, $^3J_{C-Pt}$ = 36 Hz, C_o), 163.38 (m, $^1J_{C-Pt}$ = 558 Hz, $C_{a/m}$), 163.97 (m, $^1J_{C-Pt}$ = 556 Hz, $C_{a/m}$) ppm.

δ_F = -108.61 ($^4J_{F-Pt}$ = 19 Hz, F_c), -111.30 ($^4J_{F-Pt}$ = 22 Hz, F_o) ppm.

δ_P = 19.76 ($^1J_{P-Pt}$ = 2657 Hz) ppm.

δ_{Pt} = -2885 (d, $^1J_{Pt-P}$ = ~2700 Hz) ppm.

HR-MS (ESI): found 776.1787 m/z, calculated 776.1784 m/z = $C_{39}H_{31}F_2NP^{194}Pt$ = $[M-Cl]^+$.

Elemental analysis found (calculated.EtOAc): C 45.16 (51.00), H 2.94 (3.29), N 1.33 (1.52).

6.6.3. Synthesis of **25** and **26**

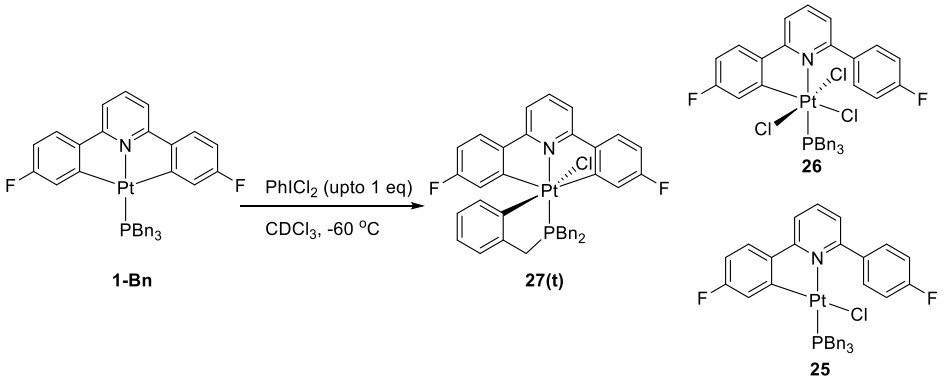

To a solution of **1-Bn** (20 mg, 2.62 x 10^{-5} mol) in chloroform (10 ml), was added $PhICl_2$ (3.6 mg, 1.31 x 10^{-5} mol, 0.5 eq) at room temperature. After addition of the final drop, solvent was removed, and the crude mixture washed with hexane. Acetone was used to dissolve the **25**, leaving behind **27(t)**. To a sample of the **25** (9 mg) in chloroform (0.6 ml) was added $PhICl_2$ (4 mg, excess) at room temperature. Full conversion to **26** was observed, though it was not isolated.

Complex - **25**

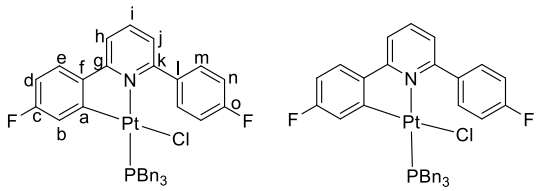

δ_H = 7.94 (1H, t, $^3J_{H\text{-}H}$ = 7.5 Hz, H_i), 7.90 (2H, dd, $^3J_{H\text{-}H}$ = 8 Hz, $^4J_{H\text{-}F}$ = 4.5 Hz, H_e), 7.72 (1H, d, $^3J_{H\text{-}H}$ = 7.5 Hz, H_h), 7.52 (2H, dd, $^3J_{H\text{-}H}$ = 8 Hz, $^4J_{H\text{-}F}$ = 5.5 Hz, H_m), 7.47 (1H, d, $^3J_{H\text{-}H}$ = 7.5 Hz, H_j), 7.37 (1H, m, Bn-*o*), 7.25 (9H, m, Bn-*m,p*), 7.10 (2H, t, $^3J_{H\text{-}H}$ = $^3J_{H\text{-}F}$ = 8.5 Hz, H_n), 6.73 (1H, td, $^3J_{H\text{-}H}$ = $^3J_{H\text{-}F}$ = 8.5 Hz, $^4J_{H\text{-}H}$ = 2.5 Hz, H_d), 6.66 (1H, dt, $^3J_{H\text{-}F}$ = 10 Hz, $^4J_{H\text{-}H}$ = $^4J_{H\text{-}P}$ = 2 Hz, $^3J_{H\text{-}Pt}$ = ~55 Hz, H_b), 3.46 (6H, d, $^2J_{H\text{-}P}$ = 11 Hz, $^3J_{H\text{-}Pt}$ = 30 Hz, Ph*CH₂*) ppm.

δ_C = 29.53 (d, $^1J_{C\text{-}P}$ = 34.5 Hz, $^2J_{C\text{-}Pt}$ = 34.5 Hz, Ph*CH₂*), 110.23 (d, $^2J_{C\text{-}F}$ = 23.5 Hz, C_d), 114.90 (d, $^2J_{C\text{-}F}$ = 23.5 Hz, C_n), 115.96 (s, C_h), 121.66 (dd, $^2J_{C\text{-}F}$ = 20 Hz, $^3J_{C\text{-}P}$ = 2 Hz, C_b), 122.76 (d, $^4J_{C\text{-}P}$ = 2 Hz, C_j), 126.15 (d, $^3J_{C\text{-}F}$ = 9.5 Hz, $^3J_{C\text{-}Pt}$ = 44 Hz, C_e), 126.82 (s, Bn-*p*), 128.38 (s, Bn-*m*), 130.40 (d, $^3J_{C\text{-}P}$ = 5.5 Hz, Bn-*o*), 131.175 (d, $^3J_{C\text{-}F}$ = 8 Hz, C_m), 133.71 (d, $^2J_{C\text{-}P}$ = 5.5 Hz, Bn-*i*), 136.66 (s, C_l), 139.19 (s, C_i), 142.76 (s, C_f), 146.19 (t, $^2J_{C\text{-}P}$ = $^3J_{C\text{-}F}$ = 6 Hz, C_a), 160.71 (s, C_k), 162.09 (d, $^1J_{C\text{-}F}$ = 253 Hz, C_c), 163.83 (d, $^1J_{C\text{-}F}$ = 250 Hz, C_o), 164.51 (s, C_g) ppm.

δ_F = -110.84 ($^4J_{F\text{-}Pt}$ = 64 Hz), -111.36 ppm.

δ_P = -1.76 ($^1J_{P\text{-}Pt}$ = 4272 Hz) ppm.

δ_{Pt} = -3807 (d, $^1J_{Pt\text{-}P}$ = ~4300 Hz) ppm.

HR-MS (ESI): found 764.1779 m/z, calculated 764.1784 m/z = $C_{38}H_{31}F_2NP^{194}Pt$ = $[M\text{-}Cl]^+$.

Crystals suitable for X-ray analysis were grown by the slow evaporation of solvent from a chloroform solution – ps34.

Complex - **26**

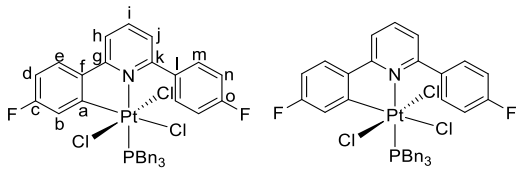

Data taken from a reaction mixture containing also **25** and **27t**.

δ_H = 7.91 (1H, t, $^3J_{H\text{-}H}$ = 8 Hz, Hi), 7.83 (1H, d, $^3J_{H\text{-}H}$ = 8 Hz, $H_{h/j}$), 7.78 (2H, dd, $^3J_{H\text{-}H}$ = 8 Hz, $^4J_{H\text{-}F}$ = 5 Hz, H_m), 7.33 (1H, d, $^3J_{H\text{-}H}$ = 8 Hz, $H_{h/j}$), 7.16 (6H, m, Bn-*p*), 7.10 (9H, m, $H_{b,n}$, Bn-*m*), 7.04 (1H, m, C_e), 6.93 (1H, td, $^3J_{H\text{-}H}$ = $^3J_{H\text{-}F}$ = 8.5 Hz, $^4J_{H\text{-}H}$ = 2 Hz, H_d), 6.41 (6H, d, $^3J_{H\text{-}H}$ = 7.5 Hz, Bn-*o*), 3.94 (6H, d, $^2J_{H\text{-}H}$ = 13 Hz, $^3J_{H\text{-}Pt}$ = 11 Hz, Ph*CH*$_2$) ppm.

δ_C = 31.63 (d, $^1J_{C\text{-}P}$ = 32 Hz, $^2J_{C\text{-}Pt}$ = 26 Hz, Ph*CH*$_2$), 113.62 (d, $^2J_{C\text{-}F}$ = 20 Hz, C_d), 114.9562 (d, $^2J_{C\text{-}F}$ = 23 Hz, C_n), 119.26, (s, $C_{h/j}$), 122.35 (d, $^2J_{C\text{-}F}$ = 21 Hz, $^2J_{C\text{-}Pt}$ = 35 Hz, C_b), 126.66 (d, $^4J_{C\text{-}P}$ = 5 Hz, $C_{h/j}$), 127.65 (d, $^5J_{C\text{-}P}$ = 4 Hz, Bn-*p*), 128.90 (d, $^4J_{C\text{-}P}$ = 3 Hz, Bn-*m*), 130.03 (d, $^3J_{C\text{-}F}$ = 5 Hz, C_e), 131.07 (d, $^3J_{C\text{-}P}$ = 6.5 Hz, Bn-*o*), 131.73 (d, $^2J_{C\text{-}P}$ = 9.5 Hz, Bn-*i*), 132.36 (d, $^3J_{C\text{-}F}$ = 8 Hz, C_m), 130.60 (s, $C_{f/l}$), 139.97 (s, C_i), 140.89 ($C_{f/l}$), 141.36 (d, $^3J_{C\text{-}F}$ = 6 Hz, C_a), 161.75 (d, $^1J_{C\text{-}F}$ = 255 Hz, C_c), 163.47 (s, C_k), 163.93 (d, $^1J_{C\text{-}F}$ = 248 Hz, C_o), 164.31 (d, $^3J_{C\text{-}P}$ = 4 Hz, C_g) ppm.

δ_F = -107.92 ($^4J_{F\text{-}Pt}$ = 29.5 Hz), -111.26 ppm.

δ_P = 9.14 ($^1J_{P\text{-}Pt}$ = 2434 Hz) ppm.

δ_{Pt} = -1719 (d, $^1J_{Pt\text{-}P}$ = ~2450 Hz) ppm.

6.6.4. Synthesis of **Me-25(b)** and **Me26(b)**

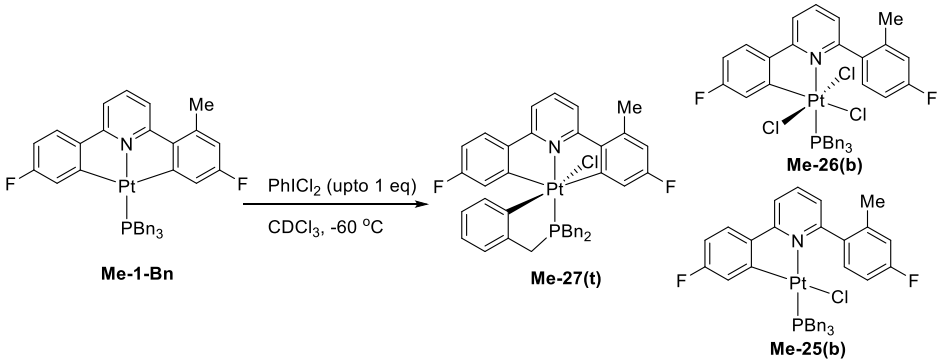

To a chloroform solution of **Me-1-Bn** (10 mg, 1.29 x 10^{-5} mol) was added $PhICl_2$ (1.8 mg, 6.43x 10^{-6} mol, 0.5eq) which gave a 50/50 mixture of **Me-27(t)** and **Me-25(b)**. The complexes were not physically separated, but the spectroscopic data acquired on pure **Me-**

27(t) allowed the identification of data from **Me-25(b)**. The addition of a further 0.5 eq of $PhICl_2$ gave an equivalent mixture of **Me-27(t)** and **Me-26(b)**.

Complex - **Me-25(b)**

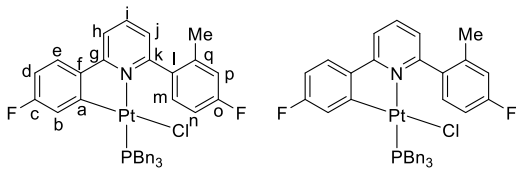

Data taken from a mixture

δ_H = 7.89 (1H, t, $^3J_{H\text{-}H}$ = 8 Hz, H_i), 7.70 (1H, d, $^3J_{H\text{-}H}$ = 8 Hz, $H_{h/j}$), 7.53 (1H, dd, $^3J_{H\text{-}H}$ = 8.5 Hz, $^4J_{H\text{-}F}$ = 5.5 Hz, H_m), 7.48 (1H, dd, $^3J_{H\text{-}H}$ = 8 Hz, $^4J_{H\text{-}F}$ = 5 Hz, H_e), 7.32 (6H, d, $^3J_{H\text{-}H}$ = 7.5 Hz, Bn-*o*), 7.30 (1H, d, $^3J_{H\text{-}H}$ = 8 Hz, $H_{h/j}$), 7.22 (9H, m, Bn-*m,p*), 7.01 (1H, dd, $^3J_{H\text{-}F}$ = 10 Hz, $^4J_{H\text{-}H}$ = 2.5 Hz, H_p), 6.92 (1H, td, $^3J_{H\text{-}H}$ = $^3J_{H\text{-}F}$ = 8.5 Hz, $^4J_{H\text{-}H}$ = 2.5 Hz, H_n), 6.67 (1H, td, $^3J_{H\text{-}H}$ = $^3J_{H\text{-}F}$ = 8 Hz, $^4J_{H\text{-}H}$ = 2 Hz, H_d), 6.42 (1H, dt, $^3J_{H\text{-}F}$ = 8.5 Hz, $^4J_{H\text{-}H}$ = $^4J_{H\text{-}P}$ = 2 Hz, $^3J_{H\text{-}Pt}$ = 54 Hz, H_b), 3.43 (6H, m, Ph*CH*$_2$), 2.61 (3H, s, Me) ppm.

δ_F = -110.96 ($^4J_{F\text{-}Pt}$ = 63 Hz), -112.78 ppm.

δ_P = -1.96 ($^1J_{P\text{-}Pt}$ = 4253 Hz) ppm.

δ_{Pt} = -3821 (d, $^1J_{Pt\text{-}P}$ = ~4300 Hz) ppm.

Complex - **Me-26(b)**

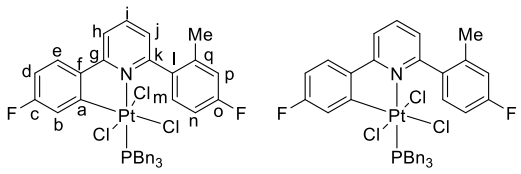

Data taken from a mixture

δ_H = 2.41 (3H, s, Me) ppm.

δ_F = -107.90 ($^4J_{F\text{-}Pt}$ = 63 Hz), -112.52 ppm.

δ_P = 7.50 ($^1J_{P\text{-}Pt}$ = 2432 Hz) ppm.

6.6.5. Synthesis of **27(c)** and **28**

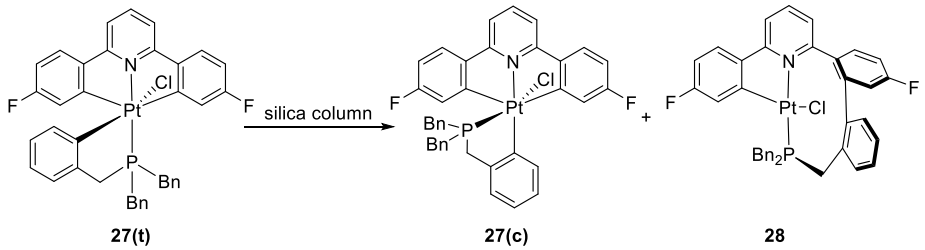

Solid complex **27(t)** (60 mg, 7.52 x 10^{-5} mol) was added to the top of a silica column and chloroform run through. After 20 column volumes of chloroform, the solvent system was changed to 40:60 EtOAC:hexane which cleanly eluted first **28** (yield 47 mg, 5.87 x 10^{-5} mol 78 %). This was then followed by 100:0 EtOAC:hexane, used to elute **27(c)** (yield 12 mg, 1.50 x 10^{-5} mol 20 %).

Complex - **27(c)**

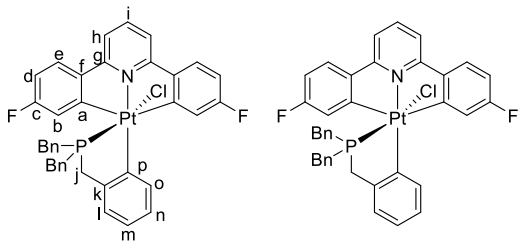

δ_H = 8.34 (1H, d, $^4J_{H\text{-}P}$ = 7.5 Hz, $^3J_{H\text{-}Pt}$ = 31 Hz, H_o), 7.84 (1H, t, $^3J_{H\text{-}H}$ = 8 Hz, H_i), 7.80 (2H, dd, $^3J_{H\text{-}H}$ = 8.5 Hz, $^4J_{H\text{-}F}$ = 5 Hz, H_e), 7.60 (2H, d, $^3J_{H\text{-}H}$ = 8 Hz, H_h), 7.27 (1H, m, $H_{l/m}$), 7.24 (2H, m, $H_{l/m}$), 7.15 (2H, t, $^3J_{H\text{-}H}$ = 7.5 Hz, Bn-*p*), 7.07 (4H, t, $^3J_{H\text{-}H}$ = 7.5 Hz, Bn-*m*), 7.02 (2H, dd, $^3J_{H\text{-}F}$ = 10.5 Hz, $^4J_{H\text{-}H}$ = 2.5 Hz, $^3J_{H\text{-}Pt}$ = ~20 Hz, H_b), 6.90 (2H, td, $^3J_{H\text{-}H}$ = $^3J_{H\text{-}F}$ = 8.5 Hz, $^4J_{H\text{-}H}$ = 2.5 Hz, H_d), 6.19 (4H, d, $^3J_{H\text{-}H}$ = 7.5 Hz, Bn-*o*), 2.97 (4H, m, Ph*CH*$_2$), 2.65 (2H, m, H_j) ppm.

δ_C = 29.40 (d, $^1J_{C\text{-}P}$ = 29 Hz, $^2J_{C\text{-}Pt}$ = 34 Hz, Ph*CH*$_2$), 34.42 (d, $^1J_{C\text{-}P}$ = 47 Hz, $^2J_{C\text{-}Pt}$ = 66 Hz, C_j), 112.16 (d, $^2J_{C\text{-}F}$ = 24 Hz, C_d), 116.72 (s, $^3J_{C\text{-}Pt}$ = 13 Hz, C_h), 121.66 (d, $^2J_{C\text{-}F}$ = 18 Hz, $^2J_{C\text{-}Pt}$ = 22 Hz, H_b), 125.37 (m, $C_{l/m,n}$), 127.59 (d, $^5J_{C\text{-}Pt}$ = 3 Hz, Bn-*p*), 128.26 (m, $C_{e,l/m}$), 128.23 (d, $^4J_{C\text{-}P}$ = 3 Hz, Bn-*m*), 129.43 (d, $^3J_{C\text{-}P}$ = 5 Hz, Bn-*o*), 131.16 (d, $^2J_{C\text{-}P}$ = 10 Hz, $^2J_{C\text{-}Pt}$ = 26 Hz, C_k), 136.00 (s, C_o), 138.09 (d, $^2J_{C\text{-}P}$ = 9 Hz, $^1J_{C\text{-}Pt}$ = 50 Hz, C_p), 140.07 (s, C_i), 140.57 (s, Bn-*i*), 143.73 (m, C_f), 161.45 (s, $^2J_{C\text{-}Pt}$ = 33 Hz, C_g), 161.68 (m, $^1J_{C\text{-}Pt}$ = 532 Hz, H_a), 164.13 (d, $^1J_{C\text{-}F}$ = 40 Hz, $^4J_{C\text{-}Pt}$ = 254 Hz, C_c) ppm.

δ_F = -108.14 ($^4J_{F\text{-}Pt}$ = 21 Hz) ppm.

δ_P = 29.00 ($^1J_{P\text{-}Pt}$ = 2692 Hz) ppm.

δ_{Pt} = -3114 (d, $^{1}J_{Pt\text{-}P}$ = ~2700 Hz) ppm.

HR-MS (ESI): found 762.1627 m/z, calculated 762.1594 m/z = $C_{38}H_{29}F_2NP^{194}Pt$ = $[M\text{-}Cl]^+$.

HR-MS (ESI): found 820.1213 m/z, calculated 820.1195 m/z = $C_{38}H_{29}F_2ClNP^{194}PtNa$ = $[M+Na]^+$.

Elemental analysis found (calculated.EtOAc): C 54.32 (56.86), H 4.59 (4.20), N 1.40 (1.58).

Complex - **28**

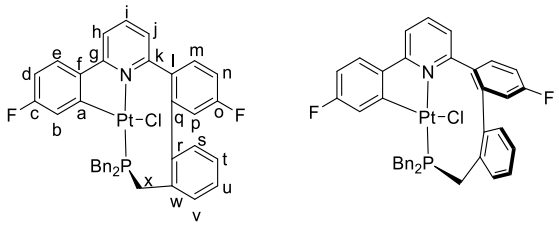

δ_H = 7.85 (1H, t, $^{3}H_{H\text{-}H}$ = 8 Hz, H_i), 7.72 (1H, dd, $^{3}J_{H\text{-}H}$ = 8.5 Hz, $^{4}J_{H\text{-}F}$ = 5.5 Hz, H_m), 7.48 (1H, d, $^{3}J_{H\text{-}H}$ = 8 Hz, H_h), 7.46 (1H, d, $^{3}J_{H\text{-}H}$ = 8 Hz, H_j), 7.35 (6H, m, H_e, Bn), 7.23 (6H, m, H_v, Bn'), 7.07 (1H, td, $^{3}J_{H\text{-}H}$ = $^{3}J_{H\text{-}F}$ = 8 Hz, $^{3}J_{H\text{-}H}$ = 2.5 Hz, H_n), 6.94 (1H, t, $^{3}J_{H\text{-}H}$ = 8 Hz, H_u), 6.88 (1H, dd, $^{3}J_{H\text{-}F}$ = 9.5 Hz, $^{4}J_{H\text{-}H}$ = 2.5 Hz, H_p), 6.68 (1H, t, $^{3}J_{H\text{-}H}$ = 8 Hz, H_t), 6.61 (1H, td, $^{3}J_{H\text{-}H}$ = $^{3}J_{H\text{-}F}$ = 8 Hz, $^{3}J_{H\text{-}H}$ = 2.5 Hz, H_d), 6.55 (1H, dt, $^{3}J_{H\text{-}F}$ = 10.5 Hz, $^{4}J_{H\text{-}H}$ = $^{4}J_{H\text{-}P}$ = 2.5 Hz, $^{3}J_{H\text{-}Pt}$ = ~60 Hz, H_b), 6.28 (1H, d, $^{3}J_{H\text{-}H}$ = 8 Hz, H_s), 4.12 (1H, dd, $^{2}J_{H\text{-}H}$ = 14 Hz, $^{2}J_{H\text{-}P}$ = 9 Hz, $H_{Bn'}$), 4.03 (1H, dd, $^{2}J_{H\text{-}H}$ = 13.5 Hz, $^{2}J_{H\text{-}P}$ = 11 Hz, H_x), 3.49 (1H, dd, $^{2}J_{H\text{-}H}$ = 15.5 Hz, $^{2}J_{H\text{-}P}$ = 8.5 Hz, H_{Bn}), 3.35 (2H, m, $H_{x,Bn}$), 3.09 (1H, t, $^{2}J_{H\text{-}P}$ = $^{2}J_{H\text{-}H}$ = 14 Hz, $H_{Bn'}$) ppm.

δ_C = 24.82 (d, $^{1}J_{C\text{-}P}$ = 20 Hz, C_{Bn}), 25.78 (d, $^{1}J_{C\text{-}P}$ = 30 Hz, $C_{Bn'}$), 33.33 (d, $^{1}J_{C\text{-}P}$ = 36 Hz, C_x), 110.12 (d, $^{2}J_{C\text{-}F}$ = 22.5 Hz, C_d), 113.60 (d, $^{2}J_{C\text{-}F}$ = 22.5 Hz, C_n), 116.59 (s, C_h), 118.00 (d, $^{2}J_{C\text{-}F}$ = 20 Hz, C_p), 121.78 (dd, $^{2}J_{C\text{-}F}$ = 19 Hz, $^{3}J_{C\text{-}P}$ = 5 Hz, C_b), 125.24 (m, $C_{j,e}$), 126.209 (d, $^{5}J_{C\text{-}P}$ = 4 Hz, C_t), 126.69 (d, $^{5}J_{C\text{-}P}$ = 3 Hz, Bn-*p*), 127.04 (d, $^{4}J_{C\text{-}P}$ = 3.5 Hz, C_u), 127.48 (s, Bn'-*p*), 128.44 (s, Bn-*m*), 129.00 (s, Bn'-*m*), 130.00 (d, $^{3}J_{C\text{-}P}$ = 7.5 Hz, Bn'-*o*), 130.10 (d, $^{3}J_{C\text{-}P}$ = 5 Hz, C_v), 130.42 (d, $^{3}J_{C\text{-}P}$ = 6 Hz, Bn-*o*), 131.47 (d, $^{4}J_{C\text{-}P}$ = 3.5 Hz, C_s), 133.09 (d, $^{2}J_{C\text{-}P}$ = 10 Hz, C_{Bn}), 133.54 (d, $^{2}J_{C\text{-}P}$ = 4.5 Hz, $C_{Bn'}$), 134.41 (d, $^{3}J_{C\text{-}F}$ = 9 Hz, C_m), 135.70 (m, C_l), 135.97 (d, $^{2}J_{C\text{-}P}$ = 3 Hz, C_w), 136.16 (s, C_i), 141.33 (d, $^{3}J_{C\text{-}P}$ = 5 Hz, C_r), 141.68 (s, C_f), 144.36 (d, $^{3}J_{C\text{-}F}$ = 8 Hz, C_q), 144.78 (dd, $^{3}J_{C\text{-}F}$ = 6 Hz, $^{2}J_{C\text{-}P}$ = 3.5 Hz,

C_a), 159.72 (s, C_k), 162.50 (dd, $^1J_{C\text{-}F}$ = 253 Hz, $^4J_{C\text{-}P}$ = 3.5 Hz, H_c), 163.03 (d, $^1J_{C\text{-}F}$ = 249 Hz, C_o), 163.30 (d, $^3J_{C\text{-}P}$ = 3.5 Hz, C_g) ppm.

δ_F = -110.38 ($^4J_{F\text{-}Pt}$ = 57 Hz), -112.08 ppm.

δ_P = -9.29 ($^1J_{P\text{-}Pt}$ = 4552 Hz) ppm.

δ_{Pt} = -3985 (d, $^1J_{Pt\text{-}P}$ = ~4500 Hz) ppm.

HR-MS (ESI): found 762.1622 m/z, calculated 762.1627 m/z = $C_{38}H_{29}F_2NP^{194}Pt$ = $[M\text{-}Cl]^+$.

Elemental analysis found (calculated.$CHCl_3$): C 52.10 (51.52), H 3.44 (3.46), N 1.51 (1.50).

Crystals suitable for X-ray analysis were grown by the slow evaporation of solvent from a chloroform solution – ps38.

6.6.6. Synthesis of **Me-27(c)**, **Me-28(a)** and **Me-28(b)**

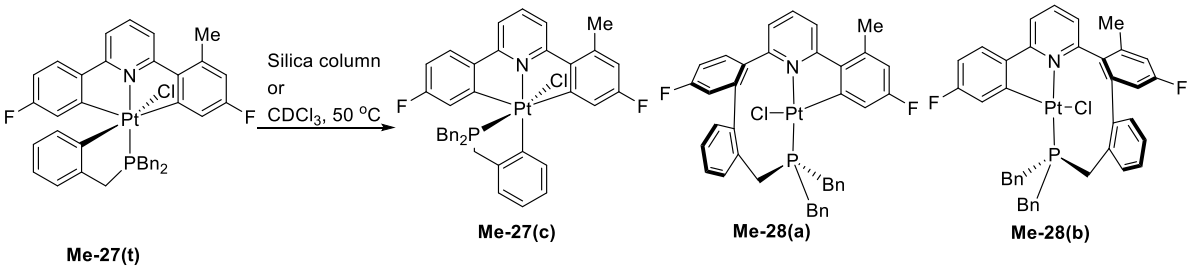

Me-27(t) **Me-27(c)** **Me-28(a)** **Me-28(b)**

Me-27(t) (20 mg, 2.46 x 10^{-5} mol) was dissolved in chloroform (5 ml) and heated to 50°C (5 days). The solvent was then removed, **Me-28(a)** and **Me-28(b)** extracted with acetone, leaving the less soluble **Me-27(c)**. **Me-27(c)** was purified by column chromatography on silica, loading with dichloromethane and eluting with EtOAc (yield 10 mg, 1.23 x 10^{-5} mol, 50%). **Me-28(a)** and **Me-28(b)** could not be separated from each other, but it was possible to separate their spectroscopic data.

Complex - **Me27(c)**

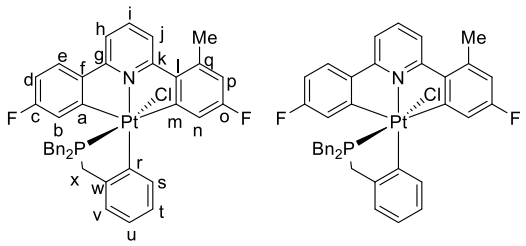

δ_H = 8.27 (1H, d, $^3J_{H\text{-}H}$ = 8 Hz, $^3J_{H\text{-}Pt}$ = 31.5 Hz, H_s), 7.80 (1H, d, $^3J_{H\text{-}H}$ = 8 Hz, H_j), 7.76 (1H, t, $^3J_{H\text{-}H}$ = 8 Hz, H_i), 7.73 (1H, dd, $^3J_{H\text{-}H}$ = 8 Hz, $^4J_{H\text{-}F}$ = 3 Hz, H_e), 7.56 (1H, d, $^3J_{H\text{-}H}$ = 8 Hz, H_h), 7.20 (1H, m, H_t), 7.14 (2H, m, $H_{u,v}$), 7.08 (2H, m, Bn-*p*), 7.00 (4H, m, Bn-*m*), 6.92 (1H, dd, $^3J_{H\text{-}F}$ = 8 Hz, $^4J_{H\text{-}H}$ = 2.5 Hz, $^3J_{H\text{-}Pt}$ = 22 Hz, H_b), 6.87 (1H, dd, $^3J_{H\text{-}F}$ = 7 Hz, $^4J_{H\text{-}H}$ = 2.5 Hz, $^3J_{H\text{-}Pt}$ = 24 Hz, H_n), 6.82 (1H, td, $^3J_{H\text{-}H}$ = $^3J_{H\text{-}F}$ = 8.5 Hz, $^4J_{H\text{-}H}$ = 2.5 Hz, H_d), 6.65 (1H, dd, $^3J_{H\text{-}F}$ = 9 Hz, $^4J_{H\text{-}H}$ = 2.5 Hz, H_p), 6.15 (2H, dd, $^3J_{H\text{-}H}$ = 7.5 Hz, Bn-*o*), 6.12 (2H, dd, $^3J_{H\text{-}H}$ = 7.5 Hz, Bn-*o*), 2.83 (4H, m, H_x, Ph*CH*$_2$), 2.69 (3H, s, Me) 2.56 (2H, m, Ph*CH*$_2$) ppm.

δ_C = 24.36 (s, Me), 29.27 (m, Ph*CH*$_2$), 34.38 (d, $^1J_{C\text{-}P}$ = 47 Hz, $^2J_{C\text{-}Pt}$ = 64 Hz, C_x), 112.08 (d, $^2J_{C\text{-}F}$ = 23 Hz, C_d), 116.13 (d, $^2J_{C\text{-}F}$ = 25 Hz, C_p), 116.51 (s, $^3J_{C\text{-}Pt}$ = 15 Hz, C_h), 119.24 (d, $^2J_{C\text{-}F}$ = 17 Hz, $^2J_{C\text{-}Pt}$ = 22 Hz, C_n), 120.58 (s, $^3J_{C\text{-}Pt}$ = 14.5 Hz, C_j), 121.50 (d, $^2J_{C\text{-}F}$ = 18 Hz, $^2J_{C\text{-}Pt}$ = 26 Hz, C_b), 125.27 (m, $C_{u,v}$), 127.56 (s, Bn-*p*), 128.31 (m, $C_{e,t}$), 128.91 (s, Bn-*m*), 129.41 (m, Bn-*o*), 131.24 (m, Bn-*i*), 136.04 (s, C_s), 138.15 (d, $^2J_{C\text{-}P}$ = 8 Hz, $^1J_{C\text{-}Pt}$ = 25.5 Hz, C_r), 139.83 (s, C_i), 141.20 (d, $^2J_{C\text{-}P}$ = 7 Hz, $^2J_{C\text{-}Pt}$ = 23 Hz, C_w), 141.43 (s, C_q), 142.32 (m , C_l), 143.80 (m, C_f), 162.06 (s, $^2J_{C\text{-}Pt}$ = 30 Hz, C_k), 162.35 (s, $^2J_{C\text{-}Pt}$ = 29.5 Hz, C_g), 162.59 (m, $^1J_{C\text{-}Pt}$ = 528 Hz, $C_{b/m}$), 162.73 (d, $^1J_{C\text{-}F}$ = 259 Hz, $^3J_{C\text{-}Pt}$ = 35 Hz, C_o), 163.23 (m, $^1J_{C\text{-}Pt}$ = 530 Hz, $C_{b/m}$), 164.04 (d, $^1J_{C\text{-}F}$ = 259 Hz, $^3J_{C\text{-}Pt}$ = 36 Hz, C_c) ppm.

δ_F = -108.24 ($^4J_{F\text{-}Pt}$ = 20 Hz), -110.53 ($^4J_{F\text{-}Pt}$ = 23 Hz) ppm.

δ_P = 29.06 ($^1J_{P\text{-}Pt}$ = 2723 Hz) ppm.

δ_{Pt} = -3120 (d, $^1J_{Pt\text{-}P}$ = ~3100 Hz) ppm.

HR-MS (ESI): found 776.1787 m/z, calculated 776.1784 m/z = $C_{39}H_{31}F_2PN^{194}Pt$ = $[M\text{-}Cl]^+$.

Elemental analysis found (calculated): C 52.75 (57.60), H 3.77 (3.84), N 1.72 (1.84).

Complex - **Me-28(a)**

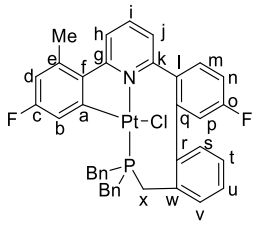

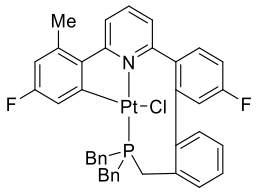

δ_H = 7.85 (1H, t, $^3J_{H\text{-}H}$ = 8 Hz, H_i), 7.68 (2H, m, $H_{h,m}$), 7.46 (1H, d, $^3J_{H\text{-}H}$ = 8 Hz, H_j), 7.34 (5H, m, Bn), 7.15 (6H, H_v, Bn), 7.07 (1H, td, $^3J_{H\text{-}H}$ = $^3J_{H\text{-}F}$ = 8.5 Hz, $^4J_{H\text{-}H}$ = Hz, H_n), 6.95 (1H, t, $^3J_{H\text{-}H}$ = 7.5 Hz, H_u), 6.87 (1H, dd, $^3J_{H\text{-}F}$ = 9.5 Hz, $^4J_{H\text{-}H}$ = 2.5 Hz, H_p), 6.70 (1H, t, $^3J_{H\text{-}H}$ = 7.5 Hz, H_t), 6.44 (1H, dd, $^3J_{H\text{-}F}$ = 9.5 Hz, $^4J_{H\text{-}H}$ = 2.5 Hz, H_d), 6.39 (1H, dt, $^3J_{H\text{-}F}$ = 9.5 Hz, $^4J_{H\text{-}H}$ = $^4J_{H\text{-}P}$ = 2.5 Hz, H_b), 6.29 (1H, d, $^3J_{H\text{-}H}$ = 7.5 Hz, H_s), 4.04 (2H, m, H_x, Ph*CH₂*)*, 3.48 (1H, dd, $^2J_{H\text{-}H}$ = 15.5 Hz, $^2J_{H\text{-}P}$ = 8 Hz, Ph*CH₂*), 3.30 (2H, m, H_x, Ph*CH₂*), 3.16 (1H, t, $^2J_{H\text{-}H}$ = $^2J_{H\text{-}P}$ = 14 Hz, Ph*CH₂*)*, 2.53 (3H, s, Me) ppm.

* Attached to the same carbon

δ_C = 23.87 (s, Me), 24.69 (d, $^1J_{C\text{-}P}$ = 21 Hz, Ph*CH₂*), 26.05 (d, $^1J_{C\text{-}P}$ = 28 Hz, Ph*CH₂*)*, 33.22 (d, $^1J_{C\text{-}P}$ = 37 Hz, C_x), 113.51 (d, $^2J_{C\text{-}F}$ = 23 Hz, C_d), 114.10 (d, $^2J_{C\text{-}F}$ = 22.5 Hz, C_n), 117.79 (d, $^2J_{C\text{-}F}$ = 22 Hz, C_p), 119.88(dd, $^2J_{C\text{-}F}$ = 19 Hz, $^3J_{C\text{-}P}$ = 6 Hz, C_b), 120.26 (s, C_h), 125.27 (s, C_j), 126.28 (d, $^5J_{C\text{-}P}$ = 4 Hz, C_t), 126.43 (d, $^5J_{C\text{-}P}$ = 2 Hz, Bn-*p*), 127.03 (d, $^4J_{C\text{-}P}$ = 3 Hz, C_u), 127.38 (m, Bn-*p*), 128.39 (s, Bn-*m*), 128.96 (s, Bn-*m*), 130.04 (m, Bn-*o*), 130.39 (m, C_v, Bn-*o*), 131.29 (d, $^4J_{C\text{-}P}$ = 3.5 Hz, C_s), 133.13 (d, $^3J_{C\text{-}F}$ = 9 Hz, C_m), 133.62 (m, Bn-*i*), 134.58 (d, $^3J_{C\text{-}F}$ = 8.5 Hz, C_m), 135.97 (m, $C_{l,w}$), 137.56 (s, C_i), 140.66 (s, C_r), 141.32 (m, C_f), 144.06 (d, $^3J_{C\text{-}F}$ = 8.5 Hz, C_q), 148.23 (m, C_a), 159.86 (s, C_k), 162.92 (d, $^1J_{C\text{-}F}$ = 249 Hz, C_o), 162.99 (d, $^1J_{C\text{-}F}$ = 246 Hz, $^4J_{C\text{-}P}$ = 5 Hz, C_c), 164.08 (s, C_g) ppm.

δ_F = -112.37, -113.51 ($^4J_{F\text{-}Pt}$ = 52 Hz) ppm.

δ_P = -8.22 ($^1J_{P\text{-}Pt}$ = 4527 Hz) ppm.

δ_{Pt} = -3439 (d, $^1J_{Pt\text{-}P}$ = ~4800 Hz) ppm.

Complex - **Me-28(b)**

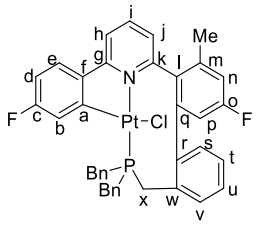

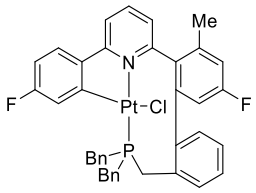

δ_H = 7.79 (1H, t, $^3J_{H\text{-}H}$ = 8 Hz, H_i), 7.44 (1H, d, $^3J_{H\text{-}H}$ = 8 Hz, H_h), 7.34 (7H, m, $H_{e,j}$, Bn), 7.15 (6H, m, H_v, Bn), 6.93 (1H, dd, $^3J_{H\text{-}F}$ = 9.5 Hz, $^4J_{H\text{-}H}$ = 2.5 Hz, H_n), 6.89 (1H, t, $^3J_{H\text{-}H}$ = 7.5 Hz, H_u), 6.69 (1H, dd, $^3J_{H\text{-}F}$ = 9.5 Hz, $^4J_{H\text{-}H}$ = 2.5 Hz, H_p), 6.66 (1H, t, $^3J_{H\text{-}H}$ = 7.5 Hz, H_t), 6.61 (1H, td, $^3J_{H\text{-}H}$ = $^3J_{H\text{-}F}$ = 8 Hz, $^4J_{H\text{-}H}$ = 2.5 Hz, H_d), 6.51 (1H, dt, $^3J_{H\text{-}F}$ = 10.5 Hz, $^4J_{H\text{-}H}$ = $^4J_{H\text{-}P}$ = 2.5 Hz, $^3J_{H\text{-}Pt}$ = ~28 Hz, H_b), 6.32 (1H, d, $^3J_{H\text{-}H}$ = 7.5 Hz, H_s), 4.25 (1H, dd, $^2J_{H\text{-}H}$ = 15 Hz, $^2J_{H\text{-}P}$ = 10 Hz, Ph*CH₂*)*, 3.96 (1H, dd, $^2J_{H\text{-}H}$ = 13 Hz, $^2J_{H\text{-}P}$ = 10.5 Hz, H_x), 3.37 (3H, m, H_x, Ph*CH₂*), 2.89 (1H, t, $^2J_{H\text{-}H}$ = $^2J_{H\text{-}P}$ = 15 Hz, Ph*CH₂*)*, 2.42 (3H, s, Me) ppm.

* Shows same carbon

δ_C = 22.38 (s, Me), 24.76 (d, $^1J_{C\text{-}P}$ = 21 Hz, Ph*CH₂*), 25.69 (d, $^1J_{C\text{-}P}$ = 28.5 Hz, Ph*CH₂*)*, 33.17 (d, $^1J_{C\text{-}P}$ = 35 Hz, C_x), 110.05 (d, $^2J_{C\text{-}F}$ = 24 Hz, C_d), 115.22 (d, $^2J_{C\text{-}F}$ = 21 Hz, C_p), 115.80 (d, $^2J_{C\text{-}F}$ = 22 Hz, C_n), 117.00 (s, C_h), 121.91 (dd, $^2J_{C\text{-}F}$ = 19 Hz, $^3J_{C\text{-}P}$ = 5 Hz, C_b), 125.02 (d, $^3J_{C\text{-}F}$ = 10 Hz, C_e), 125.82 (d, $^5J_{C\text{-}P}$ = 4 Hz, C_t), 126.82 (m, C_u, Bn-*p*), 127.40 (m, C_j Bn-*p*), 128.42 (s, Bn-*m*), 129.03 (s, Bn-*m*), 130.04 (d, $^3J_{C\text{-}P}$ = 7 Hz, Bn-*p*), 130.39 (d, $^3J_{C\text{-}P}$ = 5 Hz, Bn-*p*), 130.94 (m, $C_{s,v}$), 133.21 (d, $^3J_{C\text{-}F}$ = 11 Hz, C_m), 133.49 (m, Bn-*i*), 135.42 (s, C_l), 135.94 (s, C_w), 136.78 (s, C_i), 141.29 (s, C_r), 141.81 (m, C_f), 143.81 (d, $^3J_{C\text{-}F}$ = 9.5 Hz, C_q), 145.36 (m, C_a), 157.98 (s, C_k), 162.32 (d, $^1J_{C\text{-}F}$ = 249.5 Hz, C_o), 162.69 (d, $^1J_{C\text{-}F}$ = 254.5 Hz, $^4J_{C\text{-}P}$ = 5 Hz, C_c), 164.11 (s, C_g) ppm.

δ_F = -110.49 ($^4J_{F\text{-}Pt}$ = 53 Hz), -113.73 ppm.

δ_P = -6.91 ($^1J_{P\text{-}Pt}$ = 4622 Hz) ppm.

δ_{Pt} = -3466 (d, $^1J_{Pt\text{-}P}$ = ~4750 Hz) ppm.

HR-MS (ESI mixture): found 776.1781 m/z, calculated 776.1784 m/z = $C_{39}H_{31}F_2PN^{194}Pt$ = $[M\text{-}Cl]^+$.

6.6.7. Synthesis of **29**

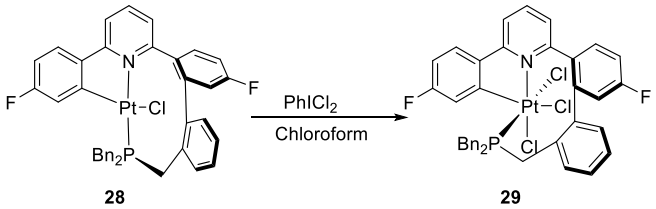

To a chloroform (1 ml) solution of **28** (10 mg, 1.25 x 10^{-5} mol) was added $PhICl_2$ (4 mg, 1.50 x 10^{-5} mol, 1.2 eq) at room temperature. The solvent was removed under vacuum, and the crude product washed with hexane (10.8 mg, 1.24 x 10^{-5} mol, 99%).

Complex - **29**

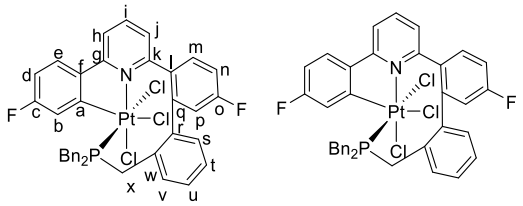

δ_H = 8.11 (1H, dd, $^3J_{H\text{-}H}$ = 9 Hz, $^4J_{H\text{-}F}$ = 5.5 Hz, H_m), 7.89 (1H, dd, $^3J_{H\text{-}F}$ = 9.5 Hz, $^4J_{H\text{-}H}$ = 2.5 Hz, $^3J_{H\text{-}Pt}$ = 23 Hz, H_b), 7.70 (1H, t, $^3J_{H\text{-}H}$ = 7.5 Hz, H_i), 7.40 (6H, m, $H_{e,h/j,n}$, Bn), 7.23 (2H, d, $^3J_{H\text{-}H}$ = Hz, Bn-*o*), 7.10 (4H, $H_{h/j}$, Bn), 6.96 (4H, m, $H_{d,t,u,v}$), 6.73 (1H, dd, $^3J_{H\text{-}F}$ = 9 Hz, $^4J_{H\text{-}H}$ = 2.5 Hz, H_q), 6.55 (1H, d, $^3J_{H\text{-}H}$ = 7 Hz, H_s), 6.34 (2H, d, $^3J_{H\text{-}H}$ = 8 Hz, Bn-*o*), 4.76 (1H, t, $^2J_{H\text{-}H}$ = $^2J_{H\text{-}P}$ = 15 Hz, Ph*CH₂*)*, 3.86 (1H, dd, $^2J_{H\text{-}H}$ = 16 Hz, $^2J_{H\text{-}P}$ = 9.5 Hz, Ph*CH₂*)*, 3.75 (1H, t, $^2J_{H\text{-}H}$ = $^2J_{H\text{-}P}$ = 14 Hz, H_x), 3.54 (1H, t, $^2J_{H\text{-}H}$ = $^2J_{H\text{-}P}$ = 15 Hz, Ph*CH₂*)**, 3.15 (1H, dd, $^2J_{H\text{-}H}$ = 15 Hz, $^2J_{H\text{-}P}$ = 11 Hz, Ph*CH₂*)**, 2.66 (1H, t, $^2J_{H\text{-}H}$ = $^2J_{H\text{-}P}$ = 14 Hz, H_x) ppm.

*,** protons attached to the same carbon.

δ_C = 26.69 (d, $^1J_{C\text{-}P}$ = 30 Hz, C_x), 30.04 (d, $^1J_{C\text{-}P}$ = 27 Hz, Ph*CH₂*), 31.62 (d, $^1J_{C\text{-}P}$ = 36 Hz, Ph*CH₂*), 114.25 (m, $C_{d,p}$), 115.24 (d, $^2J_{C\text{-}F}$ = 22.5 Hz, C_n), 118.33 (d, $^2J_{C\text{-}F}$ = 24.5 Hz, $^2J_{C\text{-}Pt}$ = 24.5 Hz, C_n), 126.87 (d, $^3J_{C\text{-}F}$ = 9.5 Hz, C_e), 127.07 (d, $^5J_{C\text{-}P}$ = 3 Hz, Bn-*p*), 127.30 (d, $^4J_{C\text{-}P}$ = 3 Hz, C_u), 127.93 (d, $^5J_{C\text{-}P}$ = 2.5 Hz, Bn-*p*), 128.35 (d, $^3J_{C\text{-}P}$ = 2.5 Hz, C_v), 128.47 (d, $^4J_{C\text{-}P}$ = 3.5 Hz, Bn-*m*), 129.27 (s, $^3J_{C\text{-}Pt}$ = 18 Hz, $C_{h/j}$), 129.69 (d, $^4J_{C\text{-}P}$ = 3.5 Hz, Bn-*m*), 130.26 (s, C_s), 130.62 (m, Bn-*o*), 130.94 (d, $^2J_{C\text{-}P}$ = 9.5 Hz, Bn-*i*), 131.60 (s, $C_{h/j}$), 131.90 (d, $^2J_{C\text{-}P}$ = 9.5 Hz, Bn-*i*), 133.48 (d, $^3J_{C\text{-}F}$ = 10 Hz, C_m), 135.82 (d, $^4J_{C\text{-}F}$ = 3.5 Hz, C_l), 138.68 (d, $^4J_{C\text{-}F}$ = 1.5 Hz, C_l), 139.00 (s, C_i), 140.51 (d, $^3J_{C\text{-}F}$ = 8 Hz, C_q), 140.74 (d, $^3J_{C\text{-}P}$ = 6 Hz, C_r), 141.44 (d, $^2J_{C\text{-}P}$ = 6.5 Hz, C_w), 162.42 (s, $C_{g/k}$), 162.47 (d, $^1J_{C\text{-}F}$ = 275.5 Hz, C_c), 163.07 (d, $^1J_{C\text{-}F}$ = 249.5 Hz, C_o), 165.05 (s, $C_{g/k}$) ppm.

δ_F = -103.68 ($^4J_{F\text{-}Pt}$ = 28.5 Hz), -111.13 ppm.

δ_P = -0.41 ($^1J_{P\text{-}Pt}$ = 2271 Hz) ppm.

δ_{Pt} (213 K) = -1902 (d, $^1J_{Pt\text{-}P}$ = ~2300 Hz) ppm.

Elemental analysis found (calculated): C 49.94 (52.46), H 3.12 (3.36), N 1.42 (1.61).

Crystals suitable for X-ray analysis were grown by the slow evaporation of solvent from a chloroform solution – ps39.

6.6.8. Synthesis of **30**

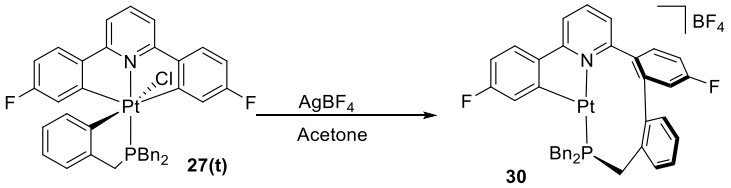

$AgBF_4$ (4.8 mg, 2.50 x 10^{-5} mol, 2eq) was added to a slurry of the complex **27(t)** (10 mg, 1.25 x 10^{-5} mol, 1eq) in acetone (0.6 ml). AgCl was removed by filtration, giving a clear, deep yellow solution of **30**.

Complex - **30**

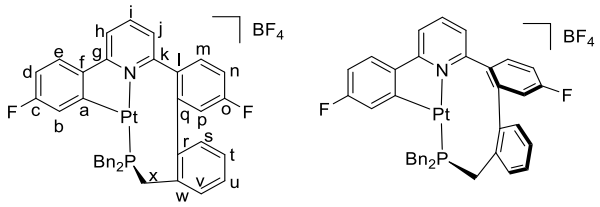

δ_H (Acetone-d_6) = 8.30 (1H, t, $^3J_{H\text{-}H}$ = 8 Hz, H_i), 8.01 (1H, d, $^3J_{H\text{-}H}$ = 8 Hz, H_h), 7.88 (1H, d, $^3J_{H\text{-}H}$ = 8 Hz, H_j), 7.76 (1H, dd, $^3J_{H\text{-}H}$ = 9 Hz, $^4J_{H\text{-}F}$ = 5.5 Hz, H_m), 7.73 (1H, dd, $^3J_{H\text{-}H}$ = 8.5 Hz, $^4J_{H\text{-}F}$ = 5.5 Hz, H_e), 7.60 (1H, d, $^3J_{H\text{-}H}$ = 7 Hz, H_v)*, 7.52 (2H, d, $^3J_{H\text{-}H}$ = 7 Hz, H_{Bn}), 7.39 (7H, m, $H_{u,n,Bn,Bn'}$), 7.23 (1H, dd, $^3J_{H\text{-}F}$ = 9.5 Hz, $^4J_{H\text{-}H}$ = 2.5 Hz, H_p), 7.22 (3H, m, $H_{Bn'}$), 7.17 (1H, t, $^3J_{H\text{-}H}$ = 8 Hz, H_t), 7.08 (1H, d, $^3J_{H\text{-}H}$ = 8 Hz, H_s), 6.87 (1H, td, $^3J_{H\text{-}H}$ = $^3J_{H\text{-}F}$ = 8.5 Hz, $^4J_{H\text{-}H}$ = 2.5 Hz, H_d), 6.46 (1H, dt, $^3J_{H\text{-}F}$ = 9 Hz, $^4J_{H\text{-}H}$ = $^4J_{H\text{-}P}$ = 2.5 Hz, $^3J_{H\text{-}Pt}$ = ~90 Hz, H_b)**, 4.32 (1H, dd, $^2J_{H\text{-}H}$ = 15 Hz, $^2J_{H\text{-}P}$ = 9.5 Hz, H_x), 3.98 (3H, m, $H_{x,Bn}$), 3.49 (2H, d, $^2J_{H\text{-}H}$ = 12.5 Hz, $H_{Bn'}$) ppm.

*At 298 K, irradiating this proton strongly affects Bn_{alkyl} protons, and weakly affects Bn'_{alkyl}, with no effect on H_x.

**At 298 K, irradiating this proton affects one H_x proton, and both Bn_{alkyl}, but no effect on Bn'_{alkyl} protons.

δ_C (Acetone-d_6) = 27.03 (d, $^1J_{C\text{-}P}$ = 25 Hz, C_{Bn}), 27.99 (d, $^1J_{C\text{-}P}$ = 27 Hz, $C_{Bn'}$), 28.90 (m, C_x), 112.56 (d, $^2J_{C\text{-}F}$ = 25 Hz, C_d), 116.60 (d, $^2J_{C\text{-}F}$ = 25 Hz, C_n), 118.37 (m, $C_{h,p}$), 123.00 (dd, $^2J_{C\text{-}F}$ = 21 Hz, $^3J_{C\text{-}P}$ = 6 Hz, H_b), 125.15 (s, C_j), 126.05 (m, C_a), 126.49 (d, $^3J_{C\text{-}F}$ = 9 Hz, C_e), 127.30 (d, $^5J_{C\text{-}P}$ = 3 Hz, $C_{Bn'}$), 127.77 (d, $^5J_{C\text{-}P}$ = 3 Hz, C_{Bn}), 128.37 (s, C_t), 128.63 (d, $^1J_{C\text{-}P}$ = 1.5 Hz, $C_{Bn'}$), 129.11 (d, $^1J_{C\text{-}P}$ = 1.5 Hz, C_{Bn}), 129.76 (d, $^3J_{C\text{-}P}$ = 7 Hz, $C_{Bn'}$), 129.96 (m, C_{Bn}), 130.57 (d, $^3J_{C\text{-}P}$ = 5 Hz, C_{Bn}), 130.89 (s, C_u), 131.80 (d, $^3J_{C\text{-}F}$ = 8 Hz, C_q), 132.18 (d, $^3J_{C\text{-}P}$ = 5 Hz, C_v), 132.83 (m, $C_{l,Bn}$), 134.63 (d, $^3J_{C\text{-}F}$ = 9.5 Hz, C_m), 135.31 (d, $^2J_{C\text{-}P}$ = 3.5 Hz, C_w), 136.53 (s, C_s), 139.27 (br s, C_r), 140.90 (s, C_f), 142.49 (s, C_i)158.66 (s, C_k), 160.71 (d, $^3J_{C\text{-}P}$ = 3 Hz, C_g), 161.56 (dd, $^1J_{C\text{-}F}$ = 255 Hz, $^4J_{C\text{-}P}$ = 5 Hz, C_c), 163.08 (d, $^1J_{C\text{-}F}$ = 250 Hz, C_o) ppm.

δ_F (Acetone-d_6) = -108.51 ($^4J_{F\text{-}Pt}$ = 65 Hz), -110.60 ppm.

δ_P (Acetone-d_6) = -9.49 ($^1J_{P\text{-}Pt}$ = 4119 Hz) ppm.

δ_{Pt} (Acetone-d_6) = -3612 (d, $^1J_{Pt\text{-}P}$ = ~4200 Hz) ppm.

HR-MS (ESI): found 762.1637 m/z, calculated 762.1627 m/z = $C_{38}H_{29}F_2NP^{194}Pt$ = $[M]^+$.

6.6.9. Synthesis of **Me-30(a)** and **Me-30(b)**

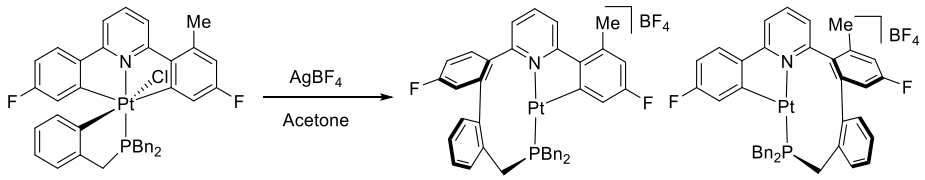

Me-27(t) **Me-30(a)** **Me-30(b)**

To a slurry of **Me-2(t)** (10 mg, 1.23 x 10^{-5} mol) in acetone (0.6 ml) was added $AgBF_4$ (3 mg, 1.48 x 10^{-5} mol, 1.2 eq). AgCl was removed by filtration, leaving a clear deep yellow solution of the two isomeric products.

Complex - **Me-30(a)**

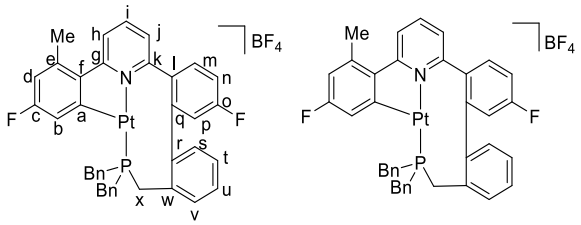

δ_H (Acetone-d_6) = 8.22 (1H, t, $^3J_{H\text{-}H}$ = 8 Hz, H_i), 7.97 (1H, d, $^3J_{H\text{-}H}$ = 8 Hz, $H_{h/j}$), 7.77 (1H, d, $^3J_{H\text{-}H}$ = 8 Hz, $H_{h/j}$), 7.51 (1H, dd, $^3J_{H\text{-}H}$ = 8.5 Hz, $^4J_{H\text{-}F}$ = 5.5 Hz, H_m), 7.27 (H_n), 6.63 (1H, dd, $^3J_{H\text{-}F}$ = 9.5 Hz, $^4J_{H\text{-}H}$ = 3 Hz, H_d), 6.19 (1H, m, $^3J_{H\text{-}Pt}$ = 110 Hz, H_b), 2.53 (3H, s, Me) ppm.

δ_F (Acetone-d_6) = -109.64, -110.18 ($^4J_{F\text{-}Pt}$ = 72 Hz) ppm.

δ_P (Acetone-d_6) = -7.73 ($^1J_{P\text{-}Pt}$ = 4043 Hz) ppm.

δ_{Pt} (Acetone-d_6) = -3632 (d, $^1J_{Pt\text{-}P}$ = ~4050 Hz) ppm.

Complex - **Me-30(b)**

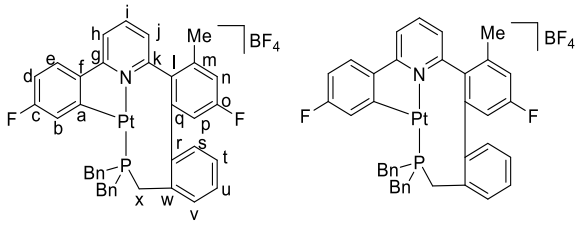

δ_H (Acetone-d_6) = 8.15 (1H, t, $^3J_{H\text{-}H}$ = 8 Hz, H_i), 7.91 (1H, d, $^3J_{H\text{-}H}$ = 8 Hz, $H_{h/j}$), 7.76 (1H, d, $^3J_{H\text{-}H}$ = 8 Hz, $H_{h/j}$), 7.51 (1H, dd, $^3J_{H\text{-}H}$ = 8.5 Hz, $^4J_{H\text{-}F}$ = 5.5 Hz, H_m), 7.47 (1H, d, $^3J_{H\text{-}H}$ = 8 Hz, H_v), 7.27 (H_n), 6.84 (1H, t, $^3J_{H\text{-}H}$ = 7.5 Hz, H_t), 6.76 (1H, td, $^3J_{H\text{-}H}$ = $^3J_{H\text{-}F}$ = 8.5 Hz, $^4J_{H\text{-}H}$ = 2.5 Hz, H_d), 6.58 (2H, m, $H_{b,s}$) 2.32 (3H, s, Me) ppm.

δ_F (Acetone-d_6) = -109.95 ($^4J_{F\text{-}Pt}$ = 63 Hz), -112.68 ppm.

δ_P (Acetone-d_6) = -0.55 ($^1J_{P\text{-}Pt}$ = 4463 Hz) ppm.

δ_{Pt} (Acetone-d_6) = -3478 (d, $^1J_{Pt\text{-}P}$ = ~4450 Hz) ppm.

HR-MS (ESI mixture): found 776.1788 m/z, calculated 776.1784 m/z = $C_{39}H_{31}F_2PN^{194}Pt$ = $[M]^+$.

6.6.10. Synthesis of **31**

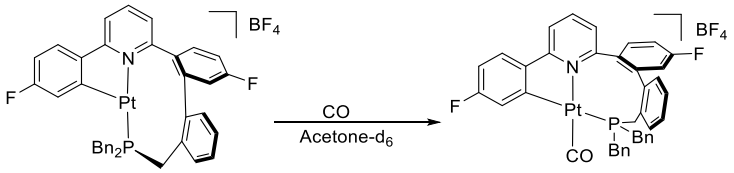

Complex **30** was dissolved in acetone (0.6 ml) in an NMR tube with a J Young valve. The solvent was then frozen by immersion in liquid nitrogen, and the air atmosphere then removed by vacuum. The atmosphere was replaced with CO gas, the tube sealed, and then the solvent was allowed to thaw. The yellow solution became almost colourless within one minute indicating the reaction was complete.

Complex - **31**

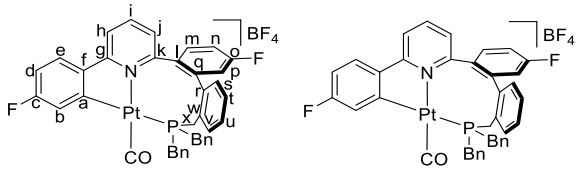

δ_H (Acetone-d_6) = 8.00 (2H, m, $H_{e,h}$), 7.96 (1H, t, $^3J_{H\text{-}H}$ = 8 Hz, H_i), 7.71 (1H, d, $^3J_{H\text{-}H}$ = 7.5 Hz, H_s), 7.50 (1H, dd, $^3J_{H\text{-}H}$ = 5.5 Hz, $^4J_{H\text{-}F}$ = 8.5 Hz, H_m), 7.39 (1H, t, $^3J_{H\text{-}H}$ = 7 Hz, H_t), 7.26 (7H, m, $H_{j,n,u,v}$, Bn-*m*,*p*), 7.19 (1H,dd, $^3J_{H\text{-}F}$ = 9 Hz, $^4J_{H\text{-}H}$ = 2.5 Hz, H_p), 7.14 (1H, td, $^3J_{H\text{-}F}$ = $^4J_{H\text{-}P}$ = 8 Hz, $^4J_{H\text{-}H}$ = 2.5 Hz, H_b), 7.08 (5H, m, H_d, Bn-*o*), 7.02 (1H, t, $^3J_{H\text{-}H}$ = 7.5 Hz, Bn-*p*), 6.91 (2H, t, $^3J_{H\text{-}H}$ = 7.5 Hz, Bn-*m*), 3.66 (2H, d, $^2J_{H\text{-}P}$ = 10 Hz, $^3J_{H\text{-}Pt}$ = 15 Hz, Ph*CH*$_2$), 3.53 (1H, dd, $^2J_{H\text{-}H}$ = 14 Hz, $^2J_{H\text{-}P}$ = 6.5 Hz, Ph*CH*$_2$)*, 3.41 (1H, t, $^2J_{H\text{-}H}$ = $^2J_{H\text{-}P}$ = 14.5 Hz, H_x)**, 3.36 (1H, dd, $^2J_{H\text{-}H}$ = 14 Hz, $^2J_{H\text{-}P}$ = 12 Hz, Ph*CH*$_2$)*, 3.04 (1H, dd, $^2J_{H\text{-}H}$ = 14.5 Hz, $^2J_{H\text{-}P}$ = 11 Hz, H_x)** ppm. *,** Coupled protons.

δ_C (Acetone-d_6) = 33.55 (d, $^1J_{C\text{-}P}$ = 18 Hz, C_x), 34.47 (d, $^1J_{C\text{-}P}$ = 23.5 Hz, Ph*CH*$_2$), 36.29 (d, $^1J_{C\text{-}P}$ = 25.5 Hz, Ph*CH*$_2$), 114.10 (d, $^2J_{C\text{-}F}$ = 21 Hz, C_d), 116.06 (d, $^2J_{C\text{-}F}$ = 21 Hz, C_n), 117.40 (d, $^2J_{C\text{-}F}$ = 24.5 Hz, C_p), 119.37 (s, $^3J_{H\text{-}Pt}$ = 35 Hz, C_h), 122.43 (d, $^2J_{C\text{-}F}$ = 21 Hz, $^2J_{C\text{-}Pt}$ = 98 Hz, C_n), 126.91 (s, $^3J_{H\text{-}Pt}$ = 24.5 Hz, C_j), 127.72 (m, C_t, Bn-*p*), 128.21 (dd, $^3J_{C\text{-}F}$ = 8.5 Hz, $^4J_{C\text{-}P}$ = 6 Hz, C_e), 128.83 (s, Bn-*m*), 129.18 (s, C_u), 129.38 (s, Bn-*m*), 129.84 (d, $^3J_{C\text{-}P}$ = 6.5 Hz, Bn-*o*), 130.27 (s, C_s), 130.49 (d, $^3J_{C\text{-}P}$ = 4.5 Hz, Bn-*o*), 131.61 (d, $^2J_{C\text{-}P}$ = 6 Hz, Bn-*i*), 132.09 (d, $^3J_{C\text{-}P}$ = 6 Hz, C_v), 132.20 (d, $^3J_{C\text{-}P}$ = 6 Hz, C_r), 133.11 (d, $^2J_{C\text{-}P}$ = 4 Hz, Bn-*i*), 135.26 (d, $^3J_{C\text{-}F}$ = 9 Hz, C_m), 135.53 (s, C_l), 138.81 (s, C_w), 140.63 (d, $^3J_{C\text{-}F}$ = 9 Hz, C_q), 140.94 (s, C_f), 141.88 (s, C_i), 158.37 (dd, $^2J_{C\text{-}P}$ = 95 Hz, $^3J_{C\text{-}F}$ = 5 Hz, C_a), 161.35

(d, $^{3}J_{C\text{-}P}$ = 5 Hz, C_g), 162.84 (d, $^{1}J_{C\text{-}F}$ = 255 Hz, $^{4}J_{C\text{-}P}$ = 10.5 Hz, C_c), 163.60 (d, $^{2}J_{C\text{-}P}$ = 9 Hz, CO), 163.78 (d, $^{1}J_{C\text{-}F}$ = 254 Hz, C_o), 165.73 (d, $^{3}J_{C\text{-}P}$ = 4 Hz, C_k) ppm.

δ_F (Acetone-d_6) = -105.85, -109.55 (d, $^{5}J_{F\text{-}P}$ = 5.5 Hz, $^{4}J_{F\text{-}Pt}$ = 36 Hz) ppm.

δ_P (Acetone-d_6) = 11.50 (d, $^{5}J_{P\text{-}F}$ = 5.5 Hz, $^{1}J_{P\text{-}Pt}$ = 1694 Hz) ppm.

δ_{Pt} (Acetone-d_6) = -3976 (d, $^{1}J_{Pt\text{-}P}$ = ~1700 Hz) ppm.

HR-MS (ESI): found 762.1606m/z, calculated 762.1627m/z = $C_{38}H_{29}F_2PN^{194}Pt$ =$[M\text{-}CO]^+$.

HR-MS (ESI): found 790.1560 m/z, calculated 790.1576 m/z = $C_{39}H_{29}F_2PNO^{194}Pt$ = $[M]^+$.

IR solid: 2097 cm^{-1} (CO stretch).

6.6.11. Synthesis of **32**

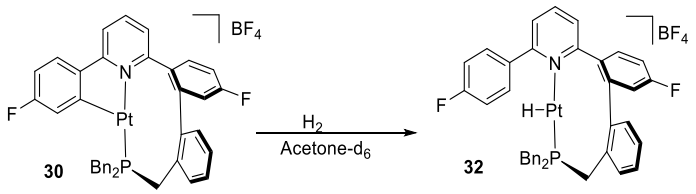

Complex **30** was dissolved in acetone (0.6 ml) in an NMR tube with a J Young valve. The solvent was then frozen by immersion in liquid nitrogen, and the atmosphere removed with vacuum. The atmosphere was replaced with H_2 gas, the tube sealed, and then the solvent allowed to thaw. The yellow solution became almost colourless within one minute indicating the reaction was complete.

Complex - **32**

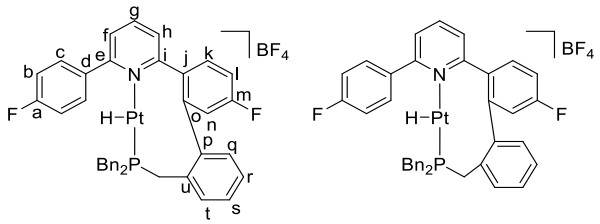

δ_H (Acetone-d_6) = 8.02 (1H, t, $^{3}J_{H\text{-}H}$ = 8.5 Hz, H_g), 7.58 (3H, m, $H_{h,k,t}$), 7.36 (1H, d, $^{3}J_{H\text{-}H}$ = 8.5 Hz, H_f), 7.29 (1H, t, $^{3}J_{H\text{-}H}$ = 8.5 Hz, H_s), 7.20 (2H, t, $^{3}J_{H\text{-}H}$ = $^{3}J_{H\text{-}F}$ = 9 Hz, H_b), 7.06 (8H, m, $H_{c,l}$, Bn-*m*,*p*), 6.96 (1H, t, $^{3}J_{H\text{-}H}$ = 7 Hz, H_r), 6.90 (2H, t, $^{3}J_{H\text{-}H}$ = 7 Hz, Bn-*o*), 6.84 (1H, m, H_n), 6.78 (2H, t, $^{3}J_{H\text{-}H}$ = 6 Hz, Bn-*o*), 6.49 (1H, t, $^{3}J_{H\text{-}H}$ = 8 Hz, H_n), 3.74 (1H, m, H_v), 3.35 (3H, m, H_v, PhCH_2), 2.40 (1H, dd, $^{2}J_{H\text{-}P}$ = 13 Hz, $^{2}J_{H\text{-}H}$ = 11 Hz, PhCH_2), -24.34 (1H, m, $^{1}J_{H\text{-}Pt}$ = 1230 Hz, PtH) ppm.

δ_C (Acetone-d_6) = 29.04 (m, C_v), 35.01 (d, $^{1}J_{C\text{-}P}$ = Hz, PhCH_2), 37.88 (m, PhCH_2), 115.18 (d, $^{2}J_{C\text{-}F}$ = 19.5 Hz, C_l), 115.77 (d, $^{2}J_{C\text{-}F}$ = 24 Hz, C_b), 116.70 (d, $^{2}J_{C\text{-}F}$ = 26 Hz, C_n), 125.46

(m, C_f), 126.62 (m, C_h), 126.80 (d, $^5J_{C-P}$ = 2 Hz, Bn-*p*), 126.87 (d, $^5J_{C-P}$ = 3 Hz, Bn-*p*), 127.13 (m, C_r), 128.13 (d, $^4J_{C-P}$ = 2 Hz, Bn-*m*), 128.31 (m, C_s, Bn-*m*), 129.82 (d, $^3J_{C-P}$ = 5 Hz, Bn-*o*), 130.26 (d, $^4J_{C-P}$ = 3 Hz, C_q), 130.51 (d, $^3J_{C-P}$ = 6 Hz, Bn-*o*), 130.76 (d, $^3J_{C-P}$ = 4.5 Hz, C_t), 131.01 (d, $^3J_{C-F}$ = 9.5 Hz, C_k), 131.31 (d, $^3J_{C-F}$ = 9 Hz, C_c), 132.60 (m, C_j), 132.78 (d, $^2J_{C-P}$ = 6.5 Hz, Bn-*i*), 133.23 (d, $^2J_{C-P}$ = 6 Hz, Bn-*i*), 136.08 (m, C_d), 136.38 (d, $^3J_{C-P}$ = 3.5 Hz, C_p), 131.71 (m, C_u), 139.85 (s, C_g), 141.37 (d, $^3J_{C-F}$ = 8.5 Hz, C_o), 160.27 (s, C_i), 160.82 (s, C_e), 162.42 (d, $^1J_{C-F}$ = 248 Hz, H_m), 163.41 (d, $^1J_{C-F}$ = 247 Hz, H_a) ppm.

δ_F (Acetone-d_6) = -110.40, -112.62 ppm.

δ_P (Acetone-d_6) = 1.31 ($^1J_{P-Pt}$ = 5015 Hz) ppm.

δ_{Pt} (Acetone-d_6) = -4419 (dd, $^1J_{Pt-P}$ = ~5000 Hz, $^1J_{Pt-H}$ = ~1500 Hz) ppm.

HR-MS (ESI): found 764.1772 m/z, calculated 764.1784 m/z = $C_{38}H_{31}F_2PN^{194}Pt$ = $[M]^+$.

6.6.12. Synthesis of **33**

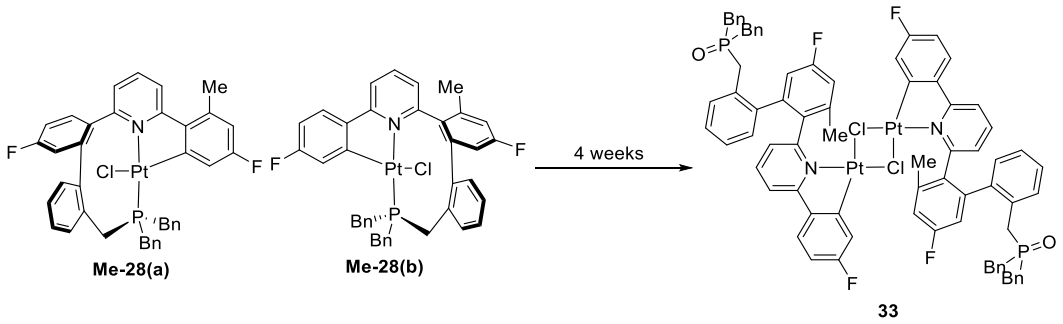

A solution of **a-Me-7** and **b-Me-7** in chloroform was left to stand for 4 weeks, after which crystals suitable for X-ray analysis formed – ps40

Complex - **33**

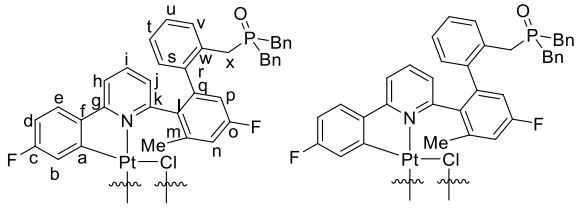

δ_H = 7.74 (1H, t, $^3J_{H-H}$ = 7 Hz, H_i), 6.99 (4H, d, $^3J_{H-H}$ = 7.5 Hz, Bn-*o*), 6.67 (1H, td, $^3J_{H-H}$ = $^3J_{H-F}$ = 8.5 Hz, $^4J_{H-H}$ = 2 Hz, H_d), 1.95 (3H, s, Me) ppm.

δ_F = -108.83 ($^4J_{F-Pt}$ = 49 Hz), -112.66 ppm.

δ_P = 59.78 ppm.

7.0 References

1 S. J. McLain, C. D. Wood, L. W. Messerle, R. R. Schrock, F. J. Hollander, W. J. Youngs and M. R. Churchill, *J. Am. Chem. Soc.*, 1978, **99**, 5962–5964.

2 R. R. Schrock, *J. Am. Chem. Soc.*, 1976, **98**, 5399–5400.

3 E. O. Fischer, G. Kreis, C. G. Kreiter, J. Müller, G. Huttner and H. Lorenz, *Angew. Chem. Int. Ed.*, 1973, **85**, 618–620.

4 W. C. Zeise, *Annu. Rev. Phys. Chem.*, 1831, **97**, 497.

5 G. Stephan, C. Näther, G. Peters and F. Tuczek, *Inorg. Chem.*, 2013, **52**, 5931–5942.

6 G. B. Kauffman, *J. Chem. Educ.*, 1983, **60**, 185–186.

7 T. J. Kealy and P. L. Paulson, *Nature*, 1951, **168**, 1039–1040.

8 J. D. Dunitz and L. E. Orgel, *Nature*, 1953, **171**, 121–122.

9 R. Noyori, T. Ohkuma, M. Kitamura, H. Takaya, N. Sayo, H. Kumobayashi and S. Akutagawa, *J. Am. Chem. Soc.*, 1987, **109**, 5856–5858.

10 J. A. Labinger, *Organometallics*, 2015, **34**, 4784–4795.

11 J. Halpern, *Acc. Chem. Res.*, 1970, **3**, 386–392.

12 M. P. Brown, R. J. Puddephatt and C. E. E. Upton, *J. Chem. Soc. Dalton Trans.*, 1974, **22**, 2457–2465.

13 J. F. Hartwig, *Organotransition Metal Chemistry: From Bonding to Catalysis*, University Science Books, Mill Valley, California, 2009.

14 N. Miyaura, K. Yamada and A. Suzuki, *Tetrahedron Lett.*, 1979, **20**, 3437–3440.

15 A. Suzuki, *Angew. Chem. Int. Ed.*, 2011, **50**, 6723–6733.

16 J. P. Nolley and R. F. Heck, *J. Org. Chem.*, 1972, **37**, 2320–2322.

17 C. C. C. Johansson Seechurn, M. O. Kitching, T. J. Colacot and V. Snieckus, *Angew. Chem. Int. Ed.*, 2012, **51**, 5062–5085.

18 M. Crespo, M. Martínez, S. M. Nabavizadeh and M. Rashidi, *Coord. Chem. Rev.*, 2014, **279**, 115–140.

19 J. R. Khusnutdinova, L. L. Newman, P. Y. Zavalij, Y. F. Lam and A. N.

Vedernikov, *J. Am. Chem. Soc.*, 2008, **130**, 2174–2175.

20 B. S. Williams, A. W. Holland and K. I. Goldberg, *J. Am. Chem. Soc.*, 1999, **121**, 252–253.

21 L. Abis, A. Senn and J. Halpern, *J. Am. Chem. Soc.*, 1978, **100**, 2915–2916.

22 K. Tatsumi, R. Hoffmann, A. Yamamoto and J. K. Stille, *Bull. Chem. Soc. Jpn.*, 1981, **54**, 1857–1867.

23 T. A. Albright, J. K. Burdett and M.-H. Whangbo, *Orbital Interactions in Chemistry*, Wiley and Sons Inc, New York, 2nd edn., 1885.

24 D. M. Crumpton-Bregel and K. I. Goldberg, *J. Am. Chem. Soc.*, 2003, **125**, 9442–9456.

25 J. B. Gary and M. S. Sanford, *Organometallics*, 2011, **30**, 6143–6149.

26 M. H. Pérez-Temprano, J. M. Racowski, J. W. Kampf and M. S. Sanford, *J. Am. Chem. Soc.*, 2014, **136**, 4097–4100.

27 M. J. Geier, M. Dadkhah Aseman and M. R. Gagne, *Organometallics*, 2014, **33**, 4353–4356.

28 C. M. Norris, J. L. Templeton, C. Hill and N. Carolina, *Organometallics*, 2004, **23**, 3101–3104.

29 R. J. Puddephatt, *Angew. Chem. Int. Ed.*, 2002, **41**, 261–263.

30 U. Fekl, W. Kaminsky and K. I. Goldberg, *J. Am. Chem. Soc.*, 2001, **123**, 6423–6424.

31 M. Rosello-Merino, O. Rivada-Wheelaghan, M. A. OrtuNo, P. Vidossich, J. Diez, A. Lledos and S. Conejero, *Organometallics*, 2014, **33**, 3746–3756.

32 R. H. Crabtree, *Chem. Rev.*, 2016, **116**, 8750–8769.

33 G. J. Kubas, R. R. Ryan, B. I. Swanson, P. J. Vergamini and H. J. Wasserman, *J. Am. Chem. Soc.*, 1984, **106**, 451–452.

34 G. J. Kubas, *J. Organomet. Chem.*, 2014, **751**, 33–49.

35 R. G. Pearson, *Inorg. Chem.*, 1973, **12**, 712–713.

36 L. Vaska and J. W. DiLuzio, *J. Am. Chem. Soc.*, 1962, **84**, 679–680.

37 S. J. Blanksby and G. B. Ellison, *Acc. Chem. Res.*, 2003, **36**, 255–263.

38 2017, 2017.

39 J. F. Hartwig, *J. Am. Chem. Soc.*, 2016, **138**, 2–24.

40 A. E. Shilov and G. B. Shul'pin, *Activation And Catalytic Reactions of Saturated Hydrocarbons in the Presence of Metal Complexes*, Kluwer Academic Publishers, Boston, 2000.

41 J. A. Labinger and J. E. Bercaw, *Nature*, 2002, **417**, 507–514.

42 M. Lersch and M. Tilset, *Chem. Rev.*, 2005, **105**, 2471–2526.

43 A. E. Shilov and G. B. Shul'pin, *Chem. Rev.*, 1997, **97**, 2879–2932.

44 B. A. Arndtsen, R. G. Bergman, T. A. Mobley and T. H. Peterson, *Acc. Chem. Res.*, 1995, **28**, 154–162.

45 G. R. Newkome, W. E. Puckett, V. K. Gupta and G. E. Kiefer, *Chem. Rev.*, 1986, **86**, 451–489.

46 R. H. Crabtree, *Chem. Rev.*, 1995, **95**, 987–1007.

47 A. D. Ryabov, *Chem. Rev.*, 1990, **90**, 403–424.

48 C. Hall and R. N. Perutz, *Chem. Rev.*, 1996, **96**, 3125–3146.

49 R. D. Young, *Chem-Eur. J.*, 2014, **20**, 12704–12718.

50 S. A. Macgregor and A. S. Weller, *Science*, 2012, **337**, 1648–1652.

51 A. I. McKay, T. Krämer, N. H. Rees, A. L. Thompson, K. E. Christensen, S. A. Macgregor and A. S. Weller, *Organometallics*, 2017, **36**, 22–25.

52 S. D. Pike, F. M. Chadwick, N. H. Rees, M. P. Scott, A. S. Weller, T. Krämer and S. A. Macgregor, *J. Am. Chem. Soc.*, 2015, **137**, 820–833.

53 F. M. Chadwick, N. H. Rees, A. S. Weller, T. Kramer, M. Iannuzzi and S. A. Macgregor, *Angew. Chem. Int. Ed.*, 2016, **55**, 3677–3681.

54 I. Castro-Rodriguez, H. Nakai, P. Gantzel, L. N. Zakharov, A. L. Rheingold and K. Meyer, *J. Am. Chem. Soc.*, 2003, **125**, 15734–15735.

55 D. R. Evans, T. Drovetskaya, R. Bau, C. A. Reed and P. D. W. Boyd, *J. Am. Chem. Soc.*, 1997, **119**, 3633–3634.

56 D. J. Lawes, S. Geftakis and G. E. Ball, *J. Am. Chem. Soc.*, 2005, **127**, 4134–4135.

57 S. E. Bromberg, H. Yang, M. C. Asplund, T. Lian, B. K. McNamara, K. T. Kotz, J. S. Yeston, M. Wilkens, H. Frei, R. G. Bergman and C. B. Harris, *Science*, 1997, **278**, 260–263.

58 D. J. Lawes, T. A. Darwish, T. Clark, J. B. Harper and G. E. Ball, *Angew. Chem. Int. Ed.*, 2006, **45**, 4486–4490.

59 T. Lian, S. E. Bromberg, H. Yang, G. Proulx, R. G. Bergman and C. B. Harris, *J. Am. Chem. Soc.*, 1996, **118**, 3769–3770.

60 A. H. Janowicz and R. G. Bergman, *J. Am. Chem. Soc.*, 1982, **104**, 352–354.

61 I. a I. Mkhalid, J. H. Barnard, T. B. Marder, J. M. Murphy and J. F. Hartwig, *Chem. Rev.*, 2009, **110**, 890–931.

62 J. I. Ito, T. Kaneda and H. Nishiyama, *Organometallics*, 2012, **31**, 4442–4449.

63 D. Lapointe and K. Fagnou, *Chem. Lett.*, 2010, **39**, 1118–1126.

64 D. R. Pahls, K. E. Allen, K. I. Goldberg and T. R. Cundari, *Organometallics*, 2014, **33**, 6413–6419.

65 K. E. Allen, D. M. Heinekey, A. S. Goldman and K. I. Goldberg, *Organometallics*, 2013, **32**, 1579–1582.

66 K. E. Allen, D. M. Heinekey, A. S. Goldman and K. I. Goldberg, *Organometallics*, 2014, **33**, 1337–1340.

67 J. Chatt and J. M. Davidson, *J. Chem. Soc.*, 1965, **111**, 843–855.

68 J. R. Sweet and W. A. G. Graham, *Organometallics*, 1983, **2**, 135–140.

69 W. D. Harman, M. Sekine and H. Taube, *J. Am. Chem. Soc.*, 1988, **110**, 5725–5731.

70 R. M. Chin, L. Dong, S. B. Duckett and W. D. Jones, *Organometallics*, 1992, **11**, 871–876.

71 W. D. Harman and H. Taube, *J. Am. Chem. Soc.*, 1988, **110**, 7555–7557.

72 M. Brookhart and M. L. H. Green, *J. Organomet. Chem.*, 1983, **250**, 395–408.

73 M. Brookhart, M. L. H. Green and G. Parkin, *Proc. Natl. Acad. Sci. U. S. A.*, 2007, **104**, 6908–6914.

74 S. J. La Placa and J. A. Ibers, *Inorg. Chem.*, 1965, **4**, 778–783.

75 Y. W. Yared, S. L. Miles, R. Bau and C. A. Reed, *J. Am. Chem. Soc.*, 1977, **99**, 7076–7078.

76 N. A. Bailey, J. M. Jenkins, R. Mason and B. L. Shaw, *Chem. Commun.*, 1965, **11**, 237–238.

77 R. F. Jordan, P. K. Bradley, N. C. Baenziger and R. E. Lapointe, *J. Am. Chem. Soc.*,

1990, **112**, 1289–1291.

78 R. H. Grubbs and G. W. Coates, *Acc. Chem. Res.*, 1996, **29**, 85–93.

79 W. Scherer, A. C. Dunbar, J. E. Barquera-Lozada, D. Schmitz, G. Eickerling, D. Kratzert, D. Stalke, A. Lanza, P. Macchi, N. P. M. Casati, J. Ebad-Allah and C. Kuntscher, *Angew. Chem. Int. Ed.*, 2015, **54**, 2505–2509.

80 I. Omae, *Coord. Chem. Rev.*, 2016, **310**, 154–169.

81 S. I. Gorelsky, D. Lapointe and K. Fagnou, *J. Am. Chem. Soc.*, 2008, **130**, 10848–10849.

82 A. McNally, B. Haffemayer, B. S. L. Collins and M. J. Gaunt, *Nature*, 2014, **510**, 129–133.

83 A. C. Cope and R. W. Siekman, *J. Am. Chem. Soc.*, 1965, **87**, 3272–3273.

84 B. J. Burke and L. E. Overman, *J. Am. Chem. Soc.*, 2004, **126**, 16820–16833.

85 G. Aullón, M. Crespo, M. Font-Bardia, J. Jover, M. Martinez and J. Pike, *Dalton Trans.*, 2015, **44**, 17968–17979.

86 M. M. Mdleleni, J. S. Bridgewater, R. J. Watts and P. C. Ford, *Inorg. Chem.*, 1995, **23**, 2334–2342.

87 A. Maleckis, J. W. Kampf and M. S. Sanford, *J. Am. Chem. Soc.*, 2013, **135**, 6618–6625.

88 G. B. Caygill and P. J. Steel, *J. Organomet. Chem.*, 1987, **327**, 115–123.

89 M. Nonoyama and H. Takayanagi, *Transit. Metal. Chem.*, 1975, **1**, 10–15.

90 D. V Howe and T. Keating, *J. Am. Chem. Soc.*, 1968, **90**, 404–410.

91 A. Kasahara, *Bull. Chem. Soc. Jpn.*, 1968, **41**, 1272.

92 L. Chassot, E. Mueller and A. Von Zelewsky, *Inorg. Chem.*, 1984, **23**, 4249–4253.

93 D. Sandrini, M. Maestri, V. Balzani, L. Chassot and A. Von Zelewsky, *J. Am. Chem. Soc.*, 1987, **109**, 7720–7724.

94 A. von Zelewsky, A. P. Suckling and H. Stoeckli-Evans, *Inorg. Chem.*, 1993, **32**, 4585–4593.

95 S. W. Thomas, K. Venkatesan, P. Müller and T. M. Swager, *J. Am. Chem. Soc.*, 2006, **128**, 16641–16648.

96 N. M. Mews, A. Berkefeld, G. Hörner and H. Schubert, *J. Am. Chem. Soc.*, 2017,

139, 2808–2815.

97 M. Hebenbrock, L. Stegemann, J. Kösters, N. L. Doltsinis, J. Müller and C. A. Strassert, *Dalton Trans.*, 2017, **46**, 3160–3169.

98 L. Zhang, L. Tian, M. Li, R. He and W. Shen, *Dalton Trans.*, 2014, **43**, 6500–6512.

99 S. Reinartz, M. Brookhart and J. L. Templeton, *Organometallics*, 2002, **21**, 247–249.

100 M. Albrecht, R. A. Gossage, U. Frey, A. W. Ehlers, E. J. Baerends, A. E. Merbach and G. Van Koten, *Inorg. Chem.*, 2001, **40**, 850–855.

101 M. Serratrice, L. Maiore, A. Zucca, S. Stoccoro, I. Landini, E. Mini, L. Massai, G. Ferraro, A. Merlino, L. Messori and M. A. Cinellu, *Dalton Trans.*, 2016, **45**, 579–590.

102 J. Ruiz, C. Vicente, C. De Haro and A. Espinosa, *Inorg. Chem.*, 2011, **50**, 2151–2158.

103 H. Schmidbaur and A. Schier, *Organometallics*, 2010, **29**, 2–23.

104 D. A. Roşca, D. A. Smith and M. Bochmann, *Chem. Commun.*, 2012, **48**, 7247–7249.

105 N. Savjani, D. A. Roşca, M. Schormann and M. Bochmann, *Angew. Chem. Int. Ed.*, 2013, **52**, 874–877.

106 D. A. Rosca, J. Fernandez-Cestau, D. L. Hughes and M. Bochmann, *Organometallics*, 2015, **34**, 2098–2101.

107 M. Kriechbaum, D. Otte, M. List and U. Monkowius, *Dalton Trans.*, 2014, **43**, 8781–8791.

108 M. Joost, A. Amgoune and D. Bourissou, *Angew. Chem. Int. Ed.*, 2015, **54**, 15022–15045.

109 L. C. Leitch, *Can. J. Chem.*, 1954, **32**, 813–814.

110 R. J. Hodges and J. L. Garnett, *J. Catal.*, 1969, **98**, 83–98.

111 J. L. Garnett and R. J. Hodges, *J. Chem. Soc. Chem. Commun.*, 1967, 1001–1003.

112 J. L. Garnett and W. A. Sollich, *Aust. J. Chem.*, 1961, **14(3)**, 441–448.

113 W. G. Brown and J. L. Garnett, *J. Am. Chem. Soc.*, 1958, **80**, 5272–5274.

114 R. H. Crabtree, *J. Organomet. Chem.*, 2015, **793**, 41–46.

115 A. A. Shteinman, *J. Organomet. Chem.*, 2015, **793**, 34–40.

116 P. F. Richardson, C. K. Chang and J. Fajer, *J. Am. Chem. Soc.*, 1979, **101**, 7738–7740.

117 M. J. Burk, R. H. Crabtree and D. V. McGrath, *J. Chem. Soc. Chem. Commun.*, 1985, **5**, 1829–1830.

118 W. D. Jones, *Acc. Chem. Res.*, 2003, **36**, 140–146.

119 D. G. Churchill, K. E. Janak, J. S. Wittenberg and G. Parkin, *J. Am. Chem. Soc.*, 2003, **125**, 1403–1420.

120 V. Uni, S. M. Kloek and K. I. Goldberg, *J. Am. Chem. Soc.*, 2007, **9**, 3460–3461.

121 U. Fekl and K. I. Goldberg, *J. Am. Chem. Soc.*, 2002, **124**, 6804–6805.

122 G. A. Luinstra, L. Wang, S. S. Stahl, J. A. Labinger and J. E. Bercaw, *J. Organomet. Chem.*, 1995, **504**, 75–91.

123 G. A. Luinstra, L. Wang, S. S. Stahl, J. A. Labinger and J. E. Bercaw, *Organometallics*, 1994, **13**, 755–756.

124 V. V Rostovtsev, J. A. Labinger, J. E. Bercaw, T. L. Lasseter and K. I. Goldberg, *Organometallics*, 1998, **17**, 4530–4531.

125 V. V Rostovtsev, L. M. Henling, J. A. Labinger and J. E. Bercaw, *Inorg. Chem.*, 2002, **41**, 3608–3619.

126 K. Thorshaug, I. Fjeldahl, C. Rømming and M. Tilset, *Dalton Trans.*, 2003, **2**, 4051–4056.

127 P. Murray, K. R. Koch and R. van Eldik, *Dalton Trans.*, 2014, **43**, 6308–6314.

128 D. R. Weinberg, J. A. Labinger and J. E. Bercaw, *Organometallics*, 2007, **26**, 167–172.

129 R. A. Periana, D. J. Taube, S. Gamble, H. Taube, T. Satoh and H. Fujii, *Science*, 1998, **280**, 560–564.

130 T. Zimmermann, M. Soorholtz, M. Bilke and F. Schuth, *J. Am. Chem. Soc.*, 2016, **138**, 12395–12400.

131 J. L. Look, U. Fekl and K. I. Goldberg, *ACS Sym. Ser.*, 2004, **17**, 283–302.

132 J. A. Labinger and J. E. Bercaw, *J. Organomet. Chem.*, 2015, **793**, 47–53.

133 B. S. Williams and K. I. Goldberg, *J. Am. Chem. Soc.*, 2001, **123**, 2576–2587.

134 M. L. Scheuermann, A. T. Luedtke, S. K. Hanson, U. Fekl, W. Kaminsky and K. I. Goldberg, *Organometallics*, 2013, **32**, 4752–4758.

135 A. V. Sberegaeva, W. Liu, R. J. Nielsen, W. a Goddard and A. N. Vedernikov, *J. Am. Chem. Soc.*, 2014, **136**, 4761–4768.

136 D. Devarajan, N. Gunsalus, D. H. Ess and R. a Periana, *Nature*, 2014, **343**, 1232–1237.

137 C. Liu, N. Han, X. Song and J. Qiu, *Eur. J. Org. Chem.*, 2010, **2010**, 5548–5551.

138 G. W. V Cave, N. W. Alcock and J. P. Rourke, *Organometallics*, 1999, **18**, 1801–1803.

139 G. W. V Cave, F. P. Fanizzi, R. J. Deeth, W. Errington and J. P. Rourke, *Organometallics*, 2000, **19**, 1355–1364.

140 C. P. Newman, G. W. V. Cave, M. Wong, W. Errington, N. W. Alcock and J. P. Rourke, *J. Chem. Soc. Dalton Trans.*, 2001, **18**, 2678–2682.

141 P. A. Shaw, J. M. Phillips, C. P. Newman, G. J. Clarkson and J. P. Rourke, *Chem. Commun.*, 2015, **51**, 8365–8368.

142 S. H. Crosby, G. J. Clarkson and J. P. Rourke, *J. Am. Chem. Soc.*, 2009, **131**, 14142–14143.

143 H. R. Thomas, R. J. Deeth, G. J. Clarkson and J. P. Rourke, *Organometallics*, 2011, **30**, 5641–5648.

144 B. M. Still, P. G. A. Kumar, J. R. Aldrich-Wright and W. S. Price, *Chem. Soc. Rev.*, 2007, **36**, 665–686.

145 S. H. Crosby, G. J. Clarkson, R. J. Deeth and J. P. Rourke, *Organometallics*, 2010, **29**, 1966–1976.

146 J. Forniés, A. Martín, R. Navarro, V. Sicilia and P. Villarroya, *Organometallics*, 1996, **15**, 1826–1833.

147 L. Rendina and R. Puddephatt, *Chem. Rev.*, 1997, **97**, 1735–1754.

148 J. Vicente, J. A. Abad, E. Martinez-Viviente and P. G. Jones, *Organometallics*, 2002, **21**, 4454–4467.

149 J. M. Phillips, University of Warwick, 2013.

150 P. A. Shaw, J. M. Phillips, G. J. Clarkson and J. P. Rourke, *Dalton Trans.*, 2016, **45**, 11397–11406.

151 H. Tan, University of Warwick, 2009.

152 O. Mitsunobu and M. Yamada, *Bull. Chem. Soc. Jpn.*, 1967, **40**, 2380–2382.

153 C. a Tolman, *Chem. Rev.*, 1977, **77**, 313–348.

154 S. Hietkamp, D. J. Stufkens and K. Vrieze, *J. Organomet. Chem.*, 1979, **169**, 107–113.

155 O. Rivada-Wheelaghan, M. Rosello-Merino, J. Diez, C. Maya, J. Lopez-Serrano and S. Conejero, *Organometallics*, 2014, **33**, 5944–5947.

156 T. L. Lohr, W. E. Piers, M. J. Sgro and M. Parvez, *Dalton Trans.*, 2014, **43**, 13858–13864.

157 P. A. Shaw, G. J. Clarkson and J. P. Rourke, *J. Organomet. Chem.*, 2017, **851**, 115–121.

158 S. H. Crosby, G. J. Clarkson and J. P. Rourke, *Organometallics*, 2012, **31**, 7256–7263.

159 J. K. Jawad and R. J. Puddephatt, *J. Organomet. Chem.*, 1976, **117**, 297–302.

160 J. K. Jawad and R. J. Puddephatt, *J. Chem. Soc. Dalton Trans.*, 1976, 1466–1469.

161 G. Ferguson, P. K. Monaghan, M. Parvez and R. J. Puddephatt, *Organometallics*, 1985, **4**, 1669–1674.

162 K. I. Goldberg, J. Yan and E. M. Breitung, *J. Am. Chem. Soc.*, 1995, **117**, 6889–6896.

163 G. S. Hill, G. P. A. Yap and R. J. Puddephatt, *Organometallics*, 1999, **18**, 1408–1418.

164 D. M. Crumpton and K. I. Goldberg, *J. Chem. Soc. Chem. Commun.*, 2000, **122**, 962–963.

165 P. A. Shaw, G. J. Clarkson and J. P. Rourke, *Organometallics*, 2016, **35**, 3751–3762.

166 A. Ariafard, Z. Ejehi, H. Sadrara, T. Mehrabi, S. Etaati, A. Moradzadeh, M. Moshtaghi, H. Nosrati, N. J. Brookes and B. F. Yates, *Organometallics*, 2011, **30**, 422–432.

167 A. Zucca, L. Maidich, L. Canu, G. L. Petretto, S. Stoccoro, M. A. Cinellu, G. J. Clarkson and J. P. Rourke, *Chem-Eur. J.*, 2014, **20**, 5501–5510.

168 L. Maidich, A. Zucca, G. J. Clarkson and J. P. Rourke, *Organometallics*, 2013, **32**, 3371–3375.

169 E. G. Bowes, S. Pal and J. A. Love, *J. Am. Chem. Soc.*, 2015, **137**, 16004–16007.

170 L. H. Sommer and W. D. Korte, *J. Org. Chem.*, 1970, **35**, 22–25.

171 M. Crespo, C. M. Anderson, N. Kfoury, M. Font-Bardía and T. Calvet, *Organometallics*, 2012, **31**, 4401–4404.

172 B. L. Madison, S. B. Thyme, S. Keene and B. S. Williams, *J. Chem. Soc. Chem. Commun.*, 2007, **129**, 9538–9539.

173 S. H. Crosby, G. J. Clarkson and J. P. Rourke, *Organometallics*, 2011, **30**, 3603–3609.

174 P. A. Shaw and J. P. Rourke, *Dalton Trans.*, 2017, **46**, 4768–4776.

175 E. Abada, P. Y. Zavalij and A. N. Vedernikov, *J. Am. Chem. Soc.*, 2017, **139**, 643–646.

176 H. Luo, H. Liu, C. Xingwei, K. Wang, X. Luo and K. Wang, *Chem. Commun.*, 2016, **53**, 956–958.

177 J. M. Racowski, N. D. Ball and M. S. Sanford, *J. Am. Chem. Soc.*, 2011, **133**, 18022–18025.

178 S. R. Whitfield and M. S. Sanford, *Organometallics*, 2008, **27**, 1683–1689.

179 S. R. Whitfield and M. S. Sanford, *J. Am. Chem. Soc.*, 2007, **129**, 15142–15143.

180 R. Corbo, D. C. Georgiou, D. J. D. Wilson and J. L. Dutton, *Inorg. Chem.*, 2014, **53**, 1690–1698.

181 N. Wang, T. M. McCormick, S. Ko and S. Wang, *Eur. J. Inorg. Chem.*, 2012, **28**, 4463–4469.

182 J. Mamtora, S. H. Crosby, C. P. Newman, G. J. Clarkson and J. P. Rourke, *Organometallics*, 2008, **27**, 5559–5565.

183 S. Fornarini and M. E. Crestoni, *Acc. Chem. Res.*, 1998, **31**, 827–834.

184 J. A. Bilbrey, A. H. Kazez, J. Locklin and W. D. Allen, *J. Comput. Chem.*, 2013, **34**, 1189–1197.

185 P. A. Shaw, G. J. Clarkson and J. P. Rourke, *Chem. Sci.*, 2017, **8**, 5547–5558.

186 M. Etienne and A. S. Weller, *Chem. Soc. Rev.*, 2014, **43**, 242–259.

187 S. Pal, S. Kusumoto and K. Nozaki, *Organometallics*, 2017, **2**, 502–505.

188 J. Dobson, P. C. Keller and R. Schaeffer, *J. Am. Chem. Soc.*, 1965, **87**, 3523–3524.

189 R. T. Taylor and T. A. Stevenson, *Tetrahedron Lett.*, 1988, **29**, 2033–2036.

190 O. V. Dolomanov, L. J. Bourhis, R. J. Gildea, J. A. K. Howard and H. Puschmann, *J. Appl. Crystallogr.*, 2009, **42**, 339–341.

191 G. M. Sheldrick, *Acta Crystallogr. A.*, 2008, **64**, 112–122.

8.0 Appendix

8.1. Crystal Data

8.1.1. Lookup Table for Crystal Data

Complex	Crystal name	CCDC identifier
3-Bu(t)	ps1	GUFLAW
3-Bu(c)	ps2	GUFKUP
7-Bu(c)	ps8	GUFLEA
1-Pr	ps9	
3-Pr(c)	ps10	
7-Pr(c)	ps17	
1-Tol	ps7	
3-Tol(c)	ps27	
6-Tol(t)	ps23	
9-Pr(t)	ps20	YAMGUR
9-Bu(c)	ps5	YAMHAY
15	ps18	
Me-13-Pr-I	ps25	YAMHEC
Me-13-Bu-I	ps35	YAMHIG
Me-1-Pr	ps19	YAMHOM
Me-1-Bn	ps32	JASVUX
Me2-13-Pr-I	ps37	YAMHUS
1-Bn	ps28	JASWEI
27(t)	ps29	JASWAE
25	ps34	JASWIM
28	ps38	JASWOS
29	ps39	JASWUY
33	ps40	JASWUX

Crystal structure determination of [ps1] GUFLAW

Crystal Data for $C_{59}H_{73}Cl_7F_4N_2P_2Pt_2$ (M =1586.46): monoclinic, space group $P2_1/c$ (no. 14), a = 42.5003(7) Å, b = 8.95573(17) Å, c = 15.7762(2) Å, β = 92.9490(14)°, V = 5996.83(17) Å^3, Z = 4, T = 150(2) K, μ(MoKα) = 5.078 mm^{-1}, *Dcalc* = 1.757 g/mm^3, 39740 reflections measured (6.28 ≤ 2Θ ≤ 61.63), 17255 unique (R_{int} = 0.0280, R_{sigma} = 0.0383) which were used in all calculations. The final R_1 was 0.0365 (I > 2σ(I)) and wR_2 was 0.0647 (all data).

Crystal structure determination of [ps2] GUFKUP

Crystal Data for $C_{29}H_{36}Cl_2F_2NPPt$ (M =733.55): orthorhombic, space group Pbca (no. 61), a = 14.9738(3) Å, b = 15.8809(4) Å, c = 24.6498(8) Å, V = 5861.7(3) Å^3, Z = 8, T = 150(2) K, μ(MoKα) = 5.056 mm^{-1}, *Dcalc* = 1.662 g/mm^3, 45707 reflections measured (6.016 ≤ 2Θ ≤ 62.336), 8857 unique (R_{int} = 0.0416, R_{sigma} = 0.0326) which were used in all calculations. The final R_1 was 0.0309 (I > 2σ(I)) and wR_2 was 0.0611 (all data).

Crystal structure determination of [ps5] YAMHAY

Crystal Data for $C_{29.83585}H_{38.50755}F_2I_{1.16415}NPPt$ (M =822.94 g/mol): monoclinic, space group $P2_1/n$ (no. 14), a = 10.2169(2) Å, b = 17.8558(4) Å, c = 16.3344(3) Å, β = 94.465(2)°, V = 2970.86(10) Å^3, Z = 4, T = 150(2) K, μ(MoKα) = 6.018 mm^{-1}, *Dcalc* = 1.840 g/cm^3, 34078 reflections measured (7.026° ≤ 2Θ ≤ 63.038°), 9117 unique (R_{int} = 0.0301, R_{sigma} = 0.0294) which were used in all calculations. The final R_1 was 0.0271 (I > 2σ(I)) and wR_2 was 0.0609 (all data).

Crystal structure determination of [ps7]

Crystal Data for $C_{39}H_{31}Cl_3F_2NPPt$ (M =884.06 g/mol): monoclinic, space group C2/c (no. 15), a = 36.4648(9) Å, b = 8.3932(2) Å, c = 23.2143(7) Å, β = 104.094(3)°, V = 6891.0(3) Å^3, Z = 8, T = 150(2) K, μ(MoKα) = 4.392 mm^{-1}, *Dcalc* = 1.704 g/cm^3, 27581 reflections measured (6.52° ≤ 2Θ ≤ 62.596°), 10276 unique (R_{int} = 0.0389, R_{sigma} = 0.0503) which were used in all calculations. The final R_1 was 0.0321 (I > 2σ(I)) and wR_2 was 0.0677 (all data).

Crystal structure determination of [ps8n] GUFLEA

Crystal Data for $C_{29}H_{36}Cl_2F_2NPPt$ (M =733.55 g/mol): orthorhombic, space group $Pna2_1$ (no. 33), a = 17.9634(6) Å, b = 13.9987(4) Å, c = 11.0698(4) Å, V = 2783.66(16) Å^3, Z = 4, T = 150(2) K, μ(MoKα) = 5.323 mm^{-1}, *Dcalc* = 1.750 g/cm^3, 19220 reflections measured (5.388° ≤ 2Θ ≤ 61.502°), 7402 unique (R_{int} = 0.0514, R_{sigma} = 0.0719) which were used in all calculations. The final R_1 was 0.0406 (I > 2σ(I)) and wR_2 was 0.0771 (all data).

Crystal structure determination of [ps9]

Crystal Data for $C_{26}H_{30}F_2NPPt$ (M =620.57 g/mol): triclinic, space group P-1 (no. 2), a = 8.97222(14) Å, b = 9.20765(17) Å, c = 15.2259(3) Å, α = 106.6101(16)°, β = 92.0547(13)°, γ = 106.6725(15)°, V = 1145.14(4) Å^3, Z = 2, T = 150(2) K, μ(MoKα) = 6.226 mm^{-1}, *Dcalc* = 1.800 g/cm^3, 34899 reflections measured (5.912° ≤ 2Θ ≤ 64.608°), 7678 unique (R_{int} = 0.0356, R_{sigma} = 0.0310) which were used in all calculations. The final R_1 was 0.0194 (I > 2σ(I)) and wR_2 was 0.0428 (all data).

Crystal structure determination of [ps10]

Crystal Data for $C_{26}H_{30}Cl_2F_2NPPt$ (M =691.47 g/mol): orthorhombic, space group $Pna2_1$ (no. 33), a = 18.3851(2) Å, b = 12.6327(2) Å, c = 11.03420(10) Å, V = 2562.73(5) Å^3, Z = 4, T = 150(2) K, μ(MoKα) = 5.776 mm^{-1}, *Dcalc* = 1.792 g/cm^3, 31888 reflections measured (6.45° ≤ 2Θ ≤ 61.444°), 7234 unique (R_{int} = 0.0386, R_{sigma} = 0.0346) which were used in all calculations. The final R_1 was 0.0223 (I > 2σ(I)) and wR_2 was 0.0412 (all data).

Crystal structure determination of [ps17]

Crystal Data for $C_{29.5}H_{34}Cl_2F_2NPPt$ (M =737.53 g/mol): orthorhombic, space group Aea2 (no. 41), a = 18.2105(2) Å, b = 17.91980(10) Å, c = 17.59350(10) Å, V = 5741.26(8) Å^3, Z = 8, T = 150(2) K, μ(CuKα) = 11.649 mm^{-1}, *Dcalc* = 1.707 g/cm^3, 16968 reflections measured (8.554° ≤ 2Θ ≤ 157.898°), 4983 unique (R_{int} = 0.0365, R_{sigma} = 0.0447) which were used in all calculations. The final R_1 was 0.0264 (I > 2σ(I)) and wR_2 was 0.0656 (all data).

Crystal structure determination of [ps18]

Crystal Data for $C_{27}H_{31}Br_2Cl_3F_2NPPt$ (M =899.76 g/mol): monoclinic, space group $P2_1/n$ (no. 14), a = 19.1246(6) Å, b = 8.5345(2) Å, c = 19.3830(5) Å, β = 108.604(3)°, V = 2998.35(15) Å^3, Z = 4, T = 150(2) K, μ(MoKα) = 7.697 mm^{-1}, *Dcalc* = 1.993 g/cm^3, 24104 reflections measured (5.264° ≤ 2Θ ≤ 61.344°), 8335 unique (R_{int} = 0.0259, R_{sigma} = 0.0298) which were used in all calculations. The final R_1 was 0.0331 (I > 2σ(I)) and wR_2 was 0.1177 (all data).

Crystal structure determination of [ps19] YAMHOM

Crystal Data for $C_{27}H_{32}F_2NPPt$ (M =634.59 g/mol): monoclinic, space group $P2_1/c$ (no. 14), a = 9.9623(3) Å, b = 9.2215(3) Å, c = 27.2996(8) Å, β = 100.217(3)°, V = 2468.17(14) Å^3, Z = 4, T = 150(2) K, μ(MoKα) = 5.780 mm^{-1}, *Dcalc* = 1.708 g/cm^3, 24451 reflections measured (4.688° ≤ 2Θ ≤ 65.326°), 8370 unique (R_{int} = 0.0602, R_{sigma} = 0.0681) which were used in all calculations. The final R_1 was 0.0535 (I > 2σ(I)) and wR_2 was 0.1525 (all data).

Crystal structure determination of [ps20] YAMGUR

Crystal Data for $C_{27}H_{33}F_2INPPt$ (M =762.50 g/mol): monoclinic, space group $P2_1/n$ (no. 14), a = 12.70561(18) Å, b = 14.9295(3) Å, c = 13.7143(2) Å, β = 93.1156(13)°, V = 2597.58(7) Å^3, Z = 4, T = 150(2) K, μ(MoKα) = 6.682 mm^{-1}, *Dcalc* = 1.950 g/cm^3, 19825 reflections measured (5.056° ≤ 2Θ ≤ 65.242°), 8654 unique (R_{int} = 0.0297, R_{sigma} = 0.0414) which were used in all calculations. The final R_1 was 0.0271 (I > 2σ(I)) and wR_2 was 0.0867 (all data).

Crystal structure determination of [ps23]

Crystal Data for $C_{41}H_{36}Cl_2F_2NOPPt$ (M =893.67 g/mol): triclinic, space group P-1 (no. 2), a = 9.33343(14) Å, b = 12.19811(14) Å, c = 16.57528(15) Å, α = 99.8343(9)°, β = 105.1171(10)°, γ = 101.2367(11)°, V = 1737.24(4) Å^3, Z = 2, T = 150(2) K, μ(MoKα) = 4.284 mm^{-1}, *Dcalc* = 1.708 g/cm^3, 97999 reflections measured (4.608° ≤ 2Θ ≤ 62.994°), 11081 unique (R_{int} = 0.0395, R_{sigma} = 0.0239) which were used in all calculations. The final R_1 was 0.0216 (I > 2σ(I)) and wR_2 was 0.0802 (all data).

Crystal structure determination of [ps25] YAMHEK

Crystal Data for $C_{27}H_{33}F_2INPPt$ (M =762.50 g/mol): monoclinic, space group $P2_1/c$ (no. 14), a = 17.1855(2) Å, b = 12.17889(16) Å, c = 13.62801(18) Å, β = 106.9357(13)°, V = 2728.64(6) Å^3, Z = 4, T = 150(2) K, μ(CuKα) = 19.291 mm^{-1}, *Dcalc* = 1.856 g/cm^3, 26064 reflections measured (9.036° ≤ 2Θ ≤ 156.396°), 5784 unique (R_{int} = 0.0576, R_{sigma} = 0.0366) which were used in all calculations. The final R_1 was 0.0364 (I > 2σ(I)) and wR_2 was 0.1012 (all data).

Crystal structure determination of [ps27]

Crystal Data for $C_{40}H_{32}Cl_8F_2NPPt$ (M =1074.32 g/mol): monoclinic, space group $P2_1$ (no. 4), a = 10.79805(3) Å, b = 15.69187(7) Å, c = 11.92493(4) Å, β = 96.2700(3)°, V = 2008.495(12) Å^3, Z = 2, T = 150(2) K, μ(CuKα) = 12.147 mm^{-1}, *Dcalc* = 1.776 g/cm^3, 40986 reflections measured (7.458° ≤ 2Θ ≤ 156.128°), 8320 unique (R_{int} = 0.0406, R_{sigma} = 0.0320) which were used in all calculations. The final R_1 was 0.0356 (I > 2σ(I)) and wR_2 was 0.0948 (all data).

Crystal structure determination of [ps28] JASWEI

Crystal Data for $C_{41}H_{36}Cl_2F_2NOPPt$ (M =893.67 g/mol): triclinic, space group P-1 (no. 2), a = 9.91020(15) Å, b = 10.80576(13) Å, c = 16.7846(2) Å, α = 78.1754(11)°, β = 80.8448(12)°, γ = 89.9308(11)°, V = 1735.95(4) Å^3, Z = 2, T = 150(2) K, μ(CuKα) = 9.786 mm^{-1}, *Dcalc* = 1.710 g/cm^3, 68689 reflections measured (8.364° ≤ 2Θ ≤ 156.784°), 7386 unique (R_{int} = 0.0595, R_{sigma} = 0.0270) which were used in all calculations. The final R_1 was 0.0234 (I > 2σ(I)) and wR_2 was 0.0588 (all data).

Crystal structure determination of [ps29] JASWAE

Crystal Data for $C_{38}H_{29}ClF_2NPPt$ (M =799.13 g/mol): triclinic, space group P-1 (no. 2), a = 11.3911(3) Å, b = 11.7933(4) Å, c = 12.8630(3) Å, α = 100.845(2)°, β = 97.595(2)°, γ = 117.163(3)°, V = 1462.18(7) Å^3, Z = 2, T = 150(2) K, μ(CuKα) = 10.686 mm^{-1}, *Dcalc* = 1.815 g/cm^3, 27557 reflections measured (7.226° ≤ 2Θ ≤ 156.402°), 6188 unique (R_{int} = 0.0564, R_{sigma} = 0.0440) which were used in all calculations. The final R_1 was 0.0257 (I > 2σ(I)) and wR_2 was 0.0619 (all data).

Crystal structure determination of [ps32] JASVUX

Crystal Data for $C_{40.4}H_{33.2}Cl_{4.2}F_2NPPt$ (M =945.63 g/mol): monoclinic, space group I2/a (no. 15), a = 14.61871(18) Å, b = 17.9381(3) Å, c = 28.6293(4) Å, β = 98.6391(12)°, V = 7422.36(19) Å^3, Z = 8, T = 150(2) K, μ(MoKα) = 4.167 mm^{-1}, *Dcalc* = 1.692 g/cm^3, 113385 reflections measured (4.878° ≤ 2Θ ≤ 64.756°), 12768 unique (R_{int} = 0.0573, R_{sigma} = 0.0396) which were used in all calculations. The final R_1 was 0.0393 (I > 2σ(I)) and wR_2 was 0.0958 (all data).

Crystal structure determination of [ps34] JASWIM

Crystal Data for $C_{38}H_{31}ClF_2NPPt$ (M =801.15 g/mol): triclinic, space group P-1 (no. 2), a = 8.51403(11) Å, b = 10.31938(18) Å, c = 18.7511(3) Å, α = 83.1662(13)°, β = 79.6553(12)°, γ = 76.3618(13)°, V = 1569.92(4) Å^3, Z = 2, T = 150(2) K, μ(MoKα) = 4.646 mm^{-1}, *Dcalc* = 1.695 g/cm^3, 54759 reflections measured (4.792° ≤ 2Θ ≤ 67.348°), 11737 unique (R_{int} = 0.0370, R_{sigma} = 0.0305) which were used in all calculations. The final R_1 was 0.0210 (I > 2σ(I)) and wR_2 was 0.0435 (all data).

Crystal structure determination of [ps35] YAMHIG

Crystal Data for $C_{30}H_{39}F_2INPPt$ (M =804.58 g/mol): monoclinic, space group $P2_1/c$ (no. 14), a = 17.9485(2) Å, b = 12.31107(18) Å, c = 13.88543(18) Å, β = 110.0913(15)°, V = 2881.48(7) Å^3, Z = 4, T = 150(2) K, μ(MoKα) = 6.029 mm^{-1}, *Dcalc* = 1.855 g/cm^3, 56183 reflections measured (6.454° ≤ 2Θ ≤ 69.214°), 11614 unique (R_{int} = 0.0429, R_{sigma} = 0.0369) which were used in all calculations. The final R_1 was 0.0295 (I > 2σ(I)) and wR_2 was 0.0652 (all data).

Crystal structure determination of [ps37] YAMHUS

Crystal Data for $C_{28}H_{35}F_2INPPt$ (M =776.53 g/mol): monoclinic, space group $P2_1/c$ (no. 14), a = 8.56227(7) Å, b = 17.96588(15) Å, c = 18.24470(15) Å, β = 96.9421(8)°, V = 2785.98(4) Å^3, Z = 4, T = 150(2) K, μ(MoKα) = 6.232 mm^{-1}, *Dcalc* =

1.851 g/cm^3, 85124 reflections measured (4.792° ≤ 2Θ ≤ 64.83°), 9618 unique (R_{int} = 0.0428, R_{sigma} = 0.0258) which were used in all calculations. The final R_1 was 0.0223 (I > 2σ(I)) and wR_2 was 0.0437 (all data).

Crystal structure determination of [ps38] JASWOS

Crystal Data for $C_{39}H_{30}Cl_4F_2NPPt$ (M =918.50 g/mol): triclinic, space group P-1 (no. 2), a = 10.06885(9) Å, b = 10.97968(11) Å, c = 17.46056(18) Å, α = 107.6381(9)°, β = 97.2289(9)°, γ = 105.2604(8)°, V = 1729.76(3) Å^3, Z = 2, T = 150(2) K, μ(CuKα) = 11.208 mm^{-1}, *Dcalc* = 1.763 g/cm^3, 59546 reflections measured (8.664° ≤ 2Θ ≤ 147.208°), 6645 unique (R_{int} = 0.0543, R_{sigma} = 0.0224) which were used in all calculations. The final R_1 was 0.0198 (I > 2σ(I)) and wR_2 was 0.0489 (all data).

Crystal structure determination of [ps39] JASWUY

Crystal Data for $C_{39}H_{30}Cl_6F_2NPPt$ (M =989.40 g/mol): monoclinic, space group $P2_1/n$ (no. 14), a = 11.49295(19) Å, b = 22.2749(4) Å, c = 14.2990(2) Å, β = 91.1028(14)°, V = 3659.93(10) Å^3, Z = 4, T = 150(2) K, μ(MoKα) = 4.357 mm^{-1}, *Dcalc* = 1.796 g/cm^3, 104681 reflections measured (4.504° ≤ 2Θ ≤ 63.73°), 11956 unique (R_{int} = 0.0546, R_{sigma} = 0.0334) which were used in all calculations. The final R_1 was 0.0255 (I > 2σ(I)) and wR_2 was 0.0519 (all data).

Crystal structure determination of [ps40] JASWUX

Crystal Data for $C_{42}H_{34}Cl_{10}F_2NOPPt$ (M =1187.26 g/mol): monoclinic, space group I2/a (no. 15), a = 23.6952(4) Å, b = 14.2502(3) Å, c = 27.6824(5) Å, β = 103.1991(19)°, V = 9100.3(3) Å^3, Z = 8, T = 100(2) K, μ(MoKα) = 3.749 mm^{-1}, *Dcalc* = 1.733 g/cm^3, 41772 reflections measured (5.036° ≤ 2Θ ≤ 61.916°), 12881 unique (R_{int} = 0.0299, R_{sigma} = 0.0351) which were used in all calculations. The final R_1 was 0.0404 (I > 2σ(I)) and wR_2 was 0.1033 (all data).

8.2. Chart Data

8.2.1. Table of Data for Figure 4.12 and Figure 4.13

	Amounts based on the integration of the methyl peak in the ^{1}H NMR spectrum					Relative amounts of each complex			
Time(h)	**Me-27(t)**	**Me-27(c)**	**Me-28(a)**	**Me-28(b)**	**total**	**Me-27(t)**	**Me-27(c)**	**Me-28(a)**	**Me-28(b)**
0	1.0000	0.0000	0.0000	0.0000	1.0000	100.0000	0.0000	0.0000	0.0000
1	4.6293	0.3332	0.0956	0.0579	5.1160	90.4867	6.5129	1.8686	1.1317
2	4.1761	0.5215	0.1009	0.0946	4.8931	85.3467	10.6579	2.0621	1.9333
3	4.0621	0.7406	0.1528	0.1367	5.0922	79.7710	14.5438	3.0007	2.6845
4	3.8279	0.8886	0.1895	0.1767	5.0827	75.3123	17.4828	3.7283	3.4765
5	3.5429	0.9822	0.2450	0.2289	4.9990	70.8722	19.6479	4.9010	4.5789
6	3.3684	1.0907	0.2672	0.2900	5.0163	67.1491	21.7431	5.3266	5.7812
7	3.1977	1.1683	0.3338	0.3377	5.0375	63.4779	23.1921	6.6263	6.7037
8	3.0504	1.2755	0.3411	0.3546	5.0216	60.7456	25.4003	6.7927	7.0615
9	2.8900	1.3522	0.3783	0.3743	4.9948	57.8602	27.0722	7.5739	7.4938
10	2.8206	1.4478	0.4085	0.4086	5.0855	55.4636	28.4692	8.0326	8.0346
11	2.6892	1.4928	0.4220	0.4356	5.0396	53.3614	29.6214	8.3737	8.6435
12	2.5201	1.5278	0.4356	0.4357	4.9192	51.2299	31.0579	8.8551	8.8571
13	2.5038	1.6202	0.4845	0.5060	5.1145	48.9549	31.6786	9.4731	9.8934
14	2.4020	1.7018	0.4800	0.5072	5.0910	47.1813	33.4276	9.4284	9.9627
15	2.3188	1.6956	0.5174	0.5144	5.0462	45.9514	33.6015	10.2533	10.1938
16	2.2580	1.7304	0.5477	0.5510	5.0871	44.3868	34.0155	10.7664	10.8313
17	2.1046	1.7724	0.5600	0.5557	4.9927	42.1535	35.4998	11.2164	11.1303
18	2.0857	1.8670	0.5805	0.5663	5.0995	40.9001	36.6114	11.3835	11.1050
19	1.9952	1.9102	0.5545	0.5671	5.0270	39.6897	37.9988	11.0304	11.2811
20	1.8838	1.8878	0.5786	0.5962	4.9464	38.0843	38.1651	11.6974	12.0532
21	1.8255	1.9302	0.6083	0.6066	4.9706	36.7259	38.8323	12.2380	12.2038
22	1.7897	2.0331	0.6127	0.6090	5.0445	35.4782	40.3033	12.1459	12.0726
23	1.7081	2.0094	0.6400	0.6297	4.9872	34.2497	40.2911	12.8329	12.6263
24	1.7023	2.0850	0.6262	0.6357	5.0492	33.7143	41.2937	12.4020	12.5901
26	1.6256	2.1580	0.6820	0.6672	5.1328	31.6708	42.0433	13.2871	12.9988
28	1.5580	2.1472	0.7079	0.6958	5.1089	30.4958	42.0286	13.8562	13.6194
30	1.4918	2.2295	0.7287	0.6985	5.1485	28.9754	43.3039	14.1536	13.5671
32	1.3942	2.3400	0.7245	0.6868	5.1455	27.0955	45.4766	14.0803	13.3476
34	1.3061	2.3385	0.7541	0.7257	5.1244	25.4879	45.6346	14.7159	14.1617
36	1.2202	2.4078	0.7518	0.7104	5.0902	23.9716	47.3027	14.7696	13.9562

38	1.1745	2.4345	0.7236	0.7342	5.0668	23.1803	48.0481	14.2812	14.4904
40	1.1185	2.4680	0.7561	0.7397	5.0823	22.0078	48.5607	14.8771	14.5544
42	1.0878	2.5538	0.7779	0.7786	5.1981	20.9269	49.1295	14.9651	14.9785
44	1.0086	2.4931	0.7479	0.7567	5.0063	20.1466	49.7993	14.9392	15.1150
46	0.9878	2.5291	0.8049	0.7793	5.1011	19.3645	49.5795	15.7789	15.2771
48	0.9223	2.6240	0.7973	0.7914	5.1350	17.9611	51.1003	15.5268	15.4119
50	0.8854	2.7015	0.7909	0.7959	5.1737	17.1135	52.2160	15.2869	15.3836
52	0.8377	2.7482	0.8002	0.7915	5.1776	16.1793	53.0786	15.4550	15.2870
54	0.8278	2.7323	0.8540	0.8210	5.2351	15.8125	52.1919	16.3130	15.6826
56	0.7653	2.7332	0.8110	0.7879	5.0974	15.0135	53.6195	15.9101	15.4569
58	0.5919	2.7533	0.8764	0.8257	5.0473	11.7271	54.5500	17.3637	16.3592
60	0.5011	2.7599	0.8216	0.7995	4.8821	10.2640	56.5310	16.8288	16.3761
62	0.4519	2.8485	1.0097	0.9032	5.2133	8.6682	54.6391	19.3678	17.3249
64	0.4519	2.8485	1.0097	0.9032	5.2133	8.6682	54.6391	19.3678	17.3249
88	0.3348	2.8546	0.9300	0.8840	5.0034	6.6914	57.0532	18.5874	17.6680
112	0.2567	2.8571	0.9065	0.9666	4.9869	5.1475	57.2921	18.1776	19.3828
136	0.1568	2.8742	0.9275	0.7466	4.7051	3.3326	61.0869	19.7127	15.8679

8.2.2. Table of Data for Figure 4.14

Time (h)	Me-30(a)↓	Me-30(b)↓	Sum*	relative amount of Me-30(a)‡	relative amount of Me-30(b)‡	ln([Me-30(a)]/[Me-30(a)]$_0$)‡
0	1.2705	0.3557	1.6262	0.7813	0.2187	-0.4863
1	1.2769	0.3703	1.6472	0.7752	0.2248	-0.4941
2	1.2721	0.3898	1.6619	0.7654	0.2346	-0.5067
3	1.2516	0.4131	1.6647	0.7518	0.2482	-0.5247
4	1.2102	0.4286	1.6388	0.7385	0.2615	-0.5426
5	1.2148	0.4449	1.6597	0.7319	0.2681	-0.5515
6	1.1987	0.4724	1.6711	0.7173	0.2827	-0.5717
7	1.1750	0.4959	1.6709	0.7032	0.2968	-0.5915
8	1.1724	0.4999	1.6723	0.7011	0.2989	-0.5946
9	1.1500	0.5176	1.6676	0.6896	0.3104	-0.6111
10	1.1565	0.5328	1.6893	0.6846	0.3154	-0.6184
11	1.1184	0.5515	1.6699	0.6697	0.3303	-0.6403
12	1.0827	0.5532	1.6359	0.6618	0.3382	-0.6522
13	1.0982	0.5770	1.6752	0.6556	0.3444	-0.6617
14	1.0809	0.5974	1.6783	0.6440	0.3560	-0.6794
15	1.0741	0.6019	1.6760	0.6409	0.3591	-0.6844
16	1.0517	0.6388	1.6905	0.6221	0.3779	-0.7141
17	1.0427	0.6452	1.6879	0.6177	0.3823	-0.7211
18	1.0468	0.6342	1.6810	0.6227	0.3773	-0.7131
19	1.0081	0.6459	1.6540	0.6095	0.3905	-0.7346
20	0.9913	0.6737	1.6650	0.5954	0.4046	-0.7580
21	0.9657	0.6907	1.6564	0.5830	0.4170	-0.7790
22	0.9516	0.6787	1.6303	0.5837	0.4163	-0.7778
23	0.9530	0.7056	1.6586	0.5746	0.4254	-0.7936
24	0.9404	0.7243	1.6647	0.5649	0.4351	-0.8105
26	0.8922	0.7079	1.6001	0.5576	0.4424	-0.8236
28	0.8679	0.7031	1.5710	0.5525	0.4475	-0.8328
30	0.8352	0.7335	1.5687	0.5324	0.4676	-0.8698
32	0.8008	0.7516	1.5524	0.5158	0.4842	-0.9014
34	0.7670	0.7542	1.5212	0.5042	0.4958	-0.9242
36	0.7560	0.7839	1.5399	0.4909	0.5091	-0.9509
38	0.7242	0.8193	1.5435	0.4692	0.5308	-0.9962
40	0.7149	0.8424	1.5573	0.4591	0.5409	-1.0180
42	0.7008	0.8467	1.5475	0.4529	0.5471	-1.0316
44	0.6736	0.8738	1.5474	0.4353	0.5647	-1.0711
46	0.6525	0.8785	1.5310	0.4262	0.5738	-1.0923
48	0.6268	0.8834	1.5102	0.4150	0.5850	-1.1188
50	0.6001	0.8735	1.4736	0.4072	0.5928	-1.1378

52	0.5948	0.8733	1.4681	0.4051	0.5949	-1.1429
54	0.5677	0.9016	1.4693	0.3864	0.6136	-1.1904
56	0.5567	0.9010	1.4577	0.3819	0.6181	-1.2020
58	0.5517	0.9400	1.4917	0.3698	0.6302	-1.2341
60	0.5410	0.9361	1.4771	0.3663	0.6337	-1.2439
62	0.5189	0.9117	1.4306	0.3627	0.6373	-1.2536
64	0.5019	0.9305	1.4324	0.3504	0.6496	-1.2881
75	0.4587	0.9604	1.4191	0.3232	0.6768	-1.3688
77	0.4482	0.9921	1.4403	0.3112	0.6888	-1.4068
79	0.4227	0.9556	1.3783	0.3067	0.6933	-1.4214
81	0.4242	0.9673	1.3915	0.3049	0.6951	-1.4274
83	0.4106	0.9782	1.3888	0.2957	0.7043	-1.4580
85	0.3976	0.9904	1.3880	0.2865	0.7135	-1.4896
87	0.4055	1.0277	1.4332	0.2829	0.7171	-1.5020
88	0.3921	0.9978	1.3899	0.2821	0.7179	-1.5049
93	0.3543	1.0114	1.3657	0.2594	0.7406	-1.5887
95	0.3337	0.9655	1.2992	0.2569	0.7431	-1.5987
97	0.3238	0.9989	1.3227	0.2448	0.7552	-1.6467
99	0.3242	1.0118	1.3360	0.2427	0.7573	-1.6555
101	0.3165	1.0016	1.3181	0.2401	0.7599	-1.6661
103	0.3063	0.9936	1.2999	0.2356	0.7644	-1.6849
105	0.2934	0.9969	1.2903	0.2274	0.7726	-1.7205
107	0.3039	1.0178	1.3217	0.2299	0.7701	-1.7094
110	0.2892	1.0096	1.2988	0.2227	0.7773	-1.7415
116	0.2637	0.9823	1.2460	0.2116	0.7884	-1.7923
133	0.2441	0.9768	1.2209	0.1999	0.8001	-1.8492
159	0.1924	0.9979	1.1903	0.1616	0.8384	-2.0618
170	0.1841	0.9092	1.0933	0.1684	0.8316	-2.0209

⸸ Taken from the integration of the methyl peak in the ^{1}H NMR spectrum

* The sum of the integrals of **Me-30(a)** and **Me-30(b)**

⁑ The ratio of the complex in solution

‡ Equation for straight-line graph for a first order reaction, $y=\ln([A]/[A]_o)$ vs time.

8.2.3. Table of Data for Figure 4.15

	Deuterium count (%)			
Time (h)	**0**	**1**	**2**	**3**
0	84	16	0	0
1	83	17	0	0
2	74	26	0	0
9	55	45	0	0
16	25	41	34	0
24	8	44	48	0
60	0	34	48	18
132	0	13	46	41
168	0	6	43	51
204	0	5	32	63
264	0	0	23	76
312	0	0	20	80
336	0	0	15	85